

Development of recombinant antibody fragments for mycotoxin detection and the investigation of AFB₁ and anti-AFB₁ Fab antibody fragment effects in hepatocellular carcinoma

Kara Moran B.Sc., M.Sc.

This thesis is submitted to Dublin City University for the degree of
Ph.D.

December 2017

Based on research carried out at
School of Biotechnology,
Dublin City University,
Dublin 9,
Ireland.

**Supervisors: Professor Richard O’Kennedy
Dr. Sandra O’Neill
Dr. Julie-Ann O’Reilly**

Declaration

I hereby certify that this material, which I now submit for assessment on the programme of study leading to the award of (insert title of degree for which registered) is entirely my own work, that I have exercised reasonable care to ensure that the work is original, and does not to the best of my knowledge breach any law of copyright, and has not been taken from the work of others save and to the extent that such work has been cited and acknowledged within the text of my work.

Signed: _____ (Candidate) ID No.: _____ Date: _____

Acknowledgements

Firstly, I would like to express my sincere gratitude to my supervisor Prof. Richard O' Kennedy for his patience, motivation, immense understanding and continuous support of my PhD studies and additional ambitions. His guidance helped me through all my work in the lab and in the writing of many works, most of all, this thesis. I am very grateful for an enthusiastic and kind mentor who was so generous with his time and knowledge. I have gained much confidence from this opportunity, and will always rely on what I have learned whilst under Prof. O' Kennedy's influential leadership.

Dr. Julie-Ann O' Reilly, I thank you for your encouragement, belief and discussions. To all, past and present in the Applied Biochemistry Group, Jonathan, Dan, Aoife, Arabelle, Julia, Jenny, Fay, Caroline, Sarah, Hannah, Sean, Darragh, Rory and Ivan too, I want to thank you most of all for your friendship, but, also for the advice and recommendations you have made to this work. There have been many coffees, scones, coffee-mornings, lunches, dinners, ice-creams, and even a few drinks along the way and I could not have imagined working with such a smart, talented and fun group. I also would like to acknowledge the BRS, the School of Biotechnology and the DCU Daniel O' Hare Scholarship programme for their support.

I am forever grateful to my Mam and Dad who believe in the importance of education and have made many sacrifices to ensure this was received. In life they live by the principles of honesty, hard work, perseverance and good humor, and following their example has served me well throughout this research. I am also thankful to my sister Pauline and my brothers Denis, John and David who have guided me my whole life and inspire me every day with their amazing work-ethic and outstanding achievements. To Norah, thank you for your support and encouragement in my educational goals.

Finally, I would like to thank Keith for your unending reassurance and enthusiasm for my research endeavors. I would have never embarked on this PhD journey were it not for you. Your confidence, support and belief in me are what got me through this work, and, gets me through everything else I do. I am most thankful for the infinite patience and generosity you show me, all in good-nature and with a smile. This work is dedicated to you and us.

Table of Contents

Declaration	i
Acknowledgements	ii
Table of Contents	iii
Table of Figures	ix
List of Tables	xiii
Abbreviations	xv
Units	xxi
List of Publications	xxiii
Courses, Scholarships and Awards	xxv
Abstract.....	1
1. Introduction	2
1.1. Introduction to thesis research	3
1.2. Mycotoxins.....	3
1.2.1. Mycotoxin Storage	4
1.2.2. Mycotoxin regulation	5
1.2.3. Aflatoxins	6
1.2.3.1 Human impact of aflatoxins.....	7
1.2.3.2 Aflatoxins and hepatocellular carcinoma.....	8
1.2.3.3 Hepatocellular carcinoma and cytokines	9
1.2.3.4 Aflatoxin B ₁ metabolism and mode of action.....	12
1.2.3.5 Economic impact of aflatoxins	14
1.2.4. Zearalenone	15
1.2.4.1 Animal impact of ZEN.....	16
1.2.5. Trichothecenes – T-2 toxin	18
1.2.5.1 T-2 toxin.....	19
1.2.6. Mycotoxin methods of detection.....	20
1.2.6.1 Chromatographic methods for mycotoxin detection.....	21
1.2.6.2 Immunoassay-based methods for mycotoxin detection.....	21
1.2.6.3 Immunoassays – conjugate development.....	24
1.2.6.4 Immunoassays – extraction methods	26
1.3. Antibody generation.....	27
1.3.1. Antibodies	27
1.3.2. Recombinant antibody fragments	29
1.3.3. Recombinant antibody fragment generation	30
1.3.4. Filamentous phage and phage display	31
1.3.5. Filamentous phage biology	32
1.3.6. Phagemids	34
1.3.7. Phage display and panning.....	36
1.3.8. Bacterial expression	37
1.4. Thesis aims.....	38
2. Materials and Methods	40
2.1. Materials.....	41

2.2 Methods.....	48
2.2.1 Safety precautions and protocols for handling toxin materials and waste	48
2.2.2 Preparation of T-2 Toxin-OVA and T-2 Toxin-BSA conjugates	48
2.2.3 Preparation of ZEN-OVA and AFB ₂ -OVA conjugates	51
2.2.4 BCA (Bicinchoninic Acid) assay for protein estimation	53
2.2.5 Reverse transcription of RNA to cDNA	54
2.2.6 Library building and linker selection	54
2.2.7 Amplification of avian variable heavy chain (V _H) and light chain (V _L) genes.....	55
2.2.8 Splice-by-Overlap Extension Polymerase Chain Reaction (SOE-PCR).....	57
2.2.9 Restriction digestion of SOE-PCR product and pComb3xSS Vector.....	58
2.2.10 Ligation of restriction digested SOE-PCR product into restriction digested pComb3xSS vector	60
2.2.11 Transformation of ligated pComb3xSS vector into electrocompetent XL-1 Blue <i>E. coli</i> cells.....	60
2.2.12 Selective enrichment of specific scFv displaying phage particles by panning.....	62
2.2.12.1 Library input titre	62
2.2.12.2 Library output titre	63
2.2.13 Polyclonal phage ELISA	64
2.2.14 Soluble expression of scFv antibody fragments in Top 10F' cells.....	65
2.2.15 Monoclonal ELISA of expressed soluble scFv antibody fragments	65
2.2.16 Re-amplification of polyclonal phage	66
2.2.17 Selective enrichment of specific scFv displaying phage particles by depletion panning with 0.1% (w/v) Ovalbumin buffer	67
2.2.18 Colony pick PCR	67
2.2.19 Bacterial expression.....	69
2.2.20 Protein extraction methods	69
2.2.20.1 Freeze-thawing.....	70
2.2.20.2 Periplasmic Osmotic Shock	70
2.2.20.3 Sonication	70
2.2.21 Immobilized Metal Ion Affinity Chromatography (IMAC)	70
2.2.22 Protein concentration and buffer exchange	71
2.2.23 Gel filtration/Size exclusion chromatography	72
2.2.24 SDS-PAGE (Sodium Dodecyl Sulphate Polyacrylamide Gel Electrophoresis).....	72
2.2.25 Western Blotting analysis	73
2.2.26 Indirect ELISA.....	75
2.2.27 Indirect competitive inhibition ELISA	76
2.2.28 MBio microarray printing and cartridge development	76
2.2.29 MBio assay protocol	78
2.2.29.1 MBio multiplex assay protocol.....	80
2.2.30 IC ₅₀ Value, limit of detection (LOD), dynamic range and coefficient of variance (CV) calculations.....	80

2.2.31 Extraction of AFB ₁ from dried distillers grains with solubles (1).....	82
2.2.32 Extraction of AFB ₁ from dried distillers grains with solubles (2)	83
2.2.33 Rapid extraction of AFB ₁ from Dried Distillers Grains with Solubles.....	84
2.2.34 Resuscitation of frozen cell line stocks	84
2.2.35 Sub-culturing THLE-2 cells	85
2.2.36 Sub-culturing HepG2 cells	85
2.2.37 Cell counting and Viability Assessment.....	86
2.2.38 AFB ₁ dosage and anti-AFB ₁ Fab treatment of THLE-2 cells.....	87
2.2.39 AFB ₁ dosage and anti-AFB ₁ Fab treatment of HepG2 cells.....	87
2.2.40 Scratch assay.....	88
2.2.41 MTT cell proliferation assay	88
2.2.42 Cytokine analysis.....	89
2.2.43 Long term storage of cells	90
3. Generation of avian recombinant anti-T-2 Toxin scFv antibody fragments.....	91
3.1. Introduction.....	92
3.2 Results.....	94
3.2.1 Evaluation criteria of T-2 toxin conjugates.....	94
3.2.1.1 Evaluation of T-2 toxin-OVA conjugate	95
3.2.1.2 Evaluation of T-2 toxin-BSA conjugate	96
3.2.2 Evaluation of avian RNA integrity	97
3.2.3 Anti T-2 toxin cDNA synthesis from avian RNA.....	99
3.2.4 Bone marrow V _H and V _L gene sequence amplifications and generation of SOE-PCR product.....	100
3.2.5 Spleen V _H and V _L gene sequence amplifications and generation of SOE-PCR product.	102
3.2.6 Restriction digestion of pComb3xSS vector, and anti-T-2 toxin purified bone marrow and spleen SOE-PCR products	105
3.2.7 Phage display and panning of anti-T-2 toxin library against T-2 toxin-OVA	107
3.2.8 Polyclonal phage ELISA screening against T-2 toxin-OVA and OVA.....	108
3.2.9 Monoclonal ELISA screening against T-2 toxin-OVA and OVA.....	110
3.2.10 Re-amplified polyclonal phage for phage-display and panning of anti-T-2 toxin library	111
3.2.11 Re-amplified polyclonal phage ELISA screening against T-2 toxin-OVA and OVA	112
3.2.12 Repeat bone marrow V _H and V _L gene sequence amplifications and generation of SOE-PCR product.	113
3.2.13 Phage-display and panning of anti-T-2 toxin library against T-2 toxin-BSA	115
3.2.14 Polyclonal phage ELISA screening against T-2 toxin-BSA and BSA.....	116
3.2.14.1 Indirect checkerboard ELISA to confirm functionality of T-2 toxin-BSA following polyclonal phage ELISA.....	118
3.2.15 Colony pick PCR	119

3.2.16 Indirect competitive inhibition ELISA using commercial anti-T-2 toxin polyclonal antibody	120
3.3 Discussion	123
4. The selection and characterisation of recombinant antibody fragments for detection of mycotoxins in a ‘point-of-site’ device	128
4.1. Introduction	129
4.2. Results	131
4.2.1. Expression, purification and characterisation of an anti-AFB ₁ Fab antibody fragment	131
4.2.2. SDS-PAGE and Western Blotting Analysis of an anti-AFB ₁ Fab antibody fragment	132
4.2.3. Indirect checkerboard ELISA using varying concentrations of anti-AFB ₁ Fab and AFB ₁ -BSA coating concentrations.....	135
4.2.4. Indirect competitive inhibition ELISA using anti-AFB ₁ Fab and varying concentrations of free AFB ₁ and AFB ₁ -BSA coating concentrations.....	136
4.2.5. Evaluation criteria of AFB ₂ conjugates	138
4.2.5.1 Evaluation of AFB ₂ -OVA.....	139
4.2.6. Monoclonal ELISA selection of anti-AFB ₂ scFv antibody fragments.....	141
4.2.7. Expression, purification and indirect ELISA with varying dilutions of anti-AFB ₂ scFv antibody fragments.....	143
4.2.8. SDS-PAGE and Western blotting analysis of anti-AFB ₂ scFv antibody fragments.....	144
4.2.9. Indirect ELISA of a selected anti-AFB ₁ scFv antibody fragment with varying concentrations of AFB ₂ -OVA.....	146
4.2.10. Indirect competitive inhibition ELISA using anti-AFB ₂ scFv antibody fragment and varying concentrations of free AFB ₂ and AFB ₂ -OVA coating concentrations.....	147
4.2.11. Evaluation criteria of ZEN conjugates	148
4.2.11.1 Evaluation of ZEN-OVA conjugate.....	148
4.2.12. Monoclonal ELISA selection of anti-ZEN scFv antibody fragments	150
4.2.13. Expression, purification and indirect ELISA with varying dilutions of anti-ZEN scFv antibody fragments.....	152
4.2.14. SDS-PAGE and Western blotting analysis of anti-ZEN scFv antibody fragments.....	153
4.2.15. Indirect checkerboard ELISA using varying concentrations of anti-ZEN scFv antibody fragments and ZEN-OVA coating concentrations	155
4.2.16. MBio Testing and Analysis of AFB ₁ in PBS	157
4.2.17. MBio Testing and Analysis of T-2 Toxin in PBS.....	158
4.2.18. MBio Testing and Analysis of AFB ₁ spiked in DDGS extract.....	160
4.2.19. MBio Testing and Analysis of T-2 toxin spiked in DDGS extract.....	162
4.2.20. MBio Multiplex Testing and Analysis of AFB ₁ and T-2 toxin in Contaminated DDGS samples	164
4.3 Discussion	166

5. The investigation of AFB₁ and anti-AFB₁ Effects on HepG2 hepatocellular carcinoma cells	171
5.1 Introduction.....	172
5.2 Results.....	175
5.2.1 The effects of AFB ₁ dosing and anti-AFB ₁ Fab antibody fragment treatment on HepG2 cell migration.....	175
5.2.1.1 The effects of AFB ₁ exposure on HepG2 cell migration.....	176
5.2.1.2 The effects of anti-AFB ₁ Fab antibody fragment on HepG2 cell migration	179
5.2.1.3 The effects of anti-AFB ₁ Fab antibody fragment treatment on HepG2 and THLE-2 cell migration	181
5.2.2 The effects of AFB ₁ dosing combined with anti-AFB ₁ Fab antibody fragment treatment on HepG2 cell proliferation.....	187
5.2.2.1 The effects of AFB ₁ dosing on HepG2 cell proliferation	188
5.2.2.2 The effects of AFB ₁ dosing and anti-AFB ₁ Fab antibody fragment treatment on HepG2 cell proliferation.....	191
5.2.2.3 The combined effects of AFB ₁ anti-AFB ₁ Fab antibody fragment treatments on HepG2 cell proliferation	193
5.2.2.4 SDS-PAGE and Western blotting analysis of anti-AFB ₁ scFv-dimer antibody fragment.....	194
5.2.2.5 The effects of varying anti-AFB ₁ antibody-format treatments on HepG2 cell proliferation	197
5.2.2.6 The effects of antibody fragment CDR sequences on HepG2 cell proliferation.....	198
5.2.2.7 SDS-PAGE and Western blotting analysis of anti-M3G Fab antibody fragment	200
5.2.2.8 The effects of anti-AFB ₁ and anti-M3G Fab antibody fragment treatments on HepG2 cell proliferation.....	203
5.2.2.9 The effects of varying anti-AFB ₁ antibody-format treatments on THLE-2 cell proliferation	205
5.2.2.10 Sequence analysis of anti-AFB ₁ fab antibody fragment and IGF-1R	206
5.2.3 The effects of AFB ₁ dosing combined with anti-AFB ₁ Fab antibody fragment treatment on HepG2 cell cytokine expression.....	207
5.2.3.1 The effects of AFB ₁ dosing on HepG2 cell IL-8 cytokine expression.	208
5.2.3.2 The effects of anti-AFB ₁ Fab antibody fragment treatment on HepG2 cell IL-8 cytokine expression	210
5.2.3.3 The effects of AFB ₁ dosing and anti-AFB ₁ Fab antibody fragment treatment on HepG2 cell IL-8 cytokine expression.....	212
5.3 Discussion.....	214
6. Conclusions.....	222
6.1. Overall Conclusions.....	223
Bibliography	229

Appendices.....	247
Appendix A	248
Appendix B	269

Table of Figures

Figure 1.1: Aflatoxin structures.....	7
Figure 1.2: Afatoxin B ₁ metabolism.....	14
Figure 1.3: Zearalenone metabolism	17
Figure 1.4: Deoxynivalenol and T-2 toxin structures.....	19
Figure 1.5: Competitive inhibition ELISA for mycotoxin analysis	23
Figure 1.6: Antibody and antibody fragment structures.....	29
Figure 1.7: Filamentous phage particle	32
Figure 1.8: Recombinant antibody engineering strategy, phage display and panning.....	37
Figure 2.1: T-2 toxin conjugate synthesis	49
Figure 2.2: ZEN-OVA conjugate synthesis.....	52
Figure 2.3: Sandwich format for Western blot transfer	74
Figure 2.4: (A) MBio optical-planar waveguide multiplexed immunoassay system (B) MBio disposable cartridges	78
Figure 2.5: MBio competitive inhibition assay format	79
Figure 3.1: Competitive inhibition ELISA with varying dilutions of T-2 toxin-OVA and free T-2 toxin against a 1/500 dilution of anti-T-2 toxin polyclonal antibody.....	96
Figure 3.2: Competitive inhibition ELISA with varying dilutions of T-2 toxin-BSA and free T-2 toxin against a 1/500 dilution of anti-T-2 toxin polyclonal antibody.....	97
Figure 3.3: Agarose gel (1% (w/v)) analysis of avian bone marrow and spleen RNA	98
Figure 3.4: (A) Bone marrow V _H and (B) V _L gene amplification.....	101
Figure 3.5: Bone marrow V _H and V _L chain SOE-PCR product	102
Figure 3.6: (A) Spleen V _H and (B) V _L gene amplification.....	103
Figure 3.7: Spleen V _H and V _L chain SOE-PCR product.....	104
Figure 3.8: Purified bone marrow and spleen V _H and V _L chain gene SOE-PCR product.....	105
Figure 3.9: Purified restriction digested bone marrow and spleen SOE-PCR products and pComb3xSS vector.....	106
Figure 3.10: Anti-T-2 toxin polyclonal phage ELISA (neat) screened against T-2 toxin-OVA and OVA	109
Figure 3.11: Anti-T-2 toxin polyclonal phage ELISA (diluted 1/3) screened against T-2 toxin-OVA and carrier proteins	110
Figure 3.12: Monoclonal ELISA of selected anti-T-2 toxin scFv clones screened against T-2 toxin-OVA and OVA.....	111
Figure 3.13: Re-amplified anti-T-2 toxin polyclonal phage ELISA (diluted 1/3) screened against T-2 toxin-OVA and KLH	113
Figure 3.14: Bone marrow V _H and V _L chain SOE-PCR product.....	114
Figure 3.15: Anti-T-2 toxin polyclonal phage ELISA (neat) screened against T-2 toxin-BSA, BSA and KLH.....	117
Figure 3.16: Indirect checkerboard ELISA with varying dilutions of T-2 toxin-BSA and anti-T-2 toxin polyclonal antibody.....	119

Figure 3.17: Colony pick PCR of unpanned and panned library colonies containing the pComb3xSS vector.....	120
Figure 3.18: Indirect competitive inhibition ELISA with T-2 toxin-BSA and varying dilutions of free T-2 toxin against anti-T-2 toxin polyclonal antibody.....	122
Figure 4.1: (A) SDS-PAGE analysis of IMAC-purified anti-AFB ₁ Fab antibody fragment.....	133
Figure 4.1: (B) Western blotting analysis of expressed and purified anti-AFB ₁ Fab Heavy chain and (C) Light chain	134
Figure 4.1: (D) SDS-PAGE and (E) Western blotting analysis of IMAC and gel-filtration purified anti-AFB ₁ Fab antibody fragment.....	135
Figure 4.2: Indirect checkerboard ELISA with varying dilutions of AFB ₁ -BSA and anti-AFB ₁ Fab antibody fragment.....	136
Figure 4.3: Indirect competitive inhibition ELISA with varying dilutions of AFB ₁ -BSA and free AFB ₁ against a 1/2,000 dilution of anti-AFB ₁ Fab antibody fragment.....	138
Figure 4.4: Indirect competitive inhibition ELISA with varying dilutions of AFB ₂ -OVA and free AFB ₂ toxin against a 1/200 dilution of monoclonal antibody (76% CR with AFB ₂)	141
Figure 4.5: Anti-AFB ₂ monoclonal ELISA of 384 anti-AFB ₂ scFv-expressing clones ...	142
Figure 4.6: Indirect ELISA of 8 anti-AFB ₂ scFv-producing clones neat, diluted 1/100 and 1/1,000.....	143
Figure 4.7: (A) SDS-PAGE and (B) Western blotting analysis of 5 expressed and IMAC- purified anti-AFB ₂ scFv-producing clones	145
Figure 4.8: Indirect ELISA of AFB ₂ -OVA and selected anti-AFB ₂ scFv antibody fragment at varying dilutions	146
Figure 4.9: Indirect competitive inhibition ELISA with AFB ₂ -OVA and varying dilutions of free AFB ₂ against anti-AFB ₂ scFv antibody fragment	148
Figure 4.10: Indirect competitive inhibition ELISA with varying dilutions of ZEN-OVA and free ZEN toxin against a 1/500 dilution of anti-ZEN antibody.....	150
Figure 4.11: Anti-ZEN monoclonal ELISA of 288 anti-ZEN scFv expressing clones	151
Figure 4.12: Indirect ELISA with ZEN-OVA and varying dilutions of anti-ZEN-expressing clones.....	152
Figure 4.13: SDS-PAGE and Western blotting analysis of expressed and IMAC-purified anti-ZEN scFv-producing clones.....	154
Figure 4.14: Indirect checkerboard ELISA of Clone 14 anti-ZEN scFv antibody fragment at varying dilutions against a range of ZEN-OVA coating	156
Figure 4.15: Indirect checkerboard ELISA of Clone 21 anti-ZEN scFv antibody fragment at varying dilutions against a range of ZEN-OVA coating concentrations....	157
Figure 4.16: MBio Indirect Competitive Inhibition Assay with anti-AFB ₁ Fab antibody fragment against free AFB ₁ in PBS and immobilised AFB ₁ -BSA (50 µg/mL).....	158

Figure 4.17: MBio Indirect Competitive Inhibition Assay with anti-T-2 toxin polyclonal antibody fragment against free T-2 toxin in PBS and immobilised T-2 toxin-BSA (50 µg/mL)	159
Figure 4.18: MBio Indirect Competitive Inhibition Assay with anti-AFB ₁ Fab antibody fragment against free AFB ₁ in DDGS extract and immobilised AFB ₁ -BSA (50 µg/mL)	161
Figure 4.19: MBio Indirect Competitive Inhibition Assay with anti-T-2 toxin polyclonal antibody against free T-2 toxin in DDGS extract and immobilised T-2 toxin-BSA (50 µg/mL)	163
Figure 5.1: Scratch assays to analyse the effects of AFB ₁ on HepG2 cell migration	178
Figure 5.2: Scratch assays to analyse the effects of anti-AFB ₁ Fab antibody fragment on HepG2 cell migration	180
Figure 5.3: Scratch assays to analyse the effects of the anti-AFB ₁ Fab antibody fragment and anti-EpCAM monoclonal antibody on HepG2 cell migration	183
Figure 5.4: Scratch assays to analyse the effects of the anti-AFB ₁ Fab antibody fragment and anti-EpCAM monoclonal antibody on THLE-2 cell migration	186
Figure 5.5: MTT proliferation assay to analyse the effects of AFB ₁ on the HepG2 cell proliferation.	190
Figure 5.6: MTT proliferation assay to analyse the effects of AFB ₁ and anti-AFB ₁ Fab antibody fragment treatment on the HepG2 cell proliferation.....	192
Figure 5.7: MTT proliferation assay to analyse the effects of AFB ₁ and the anti-AFB ₁ Fab antibody fragment on HepG2 cell proliferation	194
Figure 5.8: (A.) SDS-PAGE and (B.) Western blotting analysis of IMAC purified anti-AFB ₁ scFv-dimer antibody fragment.....	196
Figure 5.9: MTT proliferation assay to analyse the effects of anti-AFB ₁ antibody-formats on HepG2 cell proliferation.....	198
Figure 5.10: Anti-AFB ₁ Fab, anti-AFB ₁ scFv-dimer and anti-M3G antibody fragment sequence analysis.....	200
Figure 5.11: (A.) SDS-PAGE and (B.) Western blotting analysis of IMAC purified anti-M3G Fab antibody fragment.....	202
Figure 5.12: MTT proliferation assay to analyse the effects of Fab antibody fragments on HepG2 cell proliferation.	204
Figure 5.13: MTT proliferation assay to analyse the effects of anti-AFB ₁ antibody-formats on THLE-2 cell proliferation.....	206
Figure 5.14: Anti-AFB ₁ Fab antibody fragment and IGF-1R sequence analysis.....	207
Figure 5.15: IL-8 cytokine assay to analyse the effects of AFB ₁ on the HepG2 cell cytokine expression.....	209
Figure 5.16: IL-8 cytokine assay to analyse the effects of anti-AFB ₁ Fab antibody fragment on HepG2 cell cytokine expression	211
Figure 5.17: IL-8 cytokine assay to analyse the effects of AFB ₁ and anti-AFB ₁ Fab antibody fragment treatment on the HepG2 cell	

cytokine expression.....	213
Figure 5.18: Proposed AFB ₁ -IGF-1R interaction and mode of action in HepG2 cells....	217
Figure 5.19: Proposed Anti-AFB ₁ Fab antibody fragment-IGF-1R interaction and mode of action in HepG2 cells.....	220

List of Tables

Table 1.1: Current AFB ₁ , total aflatoxins, zearalenone, deoxynivalenol and total T-2/HT-2 toxin maximal allowable levels for food based on Commission Recommendation 1881/2006 (EC) and Commission Recommendation 2013/165/EU	6
Table 2.1: Reagents	41
Table 2.2: Commercial kits	42
Table 2.3: Bacterial strains	42
Table 2.4: Mammalian cell culture lines	42
Table 2.5: Media, additives and supplements	43
Table 2.6: General buffers	44
Table 2.7: Purification buffers	45
Table 2.8: SDS-PAGE and Western blotting buffers	46
Table 2.9: Equipment	47
Table 2.10: Molar ratios for T-2 toxin conjugate synthesis	50
Table 2.11: Molar ratios for ZEN and AFB ₂ conjugate synthesis	53
Table 2.12: Reaction mixture for avian V _H and V _L chain gene amplification	56
Table 2.13: Primers for avian V _H and V _L chain gene amplification	56
Table 2.14: PCR reaction conditions for avian V _H and V _L chain gene amplification	56
Table 2.15: Reagents and volumes for ethanol precipitation of purified PCR products	57
Table 2.16: Reaction mixture for avian V _H and V _L Chain SOE Extension PCR	57
Table 2.17: Primers for avian SOE-PCR	58
Table 2.18: PCR reaction conditions for SOE-PCR	58
Table 2.19: Reagents for SfiI restriction digest of SOE-PCR products and pComb3xSS vector	59
Table 2.20: XhoI and XbaI restriction digest and Antarctic phosphatase treatment of pComb3xSS vector	59
Table 2.21: Ligation of restrictiond SOE-PCR Products and pComb3xSS vector	60
Table 2.22: T-2 toxin-conjugate panning strategy	64
Table 2.23: Reaction mixture for colony pick PCR	68
Table 2.24: PCR reaction conditions for SOE-PCR product	68
Table 3.1: Concentration and integrity of avian RNA from bone marrow and spleen	99
Table 3.2: cDNA Synthesis from avian bone marrow and spleen RNA	99
Table 3.3: Panning Strategy for anti-T-2 toxin scFv library against T-2 toxin-OVA	107
Table 3.4: Anti-T-2 toxin scFv library size after 4 Rounds of panning	107
Table 3.5: Panning strategy for anti-T-2 toxin scFv library	112
Table 3.6: Library size after 4 rounds of panning	112
Table 3.7: Panning strategy for anti-T-2 toxin scFv library against T-2 toxin-BSA	115
Table 3.8: Anti-T-2 toxin scFv library after 5 rounds of panning	116
Table 4.1: MBio assay results for AFB ₁ and T-2 Toxin spiked PBS standard curve	160
Table 4.2: MBio assay results for AFB ₁ and T-2 Toxin spiked DDGS standard curve and spiked extract tests	163
Table 4.3: Multiplex analysis of DDGS sample to test AFB ₁ and	

	T-2 toxin concentration.....	165
Table 5.1:	Analysis of AFB ₁ exposure on HepG2 cell migration.....	179
Table 5.2:	Analysis of anti-AFB ₁ Fab antibody fragment effects on HepG2 cell migration.....	181
Table 5.3:	Analysis of anti-AFB ₁ Fab antibody fragment and anti-EpCAM monoclonal antibody effects on HepG2 cell migration	184
Table 5.4:	Analysis of anti-AFB ₁ Fab antibody fragment and anti-EpCAM monoclonal antibody effects on THLE-2 cell migration	187

Abbreviations

α	Alpha
AFB₁	Aflatoxin B ₁
AFB₂	Aflatoxin B ₂
AFG₁	Aflatoxin G ₁
AFG₂	Aflatoxin G ₂
AOAC	Association of Official Agricultural Chemists
APS	Ammonium persulphate
ATCC	American Type Culture Collection
β	Beta
BCA	Bicinchoninic Acid
BM	Bone marrow
BSC	Biological Safety Committee
BSA	Bovine serum albumin
CAC	The Codex Alimentarius
CCFAC	The Codex Committee on Food Additives and Contaminants
CD	Cluster of Differentiation
cDNA	Complementary deoxyribonucleic acid
CDR	Complementary determining region
CEN	European Committee for Standardization
C_H	Constant heavy chain
C_L	Constant light chain
CMO	O-(carboxymethyl) hydroxylamine hemihydrochloride
COOH	Carboxyl group
DCC	N,N'-Dicyclohexylcarbodiimide
DCU	Dublin City University
DON	Deoxynivalenol

dH₂O	Distilled water
DMEM	Dulbecco's modified Eagle's medium
DMF	Dimethylformamide
DMSO	Dimethyl sulphoxide
DON	Deoxynivalenol
DNA	Deoxyribonucleic acid
<i>E. coli</i>	<i>Escherichia coli</i>
EDC	N-ethyl-N'-(dimethylamioethyl) - carbodiimide
EDTA	Ethylenediaminetetraacetic acid
ELISA	Enzyme linked immunosorbent assay
EFSA	European Food Safety Authority
EPA	Environmental Protection Agency
EU	European Union
JECFA	Joint Expert Committee on Food Additives of the United Nations
Fab	Antibody binding fragment
FACS	Fluorescence activated cell sorting
FAO	Food and Agriculture Organization
FAPY	Formamidopyrimidine
FBS	Fetal bovine serum
Fc	Fragment-crystallisable region of antibody
FITC	Fluorescein isothiocyanate
FPLC	Fast protein liquid chromatography
Fv	Fragment variable
G	Acceleration
GC-MS	Gas chromatography-mass spectrometry
HA	Haemagglutinin

HCC	Hepatocellular carcinoma
HCl	Hydrochloric acid
His	Histidine
His₆	Hexa-histidine
HPLC	High performance liquid chromatography
HPLC-MS/MS	High performance liquid chromatography-tandem mass spectrometry
HRP	Horse radish peroxidase
HRPA	Health Products Regulatory Authority
HS	Hemisuccinate
HSD	Hydroxysteroid dehydrogenases
IARC	International Agency for Research on Cancer
Ig	Immunoglobulin
IgA	Immunoglobulin A
IgD	Immunoglobulin D
IgE	Immunoglobulin E
IgG	Immunoglobulin G
IgY	Immunoglobulin Y
IL	Interleukin
IMAC	Immobilised metal affinity chromatography
IPA	Isopropanol alcohol
IPTG	Isopropyl- β -D-galactopyranoside
κ	Kappa
KLH	Keyhole limpet hemocyanin
λ	Lambda
LB	Luria broth
LC-MS	Liquid chromatography-mass spectrometry

LLE	Liquid–liquid extraction
LoB	Limit of blank
LoD	Limit of detection
mAb	Monoclonal antibody
MFI	Mean fluorescence intensity
MG	Molecular grade
MgCl₂	Magnesium chloride
mRNA	Messenger ribonucleic acid
MTT	(3-(4,5-dimethylthiazol-2-yl)-2,5-diphenyltetrazolium bromide)
MWCO	Molecular weight ‘cut-off’
N₂	Nitrogen
NaCl	Sodium chloride
NaOH	Sodium hydroxide
NHS	N-hydroxysuccinimide
NH₂	Amino group
Ni⁺-NTA	Nickel-Nitrilotriacetic acid
NO	Nitric oxide
OVA	Ovalbumin
O/N	Overnight
pAb	Polyclonal antibody
PAGE	Polyacrylamide gel electrophoresis
PBS	Phosphate buffered saline
PBST	Phosphate buffered saline with tween (0.05 %, v/v)
PCR	Polymerase chain reaction
PEG	Polyethylene glycol
SPE	Solid phase extraction

RNA	Ribonucleic acid
ROS	Reactive oxygen species
RPM	Revolutions per minute
RT	Reverse transcription
scAb	Single chain antibody
scFv	Single chain variable fragment
SB	Super broth
SDS	Sodium dodecyl sulphate
SDS-PAGE	Sodium dodecyl sulphate polyacrylamide gel electrophoresis
SOC	Super optimal catabolite
SOE	Splice by overlap extension
SP	Spleen
ssDNA	Single stranded deoxyribonucleic acid
TAE	Tris base, acetic acid and EDTA
<i>Taq</i>	<i>Thermus aquaticus</i>
TDI	Tolerable daily intake
TEMED	Tetramethylethylenediamine
TGF	Transforming growth factor
TLC	Thin Layer Chromatography
TMB	3, 3', 5, 5'- tetramethylbenzidine
TMTC	Too many to count
TNF	Tumour necrosis factor
THLE	Transformed human liver epithelial cells
UV	Ultra Violet
V_H	Variable heavy chain
V_L	Variable light chain

WHO	World Health Organisation
ZAN	Zearalanone
ZAL	Zearalanol
ZEL	Zearalenol
ZEN	Zearalenone

Units

%	Percent
°C	Degrees Celsius
Abs	Absorbance
ANOVA	Analysis of Variance
bp	Base pair
cfu	Colony forming unit
CV	Coefficient of variance
Da	Dalton
g	grams
IC₁₀	Inhibitory concentration at 10%
IC₅₀	Inhibitory concentration at 50%
IC₉₀	Inhibitory concentration at 90%
kDa	Kilodalton
Kg	Kilogram
L	Litre
M	Molar
mg	Milligram
mL	Millilitre
mM	Millimolar
Mmol	Millimole
MW	Molecular weight
N	Number of observations
ng	Nanogram
OD	Optical density
pH	Log of the hydrogen ion concentration in solution
ppb	Parts per billion

ppm	Parts per million
SEM	Standard error of the mean
SD	Standard deviation
rpm	Revolutions per minute
v/v	Volume per unit volume
w/v	Weight per unit volume
μg	Microgram
μL	Microlitre

List of Publications

Moran, K.L.M., Lemass, D. and O' Kennedy R., 2018. Surface Plasmon Resonance-based Immunoassays: Approaches, Performance and Applications *in*: Paguio, J. (ed) *Handbook of Immunoassay Technologies: Approaches, Performances, and Applications*. Cambridge, Elsevier Inc. Accepted for publication.

Moran, K.L.M., Loftus, J.H., Murphy, C. and O' Kennedy R.J., 2018. Current and emerging technologies for the analysis of fungal and marine toxin contaminants in food *in*: Ram, M. and Obare, S.O. (ed) *Nano-Inspired biosensors for Improved Healthcare*. Florida, CRC Press. Accepted for publication.

Murphy, C., Fitzgerald, J., Byrne, H., Crawley, A., **Moran, K.L.M.** and O'Kennedy R., 2017. Optical Signal Transduction with an Emphasis on the Application of Surface Plasmon Resonance (SPR) in Antibody Characterisation: Development, Applications and Future Trends *in*: Murphy, C. and O'Kennedy R. (ed) *Immunoassays: Development, Applications and Future Trends*. New York, Pan Stanford. pp. 327-360.

Moran, K.L.M., Fitzgerald, J., McPartlin, D.A., Loftus, J.H. and O'Kennedy, R., 2016. Biosensor-Based Technologies for the Detection of Pathogens and Toxins *in*: Viviana Scognamiglio, V., Rea, G., Arduini, F. and Giuseppe Palleschi (eds) *Comprehensive Analytical Chemistry: Biosensors for Sustainable Food - New Opportunities and Technical Challenges*. Cambridge, Elsevier Inc. pp. 93-120.

Sanders, M., McPartlin, D., **Moran, K.L.M.**, Guo, Y., Eeckhout, M., O'Kennedy, R., De Saeger S., and Maragos, C. 2016. Comparison of Enzyme-Linked Immunosorbent Assay, Surface Plasmon Resonance and Biolayer Interferometry for screening of deoxynivalenol in wheat and wheat dust. *Toxins* 8(4):103, pp. 1-14.

O'Reilly, J.A., **Moran, K.L.M.** and O' Kennedy, R.J. 2013. Antibody-based sensors for disease detection *in*: Ozkan-Ariksoysa, D. (ed) *Biosensors and their Applications in Healthcare*. London, Future Science Ltd. pp. 6-23. [Online] Available from: <http://www.futuremedicine.com/doi/book/10.4155/9781909453647>

Invention Disclosure Application: Moran, K. and O'Kennedy R. Novel antibody-based approach for inhibiting cancer cell proliferation. Application filed with DCU Invent – Innovation and Enterprise, 12 December, 2017.

List of Posters

Incorporation of recombinant Fab antibody fragments in a ‘point-of- site’, optical-planar waveguide biosensor device for detection of aflatoxin B₁ . Kara Moran, Julie-Ann O’Reilly and Richard O’ Kennedy. World Mycotoxin Forum Conference, Winnipeg, Canada, 06 - 09/06/2016.

Development of recombinant antibody fragments to detect and analyse aflatoxin B₁, aflatoxin B₂, deoxynivalenol, zearalenone and T-2 mycotoxins in food and *in-vitro*. Kara Moran, Julie-Ann O’Reilly and Richard O’Kennedy. Safefood Biotoxins Knowledge Network Conference, Queens University Belfast, 11/06/2015.

The development of highly specific and sensitive antibodies that target, detect and measure mycotoxins. Kara Moran, Julie-Ann O’Reilly and Richard O’Kennedy. School of Biotechnology Research Day, Dublin City University 30/01/2015.

List of Presentations

Moran K. (27/01/2017) *Mycotoxins – Problems and Detection*. School of Biotechnology Research Day, Dublin City University.

Moran K. (16/11/2016) *Real World Applications of Molecular Biology. My Research: Mycotoxins, Antibodies and Genetics*. Amgen Experience (Education & Outreach), Dublin City University.

Moran K. (10/09/2016) *My Research: Mycotoxins, Antibodies and Genetics*. Education & Outreach - Maryfield College Secondary School, Drumcondra, Dublin.

Moran, K. (21/09/2015). *Catcher in The Rye*. Thesis in Three Competition, Regional Final, Dublin City University. *Third placed winner*.

Moran, K. (29/04/2015). *Catcher in The Rye*. Tell It Straight Competition, The Helix, Dublin City University. *First place winner*.

Moran, K. (30/01/2015). *Methods in Catching a Cereal Attacker*. School of Biotechnology Research Day, Dublin City University.

Courses, Scholarships and Awards

Inspire Fest & Lennox Postgraduate of the Year Award, 2016 - 2017

Antibody Engineering & Phage Display Course, Cold Spring Harbour Laboratory, Cold Spring Harbour, New York (5 - 18 November, 2014). Scholarship awarded for attendance.

Intensive Training on Mycotoxin Analysis. Laboratory of Food Analysis, Ghent University, Belgium (28 August – 10 September, 2014).

Biomedical Imaging in Diagnostics & Therapeutics – BioAt module. The Royal College of Surgeons, Dublin, Ireland (29 April, 2014).

Laboratory Animal Science and Training (LAST) Animal Handling Training Course for Ireland and UK License. Trinity College Dublin, Ireland (25 - 26 February, 2014).

Animal Cell Culture, Methods & Ethics – BioAt module. Dublin City University, Ireland (21 -22 January, 2014).

Cell Signalling and Molecular Medicine – BioAt module. The Royal College of Surgeons, Dublin, Ireland (3 December, 2013).

Daniel O’ Hare, Faculty of Science and Health PhD Scholarship Recipient, Dublin City University (October, 2013).

Abstract

Development of recombinant antibody fragments for mycotoxin detection and the investigation of AFB₁ and anti-AFB₁ Fab antibody fragment effects in hepatocellular carcinoma.

Kara Moran

Mycotoxins are toxic secondary metabolites produced by fungal species that grow on a vast array of food commodities globally. These contaminants pose a massive concern for human and animal health due to their prevalence in commonly consumed food commodities. Studies have shown that mycotoxin exposure, in particular aflatoxin B₁ (AFB₁) exposure, imparts mutagenic and carcinogenic effects in humans and animals. Accordingly, research is now focusing on methods to allow the rapid, cost-effective and simple detection of mycotoxins in food samples directly at the site of contamination. Additionally, investigations are centred on an improved understanding of the mechanisms that underpin mycotoxic carcinogenic effects.

This thesis describes the development and optimization of recombinant antibody fragments for inclusion in a ‘point-of-site’ device to allow the sensitive and specific detection of AFB₁ and T-2 toxin in the animal feed component, Dried Distillers Grain with Solubles (DDGS). A simple optical-planar waveguide cartridge and detection system that incorporated a recombinant anti-AFB₁ Fab antibody fragment and an anti-T-2 toxin polyclonal antibody, in a competitive inhibition format, was used for the successful detection of AFB₁ and T-2 toxin, to legislative limits outlined by the European Union. The system also allowed the simultaneous detection of both mycotoxins in a ‘proof-of-concept’ study.

This research also focused on investigating the effects of AFB₁ on HepG2 human hepatoma cells and hypothesised that the anti-AFB₁ Fab antibody fragment may have a cognate ligand on HepG2 cells. The findings outlined herein, demonstrate that low doses of AFB₁ have an inhibitory effect on HepG2 cell migration and proliferation after an initial 24 hours of exposure followed by increased secretion of IL-8 and recovery of the cells to normal levels of migration and proliferation. In addition, these results established that the anti-AFB₁ Fab antibody fragment interacted with, and, exerted an inhibitory effect on hepatocellular carcinoma cell migration and proliferation.

Chapter 1

Introduction

1.1.Introduction to thesis research

Mycotoxins are propagated by numerous fungal species and are known to be detrimental to human and animal health. These toxic contaminants have huge implications for food safety due to their ability to readily contaminate globally consumed food commodities.

This research describes the development and characterisation of recombinant antibody fragments for incorporation into a simple, cost-effective, rapid, ‘point-of-site’ device to allow the detection of mycotoxins in contaminated feed samples, to the legislative limits specified by the European Union (EU).

Investigations into mycotoxic effects on human hepatoma (HepG2) cells and normal transformed human liver epithelial (THLE-2) cells were also investigated. The effects of Aflatoxin B₁ (AFB₁) on HepG2 and THLE-2 cells were analysed in terms of, cell migration, proliferation and Interleukin-8 (IL-8) expression. Additionally, the effects of a recombinant anti-AFB₁ Fab antibody fragment treatment on HepG2 and THLE-2 cells were examined.

Together, these studies offer a sensitive and specific detection system for mycotoxin detection in feed to EU legislative limits, as well as, providing important insights into the complex effects of AFB₁ in HCC and elucidating the impact of an anti-AFB₁ Fab antibody fragment on HepG2 cell activity.

1.2.Mycotoxins

Mycotoxins are toxic secondary metabolites typically produced by *Aspergillus*, *Fusarium*, *Penicillium*, *Clavicep* and *Alternaria* fungal species and are recognized as harmful to human and animal health (Milićević *et al.*, 2010; Marin *et al.*, 2013). Reports indicate approximately 300 - 500 different mycotoxins have been fully characterised, however, research suggests thousands of unique mycotoxin types exist (Berthiller *et al.*, 2007; Yazdanpanah, 2011). Mycotoxins have huge implications for food safety due to their ability to readily contaminate globally consumed cereals such as rice, maize and wheat and their by-products including animal-feed and beer. However, nuts, spices, dried fruits, coffee and seeds can also be contaminated by mycotoxins. When ingested, mycotoxins may cause mycotoxicosis which can provoke acute or chronic disease. Chronic exposure has a greater impact on health stimulating carcinogenic, mutagenic, teratogenic, estrogenic,

hemorrhagic, immunotoxic, nephrotoxic, hepatotoxic, dermatotoxic and neurotoxic effects in humans and animals (Milićević *et al.*, 2010). The Food and Agriculture Organization (FAO) produced a seminal report in 1998, indicating that at least 25% of the world's food crops were contaminated with mycotoxins (Boutrif and Canet, 1998). However, it is now widely believed that this figure is grossly underestimated, as approximately 80% of 3715 finished feed and raw commodity samples sourced from 54 countries, collected and tested in the first quarter of 2017 were found to contain mycotoxins (Biomim, 2017). Furthermore, the United Nations indicated in 2013 that the global population is projected to increase by almost one billion people reaching 8.1 billion by 2025, and to further increase to 9.6 billion by 2050 (United Nations, 2013). Due to the severe mycotoxic consequences on health, and as the production of food crops is barely sustaining the increasing global population, prodigious efforts are being made to control and eliminate risks of mycotoxin-contamination for food safety. Consequently, mycotoxin analysis is now considered one of the most important areas for food quality improvement.

1.2.1. Mycotoxin Storage

Mycotoxin growth in food crops can manifest at any point in the food chain including in-field, at harvest, at drying and during storage. Improper drying, handling, packaging, storage, and transport conditions promote fungal growth, increasing the risk of mycotoxin production. Therefore, harvested agricultural crops stored under dry conditions that prevent fungal infection reduce the risk of mycotoxin production. However, when water activity increases to levels allowing fungal infection, mycotoxins can readily accrue in stored crops (Marin *et al.*, 2013; Villers, 2014). This poses massive difficulties in developing countries, where climatic and crop storage conditions are frequently conducive to fungal infection and mycotoxin production. In particular, the regions between 40°N and 40°S latitude have been defined as a 'hot zone' with approximately 4.5 billion people living in that region chronically exposed to mycotoxins (Williams *et al.*, 2004). While humans attempt to adapt to the environmental and climatic interventions that promote diminished food quality and crop production, fungal species are also adapting with the emergence of insidious 'masked' or 'modified' mycotoxins (Marroquín-Cardona *et al.*, 2014). As part of their metabolism, plants are capable of transforming mycotoxins into conjugated forms that hydrolyze the precursor toxins when digested by animals or humans. This results in the accumulation of

high levels of toxicity in animals directly attributable to the presence of unidentifiable conjugated mycotoxin forms (Milićević *et al.*, 2010; Berthiller *et al.*, 2013; Rychlik *et al.*, 2014). Considering the limitations of producers to access laboratory-based testing, a device that can be used on-site to determine the presence of multiple mycotoxins sensitively and to global mycotoxin standards is an immediate necessity. Such devices will enable producers to monitor mycotoxins cheaply, easily and quickly and ensure greater food control and quality.

1.2.2. Mycotoxin regulation

To guarantee quality food for all, we need to attain global mycotoxin standards with the realistic feasibility of achieving them. Extensive efforts have focused on the development of global organisations and harmonised standards to tackle and control the mycotoxin dilemma. The Codex Alimentarius (CAC) was established to enact legislation regarding contaminants including mycotoxins in food and feed. The Codex Committee on Food Additives and Contaminants (CCFAC) is responsible for the risk management component of the Codex Alimentarius risk analysis process in relation to mycotoxins in foods and feeds in particular. The body responsible for the risk assessment component of the Codex Alimentarius risk analysis process is the FAO/WHO Joint Expert Committee on Food Additives of the United Nations (JECFA). JECFA and the European Food Safety Authority (EFSA) provide the Codex Alimentarius with scientifically-based evaluations of the toxicity of mycotoxins to establish regulations for safe levels for human consumption. Concurrently, requirements for adequate sampling and analytical methods are developed by the Association of Official Agricultural Chemists (AOAC) International and standardised by the European Committee for Standardization (CEN). Current regulations encompass 13 different mycotoxins or groups of mycotoxins and specific limits have been established for many food and feed commodities and products (Milićević *et al.*, 2010). Table 1.1 lists a brief overview of the current maximal allowable levels and Tolerable Daily Intake (TDI) levels for total aflatoxins, aflatoxin B₁ (AFB₁), ZEN, DON and total T-2/ HT-2 toxin within the EU. Methods for mycotoxin analysis must be capable of detecting the presence of mycotoxins to these standard requirements.

Table 1.1: Current AFB₁, total aflatoxins, zearalenone, deoxynivalenol and total T-2/HT-2 toxin maximal allowable levels for food based on Commission Recommendation 1881/2006 (EC) and Commission Recommendation 2013/165/EU

Foodstuff	Maximal Levels (µg/kg = ppb)				
	AFB ₁	Total AFs	ZEN	DON	Total T-2/HT-2 Toxin
General Unprocessed Cereals	-	-	100	1250-1750	100-1000
Cereals intended for direct human consumption	2-5	4-10	75-100	750	50-200
Cereal products for feed and compound feeds	20	-	100-3000	900-12000	250-2000
Processed cereal-based foods and baby foods for infants and children	0.1	-	20	200	15
Bread, pastries, biscuits, cereal snacks and breakfast cereals	-	-	50	500	25-75
Tolerable Daily Intake (TDI) (µg/kg body weight)	0	0	0.2	1	0.1

1.2.3. Aflatoxins

In 1963, Hartley *et al.* isolated and described the toxic secondary metabolites of *Aspergillus flavus* as aflatoxins B₁, B₂, G₁ and G₂, so called due to the blue and green-yellow fluorescence elicited by the respective compounds under ultraviolet light (Figure 1.1). Aflatoxins may also be produced by strains of *Aspergillus parasiticus*, and both species are prevalent in food and animal feed crops including corn, wheat, maize and rice. Spices (turmeric, paprika, chilli, ginger, pepper), nuts (peanuts, pistachios, walnuts, coconuts), seeds and dried fruit are also subject to contamination (Bruneau *et al.*, 2013). More than 20 aflatoxins have been identified and factors that determine whether or not aflatoxins are produced include rainfall levels, drought, insect/bird damage, adaptations to crop genotype and agricultural practices. Aflatoxin synthesis typically occurs when temperatures are between 24 - 35°C and moisture content exceeds 7 %. Production also

occurs in postharvest conditions during storage, transportation or food processing (Rodgers *et al.*, 2002; Williams *et al.*, 2004; Khlangwiset and Wu, 2010).

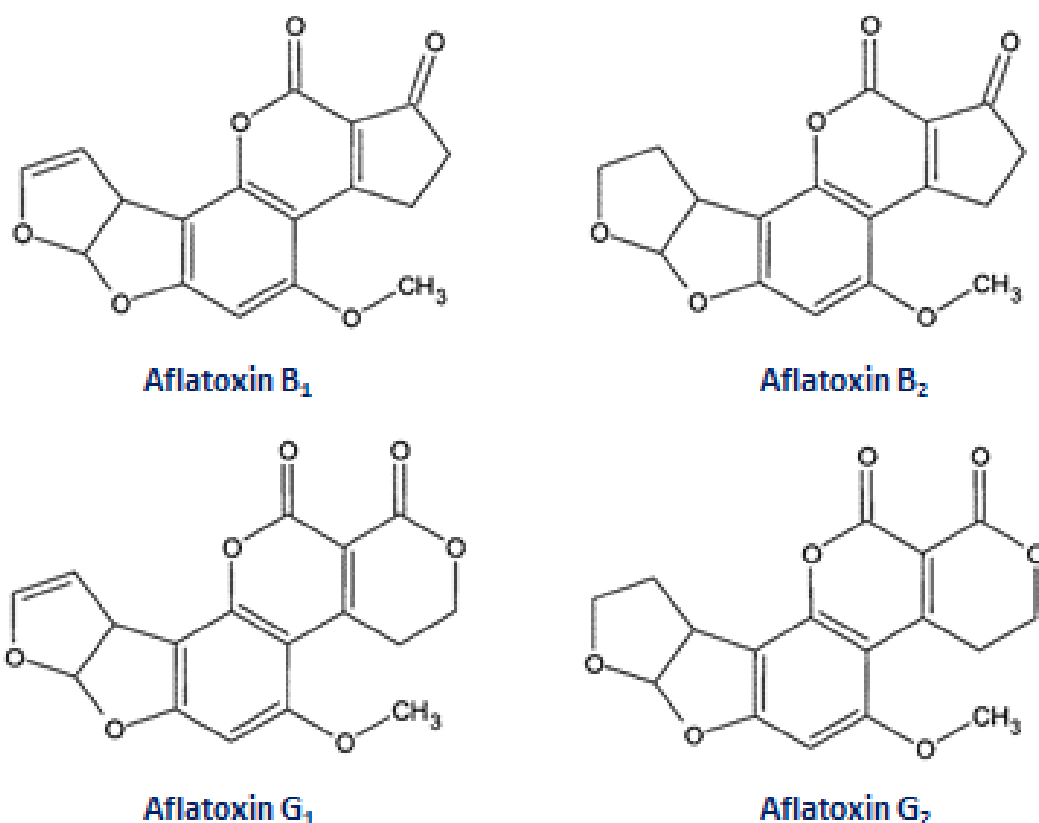


Figure 1.1: Aflatoxin structures. AFB₁, AFB₂, AFG₁, AFG₂ originally identified in 1961 are still amongst the most commonly studied mycotoxins. AFB₁ and AFB₂ and also AFG₁ and AFG₂, differ by the presence of a double bond at carbon positions 8 - 9. The presence of this double bond allows the formation of an epoxide ring making AFB₁ and AFG₁ more toxic metabolites.

1.2.3.1 Human impact of aflatoxins

Aflatoxin exposure is extremely harmful to humans. It causes immunosuppression and reduces growth rate in children resulting in interference with the bioavailability of different nutrients such as vitamin A, vitamin D, selenium and zinc (Williams *et al.*, 2004). Aflatoxin B₁ (AFB₁), the predominant isoform, is the most potent chemical hepatocarcinogen known and there is a positive association between aflatoxin exposure

and development of hepatocellular carcinoma (HCC) (Kew, 2003; Khlangwiset and Wu, 2010). The effects that arise from aflatoxin exposure are broadly referred to as aflatoxicosis. Severe cases of acute aflatoxicosis result in death, whilst, chronic aflatoxicosis results in cancer, immune suppression, and other pathological conditions that develop over time. The liver is the primary target organ with AFB₁, B₂, G₁, and G₂, grouped as human carcinogens by the International Agency for Research on Cancer (IARC). AFB₁ represents a Group 1 threat and, thus, poses very serious global health concerns (International Agency for Research on Cancer, 2002). There are significant differences in species susceptibility to aflatoxins. Effects are influenced by age, sex, weight, diet, exposure to infectious agents, and the presence of other mycotoxins and pharmacologically active substances (Bennett and Klich, 2003).

Currently, approximately 5 billion people in developing countries are at risk of chronic exposure to aflatoxins through food contamination. Lack of regulatory systems for monitoring and controlling aflatoxin contamination increases the likelihood of exposure in humans, with most cases occurring where aflatoxin exposure in food is largely uncontrolled (Liu and Wu, 2010; Wu *et al.*, 2011). Cases of acute aflatoxicosis are infrequent and the health risks associated with aflatoxin contamination are rarely seen in Europe and North America, which are mainly affected by other mycotoxin species. However, many examples can be found in developing countries. A lack of proper regulatory systems for aflatoxin detection was evident when 125 people died after consumption of AFB₁-contaminated maize in Kenya in 2004. There is also historical evidence of human loss reported from India in 1974 where 100 people who ingested contaminated corn died from aflatoxicosis. In 1967, 26 people living in a farming village in Taiwan fell ill after consumption of contaminated rice (Wu *et al.*, 2011). Recently in August 2016, it was reported that grain contaminated with AFB₁ led to the death of 14 people in Tanzania who consumed the contaminated material (Bugazi, 2016).

1.2.3.2 Aflatoxins and hepatocellular carcinoma

Hepatocellular carcinoma (HCC) is the fifth most common cancer in men and the seventh in women worldwide. However, due to poor prognosis, HCC is the third leading cause of cancer-related mortality. There is a striking geographical incidence of HCC and most of the burden is in developing countries, where over 80% of the cases occur (Ferlay *et al.*,

2010). HCC risk is up to 30 times greater in individuals suffering from both hepatitis B virus (HBV) and aflatoxin exposure compared to aflatoxin exposure in isolation (Groopman *et al.*, 2008). Although chronic infection with HBV is the major risk factor (believed to be responsible for 55% of global HCC cases), other environmental exposures namely dietary exposure to aflatoxins, tobacco smoking, liver cirrhosis caused by hepatitis C virus (HCV) and/or chronic alcohol abuse are thought to contribute to HCC incidence (Montalto *et al.*, 2002; McGlynn, 2005; Magnussen and Parsi, 2013).

1.2.3.3 Hepatocellular carcinoma and cytokines

HCC is an example of inflammation-related cancer. Chronic inflammatory appears to be essential for the initiation and development of liver cancer, affecting many cellular pathways, resulting in fibrosis, cirrhosis and finally hepatocarcinogenesis. The chronic inflammatory state is characterized by the continued expression of cytokines and recruitment of immune cells to the liver. Consequently, the activated inflammatory cells release free radicals (e.g. reactive oxygen species (ROS) and nitric oxide (NO) reactive species) which cause DNA damage and gene mutations, and, thereby promote neoplasm. In HCC, the cytokines Interleukin-6 (IL-6), Interleukin-8 (IL-8) and Transforming Growth Factor-beta (TGF- β) (in particular) favour tumour growth, Tumour Necrosis Factor-alpha (TNF- α) and IL-6 are involved in invasion and metastasis, and TGF- β , in concert with IL-10, has been shown to promote the suppression of anti-tumour immune response transformation (Capece *et al.*, 2013). Furthermore, TNF- α -induced Nuclear Factor kappa B (NF- κ B) activation is pivotal in hepatocarcinogenesis (Pikarsky *et al.*, 2004; Luedde and Schwabe, 2011). It is now becoming evident that inflammatory cytokine profiles offer prognostic value, further highlighted by the expression of inflammation-associated genes, (e.g. TNF- α and IL-6) in peritumoral liver tissue reportedly predicting late HCC recurrence (Capece *et al.*, 2013). Research is required to determine the effect of mycotoxins on cytokine secretion during HCC development. Previous work reported by Loftus *et al.*, (2016) and Bruneau *et al.* (2012) demonstrated that mycotoxins have a significant impact on cytokine secretion in J774A.1 murine macrophage. Therefore, investigations into the impact of mycotoxins on numerous cytokines involved in the modulation of HCC would be beneficial.

Tumour Necrosis Factor (TNF)

Tumour Necrosis Factor (TNF) is a pleiotropic cytokine involved in homeostasis and disease pathogenesis. The model of TNF receptor signalling has been strongly linked with different functional outcomes, such as inflammation, apoptosis and necroptosis. Identification of distinct homeostatic or pathogenic TNF-induced signalling pathways has introduced the concept of selectively inhibiting the deleterious effects of TNF while preserving its homeostatic bioactivities for therapeutic purposes in disease (Kalliolias and Ivashkiv, 2015). TNF functions by interactions with the TNF receptor superfamily, namely TNF-R1 (CD122a) and TNF-R2 (CD122b). The cytoplasmic tail of TNF-R1 contains a death domain and though vital for apoptosis, this motif is missing in TNF-R2. In the liver, TNF signalling through TNF-R1, is necessary for, normal hepatocyte proliferation during liver regeneration, induction of NF- κ B to elicit anti-apoptotic protection and in the control of the immune response. However, TNF is also the mediator of inflammation and hepatotoxicity in many animal models (Tarrats *et al.*, 2011). TNF- α is strongly involved in the pathogenesis of HCC, promoting invasion, angiogenesis and metastasis. It is also linked with cell-cycle progression, tumour development, and oxidative stress, stimulating expression of Transforming Growth Factor-alpha (TGF- α) in mouse hepatocytes and production of 8-oxodeoxyguanosine, a critical biomarker of oxidative stress and carcinogenesis (Gallucci *et al.*, 2000; Wheelhouse *et al.*, 2003; Cosgrove *et al.*, 2008). TNF- α and the cytokine IL-1 β have been shown to support tumour immune escape by inducing TNF-related Apoptosis-inducing Ligand (TRAIL) expression on liver cell surfaces and, thereby, promoting activated T-cell apoptosis (Wu *et al.*, 2008). NF- κ B is the downstream mediator of pro-tumoural TNF- α activity, and its target genes are involved in cell proliferation and survival. Furthermore, NF- κ B also induces TNF- α in a positive feedback loop (Capece *et al.*, 2013).

Interleukin-8 (IL-8)

Interleukin-8 (IL-8) is a pro-inflammatory chemokine associated with neutrophil chemotaxis and degranulation. IL-8 interacts with the C-X-C motif chemokine-receptors, CXCR1 and CXCR2, to activate multiple intracellular signalling pathways. Increased expression of IL-8 and/or its receptors has been characterized in cancer cells, endothelial cells, infiltrating neutrophils, and tumour-associated macrophages. This indicates a

significant role for the IL-8 signalling pathway at the tumour site (Waugh and Wilson, 2008). Research indicates that IL-8 is significantly upregulated in colorectal cancer (CRC) and contributes to tumour growth, invasion and metastasis (Ning and Lenz, 2012). IL-8 induces CRC cell proliferation and migration via a disintegrin and metalloprotease (ADAM)-dependent pathway. Furthermore, heparin-binding epidermal growth factor (EGF)-like growth factor (HB-EGF) was shown to exert an important role as the major ligand for this pathway (Itoh *et al.*, 2005). Studies suggest that IL-8 could be used as a prognostic indicator of HCC and its metastasis by showing significant correlations of serum IL-8 levels with tumour size and degree, and, that IL-8 may be directly or indirectly involved in the progression of HCC (Ren *et al.*, 2003) Kubo *et al.* (2005) showed that IL-8 stimulated HepG2 cell chemotactic and invasive activities opposed to cell proliferation. This research suggested that the expression of IL-8 in human HCC had more relevance to metastatic potential (i.e. vessel invasion) than to angiogenesis or cell proliferation. Despite the suggested value of IL-8 as a prognostic marker of HCC, less attention has focused on the drug-induced IL-8 signalling effects that have been shown to confer chemotherapeutic resistance in cancer cells. HCC has proven difficult to treat because of its recurrence rate and chemotherapy-resistance. Research conducted by Park *et al.* (2014) demonstrated that anti-cancer drugs (PTX and DOX) increased secretion of IL-8 expression and expression of CXCR1 in HCC *in vitro*. Furthermore, by silencing IL-8 expression, Park *et al.* reported the first evidence that IL-8 secretion induced by anti-cancer drug treatment, regulates the expression of drug resistant genes in HCC (directly or indirectly). Therefore, modulating the IL-8 signalling pathway may be of significant therapeutic value in targeting the tumour microenvironment.

Interleukin-6 (IL-6)

Interleukin-6 (IL-6) is a pleiotropic cytokine with a wide range of biological functions in immune regulation, inflammation, and oncogenesis. IL-6 plays a crucial role in the pathogenesis of HCC. IL-6 has been shown to exert its oncogenic activity in chemically-induced HCC mouse models, by triggering downstream Signal Transducer and Activator of Transcription 3 (STAT-3) and Extracellular-signal-Regulated Kinases (ERK) pathways, which in turn control target genes involved in both cell proliferation and survival (Maeda *et al.*, 2005). High IL-6 serum levels have been observed in patients with HCC, were

associated with poor prognosis (Nakagawa *et al.*, 2009) and could also be used to differentiate primary or metastatic HCC from benign lesions (Coskun *et al.*, 2004).

The most studied immunosuppressive cytokine in HCC is **IL-10**. Several studies have reported high IL-10 levels in HCC patients, with IL-10 increased in HCC tumours versus non-tumorous tissue in close proximity to tumours and versus tissues of healthy cohorts, respectively (Sachdeva *et al.*, 2015). Ryschich *et al.* have also shown the increased expression of IL-10 is correlated with high angiogenic activity in a HCC mouse model (Ryschich *et al.*, 2006).

1.2.3.4 Aflatoxin B₁ metabolism and mode of action

AFB₁ is considered a mycotoxin of serious concern globally due to its strong association with hepatocellular carcinoma. AFB₁ is digested to a toxic form during metabolism which can induce DNA dis-regulation. When AFB₁ is ingested, it is metabolised by cytochrome P450 enzymes which convert the mycotoxin to an unstable, reactive AFB₁-8-9-epoxide. The epoxide can react at the N7 position of guanine in DNA to form the primary AFB₁-N7-Gua adduct or alternatively can covalently bind protein, producing AFB₁-(lysine) albumin adducts (Figure 1.2). The AFB₁-N7-Gua adduct has a destabilised glycosidic bond which depurinates to form apurinic/apyrimidinic (AP) sites. Alternatively, the imidazole ring in AFB₁-N7-Gua adducts can be opened to produce a chemically and biologically stable formamidopyrimidine adduct, AFB₁-FAPY. The FAPY adduct itself consists of two forms, FAPY major and FAPY minor. FAPY minor is formed first, subsequently equilibrating to a 2:1 ratio of FAPY major:FAPY minor (Smela, 2002; Friedman and Rasooly, 2013).

Development of AFB₁-N7-Gua adducts is critical to induce mutations in pivotal genes and drive carcinogenic effects in animals and humans. Furthermore, AFB₁-N7-Gua adducts can result in GC to TA transversions. Moreover, liver tumor tissues with high AFB₁ exposure have been shown to develop a specific mutation at codon 249 in P53 tumour suppressing gene resulting in a G to T transversion (AGG to AGT). Therefore, the inactivation of P53 tumour suppressor gene may be a key driver in primary hepatocellular carcinoma. Significantly, the specific mutation in codon 249 of the P53 gene has been referred to as

the first example of a 'carcinogen-specific' biomarker that is fixed in tumour tissue (Bennett and Klich, 2003; Wu and Santella, 2012).

Glutathione-S-transferases (GSTs) are a family of Phase II detoxification enzymes found in the cytosol that catalyse the conjugation of reduced glutathione (GSH) to a wide variety of endogenous and exogenous electrophilic compounds e.g. activated aflatoxin (Townsend and Tew, 2003). It is suggested that variances in species glutathione and cytochrome P450 systems may attribute to differences observed in interspecies aflatoxin susceptibility (Bennett and Klich, 2003). GSTs detoxify AFB₁ to produce an AFB₁-mercapturic acid which is excreted in urine.

The metabolism of AFB₁ to dangerous DNA and protein intermediates has been proven to cause HCC in humans (International Agency for Research on Cancer, 2002). There is now justified emphasis on ensuring AFB₁ and mycotoxins are detected and monitored in foods. Accordingly, foods and feed that are found to contain mycotoxins typically are removed from the food supply chain. This in-turn projects an unavoidable effect on the global economy.

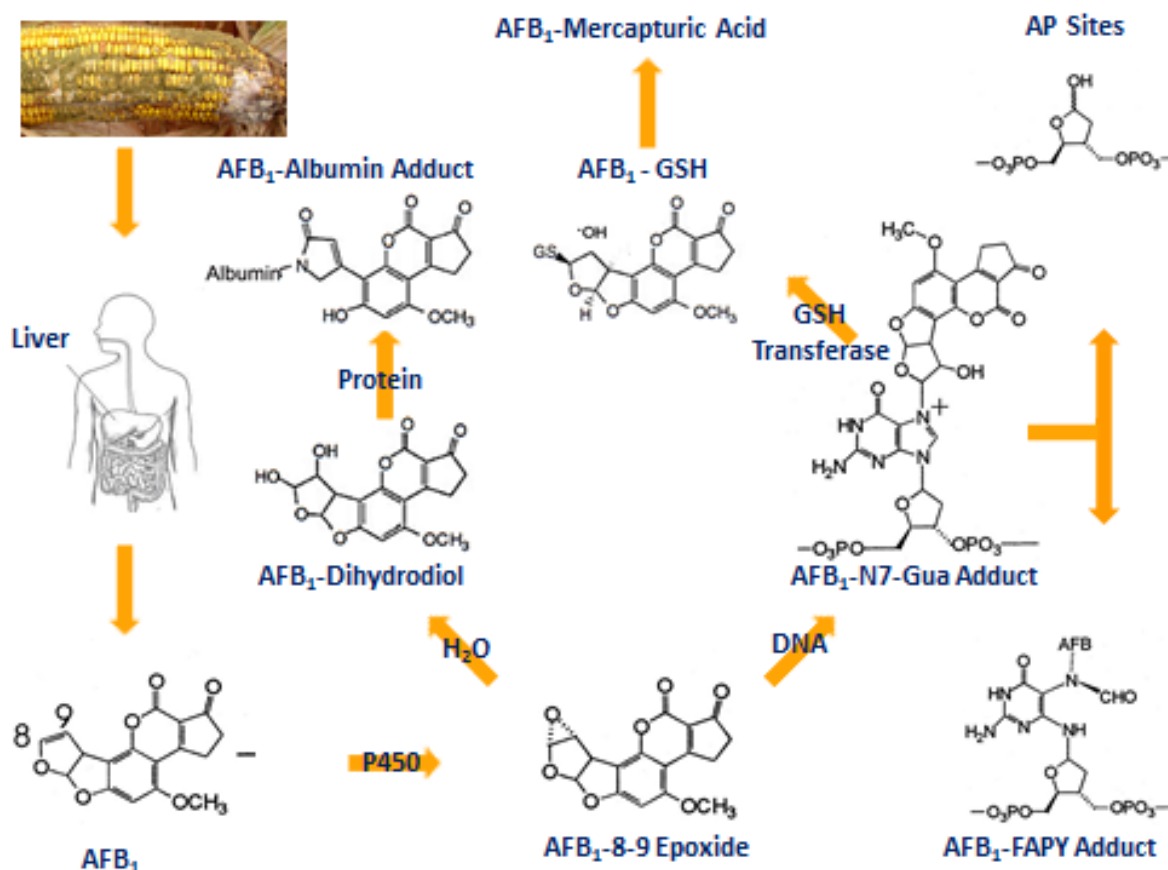


Figure 1.2: Aflatoxin B₁ metabolism. AFB₁ is ingested and converted to AFB₁-8-9-epoxides by cytochrome P450 enzymes in the liver. The AFB₁-N7-Gua adduct can be depurinated to form apurinic/aprimidinic (AP) site or its imidazole ring can be opened to produce AFB₁-FAPY products. AFB₁-N7-Gua adducts can produce G – T transversions which may be responsible for driving hepatocellular carcinoma. Alternatively AFB₁ may be detoxified by glutathione-S-transferases and excreted in urine.

1.2.3.5 Economic impact of aflatoxins

Aflatoxins are also responsible for economic problems in the food industry. Significant economic losses are associated with mycotoxin impact on human health, animal productivity and international trade. In 2013, it was reported that approximately 45 million tonnes of corn feed potentially contaminated with AFB₁ was delivered to more than 4,000 farms across Germany. This resulted in a ban on milk from dairy farms suspected of feeding animals with AFB₁-contaminated corn (Le Blond, 2013). Robust data is lacking on the true economic impact of aflatoxin exposure on markets and trade and health effects on humans and livestock. Vardon reported in 2003 that in the United States of America the estimated combined annual losses due to aflatoxin contamination in corn and peanuts,

fumonisin contamination in corn and deoxynivalenol contamination in corn and wheat was between \$0.5 billion - \$1.66 billion (Vardon, 2003). Contamination also makes crops unsuitable for export. The cost of destroying contaminated crops produced by African farmers is estimated at over \$450 million per year (Villers, 2014). More recently, commercial and financial interest in mycotoxin testing has increased. This is highlighted by the recent publication on the global market by Global QYResearch, 'Global Mycotoxin Testing Sales Market (Aflatoxins, Ochratoxins, Patulin, Fusarium toxins and Other toxin) Opportunity Analysis, Market Shares and Forecast 2017-2022' indicating the potential for the mycotoxin detection industry.

1.2.4. Zearalenone

Aflatoxins pose the most significant risk to humans and animals due to their associated carcinogenic effects. However, numerous other mycotoxins impact on food and feed consumed globally. Other mycotoxins of significant interest are discussed here in detail.

Zearalenone (ZEN, previously known as F-2 toxin and commonly known as ZEA or ZON) is a mycotoxin biosynthesised by numerous *Fusarium* species of fungi including, *F. graminearum* (also known as its anamorph *Gibberella zeae*), *F. culmorum*, *F. cerealis*, *F. equiseti*, *F. crookwellense* and *F. semitectum* (Bennett and Klich, 2003). Zearalenone was so-called as a combination of *G. zeae*, resorcylic acid lactone, -ene (for the presence of the C-1' to C-2 double bond), and -one, for the C-6' ketone (Urry *et al.*, 1966). Species producing ZEN favour temperate, warm countries, where high humidity and moisture conditions encourage proliferation on cereal crops (Da Rocha *et al.*, 2014). ZEN contamination is prevalent in corn, however, maize, wheat, sorghum, barley, oats, millet, rice and other cereal products, including flour, soybeans, malt and beer, can be affected (Zinedine *et al.*, 2007).

Though described as a mycotoxin and while biologically potent, ZEN is relatively non-toxic. It sufficiently resembles 17 β -estradiol, the principal hormone produced by the human ovary, to allow its binding to oestrogen receptors in mammalian target cells. Accordingly ZEN is more aptly described as a non-steroidal oestrogen or myco-oestrogen (Bennett and Klich, 2003). ZEN can bind both classes of oestrogen receptor with strong affinity but also interacts with hydroxysteroid dehydrogenases (HSDS) involved in the

synthesis of endogenous hormones. Therefore, ZEN can also be described as an endocrine disruptor exerting endocrine activity for which plausible links between endocrine activity and adverse effects have been demonstrated in animals and/or humans (Santos *et al.*, 2013). ZEN induces mRNA synthesis in uterine tissue by binding the oestrogen receptors (Oancea and Stoia, 2008). This affects the reproductive system causing atrophy of seminal vesicles and testes, prostate metaplasia, decreased fertility, abortion, osteoporosis, vaginal hyperkeratosis, changed progesterone and oestriol serum levels and endometrial hyperplasia. Exposure to ZEN can result in decreased fertility, still-birth and deformities in off-spring.

1.2.4.1 Animal impact of ZEN

Although the acute toxicity of ZEN is low, its metabolites have proven oestrogenic effects in animals including pigs, cattle, sheep and poultry. In addition carcinogenic, hepatotoxic, haematotoxic, genotoxic, immunotoxic, teratogenic and neurotoxic effects have been found. The consequences of ZEN metabolism in humans are poorly understood with more research required to fully elucidate the effects of ZEN on the human body (Zinedine *et al.*, 2007).

Zen - metabolism and mode of Action

Animal data indicates that ZEN biotransformation occurs in the liver (the main organ responsible for steroid metabolism), however, intestinal tissues, kidneys, testes, prostate, hypothalamus and ovaries also possess hydroxysteroid dehydrogenase (HSD) activity permitting the metabolism of five ZEN metabolites, i.e. α -zearalenol (α -ZEL), β -zearalenol (β -ZEL), α -zearalanol (zearanol, α -ZAL), β -zearalanol (teranol, β -ZAL) and zearalanone (ZAN) (Figure 1.3). In mammals, the reduction of the keto group at C-8 produces two stereoisomeric metabolites of ZEN (α - and β -isomers). These metabolites are also produced by the fungi, but at much lower concentrations than for ZEN (CCFAC, 2000).

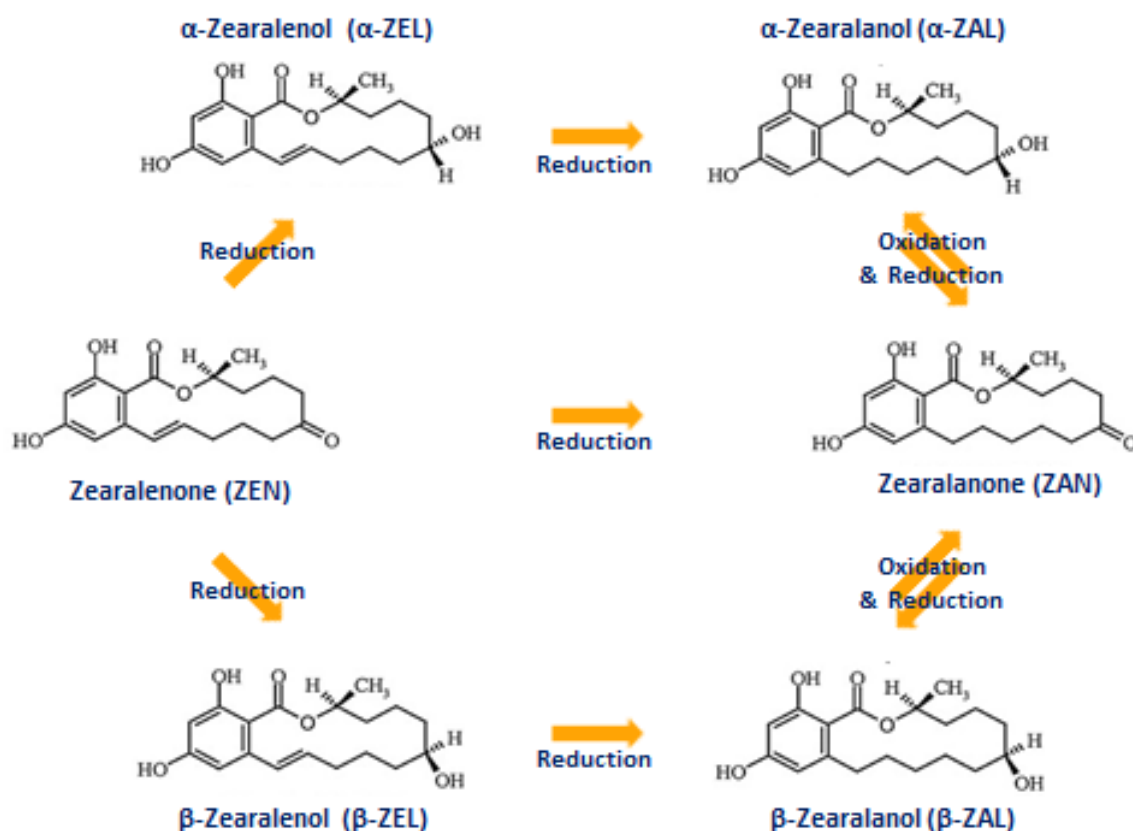


Figure 1.3: Zearalenone metabolism. ZEN is reduced predominantly to α -zearalenol (α -ZEL), and in smaller quantities to β -zearalenol (β -ZEL). Hydroxysteroid dehydrogenases (HSD) convert ZEN by reduction into the two stereoisomeric metabolites. Further reduction via 11 – 12 double bond reduction yields two minor metabolites α -zearalanol (α -ZAL) and β -zearalanol (β -ZAL). Alternatively, direct reduction of ZEN to ZAN can occur, which in turn can be further reduced to α -ZAL and β -ZAL.

ZEN is rapidly absorbed after oral administration, however, the degree of absorption can be difficult to monitor due to biliary excretion. The adverse effects of ZEN are influenced by biliary excretion and entero-hepatic cycling processes which impact the fate of ZEN. The glucuronide produced when ZEN is conjugated to glucuronic acid can be excreted in bile. It is often then re-absorbed, further metabolised by the intestinal tissue, enters the liver and, eventually, the systemic circulation by the portal blood supply. Reduced forms of ZEN have increased oestrogenic activity. The uptake of ZEN in pigs after oral administration of 10 mg/kg of body weight is approximately 80 - 85% (Biehl *et al.*, 1993). Pigs also have a low glucuronidation capacity which is responsible for ZEN inactivation. Therefore, high uptake of ZEN coupled with an inability to readily inactivate ZEN may be responsible for pig susceptibility to toxic effects of ZEN. Malekinejad *et al.* reported in

2006 that hepatic metabolism in different species results in distinct ZEN metabolites. Pigs and sheep predominantly produce α -ZEL whereas cattle produce β -ZEL more readily.

Commercial synthetic forms of reduced ZEN (zearanol) have been marketed as an anabolic agent used for animal growth promotion. It has been used to fatten cattle in the United States of America since the 1960's. However, it is banned in many other countries and the EU (Zinedine *et al.*, 2007; Belhassen *et al.*, 2015).

1.2.5. Trichothecenes – T-2 toxin

Trichothecenes are a large family of more than sixty structurally related compounds produced by a number of fungal species including *Fusarium*, *Stachbotrys*, *Myrothecium*, *Trichoderma*, *Trichothecium* and *Phomopsis* genera. The term trichothecene is derived from trichothecin, which was the one of the first members of the family identified. All trichothecenes contain a common 12, 13-epoxytrichothene skeleton and an olefinic bond with various side chain substitutions. They are classified depending on the presence of a macrocyclic ester or an ester-ether bridge between C-4 and C-15 and can be sub-divided into two groups: Type A have a hydrogen or ester type side chain at the C-8 position (T-2 toxin) or Type B group contain a ketone (deoxynivalenol) (Figure 1.4) (Bennet and Klich, 2003; Richard, 2007). They are considered mycotoxins of importance due to their prevalence in Europe and the United States of America where the moderate climate is amenable to their growth. They are of concern due to their ability to inhibit the synthesis of protein in humans and animals (Zain, 2011). It is suggested that all trichothecenes inhibit peptidyl transferase by binding to the same ribosome-binding site yet they exert different effects which can be correlated with different functional groups (Feinberg and McLaughlin, 1989). The symptoms produced by various trichothecenes include effects on almost every major system of the vertebrate body; many of these effects are due to secondary processes that are initiated by often poorly understood metabolic mechanisms related to the inhibition of protein synthesis. Currently, the most notable of the trichothecenes found in foods are deoxynivalenol (DON) and T-2 toxin.

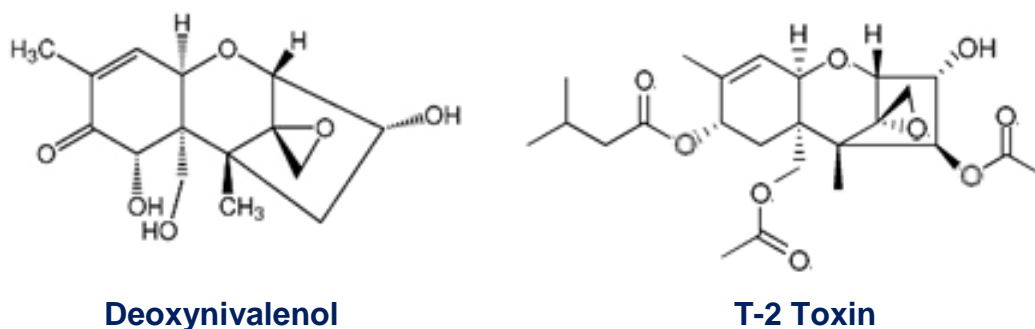


Figure 1.4: Deoxynivalenol and T-2 toxin structures. Deoxynivalenol; Type B trichothecene structure (contain a ketone group) and T-2 toxin; Type A trichothecene (contain a hydrogen or ester type side chain at the C-8 position).

1.2.5.1 T-2 toxin

T-2 toxin is a major concern as it the most toxic trichothecene, yet is less frequently detected compared to other trichothecenes like DON (Li *et al.*, 2011). The EU reported that T-2 toxin was a common contaminant in cereal samples from EU member states, and therefore EU members were at risk to dietary exposure. T-2 toxin elicits a range of toxic effects in animals with some similarities to DON, such as weight loss, vomiting and diarrhoea, however, it also causes decreases in blood cell and leukocyte count, lethargy, reduction in plasma glucose, haemorrhage, compromised immunity, necrosis, damage of cartilaginous tissues, apoptosis, pathological changes in the liver and stomach and death (Kalantari and Moosavi, 2010; Li *et al.*, 2011).

1.2.5.1.1. Human and animal impact of T-2 Toxin

T-2 toxin has been linked to the human disease called alimentary toxic aleukia (ATA). The symptoms of the disease include inflammation of the skin, vomiting and damage to hematopoietic tissues while acute symptoms are characterised by necrosis in the oral cavity, bleeding from the nose, mouth, and vagina, and central nervous system disorders. Soviet literature from the nineteenth century details disease outbreaks associated with people eating mouldy grain. During World War II large numbers of people succumbed ATA in the Orenburg region of the former U.S.S.R following consumption of overwintered grain colonized with *Fusarium sporotrichioides* and *Fusarium poae* (Joffe

and Yagen, 1978). Unlike aflatoxins and other mycotoxins, trichothecenes can act immediately upon contact. Exposure to just a few milligrams of T-2 toxin is potentially lethal. In the 1980s, the Soviet Union were accused by the United States of America of attacking Hmong tribesman in Laos and Kampuchea with a mysterious chemical-warfare agent believed to be T-2 toxin (as well as DON and nivalenon). The alleged use of this chemical warfare agent became known as yellow rain (Bennett and Klich, 2003).

T-2 toxin - metabolism and mode of action

There are a wide range of modes of action proposed for T-2 toxin. T-2 toxin reacts with the thiol groups of sulfhydryl enzymes and as a result is a potent protein and DNA synthesis inhibitor. The toxin can impair the production of antibodies, alter membrane functions, reduce lymphocyte proliferation and alter the maturation process of dendritic cells. T-2 toxin has been shown to produce, both *in vivo* and *in vitro*, single strand breaks in the DNA of lymphoid cells, as well as, inducing apoptosis in a variety of cell lines. Oxidative damage may be one of the main manifestations of cellular damage in the toxicity of several mycotoxins. The targets of oxidative damage are commonly critical biomarkers such as nucleic acids, proteins and lipids (Kalantari and Moosavi, 2010).

T-2 toxin is usually metabolized and eliminated after ingestion. In general, T-2 toxin is soluble in water, and the major metabolic reactions are usually hydrolysis, hydroxylation, de-epoxidation, and conjugation. The most typical metabolites of T-2 are HT-2 toxin (hydrolysis), T-2 triol, T-2 tetraol, neosolaniol (NEO), 30 -hydroxy HT-2, 30 -hydroxy T-2, 30 -hydroxy T-2 triol, and dihydroxy HT-2 and de-epoxy-30 -hydroxy T-2 and deepoxy-30 -hydroxy HT-2, however, more than 20 T-2 toxin metabolites are suspected. Consequently, there is a high possibility of human consumption of animal products contaminated with T-2 toxin and its metabolites (Li *et al.*, 2011).

1.2.6. Mycotoxin methods of detection

Governments throughout the world have responded to the recognition of the damaging health effects and the obvious economic consequences of mycotoxins, by introducing mycotoxin regulatory and legislative limits (Zain, 2011). As outlined many countries are

now implementing limits for a number of mycotoxins, but due to the variety of their structures and possible isoforms it is not currently possible to use one standard technique for mycotoxin analysis. There is vast research pursuing the goal of developing methods that are robust, simple, fast and suitable for ‘in-field’ analysis but to date the gold standard methods remain laboratory-based.

1.2.6.1 Chromatographic methods for mycotoxin detection

In 2009, Turner *et al.* reviewed and compared some of most commonly employed methods for mycotoxin analysis and found there was no one favourable method but that choice usually depended on: (a) the mycotoxin being analysed and, (b) the matrix being analysed (Turner *et al.*, 2009). To provide quantitative measurements of mycotoxins, analytical approaches based on the chromatographic properties of toxins have been established. Historically, Thin Layer Chromatography (TLC) was the most commonly used separation technique in mycotoxin, and specifically aflatoxin, determination. TLC has worked as a good preliminary screening technique for mycotoxins. However, it is being phased out in robust laboratory settings as it does not lend itself to accurate quantification as it is lacking in both sensitivity and the amenity for high-throughput analysis. Advances in the area of chromatography have led to a progression from TLC to more sophisticated methods based around liquid chromatographic (LC) separation coupled to detection methods such as mass spectrometry (MS) (LC-MS), fluorometric detection (FD) (HPLC-FLD) or ultra-violet detection (UVD) (HPLC-UVD) (Vilarino *et al.*, 2010). These LC-based techniques allow higher throughput and offer greater sensitivity, selectivity and more flexibility. They are now considered the gold standard for mycotoxin detection allowing multi-toxin analysis. However, chromatographic-based methods require rigorous sample pre-treatment, skilled operators and they are almost completely laboratory-based (Yeni *et al.*, 2014) so they do not facilitate rapid “on-site” analysis of mycotoxins.

1.2.6.2 Immunoassay-based methods for mycotoxin detection

Currently, immunoassay is a widely utilised tool for the analysis of toxins. It is a valuable analytical technique based on molecular recognition between antibody and antigen that allows for detection with high sensitivity and specificity. These assays are used for the

quantification of target molecules in many applications (Han *et al.*, 2013). Enzyme-linked immunosorbent assay (ELISA) is one of the most commonly used immunoassay formats as it is an inexpensive, colour-based test where the outputs may be assessed by absorbance or fluorescence determination. It is extremely useful for detecting haptens (low molecular weight molecules) such as mycotoxins that lend themselves well to competitive immunoassay detection. To achieve this, a conjugated form of the toxin is pre-coated onto multi-well plates, a mixture of toxin to be detected and detection antibody are then added to the plate. The free toxin (from the sample being analysed) and conjugated toxin compete for antibody binding, excess antibody is washed away and a labelled secondary antibody is added to detect bound anti-toxin antibody. Following addition of the substrate the absorbance of the product generated is determined. In a competitive immunoassay (Figure 1.5) the intensity of the colour signal is inversely proportional to the concentration of free-toxin present.

Commercial ELISA Kits are available from many companies including Randox, R-Biopharm, Alltech, Neogen and Sigma-Aldrich and consist of the required antibodies, reagents and materials necessary for target mycotoxin testing. These kits are also useful tools for screening and also allow some levels of quantification. Intense research in this area has resulted in the emergence of many new mycotoxin detection techniques. A highly sensitive chemiluminescence-based enzyme-linked immunoassay (CL-ELISA) was developed, using an anti-T-2 toxin monoclonal antibody against T-2 toxin and HT-2 toxin. With the benefit of a chemiluminescent substrate, IC₅₀ values of 33.28 ng/mL and 27.27 ng/mL were shown for T-2 and HT-2, respectively (Li *et al.*, 2016). Furthermore, research completed by Arola *et al.* in 2016 described the successful development of a recombinant Fab antibody fragment capable of recognizing both HT-2 and T-2 toxins selected from a phage display antibody library. A ‘point-of-site’ immunoassay based on time-resolved fluorescence resonance energy transfer (TR-FRET) was established with an IC₅₀ value of 9.6 ng/mL and a limit of detection (LOD) of 0.38 ng/mL for HT-2 toxin.

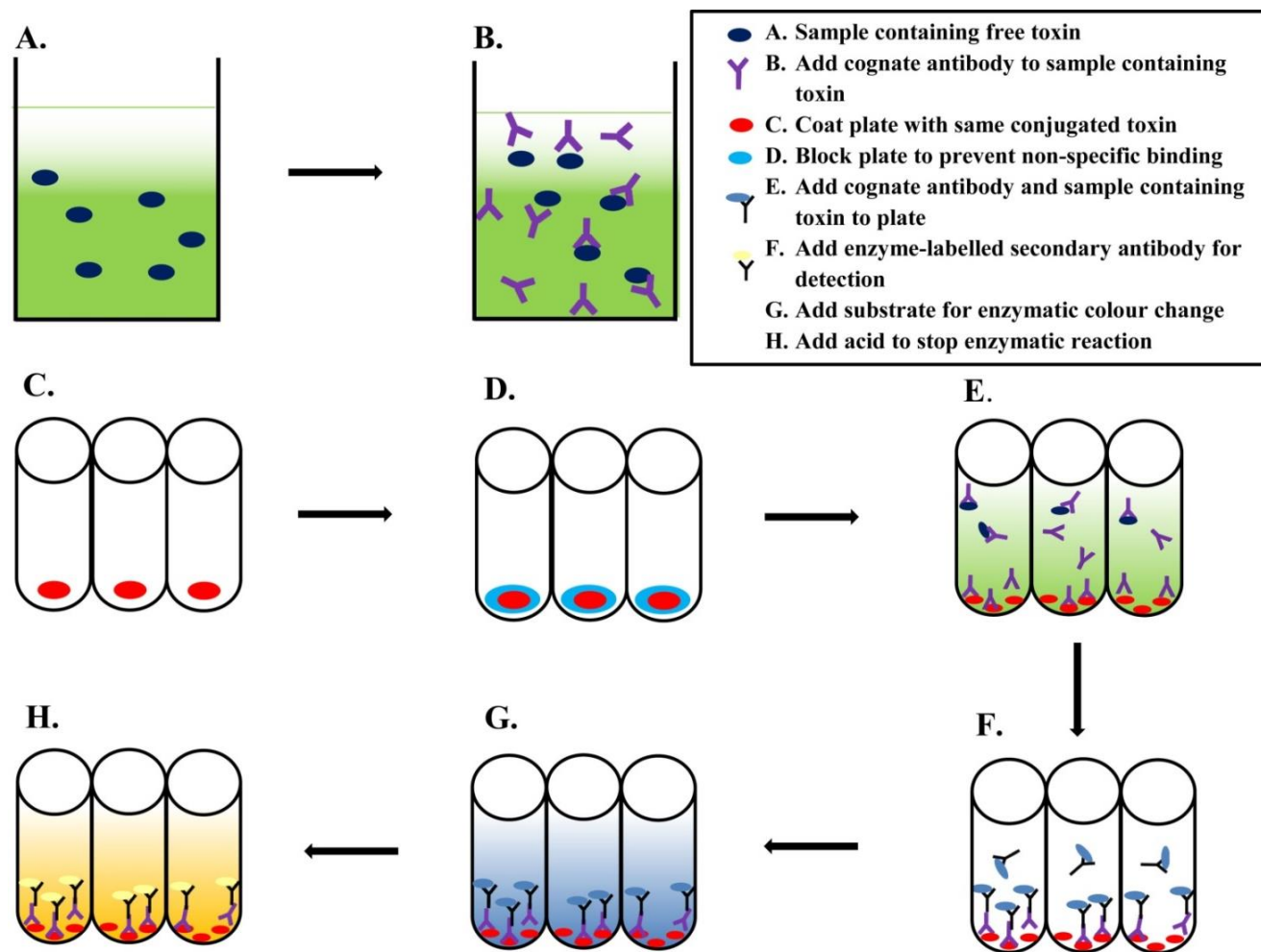


Figure 1.5: Competitive inhibition ELISA for mycotoxin analysis. A sample containing mycotoxins (A) is incubated with cognate antibody (B). Wells are coated with conjugated- mycotoxin, blocked (C-D) and mixed sample added to the plate for competition (E). Enzyme-linked secondary antibody is added, followed by substrate, the reaction is stopped with acid (F-H) and the response read on a spectrophotometer.

Recently, lateral flow devices (LFD) have also been developed for a number of different mycotoxins (R-Biopharm, Neogen, Eurofins Scientific, Vicam etc.). A sample is placed on a sample pad and moves through the system to interact with specific cognate antibodies and produce a visible colour change. The results are viewed by eye or more recently by optical readers such as mobile phone devices, making them a useful on-site screening tool. Novel qualitative and semi-quantitative rapid strip tests for screening T-2 mycotoxin in agricultural commodities were described by Molinelli *et al.* The T-2 toxin LFD presented a cut-off level of approximately 100 µg/kg for naturally contaminated wheat and oats. In this research, anti-T-2 monoclonal antibodies were immobilised on colloidal gold particles and used as the detector reagent. Test strip results were indicated by formation of up to two coloured lines (a test line was comprised of a protein conjugate of the T-2 mycotoxin and the control line was comprised of an anti-species- specific antibody) in a competitive assay format (Molinelli *et al.*, 2008). A similar approach was adapted by Lee *et al.* for the detection of AFB₁ using competition between AFB₁ and a colloidal gold-AFB₁-BSA conjugate for antibody binding sites in the test zone. The detection of AFB₁ was confirmed by use of a mobile phone device specifically, a Samsung Galaxy® S2 Smartphone, a LFIA reader, and a mobile phone device application for image acquisition and data analysis. A limit of detection of 5 µg/kg and a range of 5 to 1,000 µg/kg was established using this system (Lee *et al.*, 2013).

Many lateral flow and ELISA test kits are now commercially available for analysis of the most common mycotoxins and have been validated by organisations such as the AOAC. The use of specific antibodies within these systems to detect the mycotoxin of interest has proved very useful in screening and semi-quantitative analysis and leverage great potential for more sensitive testing with improved antibody specificity. Though chromatographic analytical techniques offer suitable, sensitive methods for determining toxin contamination within a laboratory, they have significant limitations for implementation as rapid, user-friendly, ‘on-site’ testing platforms. Therefore, the need for new cost-effective, highly sensitive, portable methods of analysis for multiple mycotoxins remains.

1.2.6.3 Immunoassays – conjugate development

The quality of mycotoxin conjugates is essential to the development and reliability of immunoassays for mycotoxins. The first step in developing an immunoassay for small

molecules is the synthesis of suitable hapten-conjugate molecules. The generation of recombinant antibody fragments against mycotoxins depends on the mycotoxin-conjugate preparation, immunization, and subsequent screening process (Lapčák *et al.*, 2003; Xu *et al.*, 2014; Zhang *et al.*, 2015). Mycotoxin-conjugates can present difficulties for immunoassay development in terms of the level of successful conjugation achievable, stability and degradation over time. Furthermore, immunization strategies are complex with the dose and concentration of the mycotoxin-conjugate playing an influential role, as well as the integrity of adjuvant and time between immunisations all being important. Immune system responses to a mycotoxin-conjugate are also complex and continue to develop with advancing age. Anatomical, physiological, and immune system differences affect responses to immunization, as do the purity and presentation of the mycotoxin-conjugate and adjuvants (Schunk and Macallum, 2005). Reducing or increasing the frequency of boosts or increasing the mycotoxin-conjugate concentration can help improve a host's immune response, however, often responses can be specific to the host's own immune system. Studies conducted by Gorelick (1990), Dyaico *et al.* (1999), Sotomayor *et al.* (1999) and Madden *et al.* (2002) have suggested that mice may exhibit natural resistance to the effects of aflatoxins, possibly due to increased levels of reduced glutathione which reacts with, and, eliminates epoxide isoforms of these mycotoxins. Therefore, selection of an alternative host (e.g. chicken or rabbit) may be required when aiming to produce recombinant antibody fragments against certain mycotoxin-conjugates.

As previously highlighted, mycotoxin detection traditionally focuses on a competitive inhibition assay format. Therefore, immunoassays methods rely on the successful immobilisation of conjugate-targets on the required test surface, and in a manner that enables correct ligand orientation, retention and reduces non-specific binding. Various methods of immobilisation include 'adsorption,' whereby the mycotoxin-conjugate is directly adsorbed onto a suitable surface, 'covalent attachment' involving direct immobilisation via a series of chemical bonds at the surface, and 'crosslinking,' whereby the mycotoxin-conjugate is chemically bonded to the immunoassay surface either directly or via the use of a bifunctional agent (Moran *et al.*, 2016). However, regardless of the immobilisation strategy, conjugate stability and retention of functionality remain critical in the ability of the immunoassay to operate successfully. Strict and vigorous testing is necessary to determine the efficacy of mycotoxin-conjugates, whilst, attention and monitoring must be exercised to ensure their continual functionality.

1.2.6.4 Immunoassays – extraction methods

A major issue for any assay is matrix effects. Food samples often present complex matrices and require extraction or sample clean-up prior to analysis. This is not ideal when a rapid method is desired, and sometimes the harsh conditions of the extraction procedure can have adverse effects on the assay (Wang *et al.*, 2014). Most biosensors perform optimally with buffers or spiked samples but translating preparation of real-world samples imposes a challenging bottleneck for immunoassay detection. Matrix effects in samples present an important problem for many biosensor devices and needs to be addressed with each biosensor/analyte/matrix scenario (Moran *et al.*, 2016).

The extraction of a sample depends on both physicochemical properties of the sample matrix and the mycotoxin. The sample or ground sample is typically blended with extraction solvent in a high-speed blender or mechanical shaker. The slurry is then filtered and subjected to subsequent purification procedures, if necessary. Extraction can be performed by liquid–liquid extraction (LLE) by use of 2 immiscible liquid-phases or solid phase extraction (SPE) using a solid and a liquid phase. During the extraction, the mycotoxin (and compounds with similar properties) will migrate into the extraction solvent until equilibrium is established. Due to the absence of completely specific extraction solvents, the solvents chosen are typically capable of removing as much mycotoxin as possible, with as little interfering compounds as possible. The most suitable solvents are easy to recover, stable, non-toxic, non-volatile, non-flammable and have little impact on the environment (Stecher *et al.*, 2007). The vast structural diversity of mycotoxins results in their different chemical and physical properties for example, aflatoxins are polar and zearalenone is non-polar. Mycotoxins may be classified depending on whether they possess electrical poles (polar) or not (non-polar), however, there are several that fall in between. The polarity of molecules determines if they are miscible in aqueous solution or insoluble. Polar molecules are water soluble, while non-polar molecules are fat soluble (Naehrer, 2014). Therefore, multi-mycotoxin analysis can be challenging as sample preparation and extract purification relies predominantly on the polarity and functional groups of the mycotoxins (Kralj Cigić and Prosen, 2009). For solid samples like cereals, polar solvents can dissolve mycotoxins and extract them from the ground sample. Furthermore, water is a polar solvent and can also be used for extraction of polar mycotoxins. Water helps to wet the ground sample, thereby, improving extraction efficiencies, by increasing penetration of the solvent into the hydrophilic material. The

most efficient solvents for extracting mycotoxins are the relatively polar solvents, such as methanol, acetone, acetonitrile, ethyl acetate, diethyl ether, toluene and chloroform or mixtures of them.

Purification of extracts can be further enhanced by using solid phase extraction (SPE). Extracts are ‘cleaned-up’ to remove interfering compounds which include pigments and lipids to obtain more accurate and precise results for analysis. High-coloured matrices such as licorice, black pepper, white pepper, spices and *Capsicum* spp. are extracted and treated by a washing step and/or immunoassay column application to remove pigmentation. The introduction of non-polar solvents such as hexane, to the initial extraction solvent or as a separate defatting step after homogenization and filtration, can be conducted to remove lipids in samples such as cereals and nuts (Rahmani *et al.*, 2009). However, these steps are typically completed with chromatographic methods for mycotoxin analysis and further emphasize the time-consuming processes associated with lab-based testing. In contrast rapid methods based on immunoassay techniques usually do not require any supplementary purification and ‘clean-up’ steps. Instead, the diluted extracts can be used directly for mycotoxin-analysis in methods such as ELISA (Krska and Molinelli, 2006).

1.3. Antibody generation

1.3.1. Antibodies

Recently, immunoassays have become prominent diagnostics due to their excellent functionality in ‘sample-to-answer’ analyses, high-throughput capability, rapid operation time and portability (Moran *et al.*, 2016). Antibodies have become invaluable biorecognition molecules for incorporation into lateral flow, ELISA-based detection platforms and in biosensors for analysis of pathogens and toxins (Banada and Bhunia, 2008). Antibodies are produced as monoclonal (through hybridoma technology), polyclonal (through animal immunisations) or recombinant formats (through display technology). The advent of recombinant antibody generation technology has given rise to novel formats such as single chain fragment variables (scFv) and antigen binding fragments (Fab) among others (Moran *et al.*, 2018). The development of specific antibodies or recombinant antibody fragments provides the ideal biorecognition elements for the detection of mycotoxins, and, integration in inexpensive, highly sensitive, portable device. Antibodies are made naturally in the body to defend against invading pathogens or

foreign bodies. The highly specific biorecognition property of antibodies for their cognate antigens has promoted their use in a vast range of applications in diagnosis and detection. Animal hosts are traditionally utilised for monoclonal and polyclonal antibody production, however, recombinant and phage display methods are commonly used to improve antibody specificity and to minimise animal costs associated with antibody generation. The development of recombinant antibody fragments which can be effectively incorporated into immunoassays for 'in-field' detection, present a compelling solution to 'point-of-site' mycotoxin analysis that can help reduce dependency on slow and costly analysis and ensure food safety for consumers.

Antibodies (also known as immunoglobulins) are produced by the body's adaptive immune system in response to foreign body invasion and recognise foreign materials or antigens. B-lymphocytes derived from lymphatic tissues including the bone marrow and the spleen, secrete antibodies, thus mediating the adaptive immunity response. An antibody (150 kDa) has four polypeptides comprised of two light (L) chains and two heavy (H) chains linked by disulphide bonds (Figure 1.6). Both chains have constant and variable regions with the latter responsible for antigen binding. The variable regions facilitate binding by bringing the hyper-variable regions of the antibody known as the complementary determining regions (CDRs) close together. The heavy chain has one variable and three constant domains whereas the light chain has one of each. There are 5 classes of immunoglobulin; IgA, IgG, IgM, IgD and IgE (Conroy *et al.*, 2009).

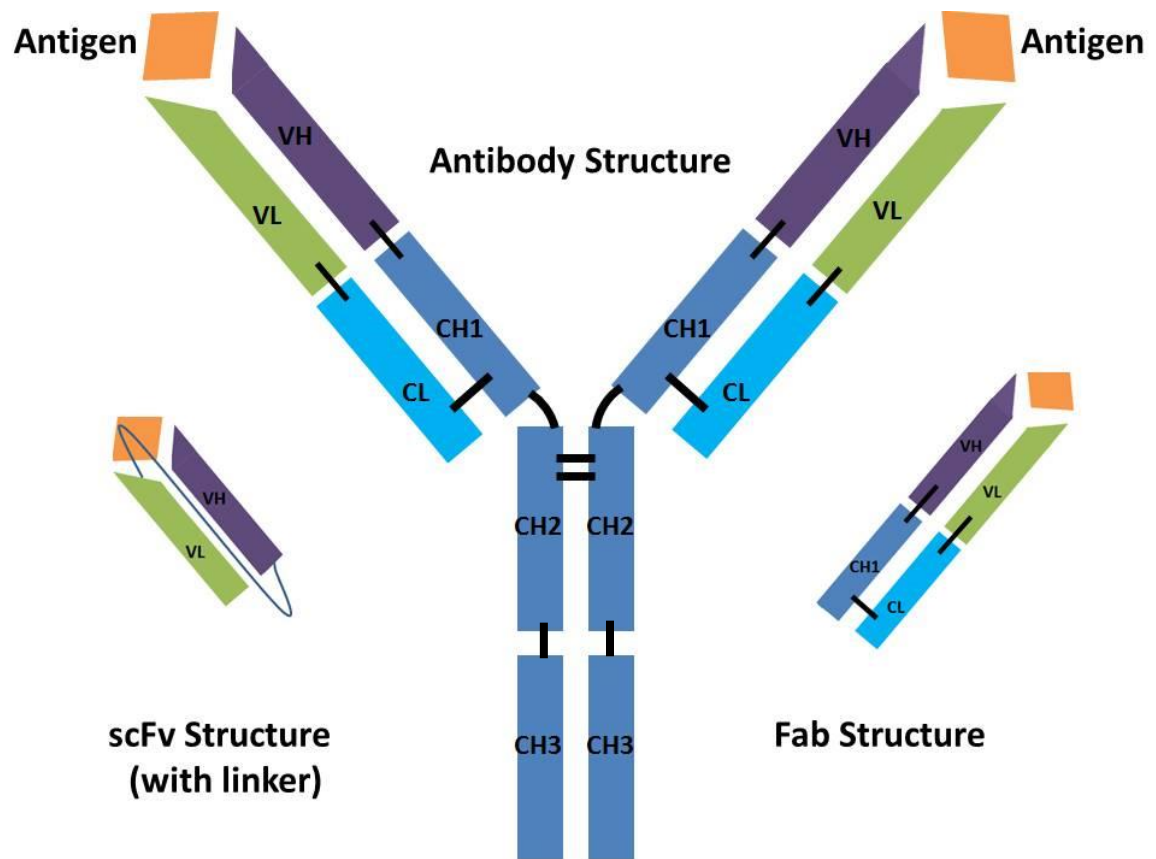


Figure 1.6: Antibody and antibody fragment structures. Full antibody structure (IgG). Antigens are presented occupying the antibody binding sites. A single-chain variable fragment (scFv) antibody fragment and a fragment antigen-binding (Fab) antibody fragment are also shown.

1.3.2. Recombinant antibody fragments

Antibodies with exquisite specificity can be generated in the laboratory and provide an area of intense research. A laboratory-generated monoclonal, polyclonal or recombinant antibody should be capable of binding with specificity to very low amounts of its antigen with a high affinity. Monoclonal antibodies are very specific and act against a single epitope. Polyclonal antibodies however bind to many different epitopes and are frequently used as capture antibodies (Byrne *et al.*, 2009; O' Reilly *et al.*, 2013). Recombinant antibodies are produced by genetic manipulation of antibody genes and deliver low-cost, rapid expression of antibody fragments in *E. coli*, as well as, the potential to use several alternative expression systems suitable for this purpose. They have further attractive attributes when compared with monoclonal or polyclonal antibodies, for example, recombinant techniques such as site-directed mutagenesis or chain shuffling offer a viable

way of optimising antibody sensitivity (Zeng *et al.*, 2012). Additionally, tags such as hexa-histidine (HIS6) for isolation or immobilisation, or labels such as green fluorescent protein for detection can be fused with the antibody fragment. Recombinant antibodies clones can also be easily renewed using sequence information and gene synthesis. Using recombinant approaches, a range of functional antibody fragments have been developed (Byrne *et al.*, 2009).

Single chain variable fragments (scFv) are the ‘simplest’ antibody fragments for cloning and expression. A scFv fragment consists of heavy and light chain variable domains of the full immunoglobulin antibody joined using a flexible glycine-serine linker (Figure 1.6). The small fragment (~25 kDa) retains the specificity and affinity of the parental antibody despite the exclusion of the constant domains. Though of greater ease to generate, a scFv frequently exhibits lower stability and can produce expression levels with low product solubility, cell culture arrest and lysis, misfolding of expressed antibody and protein aggregation. Fragment antigen binding (Fab) antibody fragments (~50 kDa) have generally been found to be a more functional and stable recombinant antibody fragment than scFv structures. The Fab fragment consists of the variable heavy and light chain genes joined with the constant heavy and light chain genes (Figure 1.6) generating a more stable antibody construct (Hayhurst, 2000; Nelson, 2010; O’Kennedy *et al.*, 2010).

1.3.3. Recombinant antibody fragment generation

Recombinant antibody generation is based upon the genetic manipulation of genes. This process allows the production of light and heavy chains of immunoglobulins as individual proteins, which can be linked together to form an immune library of various antibody fragments. The immune library can be subjected to display and panning techniques to select a specific antibody fragment against a target of interest. As well as scFv and Fab formats, several different types of recombinant antibody fragments are described in the literature including; Fv, variable fragment; (scFv)₂, fragment that consists of two scFv molecules connected by a disulfide bond; dsFv, variable fragment stabilized by additional intramolecular disulfide bond and (Fab)₂, fragments (Altshuler *et al.*, 2010).

An immune library consisting of a large pool of antibodies is generated by a host when exposed to an antigen of interest. Antigens like mycotoxins with low molecular weights

(less than 1,000 Da) are too small to elicit an immune response and therefore a suitable immunogen can be synthesised by coupling the antigen to a carrier molecule with high molecular weight (Goryacheva and De, Saeger, 2011). A recombinant antibody engineering strategy involves the construction of immune libraries from B-cell antibody-encoding genes harvested from lymphoid organs (spleen and bone marrow). Messenger RNA (mRNA) is extracted and converted into complementary DNA (cDNA) using reverse transcription. The cDNA acts as a template for amplification of antibody variable heavy and variable light chain genes using polymerase chain reactions (PCR). The amplification process has been simplified by the widespread availability of specific complementary oligonucleotide primers for the variable heavy and variable light genes for many host species including chickens, mice and rabbits. Variable heavy and variable light gene chains are then assembled using splice overlap extension PCR (SOE-PCR). These chains and a suitable vector (pComb3x series) are restriction digested at specific sites, ligated together and transformed into electrocompetent XL-1 Blue *E. coli* cells to generate multiple copies of the target antibody fragment (Barbas *et al.*, 2001). *E. coli* is the most important production system for recombinant antibody generation giving yields of protein in the gram per litre scale for extracellular production. For production of functional antibody fragments, the key to success is the secretion of both V chains into the periplasmic space of *E. coli* where the oxidizing environment allows the correct formation of disulfide bonds and the assembly to a functional Fv fragment. This strategy permitted the first expression of functional Fab fragments in *E. coli* (Frenzel *et al.*, 2013). The target antibody fragments are then subjected to suitable display and panning methods to isolate a functional, specific antibody fragment of interest.

1.3.4. Filamentous phage and phage display

More and more recombinant antibody fragments with high specificity and affinity for haptens are being isolated from immune libraries and this has been made possible by using phage display (Sheedy *et al.*, 2007). This makes phage display an obvious choice in recombinant antibody generation. The idea of phage display was first introduced by George P. Smith in 1985. *E. coli* is used as a host and filamentous bacteriophages as an expression and display system so that the encoding DNA is packaged into a single phage particle. The genetic material coding for the recombinant antibody fragment is engineered

so that it is introduced into the phage genotype and directly linked to its phenotype through expression at the surface of the phage viral coat (Smith, 1985; Leemhuis *et al.*, 2005).

1.3.5. Filamentous phage biology

Filamentous phage belong to a family of viruses called bacteriophage which infect by attaching to the F conjugative pilus of *E. coli* and injecting viral DNA directly into the host. Filamentous phage particles (Figure 1.7) are composed of a circular single-stranded DNA genome (~6,400 nucleotides) encased in a long rod like protein capsid cylinder approximately 1µm by 6.5 nm in size.

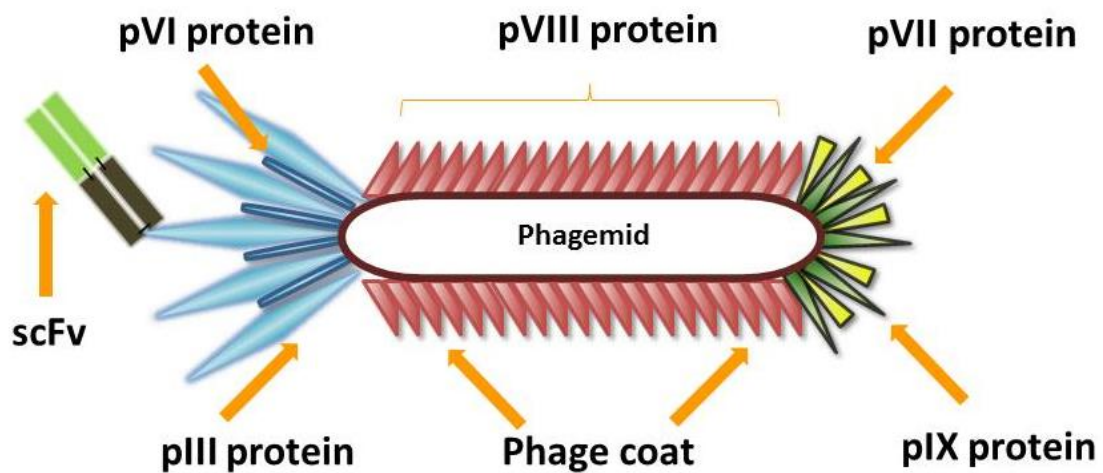


Figure 1.7: Filamentous phage particle. The filamentous phage particle is composed of five different coat proteins with pIII protein playing a critical role in the display of recombinant antibody fragments on the phage surface. The major coat protein is pVIII whilst minor proteins pVI, pVII and pIX are located at each end of the structure.

The flexible capsid consists of approximately 2,700 molecules of the major coat *gene VIII* protein (pVIII). There are 5 molecules of *gene VII* protein (pVII) and of *gene IX* protein (pIX) located at one end of the capsid while the other end is comprised of 5 molecules of *gene III* protein (pIII) and of *gene VI* protein (pVI). Infection is instigated with the binding of the bacterial F pilus to phage pIII protein. After this occurs, the pilus retracts with the pIII end of the phage particle into the bacterial periplasm. The subsequent phases of phage infection are not fully substantiated, however, the major capsid protein VIII (and possibly pVII and pIX minor capsid proteins) disassembles into the cytoplasmic membrane whilst

the phage DNA translocates into the cytoplasm. The presence of three cytoplasmic membrane Tol proteins (TolQ, R, and A) are necessary for translocation of the phage DNA into the cytoplasm and translocation of the phage coat proteins into the cytoplasmic membrane. It has also been suggested that the breakdown of the pVIII protein in the cytoplasmic membrane may be partially responsible for the translocation of the phage DNA into the cytoplasm. The phage pIII protein then merges with newly synthesised pIII within the cytoplasmic membrane and both are assembled into newly formed phage particles (Barbas *et al.*, 2001; Pande *et al.*, 2010).

The single-stranded (+) viral DNA is converted to double-stranded DNA in the cytoplasm by bacterial enzymes which synthesise a complementary (-) strand. Gyrase (type II topoisomerase) catalyses the formation of negative supercoils producing covalently closed, supercoiled double-stranded DNA called parental replicative (RF) DNA. The complementary (-) strand of the RF acts as a template for transcription with resulting mRNA translated into all phage proteins. pII, pX, and pV are the three proteins engaged in replication of DNA and are located in the cytoplasm whilst all of the other phage proteins are synthesized and located in the cytoplasmic or outer membranes. pII's function is to 'nick' the (+) strand in the RF to produce a 3'-hydroxyl that acts as a primer for synthesis of a new viral strand using the bacterial enzymes. In this process pII circularizes the displaced viral (+) strand DNA, which then is converted to supercoiled, double-stranded progeny RF molecules by the bacterial enzymes. In this way, a pool of progeny double-stranded RF molecules are produced that can direct the synthesis of the phage proteins. pV-dimers then bind to the newly synthesized viral single-stranded DNA and prevent its conversion to RF DNA and essentially switch most of the DNA replication to the synthesis of single-stranded (+) viral DNA. The pV-DNA complex is the substrate for the phage assembly reaction, which is initiated at a 78-nucleotide hairpin packaging signal exposed at the end of the DNA. pX seems to function as an inhibitor of pII function, aiding in the regulation of the amount of viral DNA produced. pVIII (major capsid protein), pVI, pVII, pIX (minor capsid proteins), pIV, pI and pXI (integral membrane proteins) are necessary for the formation of the phage particle and the membrane channels to accommodate the extruding phage particle. Phage particle-assembly occurs where the bacterial inner and outer membranes are in close contact, most likely at the sites of pIV oligomer-channel formation across the outer membrane (6-8 nm) and pI and pXI-channel formation across the cytoplasmic membrane. pV-DNA undergoes pV dimer removal and capsid protein

(pVII, pIX and pVIII) assembly around the DNA as it passes through the membrane channels before finally emerging as a phage particle through the pIV channel pore and can be continuously secreted without killing the host.

Propagation of phagemids, such as the pComb3x vector, in cells infected with helper phage results in the packaging of the phagemid DNA as phage particles in a fashion identical to that of the phage DNA itself. The helper phage provides, the phage-derived proteins which act on the phage origin of replication present in both the phagemids and helper phage and, also the enzymes required for phage replication. The structural proteins that are assembled around both the helper-phage and phagemid genomes are also supplied by helper phage.

Proteins fused to the periplasmic portion of the phage capsid can be packaged into a phage particle provided it can translocate efficiently across the inner membrane to the cytoplasm. The insertion of DNA coding for scFv and Fab antibody fragments into phage *gene III* has enabled the successful display of antibody fragments fused to the amino-terminal portion of protein pIII on filamentous phage (Smith, 1985; Barbas *et al.*, 2001).

1.3.6. Phagemids

Phagemids are filamentous phage-derived vectors that possess the recombinant coat protein genes used for display of fusion proteins. The basic components of a phagemid genome mainly includes the filamentous phage replication origin and the intergenic region (containing the packing sequence and replication origin for (-) and (+) DNA strands) for viral and complementary strand synthesis. The genome is also comprised of a plasmid origin of replication, genes encoding no or only one kind of coat protein, a gene encoding resistance to a selective antibiotic, restriction enzyme recognition sites, a promoter, and a DNA segment encoding a signal peptide (Qi *et al.*, 2012).

Additionally, a molecular tag can be included to facilitate screening of phagemid-based library. phagemid genomes can be packaged in the phage coat. Propagation of phagemids in cells infected with a helper phage such as M13KO7 provide structural and functional proteins and enzymes that result in the packaging of the phagemid DNA as phage particles in the same manner as the phage DNA. This is achieved when infection of the bacteria with helper phage activates the phage origin of replication resulting in single-stranded phagemid DNA being assembled into phage particles using helper phage proteins. The

phagemid genome carries an expression cassette that encodes the fusion-coat protein to be displayed, for example an scFv or Fab antibody fragment, thus the phagemid encodes the library to be displayed. The pComb3x phagemid vector uses the *lacZ* promoter to control expression. Expression can be suppressed by the addition of the catabolic repressor, glucose, or induced by addition of isopropyl- β -D-1- thiogalactopyranoside (IPTG). Upon induction, the scFv or Fab antibody fragment-coat fusion protein is incorporated into new phage particles and displayed on the particle surface, while the genetic information encoding the scFv remains within the phage particle. The coat-protein fusion is displayed on particles encompassing both the phagemid and the helper-phage genomes (Barbas *et al.*, 2001; Fitzgerald, 2011).

Typically, helper phage containing a defective origin of replication or packaging signal, is used for propagation as this permits preferential packaging of the phagemid genome over the helper-phage genome, and increases phagemid phage output. This is important as only phagemid phage will be able to drive the production and selection of scFv or Fab antibody fragment displayed fusion proteins.

Phagemids have become the most common vectors in phage display, and are preferred over phage for a number of reasons. The genomes of phagemids are small and can accommodate larger foreign DNA inserts. Phagemids are more efficient in transformation generating a phage display library with high diversity. A variety of restriction enzyme recognition sites are available in the genome of phagemids for convenient DNA recombination and gene manipulation. The expression level of fusion proteins can be controlled and modulated easily. Additionally, phagemids usually are genetically more stable than recombinant phage under multiple propagations (Barbas *et al.*, 2001; Qi *et al.*, 2012).

The pComb3x series of phagemid vectors are designed to contain *gene III* to express recombinant antibody fragments on their surface or as soluble proteins. The phage *gene III* allows successful display of antibody fragments fused to the amino-terminal portion of protein pIII on filamentous phage for selection. Expression is controlled using a *lacZ* promoter while *ompA* and *pelB* leader sequences are incorporated to direct expression of the recombinant antibody fragment-pIII fusion into the periplasmic space of bacteria. The pComb3x phagemid vector is particularly convenient for the soluble expression of recombinant antibodies. Usually the soluble expression of proteins requires the removal of

gene III encoding the pIII protein. However, through the addition of an amber (TAG) stop codon at the junction between the 3' SfiI restriction site at the region encoding the antibody fragment and the 5' end of *gene III* soluble expression is facilitated without *gene III* excision. Propagation of phage during selection in suppressor strains of *E. coli* such as XL-1 Blue allows for transcription of *gene III*-fusion proteins for display. However, when phage are propagated in a male non-suppressor strain such as TOP10F', the amber (TAG) stop codon is read prompting soluble expression of the recombinant antibody fragment into the periplasmic space, without continued fusion to the phage *gene III* protein. The pComb3x phagemid vector also includes two peptide tags at the carboxyl terminus of the recombinant protein. The hexa-histidine (HIS6) tag facilitates purification by immobilised metal affinity chromatography (IMAC) and the influenza haemagglutinin (HA) epitope (YPYDVPDYAS) tag, which allows for detection (Barbas *et al.*, 2001; Qi *et al.*, 2012; Hammers and Stanley, 2014).

1.3.7. Phage display and panning

Panning processes consist of several rounds of binding phage to an immobilised target antigen, a defined number of washing steps, elution processes, re-amplification of phage in *E.coli* and addition to the successive round of panning. Each successive round of panning promotes the selection and amplification of specific clones against the antigen target. The phage input of each round is typically in the 10^{12} range with phage output typically in the 10^5 to 10^8 range. The selected clones should predominate after 3-4 rounds with a 10- to 100- fold increase in output. Many factors including gradual reduction in immobilised target antigen concentrations, phage incubation time with target antigen, gradual increased wash stringency, varied elution conditions and use of competitive antigen will determine the quality of the selected antibodies during panning (Barbas *et al.*, 2001; Arbabi-Ghahroudi, 2009). A recombinant antibody engineering strategy including phage display and panning can be seen in Figure 1.8.

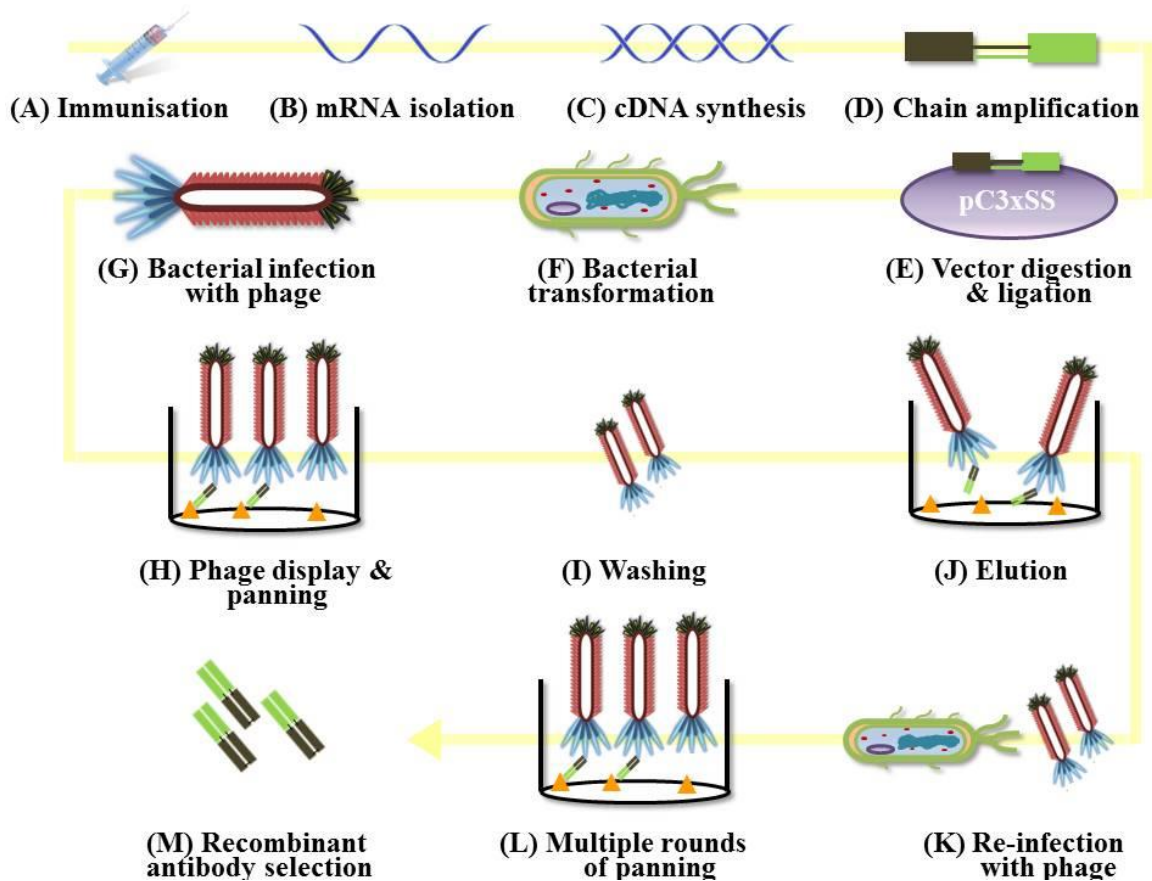


Figure 1.8: Recombinant antibody engineering strategy, phage display and panning. (A) A host animal is immunised with mycotoxin conjugated to a carrier protein. An immune response is elicited and the B cells which generate antibodies are harvested from lymphoid organs (B). mRNA is isolated and (C) converted into double stranded cDNA. (D) The cDNA acts as a template for amplification of antibody variable heavy and variable light chain genes which are linked together by SOE-PCR. (E) The SOE-PCR product is ligated into a vector. (F) The vector is transformed into *E. coli* to produce multiple copies of the target antibody. (G) *E. coli* are infected with phage displaying the antibody fragment of interest. (H) The phage are incubated with immobilised target antigen. (I) Non-specific phage are removed by washing. (J) Specifically bound phage are eluted. (K) The eluted phage are re-infected into *E. coli* and (L) re-amplified to enter further successive rounds of panning for selection and enrichment.

1.3.8. Bacterial expression

Recombinant protein expression using a pComb3xSS vector in *E. coli*, is implemented to provide a simple, fast, cheap and robust method for generating large volumes of target recombinant antibody fragments. Formerly, techniques involving bacterial expression have been hampered by the reducing nature of cytoplasm, which inhibits the formation of intradomain disulfide bridges. Consequently, antibody fragments required extraction from

inclusion bodies and refolding *in vitro* under oxidizing conditions. This method has now largely been surpassed by periplasmic expression, which allows the folding of antibody fragments in the oxidizing environment of the periplasm of *E. coli*. Periplasmic expression relies on the presence of the N-terminal pelB leader sequence in the phagemid vector that directs the recombinant protein toward protein secretion pathways. The periplasmic space of Gram-negative bacteria is rich in chaperones that aid in the production of correctly folded antibody fragments. During this process aggregation may still occur, driven by high protein concentration, however, this is less problematic for phage display-derived fragments that have encountered bacterial expression conditions during selection.

In addition to protein expression, successful purification of the desired proteins is easily facilitated through the incorporation of tags. The pComb3xSS vector incorporates a hexahistidine (HIS6) tag in the N-terminal end of the fragments, which greatly simplified protein purification when coupled with immobilized metal ion affinity chromatography (IMAC). This approach may be hampered by the selection of *E.coli* derived histidine-containing, contaminating proteins. To overcome such issues, polishing steps using size exclusion chromatography were incorporated in the purification process. Furthermore, the inclusion of an influenza haemagglutinin (HA) epitope (YPYDVPDYAS) tag permits identification and characterisation of antibody fragments with a secondary antibody using traditional methods such as ELISA and Western blotting analysis (Rouet *et al.*, 2012).

1.4. Thesis aims

Mycotoxins are of global concern due to the prevalence amongst commonly consumed foods and feed and the acute effects they elicit in humans and animals. Government and food safety authorities now recognize the need to eliminate mycotoxin-risks through food exposure. Therefore, the ability to monitor, detect and investigate these toxins is of paramount importance. The European Union (EU) has established stringent legislative levels for mycotoxins in foods and feed. Therefore, very sensitive methods for mycotoxin detection are necessary to meet the requirements laid out by the EU.

Furthermore, mycotoxin exposure is a prominent player in hepatocellular carcinoma (HCC) development, with Aflatoxin B₁ (AFB₁) proven to be a group one carcinogen. The pathway by which AFB₁ causes HCC development has been attributed to genomic

mutations, however, investigations into the exposure of AFB₁ on liver cells and liver cancer cells show the complex nature of AFB₁ exposure and further research is essential for understanding the complete effect of AFB₁ in HCC.

The aim of this research is to:

- 1.) Develop and characterise recombinant antibody fragments for the sensitive and specific detection of mycotoxins.
- 2.) Incorporate the recombinant antibody fragments into a simple, robust device for the 'point-of-site' detection of mycotoxins to EU legislative limits.
- 3.) Complete a 'proof-of-concept' study to simultaneously detect mycotoxins in a multiplex 'point-of-site' assay format.
- 4.) Complete *in vitro* studies to determine the effects of AFB₁ and an anti-AFB₁ Fab antibody fragment on normal transformed human liver epithelial (THLE-2) cells and human hepatoma (HepG2) cells in terms of migration, proliferation and IL-8 cytokine responses.

Chapter 2

Materials & Methods

2.1. Materials

All reagents and chemicals used were of analytical grade and were purchased from Sigma-Aldrich Ireland Ltd. (Vale Road, Arklow, Wicklow, Ireland) unless otherwise stated.

Table 2.1: Reagents

Reagent	Supplier & Address
Bacteriological Agar Yeast Extract Tryptone	Cruinn Diagnostics Ltd., Hume Centre, Parkwest Business Park, Nangor Road, Dublin 12, Ireland.
DNA Ligase M13K07 helper phage Restriction enzymes	Brennan and Company, 61 Birch Avenue, Stillorgan Industrial Park, Stillorgan, Co. Dublin, Ireland.
MyTaq™ Red Mix	Medical Supply Company, Damastown, Mulhuddart, Dublin 15, Ireland.
SYBR™ Safe DNA gel stain NuPAGE® LDS Sample Buffer (4X) SOC Media Glycogen EGF Recombinant Human Protein Fetal Bovine Serum Dulbecco's Modified Eagle's Medium (DMEM) LHC-8 Medium Penicillin-Streptomycin	Bio-sciences, 3 Charlemont Terrace, Crofton Road, Dun Laoghaire, Co Dublin, Ireland.
1Kb DNA Hyperladder InstantBlue Protein stain Amintra Ni-NTA	MyBio, Kilkenny Research and Innovation Centre, St. Kieran's College Road, Kilkenny, Ireland.
PCR Primers	Integrated DNA Technologies, BVBA, Interleuvenlaan 12A, B-3001 Leuven, Belgium.
Sodium Sulphate	Merck Millipore, Frankfurter, Straße 250, 64293, Darmstadt, Germany.
Hyclone Molecular Grade Water Isopropyl β-D-1-thiogalactopyranoside (IPTG) Carbenicillin Page Ruler Plus Ladder 1-Step™ Transfer Buffer Alexa Fluor 647-labelled goat anti-mouse IgG (H+L) secondary antibody Alexa Fluor 647-labelled goat anti-rabbit IgG (H+L) secondary antibody	Fisher Scientific Ireland Ltd., Suite 3, Plaza 212, Blanchardstown Corporate Park 2, Ballycoolin, Dublin 15, Ireland.

HRP-labelled anti-M13 rat secondary antibody	GE Healthcare, Amersham Pl, Little Chalfont HP7 9NA, UK.
--	---

Table 2.2: Commercial kits

Kit	Supplier & Address
NucleoSpin Plasmid DNA purification kit NucleoSpin Gel and PCR Clean-Up kit	Macherey-Nagel GmbH & Co. KG, Neumann Neander Str. 6-8, D-52355 Düren, Germany.
SuperScript® III First-Strand Synthesis System RT-PCR Kit	Bio-sciences, 3 Charlemont Terrace, Crofton Road, Dun Laoghaire, Co. Dublin, Ireland.
Pierce™ BCA Protein Assay Kit	Fisher Scientific Ireland, Suite 3, Plaza 212, Blanchardstown Corporate Park 2, Ballycoolin, Dublin 15, Ireland.
TACS® MTT Cell Proliferation Assay (MTT-CPA) R&D Systems, Cytokine DuoSet ELISA Development kit	Bio-Techne Ltd. 19 Barton Lane, Abingdon Science Park, Abingdon, OX14 3NB, UK.

Table 2.3: Bacterial strains

Strain	Genotype	Supplier & Address
XL1Blue <i>E. coli</i>	<i>recA1 endA1 gyrA96 thi- proAB lacIqZAM 5Tn 0(T tr)</i>	Agilent Technologies Ireland Ltd., Unit 3, Euro House, Euro Business, Park, Little Island, Co. Cork, Ireland.
TOP10F' <i>E. coli</i>	<i>qTn10(TetR)}m Δ(m -hsdRMS-m BC)Φ80 ZAM 5Δ X D 39Δ(ra-leu)7697galUgalKbpsLendAInupG</i>	Invitrogen/ Bio-sciences, 3 Charlemont Terrace, Crofton Road, Dun Laoghaire, Co. Dublin, Ireland

Table 2.4: Mammalian cell culture lines

Cell Line	Supplier & Address
Transformed Human Liver Epithelial-2 (THLE-2) Cells (ATCC® CRL-2706™) Human Hepatoma (HepG2) Cells (ATCC® HB-8065™)	LGC Standards, Queens Road, Teddington, Middlesex, TW11 0LY, UK.

Table 2.5: Media, additives and supplements

Media/Additives	Reagent	Composition
Luria Broth (LB)	1 Litre, pH 7.0 Tryptone Yeast Extract NaCl DH ₂ O	10 g/L 5 g/L 10 g/L Make up to 1 Litre
Super Broth (SB)	1 Litre, pH 7.0 Tryptone Yeast Extract 3-(N-morpholino) propanesulfonic acid (MOPS) 1% (w/v) Glucose DH ₂ O	30 g/L 20 g/L 10 g/L 10 g/L Make up to 1 Litre
Antibiotics	Carbenicillin Kanamycin Tetracycline	100 mg/mL in dH ₂ O 70 mg/mL in dH ₂ O 5 mg/mL in dH ₂ O
Isopropyl β -D-1-thiogalactopyranoside (IPTG)	1 M IPTG	1 g/4.2 mL in dH ₂ O
LHC-8 Medium	89% (v/v) LHC-8 10% (v/v) FBS 1% (w/v) Penicillin-Streptomycin 70 ng/mL Phosphoethanolamine 5 ng/mL Epidermal Growth Factor	444.15 mL 50 mL 5 mL 35 μ L 50 μ L
Dulbecco's Modified Eagle's Medium (DMEM)	89% (v/v) DMEM 1640 10% (v/v) FBS 1% (w/v) Penicillin-Streptomycin	445 mL 50 mL 5 mL
LHC-8 Medium Supplements	Phosphoethanolamine Epidermal Growth Factor	1 mg/mL in LHC-8 Medium 50 μ g/mL in LHC-8 Medium

Table 2.6: General buffers.

All buffers were prepared by accurately weighing out reagents on a Chyo JK-180, Mettler PJ300 balance. Reagents were then dissolved in the necessary volume of diluent. The pH of each buffer was adjusted by titration with appropriate acid (1 M HCl) or base (1 M NaOH) and monitored using an Orion 3 Star pH meter.

Buffer	Reagent	Composition
PBS	1 Litre, pH 7.4 0.15 M NaCl 2.5 mM KCl 10 mM Na ₂ HPO ₄ (dibasic) 18 mM KH ₂ PO ₄ DH ₂ O	1X 10X 8 g/L 80 g/L 0.2 g/L 2 g/L 1.44 g/L 14.4 g/L 0.24 g/L 2.4 g/L Make up to 1 Litre
PBS + 1% (w/v) Lysozyme	1% (w/v) Lysozyme PBS	1 g 100 mL
PBS + 5% (w/v) Milk Marvel	5% (w/v) Milk Marvel PBS	5 g 100 mL
PBST	1 Litre, pH 7.4 0.05% (v/v) Tween PBS	1X 10X 0.5 mL 5 mL Make up to 1 Litre
PBST + 1% (w/v) Milk Marvel	1% (w/v) Milk Marvel PBST	1 g 100 mL
PBS + 20% (v/v) Methanol	20% (v/v) Methanol PBS	20 mL Make up to 100 mL
PBS + 20% (v/v) DMSO	20 % (v/v) DMSO PBS	20 mL Make up to 100 mL
TAE Buffer	1 Litre, pH 7.0 Tris Base 17.4 M Glacial Acetic Acid Ethylenediaminetetraacetic acid (EDTA) DH ₂ O	1X 10X 4.84 g/L 48.4 g/L 1.14 mL/L 11.4 mL/L 0.37 g/L 3.7 g/L Make up to 1 Litre

Table 2.7: Purification buffers

Buffer	Reagent	Composition
Equilibration Buffer	500 mL, pH 8 50 mM NaH ₂ PO ₄ (mono) 300 mM NaCl 10 mM imidazole DH ₂ O	2.99 g/500 mL 8.76 g/500 mL 0.34 g/500 mL Make up to 500 mL
Tris-EDTA sucrose buffer (TES)	100 mL, pH 8 100 mM Tris-HCl, 0.5 M Sucrose 0.5 mM EDTA	3.5 g/100 mL 17. g/100 mL 0.002 g/100 mL
Wash Buffer A	500 mL, pH 7.5 0.5 M NaCl 0.1% (v/v) Tween 40 mM Imidazole PBS	14.6 g/500 mL 0.5 mL/500 mL 1.36 g/500 mL Make up to 500 mL
Wash Buffer B	500 mL, pH 7.5 0.5 M NaCl 0.1% (v/v) Tween 50 mM Imidazole PBS	14.6 g/500 mL 0.5 mL/500 mL 1.7 g/500 mL Make up to 500 mL
Wash Buffer C	500 mL, pH 7.5 0.5 M NaCl 0.1% (v/v) Tween 20 mM Imidazole PBS	14.6 g/500 mL 0.5 mL/500 mL 0.68 g/500 mL Make up to 500 mL
Elution Buffer	500 mL, pH 7.5 50 mM NaH ₂ PO ₄ (mono) 300 mM NaCl 250 mM Imidazole DH ₂ O	2.99 g/500 mL 8.76 g/500 mL 8.51 g/500 mL Make up to 500 mL

Table 2.8: SDS-PAGE and Western blotting buffers

Buffer	Reagent	Composition
12.5% (w/v) Acrylamide Separation Gel	1 M TrisHCl, pH 8.8 30% (w/v) Acrylamide 2% (w/v) Methylamine Bisacrylamide Deionised Water 10% (w/v) SDS 10% (w/v) APS TEMED	3 mL 5 mL 2 mL 1.868 mL 60 µL 60 µL 12 µL
4.5% (w/v) Acrylamide Stacking Gel	1 M TrisHCl, pH 6.8 30% (w/v) Acrylamide 2% (w/v) Methylamine Bisacrylamide Water 10% (w/v) SDS 10% (w/v) APS TEMED	600 µL 790 µL 300 µL 3.480 mL 48 µL 48 µL 5 µL
SDS	10% (w/v) SDS DH ₂ O	1 g 100 mL
APS	10% (w/v) APS DH ₂ O	50 mg 500 µL

Table 2.9: Equipment

Instrument	Supplier & Address
Tecan Safire™ 2 plate reader	Tecan Group Ltd., Seestrasse 103, 8708 Männedorf, Switzerland.
NanoDrop™ND1000	NanoDrop Technologies, Inc., 3411 Silverside Road, Wilmington, DE 19810, USA.
Gene Pulser Xcell™ electroporator Bio-rad Mini-Protean electrophoresis system Gel Doc™ EZ system and Image Lab™	Bio-Rad Laboratories Inc., 1000 Alfred Nobel Drive, Hercules, California 9454, USA.
Balances (Chyo JK-180, Mettler PJ300) Orion 3 Star pH meter ESCO AirStream AC2-4E8 Class II Biological Safety Cabinet	Medical Supply Company Ltd., Damastown, Mulhuddart, Dublin 15, Ireland.
Heraeus Hera-safe laminar flow cabinet Thermo Scientific Heraeus BB15 Carbon Dioxide incubator Binder C170 Carbon Dioxide incubator	Thermo Scientific, 12-16 Sedgeway Business Park, Witchford, Cambridgeshire CB6 2HY, UK.
HermLe Z233 MK-2 refrigerated centrifuge	HermLe Labortechnik GmbH., Siemensstrasse, Wehingen, 78564, Germany.
Eppendorf refrigerated centrifuge 5810 R Rotars: F45-30-11 (14,000 rpm) A-4-62 (4,000 rpm)	Eppendorf UK Ltd., Endurance House, Vision Park, Histon, Cambridge CB24 9ZR, UK.
Biometra T-Gradient PCR Thermo Cycler New Brunswick Scientific Excella E25 Temperature-Controlled Shaker Branson Sonifer™ S-450 Digital Sonicator	VWR International Co., Orion Business Campus, Northwest Business Park, Ballycoolin, Dublin 15, Ireland.
Applied Biosystems Veriti 96 Well Thermo Cycler	Bio-Sciences, 3 Charlemont Terrace, Crofton Road, Dun Laoghaire, Co. Dublin, Ireland.
Stuart Roller Mixer – SRTI	Lennox Laboratory Supplies Ltd., John F. Kennedy Drive, Naas Road, Dublin 12, Ireland.
Static incubator (37°C)	Sanyo Europe Ltd., 18 Colonial Way, Watford WD24 4PT, UK.
AKTA FPLC system S75 (16/60) analytical gel filtration column	GE Healthcare, Amersham Pl, Little Chalfont HP7 9NA, UK.
MiVac (Genevac) DNA Concentrator	Genevac Ltd., Farthing Road, Ipswich, Suffolk, IP1 5AP, UK.
MBio LightDeck® Platform MBio LightDeck® Cartridges	MBio Diagnostics, 5603 Arapahoe Avenue, Suite 1, Boulder, CO, 80303, USA.
Nikon® Eclipse E400 Microscope	Nikon Instruments Inc., Melville, NY 11747-3064, USA.
OPTIKA XDS-2FL inverted HBO Fluorescence Microscope	OPTIKA SRL, Via Rigla, 30 -24010 Ponteranica (BG), Italy

2.2 Methods

2.2.1 Safety precautions and protocols for handling toxin materials and waste

Mycotoxins are highly toxic and hazardous chemicals. Therefore, all experiments, handling, protocols for safe storage and disposal were carried out in accordance with approval from the Dublin City University (DCU) Biological Safety Committee and the Environmental Protection Agency (EPA). All cell culture procedures involving mycotoxins were conducted in a mycotoxin-designated Class II biological safety cabinet. All assays were conducted in a mycotoxin-designated fume hood. Solid waste was subjected to overnight treatment in 10% (v/v) sodium hypochlorite solution before being removed to clearly labelled sharp bins or doubled-bagged for waste removal by Stericycle (SRCL). Liquid waste was also treated overnight with 10% (v/v) sodium hypochlorite solution and disposed of down the sink. Personal protective equipment was worn at all times when handling mycotoxins and included a lab coat, safety glasses and 2 pairs of gloves.

2.2.2 Preparation of T-2 Toxin-OVA and T-2 Toxin-BSA conjugates

T-2 toxin lacks the availability of suitable reactive groups for coupling reactions. Therefore, the generation of a hemisuccinate derivative of T-2 toxin using succinic anhydride was necessary to facilitate conjugation to a carrier protein (Figure 2.1). Succinic anhydride is necessary for the introduction of carboxyl groups for the purpose of cross-linking by reaction with amino groups at neutral pH to form amide-linked carboxyls (Wang *et al.*, 2010). Carbodiimides (e.g. N,N'-Dicyclohexylcarbodiimide (DCC) and 1-ethyl-3-(3-dimethylaminopropyl)carbodiimide (EDC)) are used frequently in bioconjugation, and organic synthesis for cross-linking two proteins or for activation of carboxylic acids for reaction with ligands containing amino groups (Cammarata *et al.*, 2015). This approach was employed for the synthesis of T-2 toxin-OVA and T-2 toxin-BSA.

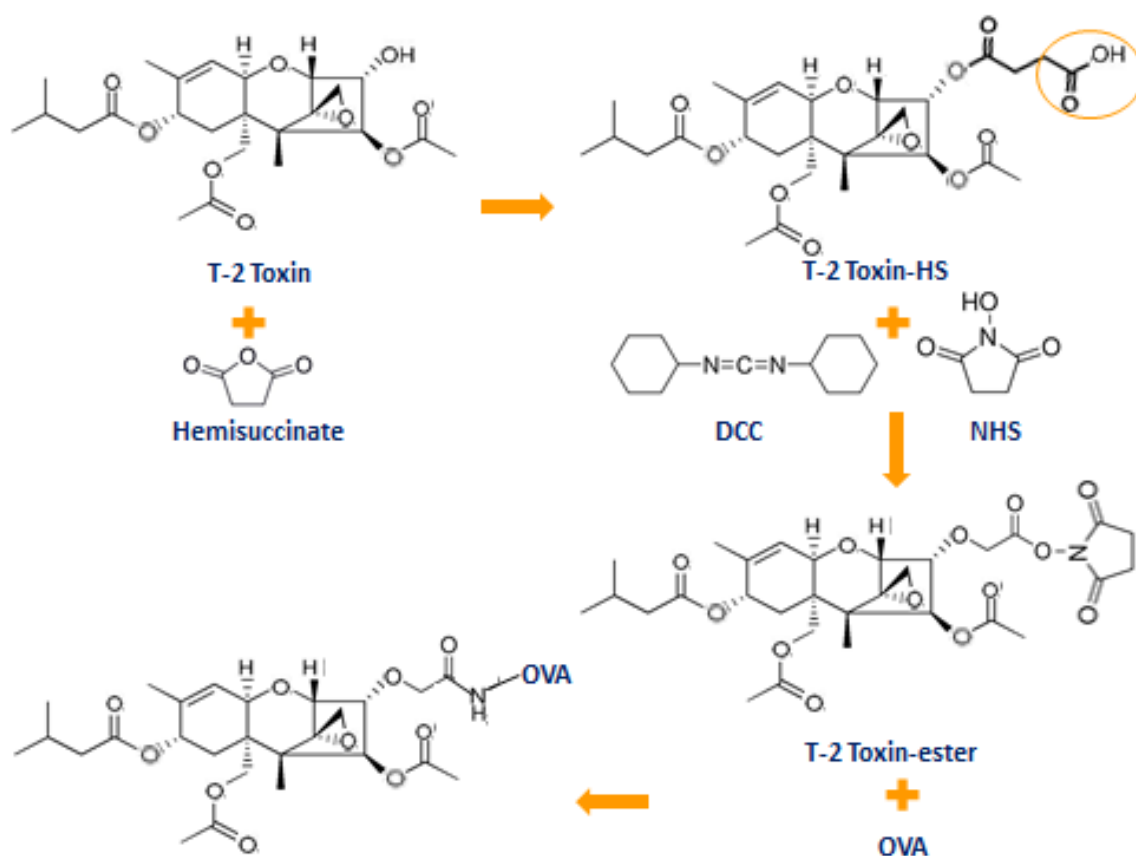


Figure 2.1: T-2 toxin conjugate synthesis. T-2 toxin lacks suitable reactive groups for conjugation. Succinic anhydride is added to generate suitable carboxyl groups. DCC and NHS are added to activate carboxyl groups generating T-2 toxin-esters for direct reaction with primary amines via amide bond formation. A carrier protein (OVA – shown) was added to the active T-2 toxin ester and underwent carbodiimide condensation to generate T-2 toxin-OVA. The same synthesis pathway was utilised for T-2 toxin-BSA.

A molar ratio (1:100) of T-2 toxin and succinic anhydride was calculated, as per Table 2.10 (Wang *et al.*, 2010; Beloglazova *et al.*, 2014). Succinic anhydride (21 mg) was added to T-2 toxin (1 mg) in 400 μ L of pyridine. The mixture was placed on a hotplate at 100°C with stirring for 4 hours. The mixture was then reduced to dryness under nitrogen at 50°C. Chloroform (1 mL) was added to re-suspend the residue and vigorously shaken by hand. Deionised water (1 mL) was added to precipitate any unreacted reagents, vigorously shaken by hand and allowed to settle. When the fractions separated, the aqueous phase was removed by gently pipetting the 1 mL fraction from the top of the chloroform liquid. This step was repeated 5 times. The extract was reduced to dryness under nitrogen at 50°C and stored at -20°C overnight. The following day the residue was re-suspended in dimethylformamide (DMF) solvent. A molar ratio (1:1.2:1.2) of T-2 toxin-HS, NHS and

DCC was calculated, as per Table 2.10. NHS (0.25 mg) and DCC (0.45 mg) were dissolved in DMF, added to the T-2 toxin-HS and mixed. The reaction was allowed to proceed for 4 hours at room temperature while rocking, and then overnight at 4°C while rocking. A molar ratio (50:1) of the T-2 toxin-ester and Ovalbumin (OVA) (2.2 mg) or Bovine Serum Albumin (BSA) (2.1 mg) carrier protein was calculated, as per Table 2.10. The carrier protein was dissolved in 3 mL of PBS and 613 µL DMF. A small volume of DMF was added to prevent precipitation of the DMF dissolved mycotoxin-ester, from the carrier protein-PBS-DMF solution, when mixed. The T-2 toxin-ester was added dropwise and shaken vigorously by hand. The reaction was allowed to proceed overnight at room temperature while rocking. The following day, the mixture was added to a Vivaspin® 10,000 MW column to buffer exchange and concentrate the sample solution. The mixture was passed through the Vivaspin® column at 3220g (Eppendorf 5810 R, Rotor A-4-62) at 4°C until the volume was ~0.5 mL. Five mL of sterile PBS was then added to the concentrator and centrifuged at 3220g (Eppendorf 5810 R, Rotor A-4-62) at 4°C until the volume was ~0.5 mL. This was completed a total of 3 times and, on last centrifugation, the volume was allowed to reach 1 mL. The concentrated mycotoxin conjugate was then carefully pipetted from the Vivaspin® column and transferred to a clean Eppendorf tube. The absorbance was read at 280 nm using a NanoDrop™ ND1000 to estimate protein concentration. Aliquots (50 µL) were prepared, labelled and stored at -20°C. Concentrated samples were retained for analysis of protein by the Bicinchoninic Acid (BCA) assay and indirect competitive inhibition ELISA to confirm the mycotoxin had been conjugated to the carrier protein on interest.

Table 2.10: Molar ratios for T-2 toxin conjugate synthesis

Reaction	Ratio	Reagent	MW	Weight (mg)	mmol
T-2 toxin: Succinic Anhydride	1: 100	T-2 toxin: Succinic Anhydride	466.52 100.07	1 21	2.14×10^{-3} 2.09×10^{-1}
T-2 toxin HS: NHS: DCC	1: 1.2: 1.2	T-2 toxin-HS NHS DCC	555.6 115.02 206.33	1 0.25 0.45	1.8×10^{-3} 2.16×10^{-3} 2.16×10^{-6}
T-2 toxin-ester: OVA	50: 1	T-2 toxin-ester OVA	395.4 42,700	1 2.2	1.8×10^{-3} 3.6×10^{-5}
T-2 toxin-ester: BSA	50: 1	T-2 toxin-ester BSA	607.6 66,463	1 2.1	1.6×10^{-3} 3.2×10^{-5}

2.2.3 Preparation of ZEN-OVA and AFB₂-OVA conjugates

ZEN and AFB₂ mycotoxins lack suitable active groups for conjugation with proteins. Therefore, carboxymethyloxime derivatives of ZEN and AFB₂ were necessary to facilitate conjugation to a suitable carrier protein. The chemical O-(carboxymethyl) hydroxylamine hemihydrochloride (CMO) has been used extensively to generate carboxyl groups for the synthesis of mycotoxin conjugates (Thouvenot and Morfin, 1983; Burkin *et al.*, 2000; Burkin *et al.*, 2002; Beloglazova *et al.*, 2013) and was employed for the synthesis of ZEN-OVA and AFB₂-OVA.

Molar ratios (1:6) of ZEN (2.5 mg) or AFB₂ (2.5 mg) and CMO (5.15 mg) were calculated, as per Table 2.11 and dissolved in 250 µL of pyridine. ZEN and AFB₂ have similar molecular weights, i.e. 318.36 and 312.27, respectively, therefore, the same molar ratios were applied to both mycotoxins. The reaction (Figure 2.2) was allowed to proceed overnight at room temperature while rocking. The following day the mixture was reduced to dryness under nitrogen at 50°C. The residue was re-suspended in 2.5 mL of deionised water. The mixture was adjusted to pH 8 with NaOH and the pH tested using pH test strips. The mixture was sonicated in a water bath for 3 minutes to re-suspend any remaining residue. Unreacted mycotoxin was extracted from the mycotoxin-CMO derivative with 5 mL of chloroform. Chloroform (1 mL) was added, vigorously shaken by hand until a foamy layer appeared and allowed to settle. When the fractions separated, the chloroform fraction was removed by gently pipetting the 1 mL fraction from the bottom of the tube leaving the aqueous phase containing the mycotoxin-CMO derivative. This step was repeated a total of 5 times. The mixture was adjusted to pH 3 using HCl to precipitate the mycotoxin-CMO derivative in the aqueous phase and the pH was tested using pH test strips. The mycotoxin-CMO derivative was extracted with 20 mL of ethyl acetate. Ethyl acetate (5 mL) was added, vigorously shaken by hand and allowed to settle. When the fractions separated, the ethyl acetate containing the mycotoxin-CMO derivative was removed by gently pipetting the 5 mL fraction from the top of the aqueous phase. This step was repeated a total of 5 times. The ethyl acetate containing the mycotoxin-CMO derivative was dried over 20 g of anhydrous sodium sulphate to remove any remaining deionised water molecules. The ethyl acetate fraction was extracted from the anhydrous sodium sulphate using a bench air vacuum. Approximately 20 mL of ethyl acetate was again added to the anhydrous sodium sulphate to wash out any remaining mycotoxin-CMO and the ethyl acetate extracted again. The extract was reduced to 2 mL in a rotary

evaporator at 50°C and then to dryness under nitrogen at 50°C. The extract was stored at -20°C overnight.

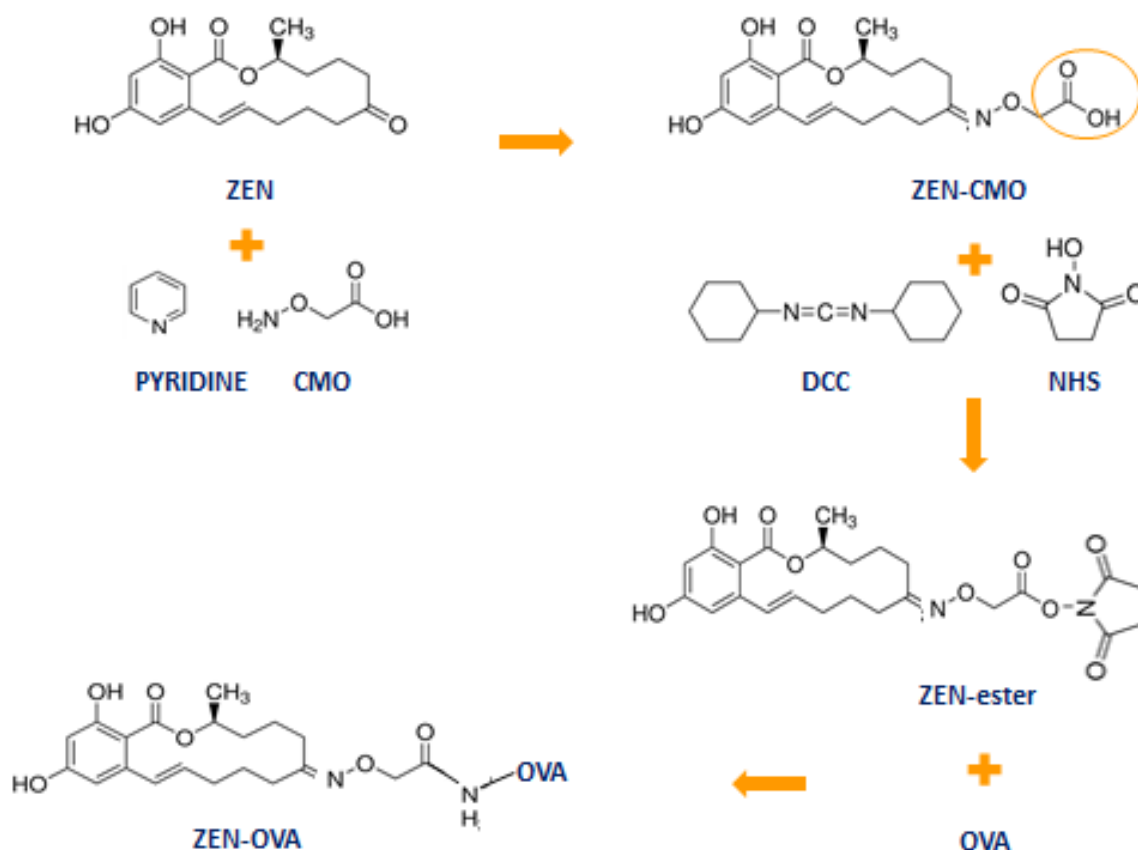


Figure 2.2: ZEN-OVA conjugate synthesis. ZEN lacks suitable reactive groups for conjugation. CMO was added to generate suitable carboxyl groups for coupling. DCC and NHS are added to activate carboxyl groups to generate ZEN-esters for direct reaction with primary amines via amide bond formation. The carrier protein (OVA) is added to the active ZEN-ester and undergoes carbodiimide condensation to generate ZEN-OVA. The same synthesis pathway was utilised for AFB₂-OVA.

The following day the residue was re-suspended in 100 µL of dimethylformamide (DMF) solvent. A molar ratio (1:2:3) of the mycotoxin-CMO derivative, NHS (1.47 mg) and DCC (3.95 mg) was calculated, as per Table 2.11. NHS and DCC were dissolved in DMF solvent, added to the extract and mixed. The reaction was allowed to proceed for 4 hours at room temperature while rocking. The reaction was then allowed to proceed overnight at 4°C. A molar ratio (56:1) of the mycotoxin-ester and Ovalbumin (OVA) (5.05 mg) carrier protein was calculated, as per Table 2.11. The carrier protein was dissolved in 3 mL of PBS and 613 µL dimethylformamide (DMF). A small volume of DMF is added to prevent

precipitation of the mycotoxin-ester dissolved in DMF when mixed. The mycotoxin-ester was added dropwise and shaken vigorously by hand. The reaction was allowed to proceed overnight at room temperature while rocking. The mixture was added to a Vivaspin® 10,000 MW column for buffer exchange and volume concentration and centrifuged at 3,220g (Eppendorf 5810 R, Rotor A-4-62) at 4°C until the volume was reduced to ~0.5 mL. Five mL of sterile PBS was added to the concentrator and centrifuged at 3,220xg (Eppendorf 5810 R, Rotor A-4-62) at 4°C until the volume was ~0.5 mL. This was completed a total of 3 times and, on last centrifugation, the volume was allowed to reach 1 mL. The concentrated conjugate was carefully pipetted from the concentrator and transferred to a clean Eppendorf tube. The absorbance was read at 280 nm using a NanoDrop™ ND1000 to estimate protein concentration. Aliquots (50 µL) were prepared, labelled and stored at -20°C. Concentrated samples were retained for analysis of protein by the Bicinchoninic Acid (BCA) assay and indirect competitive inhibition ELISA to confirm the mycotoxin had been conjugated to the carrier protein of interest.

Table 2.11: Molar ratios for ZEN and AFB₂ conjugate synthesis.

Reaction	Ratio	Reagent	MW	Weight (mg)	mmol
ZEN	1	ZEN	318.36	2.5	7.9×10^{-3}
:CMO	:6	CMO	109.30	5.15	4.71×10^{-3}
ZEN-CMO:	1:	ZEN-CMO	319.42	2.5	6.4×10^{-3}
NHS:	2:	NHS	115.02	1.47	1.28×10^{-2}
DCC	3	DCC	206.33	3.95	1.92×10^{-2}
ZEN-ester:	56:	ZEN-ester	319.42	2.5	6.4×10^{-3}
OVA	1	OVA	42,700	5.05	1.1×10^{-4}

2.2.4 BCA (Bicinchoninic Acid) assay for protein estimation

The BCA Assay was completed, as described by the manufacturer's guidelines. Briefly, standard protein (BSA) concentrations ranging from 2 - 0 mg/mL were prepared in PBS. BCA reagent was prepared by adding 50 parts reagent A (0.01 M sodium hydroxide with sodium carbonate, sodium bicarbonate, bicinchoninic acid and sodium tartate) to 1 part reagent B (4% (w/v) cupric sulphate). The mycotoxin-conjugate or protein standard (10 µL) was added to a Nunc MaxiSorp® flat-bottom 96 well plate and 200 µL of BCA reagent added. The plate was incubated at 37°C for 30 minutes and absorbance was read at

562 nm using a Tecan Safire™ 2 plate reader. A standard curve of known BSA concentration versus absorbance was constructed to determine the unknown mycotoxin-conjugate concentrations.

2.2.5 Reverse transcription of RNA to cDNA

Previously a Leghorn chicken with immunised with four boosts of 200 µg/mL of T-2 toxin-KLH. T-2 toxin was conjugated to KLH following the addition of carbonyldiimidazole (CDI) to develop a suitable immune response against a mycotoxin target of interest. The immunization schedule involved an initial administration of T-2 toxin-KLH (200 µL/mouse of 100 µg/mL conjugate with Freund's complete adjuvant in a ratio of 1:1) followed by three boosts every three weeks (200 µL/mouse of 100 µg/mL conjugate with Freund's incomplete adjuvant in a ratio of 1:1). An antibody titre of approximately 1/120,000 was achieved following the fourth immunisation and the animal was sacrificed for RNA isolation from the avian spleen and bone marrow. This work was completed by Dr. Soujanya Ratna Edupuganti (2013) and also described by Edupuganti *et al.*, 2013. Edupuganti *et al.*, reported that T-2 immunogens may induce slow immune responses in rabbits and mice due to immunosuppressive effects and accordingly they employed an immunization strategy using a T-2 toxin-KLH conjugate, prepared by a modified CDI method. The SuperScript® III First-Strand Synthesis System was used for RT-PCR and is optimized to synthesize first-strand complementary DNA (cDNA) from purified poly(A)⁺ or total RNA. The SuperScript® III kit was used, as described by the manufacturer's guidelines, to transcribe the previously isolated RNA obtained from the immunised host into cDNA. The cDNA acts as a template for the amplification of variable heavy and light chain gene fragments responsible for encoding the desired antibody fragments. Absorbance was read at 260 nm using a NanoDrop™ ND1000 to estimate cDNA concentration and the sample was then stored at -80°C.

2.2.6 Library building and linker selection

The general scheme for building libraries is similar for all species where the individual variable heavy (V_H) and variable light (V_L) chain regions are amplified separately and then linked together via a 'linker,' in a series of splice-by-overlap extension polymerase chain

reactions (SOE-PCR) steps yielding a recombinant antibody fragment product (Barbas *et al.*, 2001).

Libraries may be generated using a short (GGSSRSS) or long (GGSSRSSSSGGGSGGGG) linker. Linkers of different compositions may result in different levels of oligomerization and may also alter the interface of the V_H and V_L regions. Short chain Fragment variables (scFv) in which V_H and V_L chain variable regions are connected with a short peptide linker tend to form dimers, called bivalent diabodies, whereas scFv with long linkers tend to be monomers. Bivalent diabodies can have the advantage of binding with higher avidity to their antigen, but the use of a short linker can also lead to selection of unwanted low-affinity binders. Therefore, a balance in the degree of flexibility in the linker is required. Successful recombinant antibody construction is also dependent on avoiding interference in the folding or association of the variable domains whilst not impacting stability or recognition capabilities (Barbas *et al.*, 2001). Primers yielding a long linker were selected for building the avian scFv libraries.

2.2.7 Amplification of avian variable heavy chain (V_H) and light chain (V_L) genes

To amplify the V gene rearrangements, one V_H and one V_L amplification was performed. V_H was synthesised first, then V_L and finally both were joined together by splice-by-overlap extension polymerase chain reaction (SOE-PCR). Reactions (20X) were assembled for each type of amplification, as per Table 2.12, using avian bone marrow and spleen cDNA. The commercial primers (Integrated DNA Technologies) (Table 2.13) and PCR reaction conditions used to amplify each region (Table 2.14) in the PCR thermocycler (Biometra T-Gradient PCR Thermo Cycler) are listed below.

Table 2.12: Reaction mixture for avian V_H and V_L chain gene amplification

Reagent	1X	20X
2x MyTaq Reaction Buffer	25 µL	500 µL
Template as required	1 µL	20 µL
Primers 20 µM (<i>sense</i>)	0.5 µL each	10 µL
Primers 20 µM (<i>reverse</i>)	0.5 µL each	10 µL
Molecular Grade Water	23 µL	460 µL
Total	50 µL	1000 µL

Table 2.13: Primers for avian V_H and V_L chain gene amplification

Variable Heavy (V _H)
<i>CSCVHo-FL: (sense – long linker)</i> 5' GGT CAG TCC TCT AGA TCT TCC GGC GGT GGT GGC AGC TCC GGT GGT GGC GGT TCC GCC GTC ACG TTG GAC GAG 3'
<i>CSCG-B (reverse)</i> 5' CTG GCC GGC CTG GCC ACT AGT GGA GGA GAC GAT GAC TTC GGT CC 3'
Variable Light (V _L)
<i>CSCVK (sense)</i> 5' GTG GCC CAG GCG GCC CTG ACT CAG CCG TCC TCG GTG TC 3'
<i>CKJo-B (reverse)</i> 5' GGA AGA TCT AGA GGA CTG ACC TAG GAC GGT CAG G 3'

Table 2.14: PCR reaction conditions for avian V_H and V_L chain gene amplification

Step	Temperature	Time	Cycles
Initial Denaturation	95°C	1 minute	1
Denaturation	95°C	15 seconds	30
Annealing	55°C	15 seconds	
Extension	72°C	15 seconds (and 10 minutes)	

The amplified PCR products were resolved at 100 V for 50 minutes on a 1.5% (w/v) agarose gel and bands at approximately 400bp (V_H) and 350bp (V_L) were excised and gel-purified, as described by the manufacturer's guidelines, using a NucleoSpin Gel and a PCR Clean-Up kit. The purified PCR products were ethanol-precipitated by addition of 2 volumes of 100% (v/v) ethanol, a 1 in 10 volume of sodium acetate and 2 µL of glycogen, as per Table 2.15, and stored overnight at -80°C. The following day the sample was centrifuged at 11,752g (HermLe Z233 MK-2) at 4°C for 30 minutes. The supernatant was discarded and the pellet was air-dried and then re-suspended in 20 µL of molecular grade

water. The absorbance was read at 260 nm using a NanoDrop™ ND1000 to estimate purified PCR product yield.

Table 2.15: Reagents and volumes for ethanol precipitation of purified PCR products

Reagent	Volume
DNA Library volume	60 μ L
2X volumes 100% ice-cold ethanol	120 μ L
1/10 volume sodium acetate	6 μ L
2 μ L glycogen	2 μ L

2.2.8 Splice-by-Overlap Extension Polymerase Chain Reaction (SOE-PCR)

The purified V_H and V_L products were mixed in equal ratios to generate an overlap product. The primers used in the initial PCR amplifications, generated identical glycine-serine linker sequences that served as the overlap for the extension of the full-length product during SOE-PCR. Reactions (20X, as described in Table 2.16) were assembled for each SOE-PCR. The commercial primers (Integrated DNA Technologies) (Table 2.17) and PCR reaction conditions used for SOE-PCR (Table 2.18) in the PCR thermocycler (Biometra T-Gradient PCR Thermo Cycler) are listed below.

Table 2.16: Reaction mixture for avian V_H and V_L chain SOE-PCR product

Reagent	1 x	20X
2x MyTaq Reaction Buffer®	25 μ L	500 μ L
V_H	100 ng/50 μ L	100 ng/1000 μ L
V_L	100 ng/50 μ L	100 ng/1000 μ L
Primers 20 μ M (<i>sense</i>)	0.5 μ L	10 μ L
Primers 20 μ M (<i>reverse</i>)	0.5 μ L	10 μ L
Molecular Grade Water	Make up to 50 μ L	Make up to 1000 μ L
Total	50 μ L	1000 μ L

Table 2.17: Primers for avian SOE-PCR product

SOE-PCR Product
<i>CSC-F (sense)</i> 5' GAG GAG GAG GAG GAG GAG GTG GCC CAG GCG GCC CTG ACT CAG 3'
<i>CSC-B (reverse)</i> 5' GAG GAG GAG GAG GAG GAG CTG GCC GGC CTG GCC ACT AGT GGA GG 3'

Table 2.18: PCR reaction conditions for SOE-PCR

Step	Temperature	Time	Cycles
Initial Denaturation	95°C	1min	1
Denaturation	95°C	15s	30
Annealing	56°C	15s	
Extension	72°C	2mins (and 10mins)	

The SOE-PCR product was resolved at 100V for 50 minutes on a 2.0% (w/v) agarose gel and the band at approximately 750bp was excised and gel-purified, as described by the manufacturer's guidelines, using a NucleoSpin Gel and a PCR Clean-Up kit. The purified SOE-PCR product was ethanol-precipitated overnight at -80°C, as previously described in Section 2.2.5, and the following day centrifuged at 11,725g (HermLe Z233 MK-2) at 4°C for 30 minutes. The supernatant was discarded and the pellet air-dried and then re-suspended in 20 µL of molecular grade water. The absorbance was read at 260 nm using a NanoDrop™ ND1000 to estimate SOE-PCR purified product yield.

2.2.9 Restriction digestion of SOE-PCR product and pComb3xSS Vector

The purified SOE-PCR product and pComb3xSS vector were prepared for cloning by restriction digestion at the sites 5' GGCCNNNNNGGCC 3' and 3' CCGGNNNNNCCGG 5' using *Sfi*I restriction enzyme. Restriction digests were assembled, as per Table 2.19 and incubated at 50°C for 5 hours in the PCR thermocycler (Biometra T-Gradient PCR Thermo Cycler). The digested product was ethanol-precipitated at -80°C overnight, as previously described in Section 2.2.5.

Table 2.19: Reagents for *Sfi*I restriction digest of SOE-PCR products and pComb3xSS vector

Reagent	Spleen	Bone Marrow	pComb3xSS
SOE-PCR Product	10 µg/200 µL	10 µg/200 µL	20 µg/200 µL
<i>Sfi</i> I 20 U/µL	36 U/µg - 18 µL	36 U/µg - 18 µL	6 U/µg - 6 µL
10X NEB II Buffer	1X - 20 µL	1X - 20 µL	1X - 20 µL
Molecular Grade Water	Make up to 200 µL	Make up to 200 µL	Make up to 200 µL
Total	200 µL	200 µL	200 µL

The pComb3xSS vector was treated with *Xho*I (digestion of 5' CTCGAG 3' and 3' GAGCTC 5') and *Xba*I (5' TCTAGA 3' and 3'AGATCT 5') restriction enzymes to digest the stuffer fragment contained in the vector, as per Table 2.20. The mixture was incubated at 37°C for 1 hour followed by 65°C for 30 minutes. The pComb3xSS vector was also treated with Antarctic phosphatase, as per Table 2.20, and incubated at 37°C for 30 minutes followed by deactivation at 65°C for 15 minutes.

Table 2.20: *Xho*I and *Xba*I restriction digest and Antarctic phosphatase treatment of pComb3xSS vector

Reagent	Concentration
pComb3xSS	20 µg/200 µL
<i>Xho</i> I 20 U/µL	3 U/µg - 3 µL
<i>Xba</i> I 20 U/µL	3 U/µg - 3 µL
Antarctic Phosphatase 5 U/µL	1 U/µg - 4 µL
10X Antarctic phosphatase buffer	1X - 21 µL

The digested spleen, bone marrow and pComb3xSS vector were resolved at 100 V for 50 minutes on 1.0% (w/v) and 0.5% (w/v) agarose gels. The digested insert and digested vector were excised and gel-purified, as described by the manufacturer's guidelines, using a NucleoSpin Gel and PCR Clean-Up kit. The purified digested products were ethanol-precipitated at -80°C overnight, as described in Section 2.2.5, and on the following day centrifuged at 11,752g (HermLe Z233 MK-2) at 4°C for 30 minutes. The supernatant was discarded and the pellet air-dried and then re-suspended in 20 µL of molecular grade water. The absorbance was read at 260 nm using a NanoDrop™ ND1000 to estimate purified restriction digested SOE-PCR product and pComb3xSS yields.

2.2.10 Ligation of restriction digested SOE-PCR product into restriction digested pComb3xSS vector

The purified *Sfi*I restriction digested SOE-PCR products for spleen and bone marrow were ligated into the double-digested pComb3xSS vector using T4 DNA ligase. The ligation was prepared, as per Table 2.21, and incubated at room temperature overnight (18 hours). T4 DNA ligase was then deactivated at 65°C for 20 minutes. The ligated product was ethanol-precipitated at -80°C overnight, as described in Section 2.2.5 and the following day centrifuged at 11,752g (HermLe Z233 MK-2) at 4°C for 30 minutes. The mixture was then washed with 100 µL of 70% (v/v) ice-cold ethanol and centrifuged at 11,752g (HermLe Z233 MK-2) at 4°C for 30 minutes. The supernatant was discarded and the pellet air-dried then re-suspended in 15 µL of molecular grade water. The absorbance was read at 260 nm using a NanoDrop™ ND1000 to estimate purified ligated SOE-PCR product and pComb3xSS vector yield.

Table 2.21: Ligation of restriction digested SOE-PCR products and pComb3xSS vector

Reagent	Spleen	Bone Marrow	Control
SOE-PCR Product	0.7 µg/200 µL	0.7 µg/200 µL	-
pComb3xSS	1.4 µg/200 µL	1.4 µg/200 µL	1.4 µg/200 µL
10X Ligase Buffer	1X - 20 µL	1X - 20 µL	1X - 20 µL
T4 DNA Ligase (500 U/µL)	10 U/µL - 4 µL	10 U/µL - 4 µL	10 U/µL - 4 µL
Molecular Grade Water	Make up to 200 µL	Make up to 200 µL	Make up to 200 µL
Total	200 µL	200 µL	20 µL

2.2.11 Transformation of ligated pComb3xSS vector into electrocompetent XL-1 Blue *E. coli* cells

The successful ligation of the restriction digested SOE-PCR product into the restriction digested pComb3xSS vector enabled the cloned vector to be incorporated into electrocompetent XL-1 Blue *E. coli* cells.

Electrocompetent XL1 Blue *E. coli* cells (150 µL) (Agilent Technologies, Ireland) were placed in chilled 2.5 mm electroporation cuvettes (Bio-rad) and allowed to thaw. The

electroporation parameters on the Gene Pulser xCell Electroporation system (Bio-rad) were set at 25 μ F, 1.25 kV and the gene pulser control at 200 Ω . The cloned pComb3xSS vector (7.5 μ L) was added to the cells, mixed, tapped twice, allowed to incubate on ice for 1 minute and then pulsed in the shock-pad. The cuvette was immediately flushed with 1.25 mL of SOC media and transferred to a pre-warmed 50 mL tube. The electroporated samples from spleen and bone marrow were combined in a single 50 mL tube. The cells were rescued by incubation at 37°C for 1 hour while shaking at 220 rpm. A control ligation (digested pComb3x – no insert) was also electroporated.

A transformation titre was prepared to determine the size of the library. Two μ L of the electroporated cells and the control were added to 198 μ L SB media and used to make dilutions for plating on LB agar plates supplemented with 100 μ g/mL carbenicillin. The dilutions were plated out using the spread plate technique and the plates were incubated at 37°C overnight. Library size was calculated as follows:

$$\text{Library size} = \frac{\text{No. of colonies} \times \text{culture volume} \times \text{total ligation volume}}{\text{Plating volume} \times \text{ligation volume}}$$

The electroporated cells and the control were added to 10 mL of pre-warmed (37°C) SB media with 3 μ L carbenicillin (100 mg/mL) and 30 μ L tetracycline (5 mg/mL) and incubated at 37°C for 1 hour while shaking at 220 rpm. Carbenicillin (4.5 μ L of a 100 mg/mL stock) was added and the culture was incubated at 37°C for 1 hour while shaking at 220 rpm. Two mL of MK1307 helper-phage (1×10^{11} pfu/mL) was then added and the library was transferred to a 500 mL baffled flask containing 183 mL pre-warmed SB supplemented with 91.5 μ L (100 mg/mL) carbenicillin and 370 μ L tetracycline (5 mg/mL). This culture was incubated at 37°C for 2 hours while shaking at 220 rpm. Kanamycin (280 μ L of a 70 mg/mL stock) was added and the culture incubated at 37°C overnight while shaking at 220 rpm. This step initiated the display of the library on phage particles allowing the selective screening of the scFv-expressing clones through panning.

2.2.12 Selective enrichment of specific scFv displaying phage particles by panning

Phage rescue was carried out to select specific scFv-displaying phage particles from the transformed *E.coli* library infected with M13K07 helper phage. The rescued phage were subjected to panning which consisted of rounds of applying the phage to an immobilised target antigen, washing away non-specific phage, eluting specifically bound phage and re-amplification of the phage.

Collection of phage

The overnight culture of the transformed *E. coli* library infected with M13K07 helper phage was added to sterile 85 mL Oakridge tubes and centrifuged at 11,000g (Eppendorf 5810 R, Rotor F45-30-11) at 4°C for 30 minutes. The supernatant was transferred to sterile 85 mL Oakridge tubes, 4% (w/v) polyethylene glycol (PEG) added and the mixture incubated on ice for 30 minutes. The precipitated phage particles were centrifuged at 16,000g (Eppendorf 5810 R, Rotor F45-30-11) at 4°C for 15 minutes. The supernatant was discarded and the pellet air-dried by inverting the tubes on a paper towel for 10 minutes. The pellets were re-suspended in 2 mL of 1% (w/v) BSA in 150 mM PBS, pH 7.4, containing 0.02% (w/v) sodium azide and transferred to sterile 2 mL micro-centrifuge tubes. (**NOTE: sodium azide** is an extremely toxic and powerful poison. Ingestion can be fatal and inhalation may cause irritation to the respiratory tract and mucous membranes causing coughing, dizziness, shortness of breath, and fainting. Therefore, all work performed with sodium azide was completed in full Personal Protective Equipment using a chemical fume hood to avoid exposure.) Residual cell debris was then removed by centrifugation at 19,500 g (HermLe Z233 MK-2) at 4°C for 5 minutes and the supernatant transferred to sterile 2 mL tube at 4°C until ready to test in ELISA, denoted as Pan 0 (P0) and indicating the unpanned library.

2.2.12.1 Library input titre

At this point an input titre was prepared to determine the size of the library. Rescued phage (10 µL) was added to 90 µL SB media and used to make serial dilutions down to $\times 10^{-9}$. Electrocompetent XL-1 Blue *E. coli* cells (50 µL) at mid-exponential growth were infected with 10^{-7} , 10^{-8} and 10^{-9} dilutions of rescued phage and incubated at room temperature for

15 minutes. The dilutions were plated out, using the spread plate technique, on LB agar plates supplemented with 100 µg/mL carbenicillin and incubated at 37°C overnight. Library size was calculated, as described in Section 2.2.11.

The rescued phage were subjected to panning. Eight wells of a Nunc MaxiSorp® flat-bottom 96 well plate was coated with the target antigen (Table 2.22). The plate was incubated for 1 hour at 37°C. The plate was washed 3 times with PBS and tapped on tissue to remove excess washing fluid. The plate was blocked with 200 µL of PBS with 5% (w/v) Milk Marvel for 1 hour at 37°C. The plate was washed 3 times with PBST and 3 times with PBS and tapped on tissue to remove excess washings.

Panning steps

Rescued phage (100 µL) were added to the plate. The plate was allowed to incubate for 2 hours at 37°C. Non-specific phage were removed by pipetting up and down vigorously with PBST and waiting 5 minutes before discarding the solution. This was repeated 5 times with PBST and 5 times with PBS (Table 2.22). Specifically bound phage were eluted by pipetting up and down 10 times vigorously with 100 µL of 10 mg/mL trypsin in 150 mM PBS, pH 7.4. The plate was allowed to incubate for 30 minutes at 37°C. The eluted phage were collected and re-infected into 2 mL of electrocompetent XL-1 Blue *E. coli* cells at mid-exponential growth and incubated at room temperature for 15 minutes. Pre-warmed (37°C) SB media (6 mL) and 1.6 µL of carbenicillin (100 mg/mL) and 12 µL of tetracycline (5 mg/mL) were added and incubated at 37°C for 1 hour while shaking at 250 rpm. Carbenicillin (2.4 µL of a 100 mg/mL stock) was added and the culture was incubated at 37°C for 1 hour while shaking at 250 rpm.

2.2.12.2 Library output titre

At this point an output titre was prepared to determine the size of the phage library. Two µL of the culture was added to 198 µL SB media and used to make dilutions for plating on LB agar plates supplemented with 100 µg/mL carbenicillin. The dilutions were plated out using the spread plate technique and incubated at 37°C overnight. Library size was calculated, as described in Section 2.2.9.

Carbenicillin (2.4 μ L of a 100 mg/mL stock) was added to the culture and incubated at 37°C for 1 hour while shaking at 220 rpm. Two mL of MK1307 helper-phage (1×10^{11} pfu/mL) was then added and the library was transferred to a 500 mL sterile flask containing 183 mL pre-warmed SB supplemented with 46 μ L of (100 mg/mL) carbenicillin and 184 μ L of tetracycline (5 mg/mL). The culture was incubated at 37°C for 2 hours while shaking at 300 rpm. Kanamycin (140 μ L of a 70 mg/mL stock) was added and the culture incubated at 37°C overnight while shaking at 300 rpm.

The panning process, input/output titres and rescued phage collection were repeated for 4 rounds on successive days. The number of washes was increased and the immobilised antigen concentration on the plate decreased, as per Table 2.22, to enrich for highly specific scFv-displaying phage particles from the transformed *E. coli* library.

Table 2.22: T-2 toxin-conjugate panning strategy

Round of Panning	T-2 Toxin-Conjugate Concentration	Number of Wells	Number of Washes	Culture Volume
Round 1	50 μ g	8	5X PBST	200 mL
Round 2	25 μ g	4	8X PBST	200 mL
Round 3	12.5 μ g	4	10X PBST	200 mL
Round 4	5 μ g	4	12X PBST	200 mL

2.2.13 Polyclonal phage ELISA

A Nunc MaxiSorp® flat-bottom 96 well plate was coated with 100 μ L of T-2 toxin-conjugate diluted in PBS. The plate was incubated for 1 hour at 37°C. and then washed 3 times with PBS. The plate was blocked with 200 μ L of PBS with 5% (w/v) Milk Marvel for 1 hour at 37°C and washed 3 times with PBST and 3 times with PBS. Rescued phage inputs from the 4 rounds of panning, and the unpanned library (P0), were diluted in PBST with 1% (w/v) Milk Marvel or were added neat to the plate in triplicate (100 μ L/well). The plate was allowed to incubate for 1 hour at 37°C and washed 3 times with PBST and 3 times with PBS. PBST with 1% (w/v) Milk Marvel containing a 1 in 1,000 dilution of HRP-labelled anti-M13 rat secondary antibody was added to each well on the plate (100 μ L/well). The plate was allowed to incubate for 1 hour at 37°C. The plate was washed 3

times with PBST and 3 times with PBS. Development for detection was completed with the addition of 100 μ L of 3,3',5,5'-Tetramethylbenzidine (TMB) to each well for 10 minutes with gentle agitation. The reaction was stopped by adding 50 μ L of 1 M HCl to each well. Absorbance was read at 450 nm using a Tecan Safire™ 2 plate reader.

2.2.14 Soluble expression of scFv antibody fragments in Top 10F' cells

Soluble expression was performed by infecting the scFv-displaying phage particle clones selected from each round of panning into a non-suppressor strain of Top 10F' *E. coli* cells (Stratagene, USA) at mid-exponential growth. SB media (5 mL) with 10 μ L tetracycline (5 mg/mL) was inoculated with 5 μ L of Top 10F' cells and incubated at 37°C overnight while shaking at 220 rpm. The following day, the overnight culture was sub-cultured into fresh supplemented media. The sub-culture was incubated at 37°C and shaking at 220 rpm until an OD₆₀₀ of 0.6 was reached, at which point 50 μ L of phage from each round of panning was added and incubated at 37°C for 1 hour. Serial dilutions prepared in SB from 10⁻¹ to 10⁻⁷ were plated on LB agar plates supplemented with 100 μ g/mL carbenicillin and incubated at 37°C overnight.

2.2.15 Monoclonal ELISA of expressed soluble scFv antibody fragments

Monoclonal ELISA was completed following soluble expression of recombinant fragments for characterisation purposes. Alternatively, monoclonal ELISA was completed on murine anti-ZEN and anti-AFB₂ scFv antibody clones previously generated by Dr. Soujanya Ratna Edupuganti (2013), to select sensitive binders for ZEN and AFB₂. Anti-ZEN and anti-AFB₂ scFv antibody fragments were generated following immunization of individual mice with ZEN-KLH and AFB₂-KLH (200 μ L/mouse of 100 μ g/mL conjugate with Freund's complete adjuvant in a ratio of 1:1) followed by three boosts every three weeks (200 μ L/mouse of 100 μ g/mL conjugate with Freund's incomplete adjuvant in a ratio of 1:1) respectively.

Individual colonies from each plate, for each round of panning were picked and added to 150 μ L of SB media with 50 μ g/mL carbenicillin and 1% (w/v) glucose in a sterile Nunc flat-bottom 96 well culture plate and incubated at 37°C overnight while shaking at 220

rpm. The following day glycerol stocks were made by addition of 20% (v/v) glycerol and stocks stored at -80°C. Prior to this, SB media (370 µL) with 50 µg/mL carbenicillin and 1% (w/v) glucose was plated in a sterile Nunc round-bottom 96 deep-well plate and 30 µL of each overnight culture was added. The cultures were incubated at 37°C while shaking at 220 rpm until an OD₆₀₀ of 0.6 was reached, at which point 1 mM IPTG was added. The cultures were incubated at 30°C overnight while shaking at 220 rpm. The following day, the deep well plates were removed from the incubator and centrifuged at 4°C at 3,220g (Eppendorf 5810 R, Rotor A-4-60) for 20 minutes. The supernatant was discarded and the pellet was frozen at -80°C for 20 minutes. Each pellet was re-suspended in 100 µL of PBS with 1% (w/v) lysozyme for 20 minutes and then placed at -80°C for 20 minutes to freeze. The samples were allowed to thaw gently at ~25 - 30°C for 15 minutes. This procedure was repeated a total of 3 times. The deep well plates were centrifuged at 4°C at 3,220g (Eppendorf 5810 R, Rotor A-4-60) for 20 minutes, the lysate was removed and then diluted 1:2 in PBST with 1% (w/v) Milk Marvel.

A Nunc MaxiSorp® flat-bottom 96 well plate was coated with 100 µL of target toxin-conjugate diluted in PBS. The plate was incubated for 1 hour at 37°C. The plate was washed 3 times with PBS. The plate was blocked with 200 µL of PBS with 5% (w/v) Milk Marvel for 1 hour at 37°C. The plate was washed 3 times with PBST and 3 times with PBS. The 1:2 diluted lysate was added to the plate (100 µL/well). The plate was allowed to incubate for 1 hour at 37°C. The plate was washed 3 times with PBST and 3 times with PBS. PBST with 1% (w/v) Milk Marvel containing a 1 in 1,000 dilution of labelled secondary antibody (HRP-labelled anti-HA rat antibody) was added to each well on the plate (100 µL/well). The plate was allowed to incubate for 1 hour at 37°C. The plate was washed 3 times with PBST and 3 times with PBS. Development for detection was completed with the addition of 100 µL of 3,3',5,5'-Tetramethylbenzidine (TMB) to each well for 10 minutes with gentle agitation. The reaction was stopped by adding 50 µL of 1 M HCl to each well. Absorbance was read at 450 nm using a Tecan Safire™ 2 plate reader.

2.2.16 Re-amplification of polyclonal phage

Original phage preparations directly obtained from library ligation and transformation can be re-amplified. Electocompetent XL1-Blue *E. coli* cells (50 µL) were added to 50 mL of pre-warmed (37°C) SB media with 100 µL of tetracycline (5 mg/mL) and incubated at

37°C for 1.5-2.5 hours while shaking at 250 rpm until the OD₆₀₀ was approximately 1. The original phage library preparation (10 µL) was added to the culture and incubated at room temperature for 15 minutes. Carbenicillin (10 µL of a 100 mg/mL stock) was added and the culture was incubated at 37°C for 1 hour while shaking at 300 rpm. Carbenicillin (15 µL of a 100 mg/mL stock) was added and the culture was incubated at 37°C for an additional hour while shaking at 300 rpm. Two mL of MK1307 helper-phage (1 x10¹¹ pfu/mL) was then added and the library was transferred to a 500mL baffled flask containing 148 mL of pre-warmed SB supplemented with 75 µL (100 mg/mL) carbenicillin and 300 µL tetracycline (5 mg/mL). This culture was incubated at 37°C for 2 hours while shaking at 300 rpm. Kanamycin (280 µL of a 70 mg/mL stock) was added and the culture incubated at 37°C overnight while shaking at 300 rpm. This step re-initiates the display of the library on the phage particle coat allowing the selective screening of the scFv-expressing clones through panning and ELISA, as previously described in Sections 2.2.10 – 2.2.14.

2.2.17 Selective enrichment of specific scFv displaying phage particles by depletion panning with 0.1% (w/v) Ovalbumin Bbuffer

Depletion panning was conducted to ‘deplete’ potential ovalbumin (OVA) cross-reacting phage. Phage display and panning was completed, as previously described in Section 2.2.10, however, following each round of panning, the precipitated phage pellets were re-suspended in 2 mL of 1% (w/v) BSA in 150 mM PBS, pH 7.4, containing 0.1% (w/v) OVA and transferred to a sterile 2 mL micro-centrifuge tube. Residual cell debris was then removed by centrifugation at 19,500 g (HermLe Z233 MK-2) at 4°C for 5 minutes and the supernatant transferred to sterile 2 mL tube at 4°C until ready to test in ELISA.

2.2.18 Colony pick PCR

Molecular cloning techniques require screening bacterial colonies for the presence of the cloned insert. Colony pick PCR is a convenient high-throughput method for determining the presence or absence of insert DNA in plasmid constructs. Colony PCR can provide a simple process for identification of an insert of interest by: 1) using specific primers to detect the presence of the insert; 2) setting up a standard PCR reaction containing the bacterial vector as template; and 3) running the PCR product on a gel to analyze product

size. Individual transformants grown to calculate input and output phage titres can be picked, added directly to the PCR reaction and lysed during the initial heating step. This initial heating step causes the release of the plasmid DNA from the cell, so it can serve as template for the amplification reaction. Primers designed to specifically target the insert DNA can be used to determine if the construct contains the DNA fragment of interest. DNA insert-specific primers can provide information on both the specificity and size of the cloned insert. The presence or absence of a PCR amplicon and the size of the product are determined by electrophoresis alongside a DNA ladder on an agarose gel.

To amplify the SOE-PCR product of interest ligated into the digested pComb3xSS vector, single colonies were picked with a sterile pipette tip from the output plates produced during each round of panning. Reactions (20X, as described in Table 2.24) were assembled for each individual colony by adding a single colony into 50 μ L of the reaction mastermix and pipetting up and down 5 times. The commercial primers (Integrated DNA Technologies) listed in Table 2.23 were used to amplify the SOE-PCR insert DNA and PCR reaction conditions used for amplification (Table 2.24) in the PCR thermocycler (Biometra T-Gradient PCR Thermo Cyclers) are listed below.

Table 2.23: Reaction mixture for colony pick PCR

Reagent	1 x	20X
2x MyTaq Reaction Buffer®	25 μ L	500 μ L
Primers 20 μ M (<i>sense</i>)	0.5 μ L	10 μ L
Primers 20 μ M (<i>reverse</i>)	0.5 μ L	10 μ L
Molecular Grade Water	24 μ L	480 μ L
Total	50 μ L	1000 μ L

Table 2.24: PCR reaction conditions for SOE-PCR insert

Step	Temperature	Time	Cycles
Initial Denaturation	95°C	1min	1
Denaturation	95°C	15s	25
Annealing	56°C	15s	
Extension	72°C	2mins (and 10mins)	

The colony pick PCR product was resolved at 100V for 50 minutes on a 2.0% (w/v) agarose gel and the band at approximately 750bp was identified as the SOE-PCR insert present in the pComb3xSS vector.

2.2.19 Bacterial expression

Recombinant antibody fragments generated previously by Dr. Sharon Stapleton, 2007 (anti-AFB₁ Fab antibody fragment ligated into a pComb3xSS vector), Dr. Lynsey Dunne, 2002 (anti-AFB₁ scFv dimer antibody fragments ligated into a pAK500 vector) and Dr. Sue Townsend, 2009 (anti-Morphine-3-Glucuronide (M3G) Fab anti-body fragment ligated into a pComb3x vector) were bacterially expressed in 100 mL (small-scale) or 200 mL (large-scale) cultures.

A culture was prepared by inoculating 10 mL of SB media containing 50 µg/mL carbenicillin and 1% (w/v) glucose with 5 µL of *E. coli* containing recombinant antibody fragments ligated into the pComb3xSS or pComb3x vector and incubated at 37°C overnight while shaking at 250 rpm. The following day 100 mL (small-scale) or 200 mL (large-scale) cultures of media with 50 µg/mL carbenicillin and 1% (w/v) glucose were prepared in a 1 Litre conical flask to allow for aeration. Two mL (1% cell density) of the overnight culture were sub-cultured into the media and incubated at 37°C while shaking at 220 rpm until an OD₆₀₀ of 0.6 was reached, at which point the optimised concentration of IPTG [0.1 mM] was added to induce expression. The cultures were incubated overnight at 30°C and 220 rpm. Alternatively, a culture was prepared by inoculating 10 mL of SB media containing 25 µg/mL chloramphenicol with 5 µL of *E. coli* containing recombinant antibody fragments ligated in the pAK500 vector and incubated at 37°C overnight while shaking at 250 rpm. The following day 200 mL cultures of media with 25 µg/mL chloramphenicol were prepared in a 1 Litre conical flask to allow for aeration. One mL (0.5% cell density) of the overnight culture were sub-cultured into the media and incubated at 37°C while shaking at 220 rpm until an OD₆₀₀ of 0.5 – 0.6 was reached, at which point the optimised concentration of IPTG [1 mM] was added to induce expression. The cultures were incubated overnight at 30°C and 220 rpm.

2.2.20 Protein extraction methods

Protein was extracted from the *E. coli* cells transformed with the pComb3xSS or pComb3x vector by mechanical freeze-thaw based on methods described by Johnsen and Hecht (1994) and sonication to lyse cells. Alternatively, protein was extracted from the *E. coli*

cells transformed with the pAK500 vector by periplasmic osmotic shock methods described by Dunne (2002) and sonication to lyse cells.

2.2.20.1 Freeze-thawing

Cultures were transferred into sterile 250 mL Nalgene bottles and centrifuged at 3,220g (Eppendorf 5810 R, Rotor A-4-62) at 4°C for 40 minutes. The resulting pellets were re-suspended in equilibration buffer [50 mM NaH₂PO₄, 300 mM NaCl, 10 mM imidazole, pH 7.5] to give a final volume of 40 mL (4 x 10 mL aliquots). The suspensions were frozen at -80°C for 20 minutes and then allowed to thaw gently at room temperature for 15 minutes. This procedure was repeated a total of 3 times. The cells and cell lysate were centrifuged at 3,220g (Eppendorf 5810 R, Rotor A-4-62) at 4°C for 40 minutes. The lysate supernatant was collected and then subjected to sonication.

2.2.20.2 Periplasmic Osmotic Shock

Cultures were transferred into sterile 250 mL Nalgene bottles and centrifuged at 3,220g (Eppendorf 5810 R, Rotor A-4-62) at 4°C for 40 minutes. The resulting pellets were re-suspended in TES (100 mM Tris-HCl, 0.5M sucrose, 0.5mM EDTA, pH 8) to give a final volume of 40 mL (4 x 10 mL aliquots). The suspensions were incubated on ice for 1 hour. The lysate supernatant was collected and then subjected to sonication.

2.2.20.3 Sonication

The lysate supernatants were pooled together in 2 sterile 85 mL Oakridge tubes and placed on ice. Samples were sonicated using a Branson Sonifer™ S-450 Digital Sonicator at 40% amplitude for 4 second pulses with 2 second intervals for 1.5 minutes. The sonication procedure was repeated twice. The cells and cell lysate were centrifuged at 11,752g (Eppendorf 5810 R, Rotor F45-30-11) at 4°C for 40 minutes. The lysate supernatant was collected and passed through a 20 µM sterile filter.

2.2.21 Immobilized Metal Ion Affinity Chromatography (IMAC)

Nickel-Nitrilotriacetic acid (Ni⁺-NTA) resin (2 mL) was loaded into a Biorad™ column to give a final column volume of 1 mL. The column was equilibrated with 10 mL of

equilibration buffer [50 mM NaH₂PO₄, 300 mM NaCl, 10 mM imidazole, pH 7.5]. The filtered lysate was passed through the column, the 'flow-through' collected and re-applied to the column twice. For recombinant antibody fragments expressed from the pComb3xSS or pComb3x vector, the column was washed with 8 mL of wash buffer A [50 mM NaH₂PO₄, 300 mM NaCl, 40 mM imidazole, pH 7.5] and 8 mL of wash buffer B [50 mM NaH₂PO₄, 300 mM NaCl, 50 mM imidazole, pH 7.5] to remove non-specifically bound protein. For recombinant antibody fragments expressed from the pAK500 vector, the column was washed with 8 mL of equilibration buffer [50 mM NaH₂PO₄, 300 mM NaCl, 10 mM imidazole, pH 7.5] and 8 mL of wash buffer C [50 mM NaH₂PO₄, 300 mM NaCl, 20 mM imidazole, pH 7.5] to remove non-specifically bound protein. The histidine-tagged recombinant antibody fragments, specifically bound to the Ni-NTA resin, were eluted with 5 mL of elution buffer [50 mM NaH₂PO₄, 300 mM NaCl, 250 mM imidazole, pH 7.5]. At all steps of purification, samples were retained for SDS-PAGE and Western blotting analysis.

2.2.22 Protein concentration and buffer exchange

A Vivaspin® 6 mL 10,000 MW concentrator was washed with 5 mL of deionised water at 3,220g (Eppendorf 5810 R, Rotor A-4-62) at 4°C for 5 minutes. This step was repeated twice with PBS. To allow buffer exchange, 5 mL of eluate were added to the concentrator and centrifuged at 3,220g (Eppendorf 5810 R, Rotor A-4-62) at 4°C until the volume was reduced to ~0.5 mL. Five mL of sterile PBS 150 mM with 0.02% (w/v) sodium azide were added to the concentrator and centrifuged at 3,220g (Eppendorf 5810 R, Rotor A-4-62) at 4°C until volume was ~0.5 mL. (**NOTE: sodium azide** is an extremely toxic and powerful poison. Ingestion can be fatal and inhalation may cause irritation to the respiratory tract and mucous membranes causing coughing, dizziness, shortness of breath, and fainting. Therefore, all work performed with sodium azide was completed in full Personal Protective Equipment using a chemical fume hood to avoid exposure.) This was completed a total of 3 times and on the last centrifugation the volume was allowed to reach 1 mL. The concentrated eluate was carefully pipetted from the concentrator surface and transferred to a sterile micro-centrifuge tube. The absorbance was read at 280nm using a NanoDrop™ ND1000 to estimate protein concentration. Aliquots were prepared (50 µL), labelled and

stored at -20°C. Concentrated samples were retained for SDS-PAGE and Western blotting analysis.

2.2.23 Gel filtration/Size exclusion chromatography

Eluted protein fractions from the IMAC purification were further purified by chromatography on a size exclusion column. Gel filtration (or size exclusion chromatography) is a basic chromatography technique that separates proteins based on differences in molecular size and shape as they pass through a gel filtration medium in a packed column. This step is frequently used as a final polishing step following IMAC purification for isolation of highly pure protein (Kim *et al.*, 2011).

An AKTA FPLC system and a S75 (16/60) analytical gel filtration column (GE Healthcare) was equilibrated with 150 mM PBS, pH 7.4. Protein-containing fractions previously purified by IMAC were applied to the column at a flow rate of 1 mL/minute. Fractions were collected after 0.4 column volumes (CV) until 1 CV was reached (1CV = 50 mL). Protein was monitored online by A280 using the dedicated Unicorn control and evaluation software (GE Healthcare). Protein peaks of the eluted protein fraction from IMAC purification were analysed by SDS-PAGE and Western blotting.

2.2.24 SDS-PAGE (Sodium Dodecyl Sulphate Polyacrylamide Gel Electrophoresis)

SDS-PAGE is one of the most common methods for protein separation. Protein quality and purity can be readily investigated using SDS-PAGE whilst also providing the basis for further investigation through Western blotting analysis. In this process, sodium dodecyl sulfate (SDS) an anionic detergent, imparts a negative charge and linearizes proteins. Two-mercaptoethanol and boiling are applied to ensure proteins are fully denatured. When an electric field is applied the negatively charged proteins migrate from the cathode (negative electrode) towards the anode (positive electrode) separating the proteins as they move through the gel, based on their size.

Two 12.5% (w/v) acrylamide separation gels [1 M TrisHCl, pH 8.8, 30% (w/v) acrylamide, 2% (w/v) methylamine bisacrylamide, water, 10% (w/v) SDS, 10% (w/v)

APS, TEMED] were prepared according to Table 2.2.7. The gels were cast between Biorad™ plates and allowed to set. Two 4.5% (w/v) acrylamide stacking gels [1M TrisHCl, pH 6.8, 30% (w/v) acrylamide, 2% (w/v) methylamine bisacrylamide, water, 10% (w/v) SDS, 10% (w/v) APS, TEMED] were added and combs inserted at an angle to prevent bubbles forming. The gels were placed in the Biorad™ chamber, as described by the manufacturer's guidelines.

Electrophoresis buffer [50 mM TrisHCl, 196 mM Glycine, 0.1% (w/v) SDS] was gently poured into the inner chamber until it reached the top of the plates and combs were removed from the gels. Excess buffer was poured into the outer chamber and bubbles expelled. Protein samples were prepared in NuPAGE® LDS Sample Buffer (4X). Samples were mixed and boiled at 95°C for 5 minutes. Pageruler Plus Prestained Protein Ladder™ (5 µL) and each prepared sample (10 µL) was loaded into the wells. The lid was then placed on top of the chamber. The gels were resolved at 150 V and allowed to run for 1 - 1.5 hours. Once the current was switched off, the gels were carefully removed. One of the gels was stained with InstantBlue™ dye for 1 hour and excess stain washed away with deionised water. Images of the resulting gel were recorded by camera. The remaining gel was used for Western blotting analysis.

2.2.25 Western Blotting analysis

Western blotting was first described by Towbin *et al.* in 1979 and involves the transfer of resolved proteins in polyacrylamide gels to nitrocellulose membranes. This method uses antibodies to identify specific protein targets transferred to the nitrocellulose membrane, where the specificity of the antibody-antigen interaction enables a target protein to be identified (Figure 2.2).

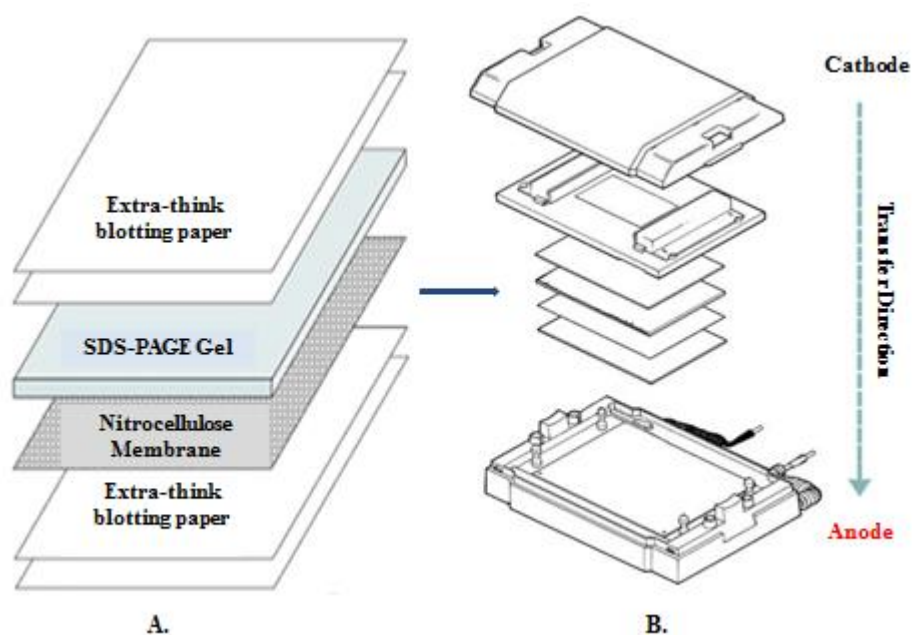


Figure 2.3: Sandwich format for Western blot transfer. (A) All components of the transfer sandwich are pre-soaked in 1-Step™ Transfer Buffer. The nitrocellulose membrane is placed on top of two layers of extra-thick blotting paper. The resolved SDS-PAGE gel is gently position on top of the membrane. Two further layers of extra-thick blotting paper are placed on top of the gel and air bubbles gently smoothed out. (B) The sandwich is applied to the transfer system, electric current is applied and the transfer of proteins to the nitrocellulose membrane occurs as the current passes from the cathode to the anode.

An acrylamide gel containing proteins resolved by SDS-PAGE, 2 sheets of extra-thick blotting paper and a nitrocellulose membrane were soaked for 10 minutes in 1-Step™ Transfer Buffer. The proteins were transferred from the gel to the nitrocellulose membrane using a sandwich format applied to the Biorad™ Trans-Blot® SD Semi-Dry Transfer System for 21 minutes at 15 V. The nitrocellulose membrane was blocked for 1 hour at room temperature in PBS with 5% (w/v) Milk Marvel [5 g/100 mL PBS] with gentle agitation. The membrane was then washed 3 times with PBS and 3 times with PBST before being incubated for 1 hour at room temperature in PBST with 1% (w/v) Milk Marvel [1 g/100 mL PBST] containing a 1 in 2,000 dilution of labelled secondary antibody (HRP-labelled anti-HA rat antibody) with gentle agitation. The membrane was washed with PBS-T for 20 minutes at room temperature with gentle agitation. Development for detection was completed with the drop-wise addition of 2 mL of 3,3',5,5'-Tetramethylbenzidine (TMB) to the nitrocellulose membrane. Images of the resulting Western blot were recorded by camera.

2.2.26 Indirect ELISA

In this ELISA format the antigen is coated onto a high protein-binding capacity polystyrene 96 well ELISA plate. Primary antibody is applied, followed by an enzyme-labelled secondary antibody which binds the first antibody. The secondary antibody is usually an anti-species antibody and is often polyclonal. The enzyme-labelled secondary antibody is reduced by the addition of a suitable substrate to elicit a colour change. This reaction is stopped with acid and the absorbance of the developed colour can be determined using a spectrophotometer. This method provides a titre for antigen-antibody complex binding. The most precise method for optimizing assay concentrations is the checkerboard ELISA method. This method was originally designed to determine antigen/antibody concentration for ELISA tests and can be used to determine optimal coating concentrations for any type of immobilized biomolecule. This method also allows selection of an optimal concentration for any or all reactants in the assay (Gibbs, 2001).

In the indirect checkerboard ELISA a Nunc MaxiSorp® flat-bottom 96 well plate was coated with 100 µL of concentrations between 0.66 - 15 µg/mL of toxin-conjugate diluted in PBS in triplicate. The plate was incubated for 1 hour at 37°C. The plate was then washed 3 times with PBS. The plate was blocked with 200 µL of PBS with 5% (w/v) Milk Marvel for 1 hour at 37°C. The plate was washed 3 times with PBST and 3 times with PBS. Doubling dilutions of antibody diluted using PBST with 1% (w/v) Milk Marvel were added to the plate in triplicate (100 µL/well). The plate was allowed to incubate for 1 hour at 37°C. The plate was washed 3 times with PBST and 3 times with PBS. PBST + 1% (w/v) Milk Marvel containing a 1 in 1,000 dilution of labelled secondary antibody (HRP-labelled anti-HA-rat antibody) was added to each well on the plate. The plate was allowed to incubate for 1 hour at 37°C. The plate was washed 3 times with PBST and 3 times with PBS. Development for detection was completed with the addition of 100 µL of 3,3',5,5'-Tetramethylbenzidine (TMB) to each well for 10 minutes with gentle agitation. The reaction was stopped by adding 50 µL of 1M HCl to each well. Absorbance was read at 450 nm using a Tecan Safire™ 2 plate reader. A negative control using a non-carrier protein, diluted in PBS to the same concentration of the immobilised toxin-conjugate, was used to test for the presence (if any) of non-specific binding.

2.2.27 Indirect competitive inhibition ELISA

Indirect competitive inhibition ELISA is an accepted, reliable, and sensitive method for measuring antibody responses against a variety of infectious pathogens in both humans and animals (Li *et al.*, 2001). A Nunc MaxiSorp® flat-bottom 96 well plate was coated with 100 μ L of 5 μ g/mL AFB₁-BSA, 3 μ g/mL AFB₂-OVA and 10 μ g/mL T-2 toxin-OVA diluted in PBS in triplicate. The plate was incubated for 1 hour at 37°C. The plate was washed 3 times with PBS. The plate was blocked with 200 μ L of PBS with 5% (w/v) Milk Marvel [5 g/100 mL PBS] for 1 hour at 37°C. The plate was washed 3 times with PBST and 3 times with PBS. Standards of decreasing concentrations of antigen were prepared in PBS. Each standard (50 μ L) was added to the plate, followed by an equal volume of cognate antibody diluted using PBST with 1% (w/v) Milk Marvel [1 g/100 mL PBST] in triplicate and allowed to incubate for 1 hour at 37°C. The plates were washed 3 times with PBST and 3 times with PBS. PBST with 1% (w/v) Milk Marvel [1 g/100 mL PBST] containing a 1 in 1,000 dilution of labelled secondary antibody (HRP labelled anti-HA rat antibody) (100 μ L) was added to each well on the plate. The plate was left to incubate for 1 hour at 37°C. The plates were washed 3 times with PBST and 3 times with PBS. Development for detection was completed with the addition of 100 μ L of 3,3',5,5'-Tetramethylbenzidine (TMB) to each well for 10 minutes with gentle agitation. The reaction was stopped by adding 50 μ L of 1 M HCl to each well. Absorbance was read at 450 nm using a Tecan Safire™ 2 plate reader. A negative control using a non-carrier protein, diluted in PBS to the same concentration of the immobilised toxin-conjugate, was used to test for the presence (if any) of non-specific binding.

2.2.28 MBio microarray printing and cartridge development

Portable optical-planar waveguide LightDeck® cartridges for the 'point-of-site' detection of AFB₁ and T-2 toxin were developed and generated by MBio Diagnostics, Colorado, USA. The system is based on a small, light-weight optical reader platform for rapid result read-out, following test completion on a simple cartridge construct (Figure 2.4 A.)). Briefly, the cartridges are composed of an optical-planar waveguide substrate which is an injection moulded, plastic component activated by proprietary silane-based surface chemistry. Immobilisation of targets in a microarray format on the waveguide surface was via a combination of covalent (lysine residues of targets) and non-specific interactions

(hydrophobic, van der Waals, electrostatic). Mycotoxin-conjugates were printed onto the waveguide surface (Figure 2.4 B.)) using a Bio-Dot AD3200 robotic arrayer at varying concentrations. The generated spots were 0.5 mm in diameter by use of the Bio-Jet print head dispensing 20 nL volumes. Replicates (2) of each spot were printed onto a grid containing 1 mm centres, blocked with 0.5% (w/v) casein in PBS (with Proclin300 antimicrobial agent) prior to spin-drying. The microarrays were then assembled in an injection-moulded cartridge containing a 5 mm fluidic channel, a single inlet port and a waste reservoir.

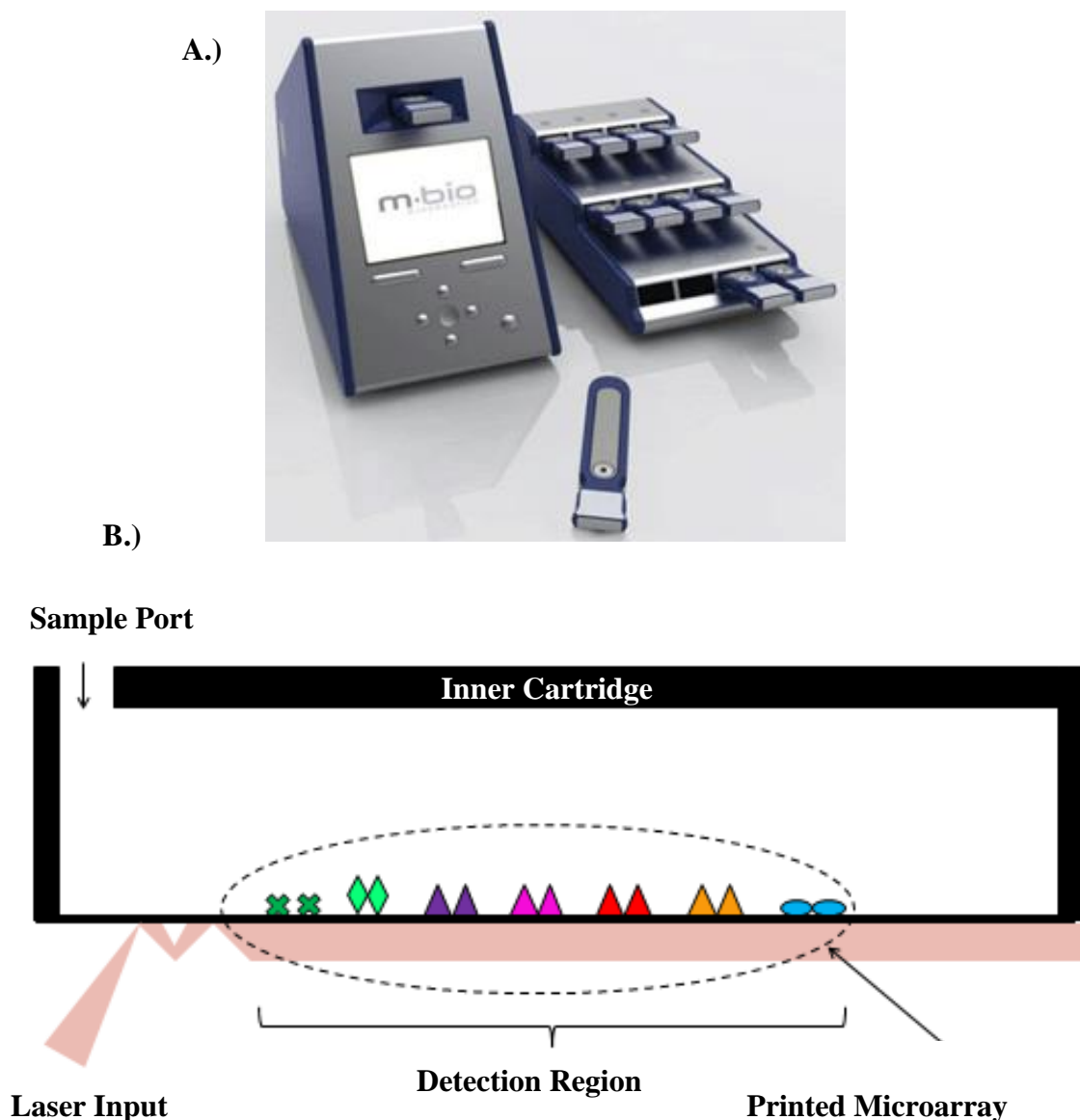


Figure 2.4 A.) MBio optical-planar waveguide multiplexed immunoassay system. This platform uses disposable cartridges and a laptop-connectable reader platform. **B.) MBio disposable cartridges.** The cartridges are comprised of injection moulded plastic spotted with an array of test antigens.

2.2.29 MBio assay protocol

The ability of free AFB₁ and T-2 toxin to compete with and inhibit, the binding of cognate anti-AFB₁ Fab antibody fragment and anti-T-2 toxin polyclonal antibodies to immobilised AFB₁ and T-2 toxin conjugates, forms the basis of the MBio competition inhibition assay (Figure 2.5). In this assay the MBio LightDeck® cartridge was spotted with 5 and 50 µg/mL of AFB₁-BSA and 50 and 100 µg/mL of T-2 toxin-BSA. Standards of decreasing concentrations of AFB₁ and T-2 toxin or test samples were prepared in PBS. Each standard

or test sample (100 μL) was added to an equal volume of anti-AFB₁ Fab antibody fragment (14 $\mu\text{g/mL}$) or anti-T-2 toxin polyclonal antibody (1/500) diluted using PBS and allowed to incubate at room temperature for 5 minutes. Then, 175 μL of the mixed sample was added to the cartridge and allowed to flow through the fluid channel for 10 minutes. A PBS wash (175 μL) was added for 3.5 minutes. An Alexa-Fluor-647 labelled anti-mouse or rabbit antibody was diluted (1/500) in PBS and 175 μL was added to the cartridge. The detection antibody was allowed to flow through the fluid channel for 5 minutes. A PBS wash (175 μL) was added for 3.5 minutes. Detection was completed by analysing fluorescent intensity using the portable MBio LightDeck® Reader platform.

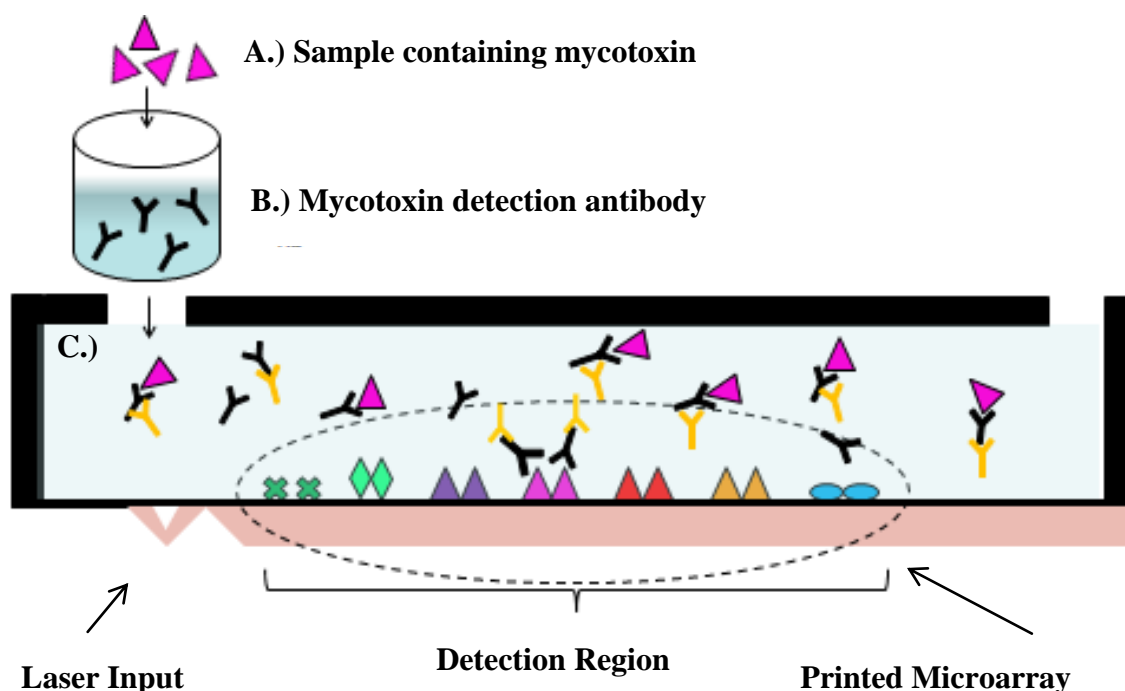


Figure 2.5: MBio Competitive Inhibition Assay Format. A.) A sample containing mycotoxins is incubated with cognate mycotoxin detection antibody. B.) This sample is applied to an MBio disposable cartridge spotted with an array of mycotoxin-conjugates. C.) The mycotoxin and cognate antibody sample are allowed to compete with the mycotoxin-conjugates immobilised on the cartridge surface. An anti-species Alexa Fluor 647-labelled secondary antibody is added and allowed to bind the mycotoxin detection antibody. The resultant fluorescence intensity is read using the optical reader platform.

2.2.29.1 MBio multiplex assay protocol

In this assay the MBio LightDeck® cartridge was spotted with 5 and 50 µg/mL of AFB₁-BSA and 50 and 100 µg/mL of T-2 toxin-BSA. Each test sample (100 µL) was added to 50 µL of anti-AFB₁ Fab antibody fragment (28 µg/mL) and 50 µL of anti-T-2 toxin polyclonal antibody (1/250) diluted using PBS and allowed to incubate at room temperature for 5 minutes. Then, 175 µL of the mixed sample was added to the cartridge and allowed to flow through the fluid channel for 10 minutes. A PBS wash (175 µL) was added for 3.5 minutes. Alexa-Fluor-647 labelled anti-mouse (1/125) and anti-rabbit antibody (1/125) were diluted together in PBS and 175 µL of the mixture was added to the cartridge. The detection antibodies were allowed to flow through the fluid channel for 5 minutes. A PBS wash (175 µL) was added for 3.5 minutes. Detection was completed by analysing fluorescence intensity using the portable MBio LightDeck® Reader platform.

2.2.30 IC₅₀ Value, limit of detection (LOD), dynamic range and coefficient of variance (CV) calculations

Purified recombinant antibody fragments were characterised for the determination of performance criteria and to indicate how sensitively they could bind and interact with their cognate antigens. The evaluation process is critical in understanding how the antibody fragments will function for quantitative analysis of their mycotoxin targets. Antibody sensitivity was evaluated in indirect competitive inhibition assays for calculation of a half maximal inhibitory concentration (IC₅₀) value, which represented the concentration of free toxin that produced 50% inhibition in response. The IC₅₀ value of an antibody was determined using GraphPad Prism 5 statistical software. The software generated a sigmoidal curve by plotting normalised response (mean response (R)/by the mean response at 0 ng/mL of free toxin (R₀)) against the concentration of free mycotoxin in log-scale and using a four parameter logistic function. The relative IC₅₀ value is the parameter 'c' in a 4-parameter logistic model and is the concentration corresponding to a response midway between the estimates of the lower and upper plateaus (Sebaugh, 2011). The equation of the obtained sigmoid curve, using the four parameter logistic function is:

$$y = A + \frac{B - A}{1 + \left(\frac{x}{C}\right)^D} \quad (1)$$

where,

Y = normalised response

x = concentration of free mycotoxin

A = maximum normalized response measured

B = minimum normalized response measured

C = point of inflection

D = slope of linear part of the curve

The IC_{50} is the concentration of free mycotoxin needed to decrease the response to half of its maximum value. This response is calculated as follows:

$$50\% \text{ maximal response} = \text{maximum response} - (0.5 \times (\text{maximum response} - \text{minimum response})) \quad (2)$$

The x-value corresponding to this y-value is the IC_{50} and can be calculated using equation (1).

The limit of detection (LoD) is also an important criterion for qualitative performance. This value represents the lowest amount of analyte in a sample that can be detected and may be used to indicate sensitivity. Determination of the LoD relies on prior identification of the limit of blank (LoB) value. The LoB is the highest value observed in a series of results from a sample that contains no analyte. It is important to note that the LoB refers to an observed test result, while all other limits refer to actual concentrations of the analyte. The LoD is the actual concentration at which an observed test/assay result is likely to exceed the LoB and, therefore, may be declared as detected (The National Committee for Clinical Laboratory Standards, 2004). The LoD is calculated using the LoB and test replicates of a sample known to contain a low concentration of analyte. The mean and standard deviation of the low concentration sample is calculated and the LoD is determined as, LoB plus 1.654 times the standard deviation of a low concentration analyte (Armbruster

and Pry, 2008). The blank produces the highest value in competitive inhibition assays, therefore, equation 1 and 2 are used to determine the LoB and LoD in this format (Tang *et al.*, 2013)

$$LoB = mean\ blank - 1.645(SD\ blank) \quad 3$$

$$LoD = LoB - 1.654(SD\ low\ concentration\ analyte) \quad 4$$

Variability in laboratory measurements are evaluated by determining the coefficient of variation (CV) and represents the extent of variability of an assay. In many laboratories it is well-accepted to summarise the variability of assays not by the standard deviation (SD) but by the CV. In assays, SD generally tends to be proportional to the sample values and therefore, increases or decreases proportionally as the mean increases or decreases. The calculation of the CV by division of the mean removes it as a factor in the variability. The CV is expressed as a percentage of deviation from the mean. The CV therefore, represents a standardization of the SD that permits comparison of variability estimations regardless of the magnitude of analyte concentration, at least throughout most of the working range of the assay. CV is defined as the SD divided by the mean and reported as a percentage. The larger the CV, the greater the error in the assay (Reed *et al.*, 2002; Hanneman *et al.*, 2011).

It is vital to determine the dynamic range of an assay. Maintaining analysis within the dynamic range indicates accurate assay readout which is proportional to the amount of target molecule in the sample. Therefore, in order to stay within the dynamic range of the assay, samples may need to be diluted or concentrated. Failure to stay within the dynamic range of the assay will return spurious results and data (Broadway, 2012). The dynamic range can be defined as the range between the IC₁₀ and IC₉₀ values, at the concentrations of an inhibitor required to reduce the response to 10% and 90% binding, compared to the response when inhibitor is not present (100% binding). The concentration range determined between these two points can be considered the dynamic range of the assay (Campbell *et al.*, 2007).

2.2.31 Extraction of AFB₁ from dried distillers grains with solubles (1)

Extraction of AFB₁ from Dried Distillers Grains with Solubles (DDGs) was based upon a Quick-Easy-Cheap-Effective-Rugged-Safe (QuEChERS). This method was first developed

by Anastassiades and Lehotay (2003) at the USDA/ARS-ERRC in Wyndmoor/Pennsylvania for the determination of pesticide residues in agricultural commodities such as fruits and vegetables. However, it has also proven amenable to the extraction of mycotoxins from various foods in numerous publications. Food commodities are blended or homogenised to increase the available surface area for extraction purposes. Typically magnesium sulphate is added to exceed the saturation point, while sodium chloride controls the polarity of the extraction solvent. Solvent extraction is completed to partition mycotoxins usually between water and the organic solvent of interest, based on their relative solubilities.

AFB₁-contaminated DDGS samples and blank, non-AFB₁-contaminated DDGS samples were extracted. One gram of ground DDGS sample was weighed out into a 50 mL polypropylene tube, to which MgSO₄H₂O (0.2g) and NaCl (0.5g) were added, followed by 10 mL of 60/20/20% (v/v) Acetonitrile/Methanol/Water solution. The sample was then shaken overnight at 300 rpm at room temperature. The following day, the sample was centrifuged at 3,220g (Eppendorf 5810 R, Rotor A-4-62) at 4°C for 10 minutes. The supernatant was transferred to a glass test tube and the organic solvents evaporated under a Nitrogen stream at 40°C. The remaining DDG residue was re-suspended in 300 µL of PBS and collected in a new tube for analysis.

2.2.32 Extraction of AFB₁ from dried distillers grains with solubles (2)

Extraction of AFB₁ from Dried Distillers Grains with Solubles (DDGS) was also completed based upon a modified Quick-Easy-Cheap-Effective-Rugged-Safe (QuEChERS). AFB₁-contaminated DDGS samples and blank, non-AFB₁-contaminated DDG samples were extracted. One gram of ground DDGS sample was weighed out into a 50 mL polypropylene tube, to which 5 mL of 2% (v/v) formic acid was added and allowed to soak for 30 minutes. MgSO₄H₂O (2g) and NaCl (0.05g) was then added to the tube and immediately shaken by hand for 30 seconds. The tube was centrifuged at 3,220g (Eppendorf 5810 R, Rotor A-4-62) at 4°C for 5 minutes. The upper organic phase (2 mL) was collected into a 15 mL polypropylene tube containing MgSO₄H₂O (0.3g) and immediately shaken by hand for 30 seconds. The sample was then centrifuged at 3,220g (Eppendorf 5810 R, Rotor A-4-62) at 4°C for 1 minute. The supernatant was removed to a glass test tube and the organic solvents evaporated under a Nitrogen stream at 40°C. The

remaining DDGS residue was re-suspended in 300 μ L of PBS, vortexed for 2 minutes and collected for analysis.

2.2.33 Rapid extraction of AFB₁ from Dried Distillers Grains with Solubles

Rapid extraction of AFB₁ from Dried Distillers Grains with Solubles (DDGS) was completed. AFB₁ contaminated DDG samples and blank, non-AFB₁ contaminated DDGS samples were extracted. Three grams of ground DDGS sample was weighed out into a 50 mL polypropylene tube to which 9 mL of 20% (v/v) methanol was added and vortexed for 10 minutes. The tube was then centrifuged at 3,220g (Eppendorf 5810 R, Rotor A-4-62) at 4°C for 20 minutes. The supernatant was filtered through Whatman 11 μ M Filter Paper and collected for analysis.

2.2.34 Resuscitation of frozen cell line stocks

Transformed human liver epithelial (THLE-2) cells (See Appendix A for Dublin City University Biological Safety Committee and Environmental Protection Agency approval) and Human hepatoma (HepG2) were obtained from ATCC. A cryovial of the THLE-2 or HepG2 cell lines were thawed at 37°C in a water bath. Appropriate medium, as described in Section 2.1 (Table 2.5) for THLE-2 cells and HepG2 cells (9 mL) pre-warmed to 37°C was added to a 15 mL polypropylene tube. The thawed cells were slowly transferred to the tube. The cells were pelleted at 2,730g (Eppendorf 5810 R, Rotor A-4-62) at 4°C for 5 minutes and the supernatant discarded to remove any cryo-preservant. The cells were re-suspended in appropriate medium (10 mL) pre-warmed to 37°C, were added to a T25 cell culture flask and incubated at 37°C overnight in a 5% CO₂ humidified atmosphere. Cell growth was monitored by examining the cells under a Nikon® Eclipse E400 Microscope. After 24 hours of cell growth, the cells were sub-cultured into a T75 cell culture flask and a sub-culture routine was implemented to ensure optimal cell growth conditions were maintained.

2.2.35 Sub-culturing THLE-2 cells

Transformed human liver epithelial (THLE-2) cells were cultured in LHC-8 medium supplemented with 10% (v/v) fetal bovine serum, 1% (w/v) penicillin-streptomycin, 70 ng/mL phosphor-ethanoalamine and 5 ng/mL epidermal growth factor, at 37°C in a 5% CO₂ humidified atmosphere. When THLE-2 cell monolayers were 80% confluent the old medium was removed and collected in a 15 mL polypropylene tube. The old medium was centrifuged at 2,730g (Eppendorf 5810 R, Rotor A-4-62) at 4°C for 5 minutes with no brake and the supernatant discarded. The collected pellet cells were retained for sub-culture. The adherent cells were washed twice with 5 mL of Dulbecco's PBS. The cell layer was rinsed with 2 mL of 0.05% (w/v) Trypsin + 0.5% (w/v) EDTA solution and incubated at 37°C in a 5% CO₂ humidified atmosphere for 5 minutes or until they were non-adherent to the flask under a Nikon® Eclipse E400 Microscope. The appropriate medium (8 mL) was added to inactivate the trypsinisation process and collected into the 15 mL polypropylene tubes containing the retained THLE-2 cells. The trypsinised cells were then pelleted at 2,730g (Eppendorf 5810 R, Rotor A-4-62) at 4°C for 5 minutes. The supernatant was removed and the pellet re-suspended in 2 mL of appropriate medium and split in a 1:2 ratio. Fresh T75 cell culture flasks were prepared with 16 mL of appropriate medium and 1 mL of the cell suspension added. The cells were incubated at 37°C in a 5% CO₂ humidified atmosphere. Cells were split approximately every 3 days when 80% confluency was achieved.

2.2.36 Sub-culturing HepG2 cells

Human hepatoma (HepG2) cells were cultured in DMEM medium supplemented with 10% (v/v) fetal bovine serum and 1% (w/v) penicillin-streptomycin at 37°C in a 5% CO₂ humidified atmosphere. When HepG2 cell monolayers were 70% confluent the old medium was removed and discarded. The adherent cells were washed twice with 5 mL of Dulbecco's PBS. The cell layer was rinsed with 2 mL of 0.5% (w/v) Trypsin + 5% (w/v) EDTA solution and incubated at 37°C in a 5% CO₂ humidified atmosphere for 5 minutes or until they were non-adherent to the flask under a Nikon® Eclipse E400 Microscope. The appropriate medium (8 mL) was added to inactivate the trypsinisation process and collected into the 15 mL polypropylene tube. The trypsinised cells were then pelleted at 2,730g (Eppendorf 5810 R, Rotor A-4-62) at 4°C for 5 minutes. The supernatant was

removed and the pellet re-suspended in 3 mL of appropriate medium and split in a 1:3 ratio. Fresh T75 cell culture flasks were prepared with 17 mL of appropriate medium and 1 mL of the cell suspension added. The cells were incubated at 37°C in a 5% CO₂ humidified atmosphere. Cells were split approximately every 2 days when 70% confluency was achieved.

2.2.37 Cell counting and Viability Assessment

Cells were counted and viability assessed using trypan blue. Trypan blue is negatively charged and therefore, is excluded from viable cells. In contrast, cells with damaged cell membranes (dead cells) take up the blue stain. Unstained cells were counted by adding 5 µL of cell suspension to 20 µL of sterile water with 25 µL 0.04% (w/v) trypan blue solution and loading the sample onto a Neubauer haemocytometer. The unstained cells were counted within 5 minutes of dye addition under a Nikon® Eclipse E400 Microscope by observing and averaging the number of unstained cells in 5 squares on the haemocytomer. The number of stained cells were also noted and totalled with unstained cells for percentage cell viability.

The number of viable cells/mL in the suspension was calculated as follows:

$$\begin{aligned} \text{Number of cells/mL} \\ = \text{average number of unstained cells} \times \text{dilution factor} \times 10^4 \end{aligned}$$

where,

Average number of unstained cells = the average of 5 squares counted

Dilution factor = 10

10^4 = volume of haemocytomer.

The percentage of viable of cells was calculated as follows:

$$\text{Percentage of viable cells} = \text{total number of } \frac{\text{counted}}{\text{unstained}} \text{ cells}$$

2.2.38 AFB₁ dosage and anti-AFB₁ Fab treatment of THLE-2 cells

AFB₁ stock was prepared in methanol at 5 mg/mL and 10 X stocks of 0.01 or 0.1 ng/mL doses of AFB₁ were prepared in THLE-2 complete culture medium, as described in Section 2.1 (Table 2.5). The cells were treated with AFB₁ for the necessary time-frame (24, 48, 72 and/or 96 hours). The negative control consisted of cells that were cultured in THLE-2 complete culture medium and 0.05% (v/v) methanol (vehicle). Positive control cells were cultured in THLE-2 complete culture medium free of AFB₁. Anti-AFB₁ Fab antibody fragment (0.14 µM) diluted in Dulbeccos PBS was also added for the necessary time-frame (24, 48, 72 and/or 96 hours) to THLE-2 cells AFB₁-dosed, as well as, a negative control (cells cultured with THLE-2 complete culture medium and 0.05% (v/v) methanol (vehicle) and a positive control (cells cultured with THLE-2 complete culture medium free of AFB₁). Dulbeccos PBS alone was also added to THLE-2 cells as a negative control. Media, AFB₁-doses and anti-AFB₁ Fab treatments were refreshed every 24 hours. Incubations and test treatments were completed in triplicate.

2.2.39 AFB₁ dosage and anti-AFB₁ Fab treatment of HepG2 cells

AFB₁ stock was prepared in methanol at 5 mg/mL and 10 X stocks of 0.01 or 0.1 ng/mL doses of AFB₁ were prepared in HepG2 complete culture medium, as described in Section 2.1 (Table 2.5). The cells were treated with AFB₁ for the necessary time-frame (24, 48, 72 and/or 96 hours). As a negative control, cells were cultured in HepG2 complete culture medium and 0.05% (v/v) methanol (vehicle) or as a positive control cells were cultured in HepG2 complete culture medium free of AFB₁. Anti-AFB₁ Fab antibody fragment (0.14 µM) diluted in Dulbeccos PBS was also added for the necessary time-frame (24, 48, 72 and/or 96 hours) to HepG2 cells AFB₁-dosed, as well as, a negative control (cells cultured with HepG2 complete culture medium and 0.05% (v/v) methanol (vehicle) and a positive control (cells cultured with HepG2 complete culture medium free of AFB₁). Media, AFB₁-doses and anti-AFB₁ Fab treatments were re-freshed every 24 hours. Dulbeccos PBS alone was also added to HepG2 cells as a negative control. Media, AFB₁-doses and anti-AFB₁ Fab treatments were refreshed every 24 hours. Incubations and test treatments were completed in triplicate.

2.2.40 Scratch assay

Cells were trypsinized and collected, as described previously in Section 2.2.33. HepG2 cells (0.5×10^6 cells/mL) and THLE-2 cells (0.25×10^6 cells/mL) were re-suspended in 2 mL of appropriate media, as described in Section 2.1 (Table 2.5) and added to a 6-well cell culture plate. The cells were incubated for 24 hours at 37°C in a 5% CO₂ humidified atmosphere until at least 80% confluency was achieved. A 1 mm scrape was placed through the middle of the confluent monolayer of cells using a 200 µL pipette tip. The cells were washed twice with PBS (2 mL) to remove cellular debris and the wash discarded. Fresh appropriate medium (2 mL) was added to each well. THLE-2 and HepG2 cells were treated with 0.01 or 0.1 ng/mL doses of AFB₁ for the necessary time-frame (24, 48, 72 or 96 hours) and/or anti-AFB₁ Fab antibody fragment (0.14 µM) for the necessary time-frame (24, 48, 72 or 96 hours) to examine induced effects on cellular migration. At various time-points (0, 24, 48, 72 and 96 hours), the migration of the wound closure was visualised using an OPTIKA XDS-2FL inverted HBO Fluorescence Microscope. The percent coverage of cells was analysed using RStudio software and a program designed by Ivan McGuire.

2.2.41 MTT cell proliferation assay

The TACS® MTT Cell Proliferation Assay (MTT-CPA) is a sensitive kit for the spectrophotometric measurement of cell proliferation based upon the reduction of the tetrazolium salt, 3,-[4,5-dimethylthiazol-2-yl]-2,5-diphenyl-tetrazolium bromide (MTT). The assay was carried out according to the manufacturer's guidelines. Briefly, THLE-2 (2.5×10^5 cells/mL) and HepG2 (5×10^5 cells/mL) were plated in 100 µL of appropriate culture medium, as described in Section 2.1 (Table 2.5), in a flat-bottomed 96 well culture plate (and a control of media alone) in triplicate. THLE-2 and HepG2 cells were treated with 0.01 or 0.1 ng/mL doses of AFB₁ for the necessary time-frame (24, 48, 72 or 96 hours) and/or anti-AFB₁ Fab antibody fragment (0.14 µM) for the necessary time-frame (24, 48, 72 or 96 hours) to examine induced effects on proliferation. Further experimentation was completed to determine the anti-AFB₁ Fab effects on proliferation. AFB₁ (0.5 ng/mL) and anti-AFB₁ Fab antibody fragment (0.14 µM) were allowed to pre-incubate for 15 minutes prior to addition to the cells. AFB₁ (1 µg/mL) and anti-AFB₁ Fab antibody fragment (0.14 µM), were allowed to pre-incubate for 1 hour to allow binding

equilibrium to be reached, prior to addition to the cells. Anti-AFB₁ monoclonal (Sigma), anti-AFB₁ polyclonal (Sigma), anti-AFB₁ scFv and anti-M3G Fab (0.14 μ M) antibodies or antibody fragments were also added to the cells. The MTT reagent was added (10 μ L) to each well and the plate was incubated at 37°C in a 5% CO₂ humidified atmosphere for 2 hours to allow for visual, intracellular reduction of the soluble yellow MTT to the insoluble purple formazan dye. Detergent reagent (100 μ L) was added to each well to solubilize the formazan dye at room temperature for 24 hours. Absorbance was read at 570 nm (reference wavelength 650 nm) using a Tecan Safire™ 2 plate reader. The control samples consisting of cells alone with media, were subtracted from the triplicate values and averaged. Normalised proliferation of all AFB₁ dosed and/or anti-AFB₁ Fab antibody fragment-treated cells were calculated and compared to cells treated with the relevant vehicle control. Each assay was completed in biological triplicate. Statistical analysis of data was completed using GraphPad Prism version 5 (GraphPad, La Jolla, CA, USA.). Significance was evaluated by 1-way ANOVA analysis and the Newman-Keuls Multiple Comparison Test with P<0.05*; P<0.01** and P<0.001***.

2.2.42 Cytokine analysis

Cytokine testing for IL-8 was completed using R&D duoset ELISA incomplete Kits according to the manufacturer's guidelines with minor changes. Briefly, THLE-2 (10 x 10⁵ cells/mL) and HepG2 (20 x 10⁵ cells/mL) were plated in 200 μ L of appropriate culture medium, as described in Section 2.1 (Table 2.5), in a flat-bottomed 96 well culture plate (and a control of media alone) in triplicate. THLE-2 and HepG2 cells were treated with 0.01 or 0.1 ng/mL doses of AFB₁ for the necessary time-frame (24, 48 or 72 hours) and/or anti-AFB₁ Fab antibody fragment (0.14 μ M) for the necessary time-frame (24, 48 or 72 hours). Supernatants were collected and frozen at -4°C to examine induced effects on cytokine expression. Cytokine ELISAs were completed by diluting the anti-human IL-8 capture antibody (1/120 dilution) in PBS and adding 50 μ L per well on a Nunc MaxiSorp® flat-bottom 96 well plate. The plate was sealed and incubated overnight at room temperature. The following day the plate was washed three times with PBS. The plate was blocked with 1% (w/v) BSA in PBS (300 μ L/well) and incubated at room temperature for 1 hour. The plate was then washed three times with PBS + 0.1% (w/v) BSA and 0.05% (v/v) Tween 20. Thawed supernatants or doubling dilutions of standards (IL-8: 2000 – 0 pg/mL)

in TBS + 0.1% (w/v) BSA and 0.05% (v/v) Tween 20 (50 μ L/well) were added. The plate was sealed and incubated for 2 hours at room temperature. The plate was then washed three times with PBS + 0.1% (w/v) BSA and 0.05% (v/v). Detection antibody was diluted (1/60) in TBS + 0.1% (w/v) BSA and 0.05% (v/v) Tween 20 and (50 μ L/well) was added. The plate was sealed and incubated at room temperature for 2 hours. Streptavidin-HRP was diluted (1/40) in TBS + 0.1% (w/v) BSA and 0.05% (v/v) Tween 20 and (50 μ L/well) was added. The plate was sealed and incubated at room temperature for 20 minutes in the dark. The plate was washed three times with PBS + 0.1% (w/v) BSA and 0.05% (v/v). Then 3,3',5,5'-Tetramethylbenzidine (TMB) (50 μ L/well) was added, the plate was sealed and incubated at room temperature for 20 minutes in the dark. The reaction was stopped by adding 50 μ L of 1 M HCl to each well and the plate gently tapped to ensure thorough mixing. AFB₁ dosed and/or anti-AFB₁ Fab antibody fragment-treated cells were compared to cells treated with the relevant vehicle control. Each assay was completed in biological triplicate. Absorbance was read at 450 nm using a Tecan Safire™ 2 plate reader. Statistical analysis of data was completed using GraphPad Prism version 5 (GraphPad, La Jolla, CA, USA.). Significance was evaluated by 1-way ANOVA analysis and the Newman-Keuls Multiple Comparison Test with $P < 0.05^*$; $P < 0.01^{**}$ and $P < 0.001^{***}$.

2.2.43 Long term storage of cells

Cells were trypsinised and collected as previously described in Section 2.2.29. Cells were diluted to 2×10^6 cells/mL in 95% (v/v) in an appropriate medium and 5% (v/v) dimethyl sulfoxide in cryovials. The aliquots were transferred to a Nalgene® Mr. Frosty container and placed at -80°C overnight for slow freezing. The following day the cryovials were placed in liquid nitrogen dewar flasks for long-term storage.

Chapter 3

Generation of avian recombinant anti-T-2 toxin scFv antibody fragments

3.1.Introduction

T-2 toxin is considered a mycotoxin of importance due to its prevalence in the United States of America and Europe. Exposure to T-2 toxin causes severe effects including inflammation of the skin, vomiting, damage to hematopoietic, necrosis in the oral cavity, bleeding from the nose, mouth, and vagina, and central nervous system disorders (Bennett and Klich, 2003). Presently, the gold-standard methods for mycotoxin detection and analysis centre on expensive, laboratory-based chromatographic methods which require time for analysis and experienced operators. Therefore, there is a need for specific and sensitive methods that allow the ‘point-of-site’ detection of T-2 toxin in food and animal feed. Recently, biosensors have become prominent due to their perceived applicability in ‘sample-to-answer’ analyses, high-throughput capability, rapid operation time and portability. Biosensors are often categorized by their biological recognition element and when antibodies or antibody fragments are applied in this role, the biosensor is termed an immunosensor (Moran *et al.*, 2016). The advent of recombinant antibody generation technology has given rise to novel formats such as single chain fragment variables (scFv) and antigen binding fragments (Fab) among others (Moran *et al.*, 2018). The development of recombinant antibody fragments, which can be effectively incorporated into immunoassays for ‘in-field’ detection, present a compelling solution to ‘point-of-site’ mycotoxin analysis that can help reduce dependency on slow and costly lab-based analysis and ensure food safety for consumers.

The aim of the research described in this chapter is to develop and select a recombinant antibody fragment against T-2 toxin through library building, phage display and panning experiments. The intended use for the anti-T-2 toxin scFv antibody fragment was for incorporation in an MBio multiplex optical-planar waveguide biosensor device to detect T-2 toxin in contaminated food or animal feed samples. Specific antibody fragments were required for this purpose, however, their selection proved challenging. Therefore, the application of a commercial anti-T-2 polyclonal antibody was also examined for sensitive T-2 toxin detection.

Library building, phage display and panning are described for the isolation of anti-T-2 toxin scFv antibody fragments in this section. This chapter focuses on the successful generation of a recombinant library from RNA (isolated from an immunised host),

reversed transcribed into cDNA and subjected to polymerase chain reaction (PCR) to amplify antibody variable heavy and variable light gene sequences that can be linked together. Subsequently, through phage display, the amplified linked sequence of the antibody construct was readily inserted into phage-coat particle-sequences and amplified in bacterial cells. This enabled the phage to ‘display’ the antibody fragment on the phage coat surface while containing the genetic sequence for the antibody inside, resulting in a link between genotype and phenotype. The antibody fragment-displaying phage were then selected using panning strategies which enriched for T-2 toxin binders (Barbas *et al.*, 2001). To ensure the selection of specific anti-T-2 toxin binders, the development of stable mycotoxin-conjugates was crucial to certify that the correct target was being bound during screening. Therefore, this chapter also discusses the process of chemically conjugating T-2 hapten molecules to Ovalbumin (OVA) and Bovine Serum Albumin (BSA). The conjugation of T-2 toxin to OVA and BSA was confirmed and monitored by indirect competitive inhibition ELISA to ensure functional conjugates were in use for screening procedures.

Panning strategies using the T-2 toxin-OVA conjugate elicited a response primarily against OVA, which was confirmed by a lack of response in OVA-depletion panning experiments. Implementation of the T-2 toxin-BSA conjugate for panning yielded a low response from anti-T-2 toxin scFv antibody fragments indicating that the scFv library was not specific for its T-2 toxin target. In the absence of a selected anti-T-2 toxin scFv antibody fragment, a commercial anti-T-2 toxin polyclonal antibody was tested in indirect ELISA and indirect competitive inhibition ELISA. This antibody proved sensitive, with an IC_{50} value of 8.5 ng/mL and limit of detection of 5.8 ng/mL, and therefore, was selected for analysis of T-2 toxin using the MBio detection system described in Chapter 4.

3.2 Results

3.2.1 Evaluation criteria of T-2 toxin conjugates

To assess the integrity of the mycotoxin-conjugates synthesised ‘in-house,’ as described in Section 2.1.2, an indirect competitive inhibition ELISA was completed. This technique was used to determine if T-2 toxin was successfully conjugated to the carrier proteins Ovalbumin (OVA) and Bovine Serum Albumin (BSA) and, to ensure their usefulness for screening libraries of recombinant antibody fragments. In accordance with Sanders (2014), the T-2 toxin-conjugates were considered functional for screening protocols if the absorbance ‘0’ (no competitor toxin) value exceeded 1 and if decreasing absorbance values were obtained in the presence of increasing standard mycotoxin concentrations. The indirect competitive inhibition ELISA was completed, as described in Section 2.2.27 and involved coating varying concentrations of the T-2 toxin conjugate on a Nunc MaxiSorp® flat-bottom 96 well plate and incubating a range of free mycotoxin concentrations with commercial anti-T-2 toxin polyclonal antibody. The cognate antibody bound the free mycotoxin in each sample, and with increasing concentrations of free mycotoxin, the antibody was inhibited differentially from binding the immobilised mycotoxin-conjugate (e.g. a high concentration of free mycotoxin saturated the cognate antibody preventing it from binding to the immobilised mycotoxin-conjugate, whilst, a low concentration of free mycotoxin did not saturate the cognate antibody and the remaining antibody was available to bind the immobilised mycotoxin-conjugate). A HRP-labelled secondary antibody was added, developed with 3,3',5,5'-Tetramethylbenzidine (TMB) and the absorbance read at 450 nm using a Tecan Safire™ 2 plate reader.

The response produced by the antibody binding to the immobilised mycotoxin-conjugate was inversely proportional to the concentration of free mycotoxin used to inhibit the commercial anti-T-2 toxin polyclonal antibody. A decreasing response could only be elicited if the mycotoxin was directly conjugated to the carrier protein and immobilised on the plate.

3.2.1.1 Evaluation of T-2 toxin-OVA conjugate

A commercial anti-T-2 toxin polyclonal antibody obtained from a rabbit immunised with a T-2 KLH conjugate (Sigma Immuno Chemicals – T-0534) was incubated with increasing concentrations of free T-2 toxin (0 - 50 ng/mL) and was then applied to a plate coated with a range of decreasing concentrations of T-2 toxin-OVA conjugate (5, 2, 1 and 0.2 µg/mL). A range of free T-2 toxin and immobilised T-2 toxin-OVA concentrations were used to indicate if an absorbance '0' (no competitor toxin) value in excess of 1 and a decreasing absorbance response could be achieved. This occurs when the free T-2 toxin binds, and, reduces availability of the anti-T-2 toxin polyclonal antibody for immobilised T-2 toxin-OVA interaction. The absorbance results in Figure 3.1 indicate a decreasing response was elicited by the binding of inhibited anti-T2 toxin polyclonal antibody, which decreased when applied to the immobilised T-2 toxin-OVA at all concentrations. The result also showed that when 5, 2 and 1 µg/mL of T-2 toxin-OVA were immobilised, the absorbance '0' (no competitor toxin) value exceeded 1. Together these results indicated that T-2 toxin was successfully conjugated to its protein carrier and was functional for screening purposes at concentrations of 5, 2 and 1 µg/mL. Polyclonal antibodies are not ideal for competitive inhibition ELISA as they are a collection of immunoglobulin molecules that react against a specific antigen, each identifying a different epitope, therefore, the response elicited by their binding to a target (T-2 toxin or T-2 toxin-OVA) may be heterogenous and not represent true competition (Hanley *et al.*, 1995; Lipman *et al.*, 2005). However, commercial monoclonal anti-T-2 toxin antibodies are not readily available and, therefore, anti-T-2 toxin polyclonal antibody was deemed useful for testing the T-2 toxin-OVA conjugate. The total protein concentration of T-2 toxin-OVA (0.96 mg/mL) was calculated using the Pierce™ BCA Protein Assay Kit, as described by the manufacturer's guidelines (Section 2.2.4.)

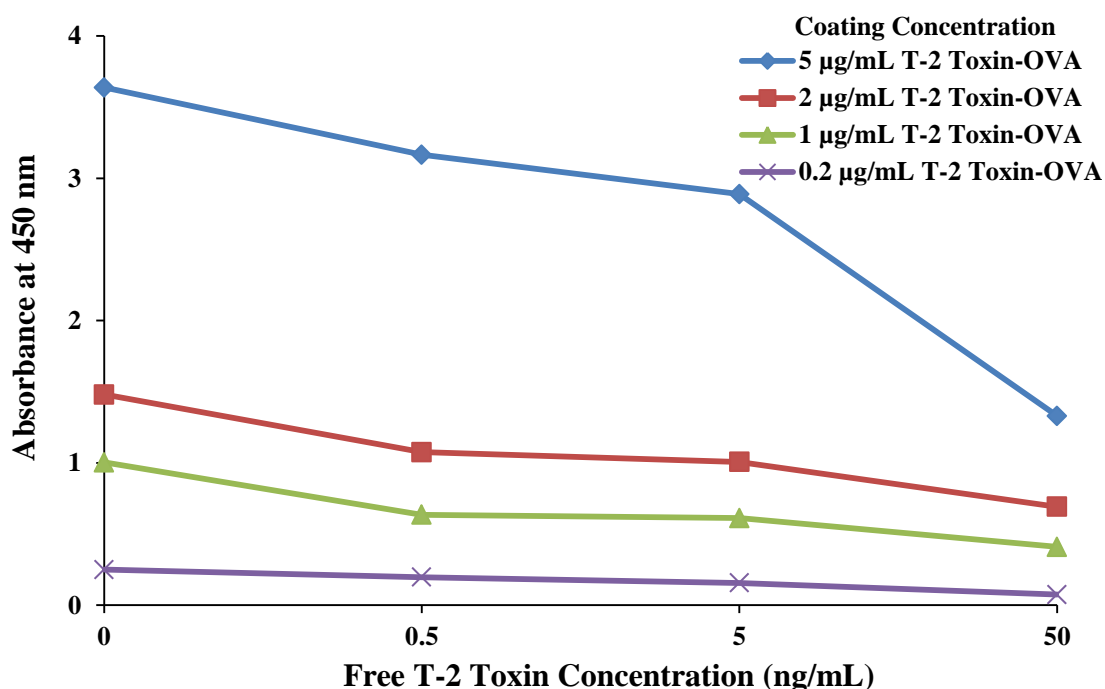


Figure 3.1: Competitive inhibition ELISA with varying dilutions of T-2 toxin-OVA and free T-2 toxin against a 1/500 dilution of anti-T-2 toxin polyclonal antibody. T-2 toxin-OVA (0.96 mg/mL) was diluted to 5, 2, 1 and 0.2 µg/mL with PBS. Free T-2 toxin (0, 0.5, 5 and 50 ng/mL) was prepared in PBST with 5% (v/v) methanol and allowed to incubate with a 1/500 dilution of anti-T-2 toxin whole antiserum polyclonal antibodies. The mixed samples were applied to the T-2 toxin-OVA coated plate. A HRP-labelled anti-rabbit secondary antibody diluted 1/10,000 in PBST with 1% (w/v) Milk Marvel was added, followed by TMB HRP substrate. The reaction was stopped with 10% (v/v) HCl and absorbance was read at 450 nm using a Tecan Safire™ 2 plate reader. Experiments were performed with three replicates and results averaged (n = 1).

3.2.1.2 Evaluation of T-2 toxin-BSA conjugate

A commercial anti-T-2 toxin polyclonal antibody was incubated with increasing concentrations of free T-2 toxin (0 - 50 ng/mL) and was then applied to a plate coated with a range of decreasing concentrations of T-2 toxin-BSA conjugate (10, 2 and 0.66 µg/mL). A range of free inhibitor T-2 toxin and immobilised T-2 toxin-BSA concentrations were used to indicate if an absorbance '0' (no competitor toxin) value in excess of 1 and a decreasing absorbance response could be achieved. The absorbance results in Figure 3.2 indicate that when 10 µg/mL of T-2 toxin-BSA was immobilised, a decreasing response was elicited by the binding of inhibited anti-T2-toxin polyclonal antibody and the absorbance '0' (no competitor toxin) value exceeded 1. Together, these results indicated that T-2 toxin was successfully conjugated to its protein carrier and was functional for screening purposes at this concentration (10 µg/mL). The total protein concentration of T-2

toxin-BSA (2.1 mg/mL) was calculated using the Pierce™ BCA Protein Assay Kit, as described by the manufacturer's guidelines (Section 2.2.4).

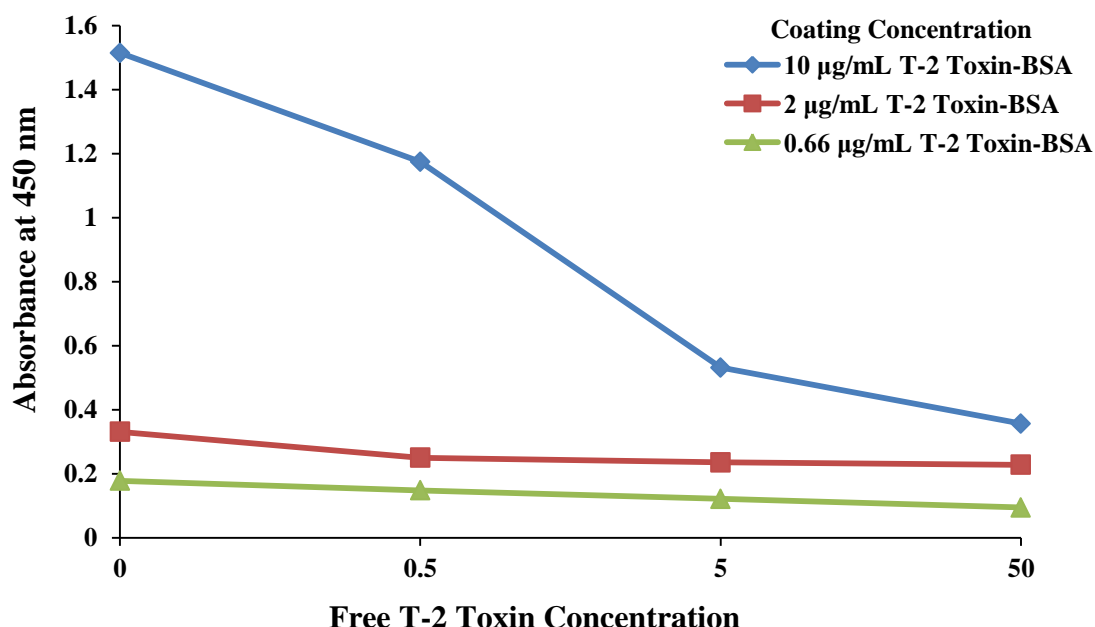


Figure 3.2: Competitive inhibition ELISA with varying dilutions of T-2 Toxin-BSA and free T-2 toxin against a 1/500 dilution of anti-T-2 toxin polyclonal antibody. T-2 toxin-BSA (2.1 mg/mL) was diluted to 10, 2 and 0.66 µg/mL with PBS. Free T-2 toxin (0, 0.5, 5 and 50 ng/mL) was prepared in PBST with 5% (v/v) methanol and allowed to incubate with a 1/500 dilution of anti-T-2 toxin whole antiserum polyclonal antibodies. The mixed samples were applied to the T-2 toxin-BSA-coated plate. A HRP-labelled anti-rabbit secondary antibody diluted 1/10,000 in PBST with 1% (w/v) Milk Marvel was added, followed by TMB HRP substrate. The reaction was stopped with 10% (v/v) HCl and absorbance was read at 450 nm using a Tecan Safire™ 2 plate reader. Experiments were performed with three replicates and results averaged (n = 1).

3.2.2 Evaluation of avian RNA integrity

RNA isolated from the bone marrow and the spleen of a Leghorn chicken immunised with T-2 toxin-KLH and stored at -80°C by Dr. Soujanya Ratna Edupuganti (2013) and also described by Edupuganti *et al.*, 2013, was used for cDNA synthesis as previously described in Section 2.2.5. The integrity of the isolated RNA was investigated before completing cDNA synthesis by running the isolated RNA on a 1% (w/v) agarose gel and by reading absorbance at 260 nm using a NanoDrop™ND1000.

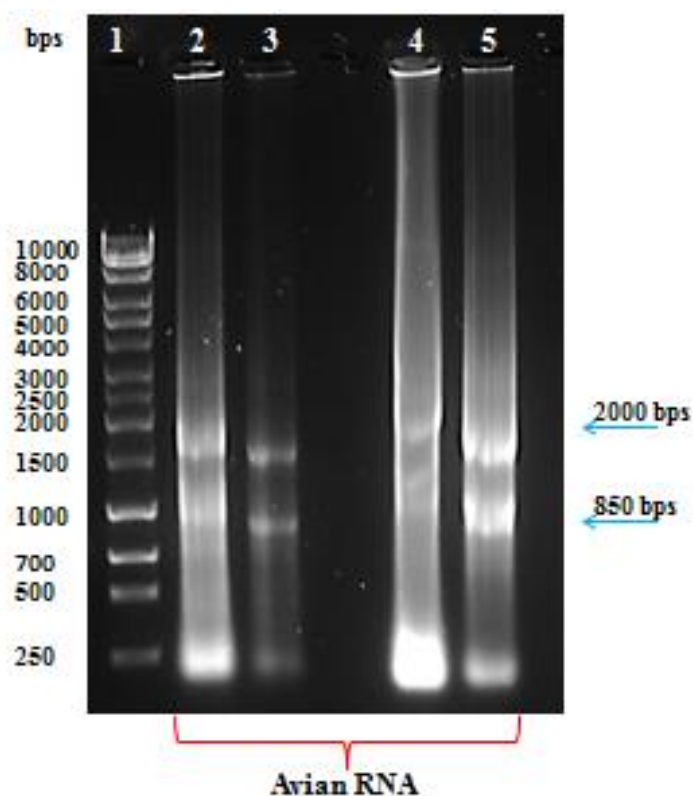


Figure 3.3: Agarose gel (1% (w/v)) analysis of avian bone marrow and spleen RNA. Major ribosomal RNA species can be seen at approximately 2000 bps and 850 bps. (Lane 1: 1 Kb DNA Ladder; Lane 2: T-2 Bone Marrow RNA (neat); Lane 3: T-2 Bone Marrow RNA (1/5); Lane 4: T-2 Spleen RNA (neat); Lane 5: T-2 Spleen RNA (1/5)).

The RNA previously harvested from the avian bone marrow and spleen was applied to a 1% (w/v) agarose gel, neat and at a 1 in 5 dilution in molecular grade water. Ribosomal RNA is expected at approximately 2000 bps and 850 bps and these bands can be seen in all fractions in Figure 3.3. This indicated the RNA samples had not degraded and were suitable for use in cDNA synthesis. Furthermore, the concentration necessary for successful cDNA synthesis was attained and the integrity of the RNA was deemed acceptable according to the ratio criterion $A_{260}/A_{280} = 1.6 - 1.9$ set out by Barbas *et al.* (2001) summarised in Table 3.1.

Table 3.1: Concentration and integrity of avian RNA from bone marrow and spleen.

RNA Type	RNA Concentration (ng/μL)	Acceptable Levels (ng/μL)	RNA A260/280	Acceptable Levels A260/280
Avian T-2 Bone Marrow	2,940	1 - 4,000	1.7	1.6 - 1.9
Avian T-2 Spleen	4,983	5 - 10,000	1.6	1.6 - 1.9

3.2.3 Anti T-2 toxin cDNA synthesis from avian RNA

A SuperScript® III First-Strand Synthesis System RT-PCR Kit was used, as described by the manufacturer's guidelines, to convert the avian RNA into cDNA. The concentration and integrity of the cDNA synthesised was determined by reading absorbance at 260 nm using a NanoDrop™ND1000 and was deemed acceptable according to criteria set out by Barbas *et al.* summarised in Table 3.2. This indicated that the required quantity of cDNA was generated, was of good integrity and was suitable for the production of an avian scFv library.

Table 3.2: cDNA Synthesis from avian bone marrow and spleen RNA.

cDNA Type	cDNA concentration (ng/μL)	Acceptable Levels (ng/μL)	cDNA A260/280	Acceptable Levels A260/280
Avian T-2 Bone Marrow	1,224	1,000	1.85	1.6 - 1.9
Avian T-2 Spleen	1,726	1,000	1.87	1.6 - 1.9

3.2.4 Bone marrow V_H and V_L gene sequence amplifications and generation of SOE-PCR product

Bone marrow V_H and V_L gene sequence amplifications for the construction of scFv antibody fragment libraries with long linkers were completed using synthesised cDNA, avian long linker primers and MyTaq polymerase, as described in Sections 2.2.5 – 2.2.7. The primers used for V_H and V_L amplification create identical linker sequences that serve as the overlap for the extension of the full-length product. CSCVHo-FL (long-linker) sense primers and CSCG-B reverse primers were used to amplify V_H sequences from the avian cDNA. The sense primer has a tail sequence that was used as the linker sequence for Splice-by-Overlap Extension polymerase chain reaction (SOE-PCR). The reverse primer has a tail sequence containing a *Sfi*I site which was recognised by the reverse extension primer during SOE-PCR. CSCVK sense primers and CKJo-B reverse primers were used to amplify V_L sequences from avian cDNA. CSCVK has a 5' sequence tail containing a *Sfi*I site which was recognised by the reverse extension primer during SOE-PCR whilst the reverse primer provided the linker sequence for overlap extension. Products at ~400 bps for V_H long linker reactions and, at ~350 bps for V_L reactions were expected from these amplifications. These bands are clearly visible in Figure 3.4: (A) and (B). Other possible V_H and V_L amplifications can be seen higher on the gels which were later removed through gel purification. Negative controls indicate the absence of V_H and V_L amplification, however, primer dimers can be seen below ~200 bps. The 400 bp band was excised, purified and found to have 6,520.2 ng total DNA for V_H gene sequence amplification. The band at ~350 - 400 bps was excised, purified, quantified and found to have 13,104 ng total DNA for V_L gene sequence amplification.

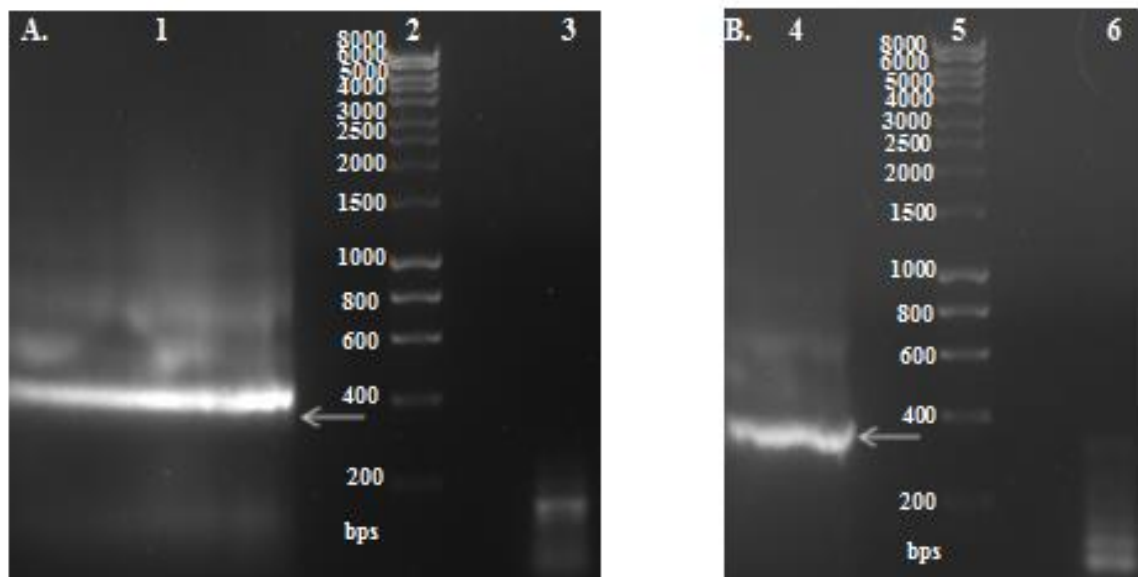


Figure 3.4: (A) Bone marrow V_H and (B) V_L gene amplification. 20X V_H chain gene amplifications can be seen at approximately 400 bps. 20X V_L chain gene amplifications can be seen at approximately 350 bps. ((A) Lane 1: V_H product; Lane 2: 1 Kb DNA Ladder; Lane 3: Negative Control. (B) Lane 4: V_L product; Lane 5: 1 Kb DNA Ladder; Lane 6: Negative Control).

Equimolar concentrations of purified bone marrow V_H and V_L gene amplifications, avian overlap extension primers and MyTaq polymerase were used to produce a bone marrow SOE-PCR product, as described in Section 2.2.8. The primers used amplified the V_H and V_L genes with an overlap linker serine-glycine sequence (GGSSRSSSSGGGSGGGG) creating a full-length fusion product. An SOE-PCR product at ~750 bps was expected from these amplifications. This band is clearly visible in Figure 3.5. A band can be seen at ~400 bps which may be residual V_H or V_L product and this band was removed for SOE-PCR product purification. A negative control indicates the absence of SOE-PCR product amplification. The band at ~750 bps was excised, purified, quantified and found to have 4,098 ng total DNA. The yield of bone marrow SOE-PCR product was deemed suitable for restriction digestion and ligation into the pComb3xSS vector.

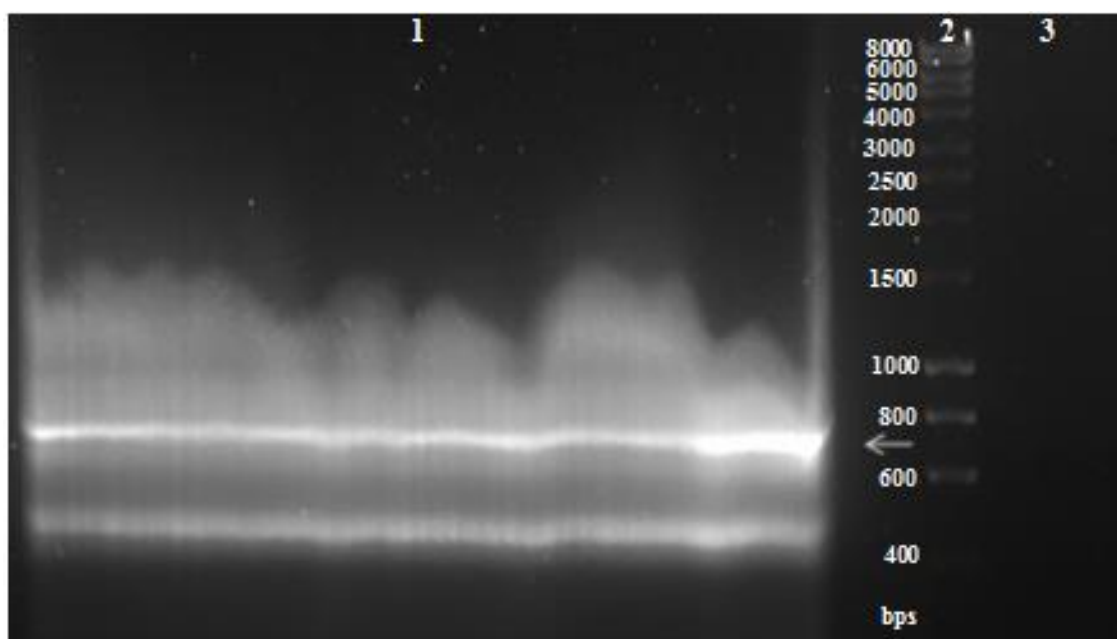


Figure 3.5: Bone marrow V_H and V_L chain SOE-PCR product. A 20X SOE-PCR product amplification can be seen at approximately 750 bps. (Lane 1: SOE-PCR Product; Lane 2: 1 Kb DNA Ladder; Lane 3: Negative Control).

3.2.5 Spleen V_H and V_L gene sequence amplifications and generation of SOE-PCR product.

Spleen V_H and V_L gene sequence amplifications for the construction of scFv libraries with long linkers were completed using synthesised cDNA, avian long linker primers and MyTaq polymerase, as described in Sections 2.2.5 – 2.2.7. The same primers described for bone marrow V_H and V_L were used to create identical linker sequences that serve as the overlap for the extension of the full-length spleen SOE-PCR product. Products at ~400 bps for V_H long linker reactions and at ~350 bps for V_L reactions were expected from these amplifications. These bands are clearly visible in Figure 3.6: (A.) and (B.). Other possible V_H and V_L amplifications can be seen higher on the gels which are excised during gel purification steps. Negative controls indicate the absence of V_H and V_L amplifications, however, primer dimers can be seen below ~200 bps in Figure 3.6: (B.). The 400 bps band was excised, purified and quantified at 6,380 ng total DNA for V_H gene sequence amplification. The band at ~350 - 400 bps was excised, purified and quantified at 12,261 ng total DNA for V_L gene sequence amplification.

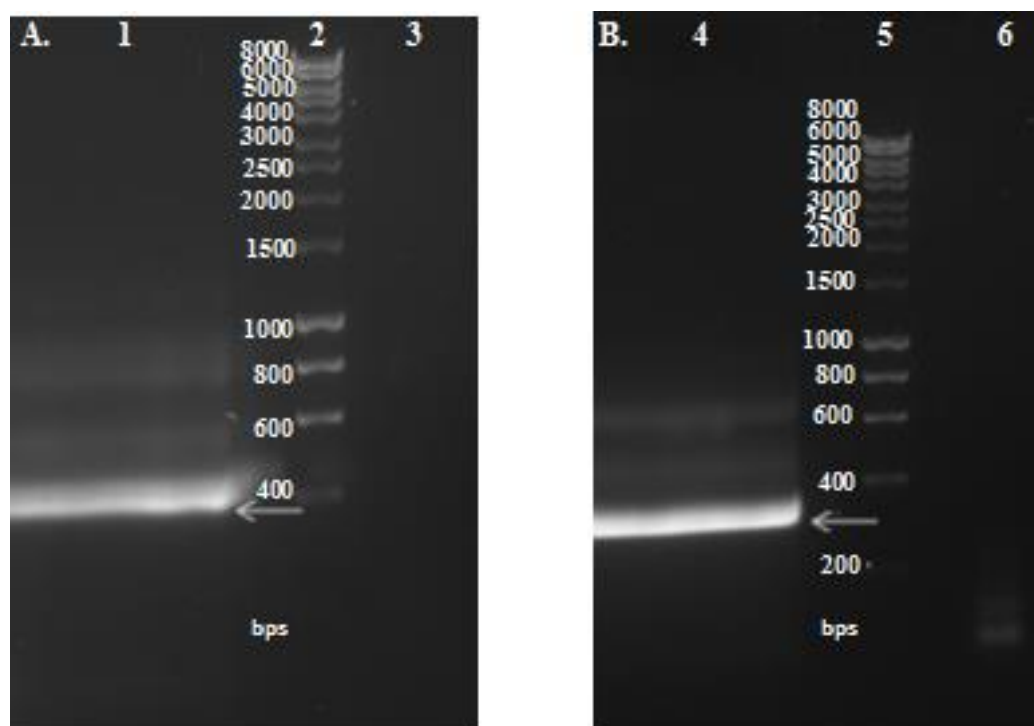


Figure 3.6: (A) Spleen V_H and (B) V_L gene amplification. A 20X V_H chain gene amplification can be seen at approximately 400 bps. V_L chain gene amplifications can be seen at approximately 350 bps. ((A) Lane 1: V_H product; Lane 2: 1 Kb DNA Ladder; Lane 3: Negative Control. (B) Lane 4: V_L product; Lane 5: 1 Kb DNA Ladder; Lane 6: Negative Control).

Equimolar concentrations of purified spleen V_H and V_L gene amplifications, avian overlap extension primers and MyTaq polymerase were used to produce a spleen SOE-PCR product, as described in Section 2.2.8. The primers allowed amplification of the V_H and V_L genes with an overlap linker serine-glycine sequence (GGSSRSSSSGGGGSGGGG) for a full-length fusion product. An SOE product at ~750 bps was expected from these amplifications. This band is clearly visible in Figure 3.7. A negative control indicates the absence of SOE product amplification. The band at ~750 bps was excised, purified, quantified and found to have 4,885 ng total DNA. The yield of spleen SOE product was deemed suitable for digest and ligation into the pComb3XSS vector.

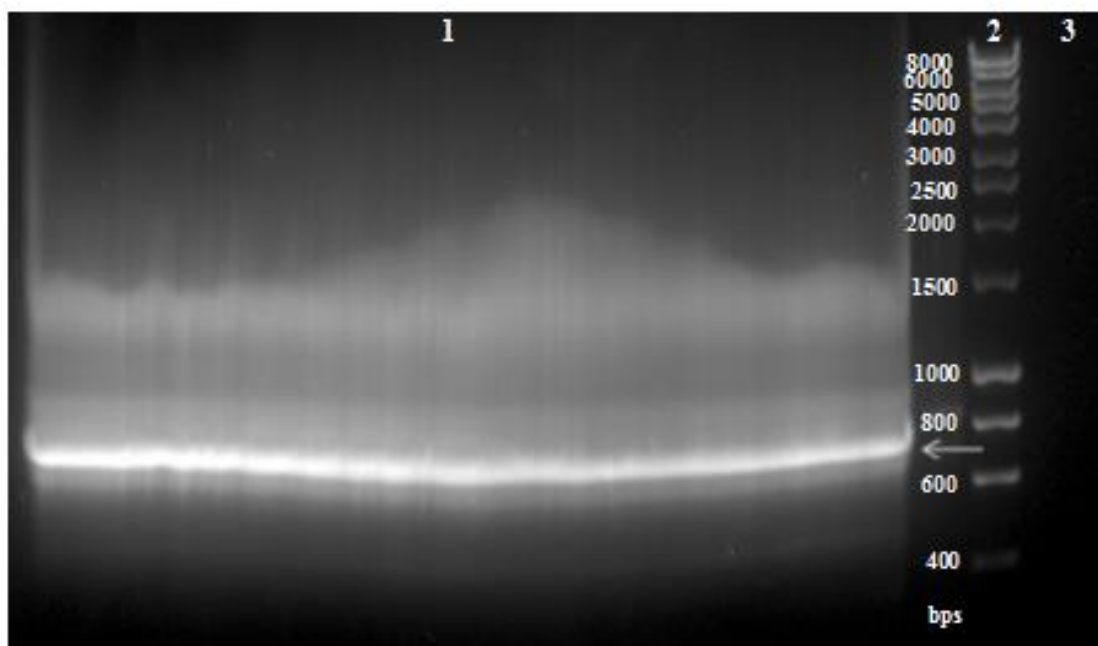


Figure 3.7: Spleen V_H and V_L chain gene SOE-PCR product. 20X SOE-PCR product gene amplification can be seen at approximately 750 bps. (Lane 1: SOE-PCR Product; Lane 2: 1 Kb DNA Ladder; Lane 3: Negative Control).

The purified bone marrow and spleen SOE-PCR products (1 in 10 dilution) can be clearly seen at a correct band size of ~750 bps in Figure 3.8. and, therefore, these were digested for ligation into the pComb3xSS vector.

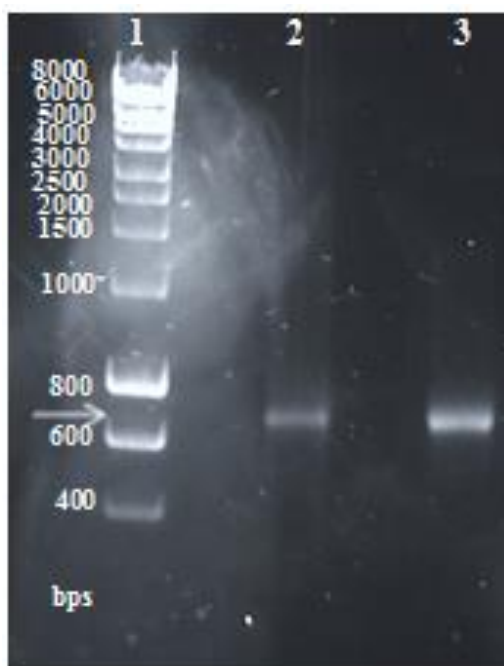


Figure 3.8: Purified bone marrow and spleen V_H and V_L chain gene SOE-PCR product. SOE-PCR product gene amplification can be seen at approximately 750 bps. (Lane 1: 1 Kb DNA Ladder; Lane 2: Bone Marrow SOE-PCR Product (1/10); Lane 3: Spleen SOE-PCR Product (1/10)).

3.2.6 Restriction digestion of pComb3xSS vector, and anti-T-2 toxin purified bone marrow and spleen SOE-PCR products

Triple restriction digestion of the pComb3xSS vector was completed with *Sfi*I, *Xba*I and *Xho*I enzymes and the vector was then treated with Antarctic phosphatase, as described in Section 2.2.9. The pComb3xSS vector contains a double stuffer fragment between two *Sfi*I sites. Digestion with *Sfi*I can result in a significant amount of intact stuffer fragment or undigested vector, which can cause library contamination, therefore, further digestion with *Xba*I and *Xho*I was necessary to fully degrade the stuffer fragment. The digested vector was then Antarctic phosphatase treated to de-phosphorylated exposed, digested ends by catalysing the removal of 5' phosphate from the DNA. Phosphatase-treated fragments lack the 5' phosphoryl termini required by ligase, thus preventing the digested vector from self-ligation in the presence of T-4 Ligase during insert ligation. Bone marrow and spleen SOE-PCR products were digested with *Sfi*I enzyme for complementary insertion and ligation into the *Sfi*I digested vector.

Figure 3.9 shows purified bone marrow SOE-PCR product (1,692 ng) and spleen SOE-PCR product (3,720 ng) successfully digested at ~800 bps. Triple digested, Antarctic phosphatase treated and purified vector (2170 ng) can be seen at ~3200 bps. The purified bone marrow and spleen SOE-PCR products and the purified digested vector were ligated using T-4 Ligase and transformed into *E. coli*, as described in Section 2.2.10 and 2.2.11, respectively. The electroporated samples from spleen and bone marrow were combined in a single 50 mL tube, allowed to recover, helper-phage added and incubation allowed to proceed overnight. The generated library was then subjected to 4 rounds of panning, as described in Section 2.2.12.

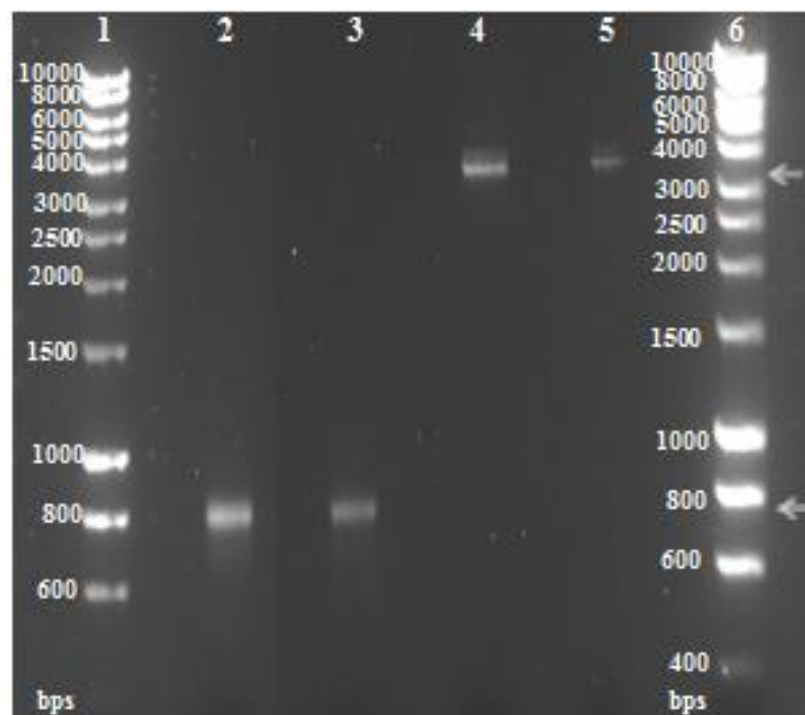


Figure 3.9: Purified restriction digested bone marrow and spleen SOE-PCR products and pComb3xSS vector. Digested SOE-PCR products can be seen at approximately 800 bps. Triple Digested pComb3xSS vector can be seen at approximately 3200 bps. (Lane 1: 1 Kb DNA Ladder; Lane 2: Digested Bone Marrow SOE-PCR Product; Lane 3: Digested Spleen SOE-PCR Product; Lane 4: Digested pComb3xSS vector (neat); Lane 5: Digested pComb3xSS vector (1/5); Lane 6: 1 Kb DNA Ladder).

3.2.7 Phage display and panning of anti-T-2 toxin library against T-2 toxin-OVA

The digested bone marrow and spleen V_H and V_L SOE-PCR constructs amplified from avian cDNA provide the engineered genetic material for generation of the scFv antibody fragment of interest. The *Sfi*I digested constructs were cloned into *Sfi*I digested pComb3xSS vector by ligation. The ligated bone marrow and spleen products were transformed into electrocompetent *E. coli* cells, combined together and allowed to grow overnight to express and produce a diverse library of multiple copies of the scFv antibody fragment. The following day the cultures were infected with M13 phage and allowed to grow overnight to initiate the process of phage display and panning, as described in Section 2.2.12. The first round of panning was completed by coating a Nunc MaxiSorp® flat-bottom 96 well plate with T-2 toxin-OVA at the concentrations outlined in Table 3.3. Phage were collected, applied to the plate, subjected to vigorous washing, eluted and used to re-infect *E. coli* cultures which were grown overnight. The following day the process was repeated. A library count of inputs and outputs was calculated each day by plating *E. coli* cells on carbenicillin-selective agar prior to and after phage infection. The size of the anti-T-2 toxin scFv library is indicated in Table 3.4 and should be a minimum of 1×10^7 , as described by Barbas *et al.* (2001).

Table 3.3: Panning strategy for anti-T-2 toxin scFv library against T-2 toxin-OVA

Round of Panning	T-2 Toxin-OVA Concentration (µg/mL)	Number of Wells	Number of Washes	Culture Volume (mL)
1	50	8	5X PBST	200
2	25	4	8X PBST	200
3	12.5	4	10X PBST	200
4	5	4	12X PBST	200

Table 3.4: Anti-T-2 toxin scFv library size after 4 rounds of panning

Round of Panning	Input (cfu/mL)	Output (cfu/mL)
0	$>1 \times 10^{11}$	2.9×10^6
1	3.84×10^{14}	1×10^6
2	1.4×10^{14}	6.1×10^5
3	8.16×10^{13}	3.2×10^5
4	6×10^{14}	1.1×10^5

3.2.8 Polyclonal phage ELISA screening against T-2 toxin-OVA and OVA

Polyclonal phage ELISA was completed, as described in Section 2.2.12, and used to select for anti-T-2 toxin-specific scFv antibody fragments. T-2 toxin is a hapten and must be conjugated to a larger carrier protein for screening methods. T-2 toxin was conjugated to Ovalbumin (OVA), as previously described in Section 2.2.2. To ensure that the response elicited by the anti-T-2 toxin phage library was specific against T-2 toxin and not OVA, polyclonal phage ELISA was completed against T-2 toxin-OVA and OVA. Phage collected from each round of panning were tested against 100 μ L per well of 2 or 5 μ g/mL of T-2 toxin-OVA (diluted in PBS) and 5 μ g/mL of OVA (diluted in PBS) coated on a Nunc MaxiSorp® flat-bottom 96 well plate. The response observed should increase with progressive rounds of panning as enrichment occurs for specific anti-T-2 toxin phage displaying scFv antibody fragments when screened against the T-2 toxin-OVA target. Similarly, if the response observed for OVA increases then selection of anti-OVA phage displaying scFv antibody fragments may be evident. Figure 3.10 indicates enrichment for both T-2 toxin-OVA and OVA in Pan 4. This result suggests that the pool of anti-T-2 toxin phage selected in Pan 4 contained antibodies enriched for both T-2 toxin and for the conjugated OVA protein. The experiment was repeated with phage diluted 1 in 3 in PBST with 1% (w/v) Milk Marvel and additional carrier proteins as controls to determine if specific enrichment for T-2 toxin was occurring. The results in Figure 3.11 indicate enrichment in Pan 4, however, again this was significant for OVA protein on its own, as well as T-2 toxin. This experiment included a positive control, KLH, and a negative control, Bovine Serum Albumin (BSA). KLH was used as the protein carrier for the T-2 toxin immunogen and, therefore, the avian immune response produces a repertoire of antibodies against KLH, as well as, the T-2 toxin target. The response decreased for KLH with successive rounds of panning as specific anti-KLH scFv antibody fragments, or, non-specific anti-T2 scFv were washed away. A low BSA response was elicited as expected. BSA was not previously introduced into this experiment and therefore, a response against BSA should not occur. The repeated polyclonal phage ELISA indicated that the panning process had been successful, as anti-KLH binders had been depleted and enrichment was evident in Pan 4. However, it remained unclear if enrichment for T-2 toxin or OVA had occurred. Polyclonal phage represents a pool of multiple scFv-producing clones, therefore, to determine if the scFv library contained specific clones against T-2 toxin, monoclonal

ELISA was used to examine individual scFv antibody fragments expressed by single clones.

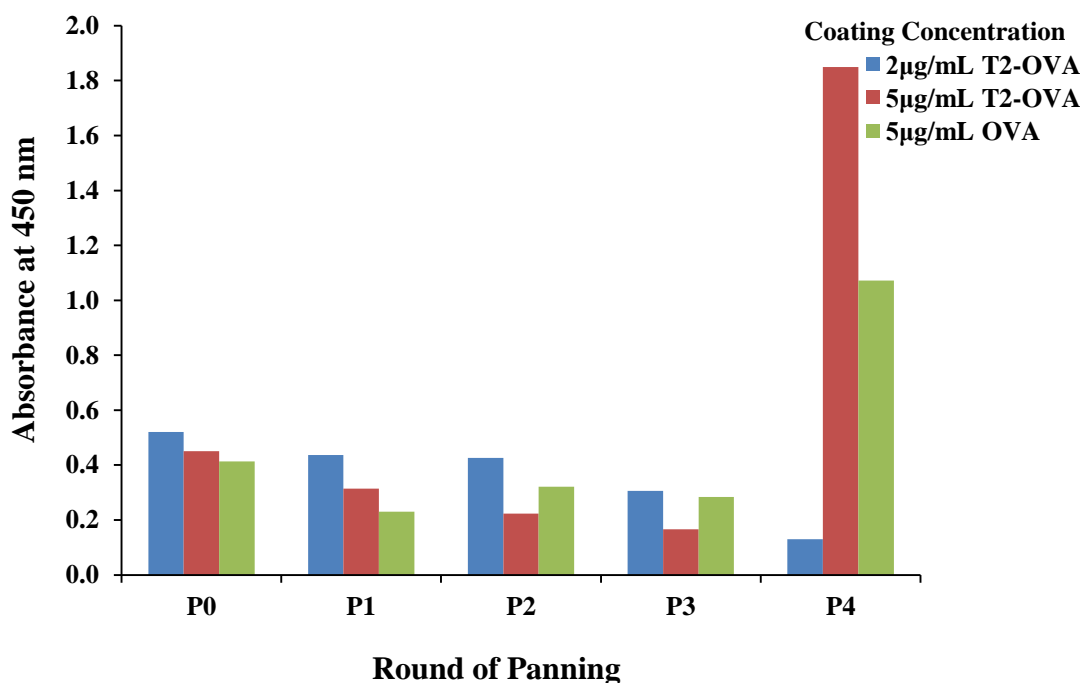


Figure 3.10: Anti-T-2 toxin polyclonal phage ELISA (neat) screened against T-2 toxin-OVA and OVA. The ELISA plate was coated with varying concentrations of T-2 toxin-OVA (2 and 5 µg/mL) and OVA (5 µg/mL) as a positive control. Anti-T-2 toxin polyclonal phage collected from each round of panning was applied (neat) to determine if enrichment for anti-T2 scFv antibody fragments had occurred in successive rounds of panning. P4 suggests enrichment for T-2 toxin-OVA and OVA. Experiments were performed with three replicates and results averaged (n = 1).

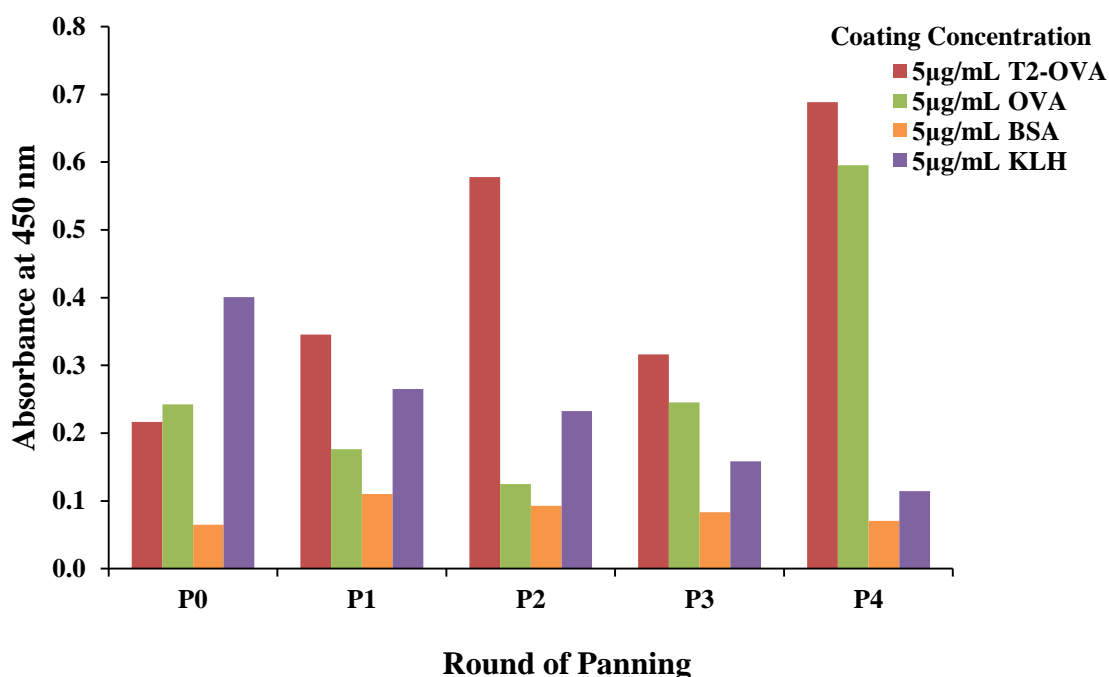


Figure 3.11: Anti-T2 Polyclonal phage ELISA (diluted 1/3) screened against T-2 Toxin-OVA and carrier proteins. The ELISA plate was coated with 5 µg/mL of T-2 toxin-OVA, OVA, BSA and KLH. Anti-T2 polyclonal phage collected from each round of panning was applied diluted 1/3 with PBST with 1% (w/v) Milk Marvel to determine if enrichment for anti-T2 scFv antibody fragments had occurred in successive rounds of panning. P2 and P4 suggest enrichment for T-2 toxin-OVA. P4 has also enrichment for OVA. A decrease in response for KLH occurred as phage displaying non-specific anti-T2 scFv fragments were washed away. BSA was included as a negative control with no significant enrichment evident. Experiments were performed with three replicates and results averaged (n = 1).

3.2.9 Monoclonal ELISA screening against T-2 toxin-OVA and OVA

Monoclonal ELISA was used to investigate if individual clones from the anti-T2 scFv library were specific against T-2 toxin or OVA. Polyclonal phage (10 µL) from Round 4 of panning were infected into mid-exponential phase TOP 10F' cells for soluble expression and plated out on carbenicillin agar plates, as described in Section 2.2.14. Single colonies (192) were picked, grown, induced with IPTG for soluble expression and lysed to release scFv antibody fragments from *E. coli* cells, as described in Section 2.2.14. The lysates from 48 clones were then applied to ELISA plates coated with 100 µL per well of 5 µg/mL of T-2 toxin-OVA (diluted in PBS) and 5 µg/mL of OVA (diluted in PBS). Figure 3.12 indicates that the highest responding anti-T-2 toxin scFv-producing clones enriched for during panning, were binding to OVA with more specificity than T-2 toxin conjugated to

OVA. Therefore, the scFv antibody fragments enriched for during panning were not T-2 toxin-specific. To overcome this issue, an OVA depletion step was developed to bind and eliminate OVA-specific scFv antibody fragments during panning and attain specific T-2 toxin antibodies. This process involved re-amplification of the un-panned polyclonal phage (Pan '0') from the previously prepared anti-T-2 toxin polyclonal phage library.

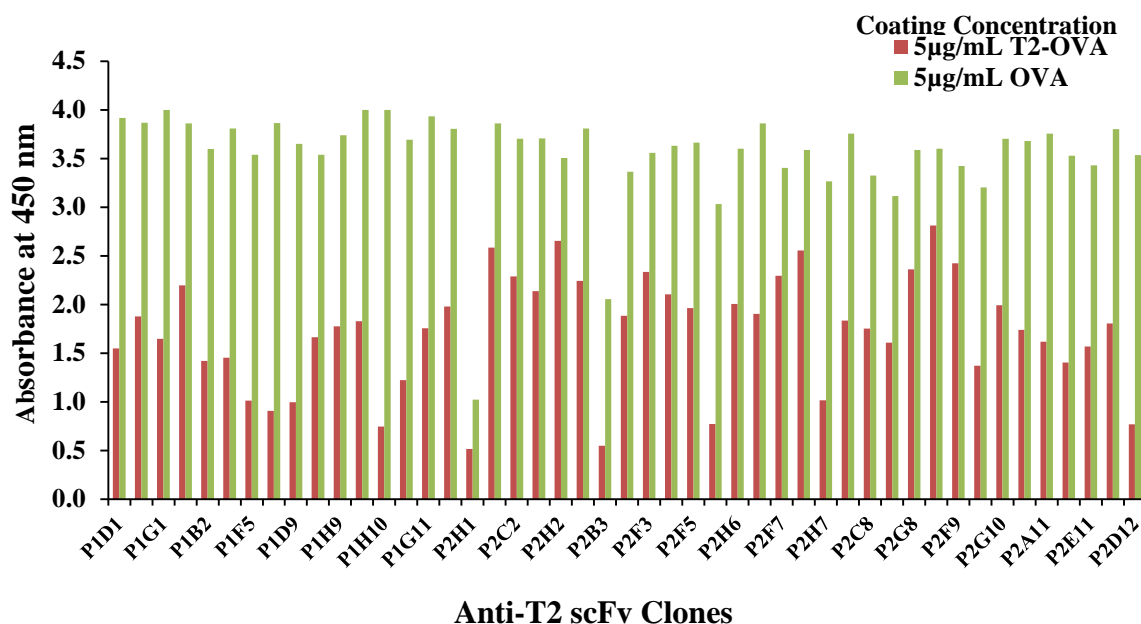


Figure 3.12: Monoclonal ELISA of selected anti-T-2 toxin scFv clones screened against T-2 toxin-OVA and OVA. The ELISA plate was coated with 5 µg/mL of T-2 toxin-OVA and OVA. The lysates from selected clones were diluted 1/2 with PBST with 1% (w/v) Milk Marvel and were applied to the coated ELISA plate. Experiments were performed once (n = 1).

3.2.10 Re-amplified polyclonal phage for phage-display and panning of anti-T-2 toxin library

Un-panned polyclonal phage (Pan '0') were re-amplified, as described in Section 2.2.16 and treated with OVA to deplete anti-OVA-specific scFv antibody fragments and select for anti-T-2 toxin-specific scFv antibody fragments. The first round of panning was completed by coating a Nunc MaxiSorp® flat-bottom 96 well plate with T-2 toxin-OVA at the concentrations outlined in Table 3.5. Re-amplified phage were collected and re-suspended in PBS with 0.1% (w/v) OVA and 1% (w/v) Milk Marvel. This was applied to the plate,

subjected to vigorous washing, eluted and used to re-infect *E. coli* cultures which were grown overnight. The following day the process was repeated. A library count of inputs and outputs was calculated each day by plating out *E. coli* cells prior to and after phage infection. The size of the anti-T-2 toxin scFv library is indicated in Table 3.6 and should be a minimum of 1×10^7 , as described by Barbas *et al.* (2001).

Table 3.5: Panning strategy for anti-T-2 toxin scFv library

Round of Panning	T-2 Toxin-OVA Concentration ($\mu\text{g/mL}$)	Number of Wells	Number of Washes	Culture Volume (mL)
1	50	8	5X PBST	200
2	25	4	8X PBST	200
3	12.5	4	10X PBST	200
4	5	4	12X PBST	200

Table 3.6: Library size after 4 rounds of panning

Round of Panning	Input (cfu/mL)	Output (cfu/mL)
0	$>1 \times 10^{11}$	3.0×10^6
1	Too many to count	8.17×10^7
2	Too many to count	2.6×10^6
3	Too many to count	8.6×10^6
4	Too many to count	5×10^6

3.2.11 Re-amplified polyclonal phage ELISA screening against T-2 toxin-OVA and OVA

Polyclonal phage ELISA was completed, as described in Section 2.2.13. The result in Figure 3.13 indicates a decrease in KLH response with successive rounds of panning. However, no significant response or enrichment for T-2 toxin was evident compared to OVA. The depletion of OVA did not lead to the enrichment of specific T-2 toxin scFv binders. Excess OVA may have been used and possibly saturated the polyclonal phage. Alternatively, degradation of the T-2 toxin-OVA conjugate may have occurred preventing the successful binding of T-2 toxin-specific scFv antibody fragments. The use of a different T-2 toxin conjugate (T-2 toxin-BSA) that eliminates the need for OVA depletion

and reduces selection of OVA binders was explored as a potential solution for selecting T-2 toxin-specific phage.

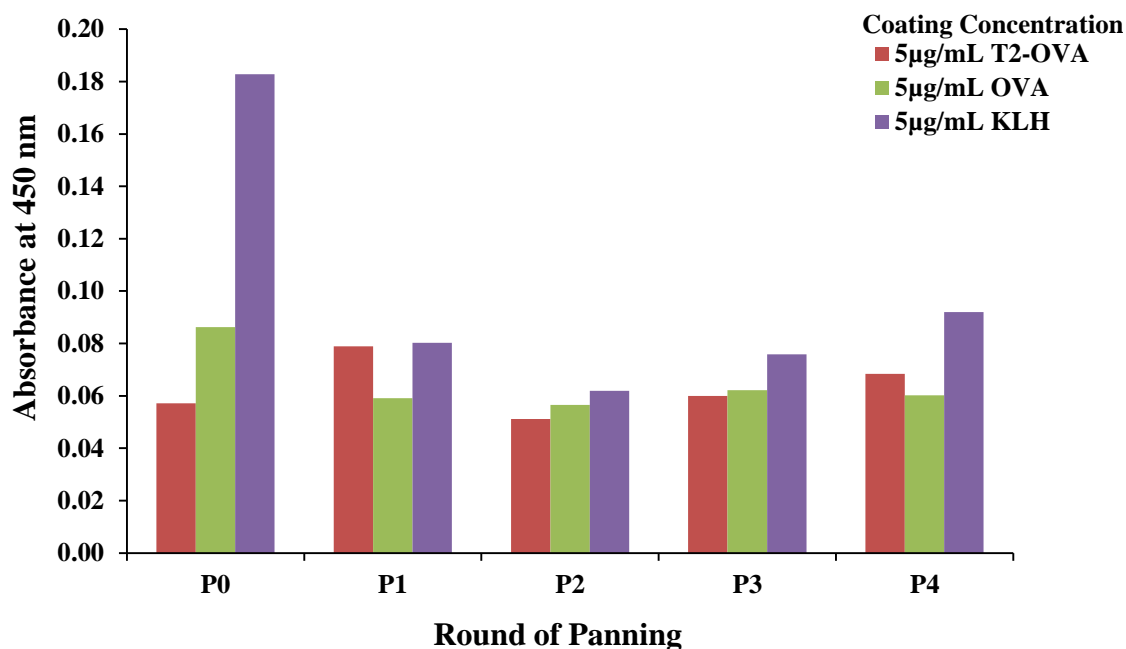


Figure 3.13: Re-amplified Anti-T-2 toxin Polyclonal phage ELISA (diluted 1/3) screened against T-2 toxin-OVA, OVA and KLH. The ELISA plate was coated with 5 µg/mL of T-2 toxin-OVA, OVA, KLH and T-2 toxin. Anti-T-2 toxin polyclonal phage collected from each round of panning was applied diluted 1/3 with PBST with 1% (w/v) Milk Marvel to determine if enrichment for anti-T-2 toxin scFv antibody fragments had occurred in successive rounds of panning. A decrease in response can be seen for KLH, as non-specific anti-T-2 toxin scFv antibody fragments are washed away. Enrichment for T-2 toxin-OVA or OVA is not evident. Experiments were performed with three replicates and results averaged ($n = 1$).

3.2.12 Repeat bone marrow V_H and V_L gene sequence amplifications and generation of SOE-PCR product.

Experiments involving the re-amplification of phage libraries can result in decreased library diversity with successive attempts (Barbas *et al.*, 2011). Prior to the phage display and panning experiments using T-2 toxin-BSA as the screening conjugate, a new anti-T-2 toxin library was built to ensure library complexity was maximised for further re-amplification of available phage preparations. Sufficient spleen SOE-PCR product was available from earlier amplifications, however, further bone marrow SOE-PCR product

was required. To achieve this bone marrow V_H and V_L gene sequence amplifications for the construction of scFv antibody fragment libraries with long linkers were completed again using synthesised cDNA, avian long linker primers and MyTaq polymerase, as described in Sections 2.2.5 – 2.2.7. Equimolar concentrations of purified spleen V_H and V_L gene amplifications, avian overlap extension primers and MyTaq polymerase were used to produce further bone marrow SOE-PCR product, as described in Section 2.2.8. An SOE product at ~750 bps was expected from these amplifications. This band is clearly visible in Figure 3.14. The band at ~750 bps was excised, purified, quantified and deemed suitable for restriction digestion and ligation into the pComb3xSS vector.

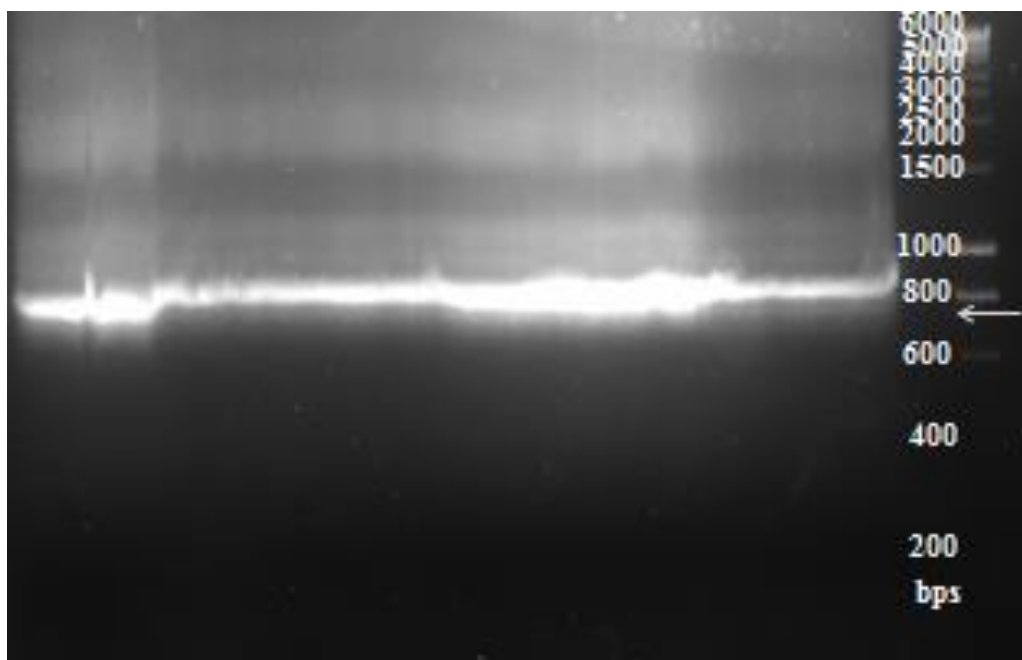


Figure 3.14: Bone marrow V_H and V_L chain SOE-PCR product. A 20X SOE-PCR product amplification can be seen at approximately 750 bps.

Triple restriction digestion of the pComb3xSS vector was completed again with *Sfi*I, *Xba*I and *Xho*I enzymes and the vector was then treated with Antarctic phosphatase, as described in Section 2.2.9. Bone marrow and spleen SOE-PCR products were digested with *Sfi*I enzyme for complementary insertion and ligation into the *Sfi*I digested vector. The purified bone marrow and spleen SOE-PCR products and the purified digested vector were ligated using T-4 Ligase and transformed into *E. coli*, as described in Section 2.2.10 and 2.2.11,

respectively. The generated library was then subjected to 5 rounds of panning, as described in Section 2.2.12.

3.2.13 Phage-display and panning of anti-T-2 toxin library against T-2 toxin-BSA

The *Sfi*I digested constructs were cloned into *Sfi*I digested pComb3xSS vector by ligation. The ligated product was transformed into electrocompetent *E. coli* cells and allowed to grow overnight to express and produce a library of multiple copies of the scFv antibody fragment. The following day the cultures were infected with M13 phage and allowed to grow overnight to initiate the process of phage display and panning, as described in Section 2.2.12. The first round of panning was completed by coating a Nunc MaxiSorp® flat-bottom 96 well plate with T-2 toxin-BSA at the concentrations outlined in Table 3.7. Phage were collected, applied to the plate, subjected to vigorous washing, eluted and used to re-infect *E. coli* cultures which were grown overnight. The following day the process was repeated. A library count of inputs and outputs was calculated each day by plating *E. coli* cells on carbenicillin-selective agar prior to and after phage infection. The size of the anti T-2 toxin scFv library is indicated in Table 3.8 and should be a minimum of 1×10^7 , as described by Barbas *et al.* (2001).

Table 3.7: Panning strategy for anti-T-2 toxin scFv library against T-2 toxin-BSA

Round of Panning	T-2 Toxin-BSA Concentration (µg/mL)	Number of Wells	Number of Washes	Culture Volume (mL)
1	100	8	5X PBST	200
2	50	4	8X PBST	200
3	25	4	10X PBST	200
4	12.5	4	12X PBST	200
5	6.1	4	12X PBST	200

Table 3.8: Anti-T-2 toxin scFv library size after 5 rounds of panning

Round of Panning	Input (cfu/mL)	Output (cfu/mL)
0	$>1 \times 10^{11}$	5.27×10^6
1	1.12×10^{15}	5.9×10^6
2	TMTC	7.6×10^6
3	1.152×10^{14}	1.68×10^5
4	TMTC	6.36×10^6
5	TMTC	4.13×10^6

3.2.14 Polyclonal phage ELISA screening against T-2 toxin-BSA and BSA

Polyclonal phage ELISA was completed, as described in Section 2.2.13, and used to select for T-2 toxin-specific scFv antibody fragments. T-2 toxin is a hapten and must be conjugated to a larger carrier protein for screening methods. T-2 toxin was conjugated to Bovine Serum Albumin (BSA), as previously described in Section 2.2.2. Previous results using OVA as the carrier molecule for screening purposes proven unsuccessful and, therefore, screening with T-2 toxin-BSA was examined. To ensure that the response elicited by the anti-T-2 toxin phage library was specific against T-2 toxin, polyclonal phage ELISA was completed against T-2 toxin-BSA, BSA and KLH. Phage collected from each round of panning were tested against 100 μ L per well of 10 μ g/mL of T-2 toxin-BSA (diluted in PBS), 10 μ g/mL of BSA (diluted in PBS) and 10 μ g/mL of KLH (diluted in PBS) coated on a Nunc MaxiSorp® flat-bottom 96 well plate. The response observed should increase with progressive rounds of panning as enrichment occurs for specific anti-T-2 toxin phage scFv antibody fragments when screened against the T-2 toxin-BSA target. In contrast, the response for KLH should decrease with successive rounds of panning as specific anti-KLH scFv antibody fragments, or, non-specific anti-T-2 toxin scFv are washed away. The BSA response should also be low to ensure that the anti-T-2 toxin scFv antibody fragments are not binding the BSA-conjugate molecule. Figure 3.15 indicates the responses elicited for T-2 toxin-BSA, BSA and KLH were low for all rounds of panning. This suggests the phage display and panning process had not been successful for the enrichment anti-T-2 toxin scFv antibody fragments. The response elicited by the binding of the anti-T-2 toxin scFv antibody fragments to T-2 toxin-BSA is not significantly higher than that of anti-T-2 toxin scFv antibody fragments to BSA. This suggests that the library does not contain phage displaying scFv antibody fragments which are specific to T-2 toxin and capable of producing a high binding response when targeted to T-2 toxin. This supports the earlier

results identified during panning, polyclonal phage ELISA and monoclonal ELISA against T-2 toxin-OVA, were the phage displayed anti-T-2 toxin scFv antibody fragments bound to the OVA conjugate molecule, however, were not shown to specifically bind T-2 toxin. Results indicating that the phage displayed anti-T-2 toxin scFv antibody fragments were not binding T-2 toxin significantly after repeating the panning and polyclonal phage ELISA experiments using T-2 toxin-BSA as the screening conjugate molecule, confirm that the anti-T-2 toxin phage library do not contain scFv antibody fragments which are specific for T-2 toxin. Further experimentation was conducted to confirm if the pComb3xSS vector contained the scFv fragment of interest. This was investigated through Colony Pick PCR.

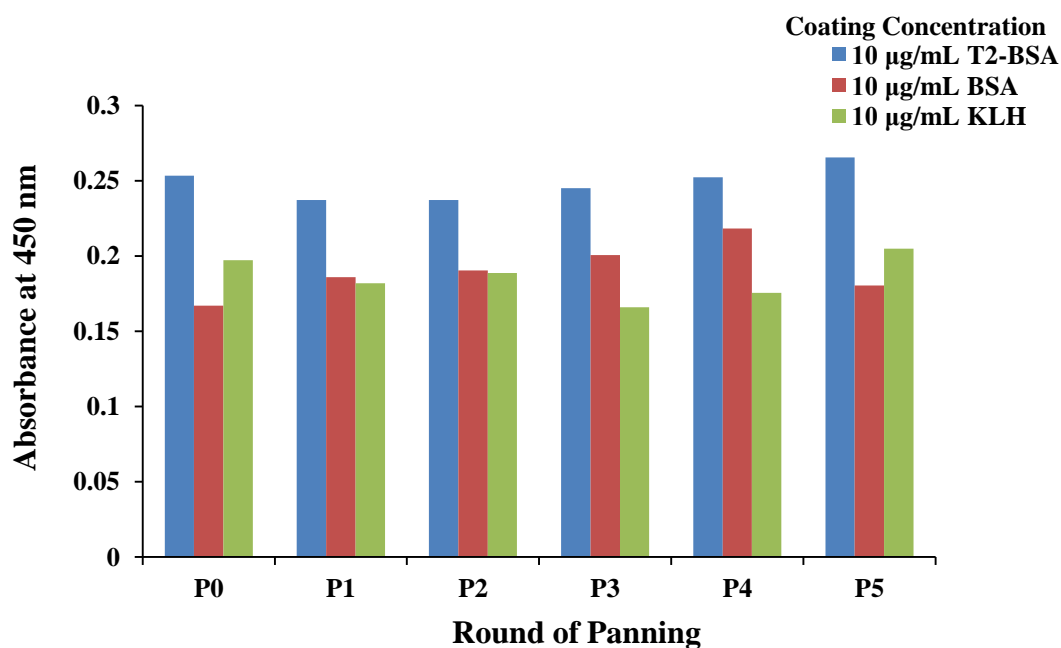


Figure 3.15: Anti-T-2 toxin polyclonal phage ELISA (neat) screened against T-2 toxin-BSA, BSA and KLH. The ELISA plate was coated with 10 µg/mL of T-2 toxin-BSA, BSA and with KLH as a positive control. Anti-T-2 toxin polyclonal phage collected from each round of panning was applied (neat) to determine if enrichment for anti-T-2 scFv antibody fragments had occurred in successive rounds of panning. Experiments were performed with three replicates and results averaged (n = 1).

3.2.14.1 Indirect checkerboard ELISA to confirm functionality of T-2 toxin-BSA following polyclonal phage ELISA

Following the use of T-2 toxin-BSA for panning experiments, an indirect checkerboard ELISA, as described in Section 2.2.26 was completed with the T-2 toxin-BSA conjugate and a commercial anti-T-2 toxin polyclonal antibody to ensure the conjugate was functional for binding purposes. The indirect ELISA involved coating an ELISA plate with varying concentrations of T-2 toxin-BSA at concentrations which were within the 100 – 6.1 µg/mL range used for panning purposes. Figure 3.16 shows that the anti-T-2 toxin polyclonal antibody bound to the T-2 toxin-BSA conjugate successfully at the tested coating concentrations of 10, 20 and 30 µg/mL. This indicates that the T-2 toxin-BSA conjugate was still stable, functional and suitable for the anti-T-2 scFv screening process. This result confirmed that the T-2 toxin conjugates produced for the anti-T-2 scFv antibody fragment panning process were not responsible for poor panning responses obtained.

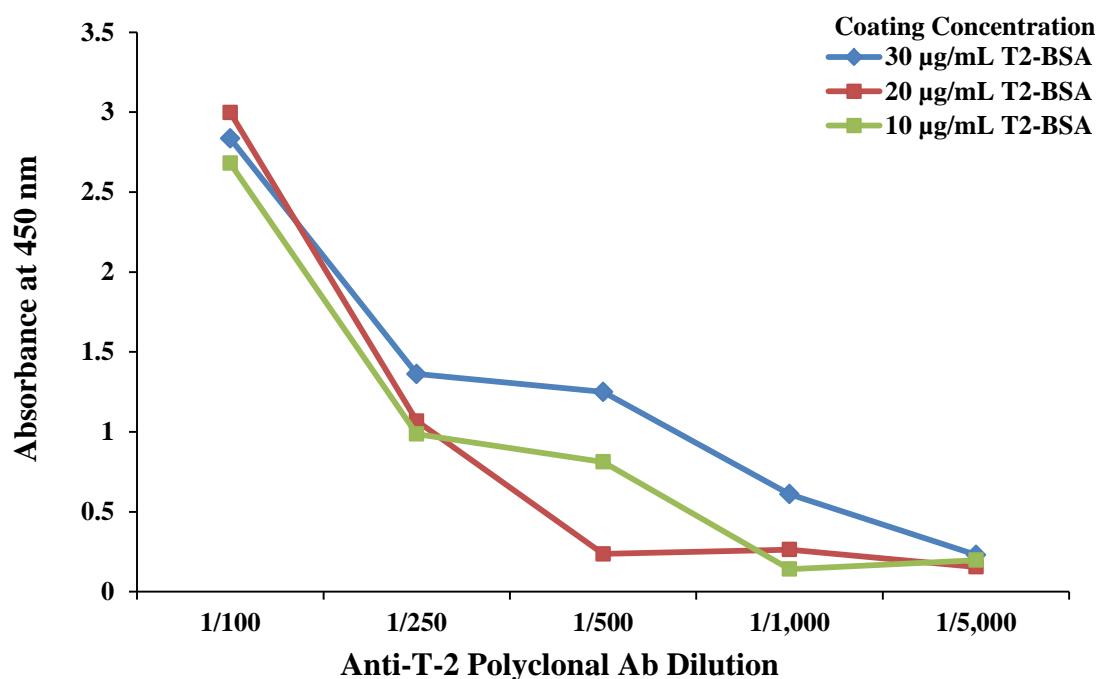


Figure 3.16: Indirect checkerboard ELISA with varying dilutions of T-2 toxin-BSA and varying dilutions of anti-T-2 toxin polyclonal antibody. T-2 toxin-BSA was diluted to 10, 20 and 30 µg/mL with PBS and used to coat an ELISA plate. Commercial polyclonal T-2 toxin antibody diluted at 1/100, 1/250, 1/500 1/1,000 and 1/5,000 in PBST with 1% (w/v) Milk Marvel was added to the plate. A HRP-labelled anti-rabbit secondary antibody diluted 1/10,000 in PBST with 1% (w/v) Milk Marvel was added to detect the commercial polyclonal T-2 toxin antibody followed by TMB. The reaction was stopped with 10% (v/v) HCl and absorbance was measured at 450 nm using a Tecan Safire™ 2 plate reader. Experiments were performed with three replicates and results averaged (n = 1).

3.2.15 Colony pick PCR

Colony pick PCR was conducted to determine the presence or absence of the constructed SOE-PCR product within the pComb3xSS vector construct. Colonies (15) were selected from plates containing bacterial colonies from the unpanned, pan 1, pan 2 and pan 5 rounds of the anti-T-2 toxin phage library, as described in Section 2.2.18. The LB agar plates contained carbenicillin (100 µg/mL) to select for colonies containing the pComb3xSS vector of interest. Colonies were picked and added to a PCR mastermix containing primers specific for the amplification of the SOE-PCR product. A SOE product at ~750 bps was expected from these amplifications. These bands were clearly visible in Figure 3.17 indicating the presence of the SOE-PCR insert of interest for each round of panning tested. This indicates that the library building process, ligation, and transformation process had

been successful, as well as, demonstrating that clones containing the SOE-PCR product had been successfully carried through the entire panning process.

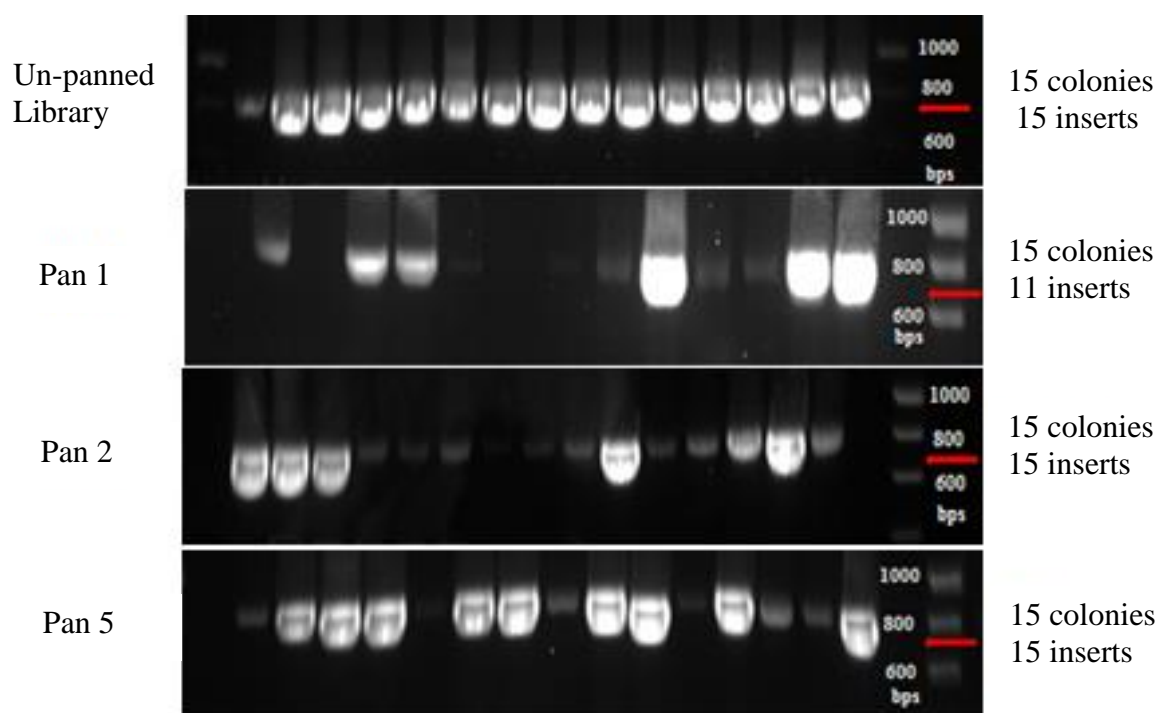


Figure 3.17: Colony pick PCR of un-panned and panned library colonies containing the pComb3xSS vector. The colonies selected were amplified using SOE-PCR primers. The majority of clones (56 out of 60) selected indicated that the amplification of the SOE-PCR product was successful and can be seen at approximately 750 bps.

3.2.16 Indirect competitive inhibition ELISA using commercial anti-T-2 toxin polyclonal antibody

A specific recombinant scFv antibody fragment against T-2 toxin could not be effectively developed despite results indicating that the RNA used was of good integrity, the V_H , V_L and SOE-PCR products and library construction were of high quality and the SOE-PCR product was evident in the majority of transformants from various rounds of panning. Therefore, a commercial anti-T-2 toxin polyclonal antibody was employed for analysis of T-2 toxin. The commercial anti-T-2 toxin polyclonal antibody obtained from a rabbit immunised with a T-2 KLH conjugate was previously used in Section 3.2.14.1, in an indirect checkerboard ELISA to test that the T-2 toxin-BSA conjugate was functional. However, this experiment was also analysed to determine the correct coating concentration

of T-2 toxin-BSA and working concentration of commercial polyclonal anti-T-2 toxin antibody. T-2 toxin-BSA coated at 10, 20 and 30 $\mu\text{g/mL}$ enabled the successful binding of commercial polyclonal anti-T-2 toxin antibody with all coatings of T-2 toxin-BSA indicating an effective antibody titre of $\sim 1/5,000$. Results from Figure 3.16 indicate a coating of 10 $\mu\text{g/mL}$ of T-2 toxin and a 1/500 dilution of the commercial anti-T-2 toxin polyclonal antibody were suitable concentrations for future commercial anti-T-2 toxin polyclonal antibody characterisation experiments.

Following the lack of successful anti-T-2 toxin scFv antibody fragment selection and the successful use of the commercial anti-T-2 toxin polyclonal ELISA for conjugate analysis, the anti-T-2 toxin polyclonal antibody was characterised in an indirect competitive inhibition ELISA, as described in Section 2.2.27. The IC_{50} value, limit of detection value and dynamic range were investigated, as described in Section 2.1.30, to establish the sensitivity of the antibody. Normalized absorbances were plotted against a range of free T-2 toxin concentrations to determine the IC_{50} value of the antibody using GraphPad Prism 5 software. The IC_{50} value is the free toxin concentration corresponding with the half maximum absorbance value was determined from Figure 3.18 and serves as a measure of the effectiveness of free T-2 toxin in inhibiting the specific biological interaction of commercial polyclonal anti-T-2 toxin antibody with immobilized T-2 toxin-BSA on an ELISA plate. The IC_{50} value was calculated at 8.5 ng/mL . The limit of detection was calculated using the indirect competitive inhibition ELISA format to test 20 blank replicates and 20 low concentration analyte replicates, according to the equations described by Armbruster and Pry (2008) and Tang *et al.* (2013). The limit of detection was determined as 5.8 ng/mL . These results indicated that the anti-T-2 toxin polyclonal antibody was functioning to below stringent E.U. legislative limits for T-2 toxin in this assay format and was a suitable candidate for use in the MBio multiplex mycotoxin detection system. The dynamic range of the T-2 toxin indirect competitive inhibition ELISA was determined based on the IC_{10} – IC_{90} of the assay and was calculated as 0.3 – 327 ng/mL .

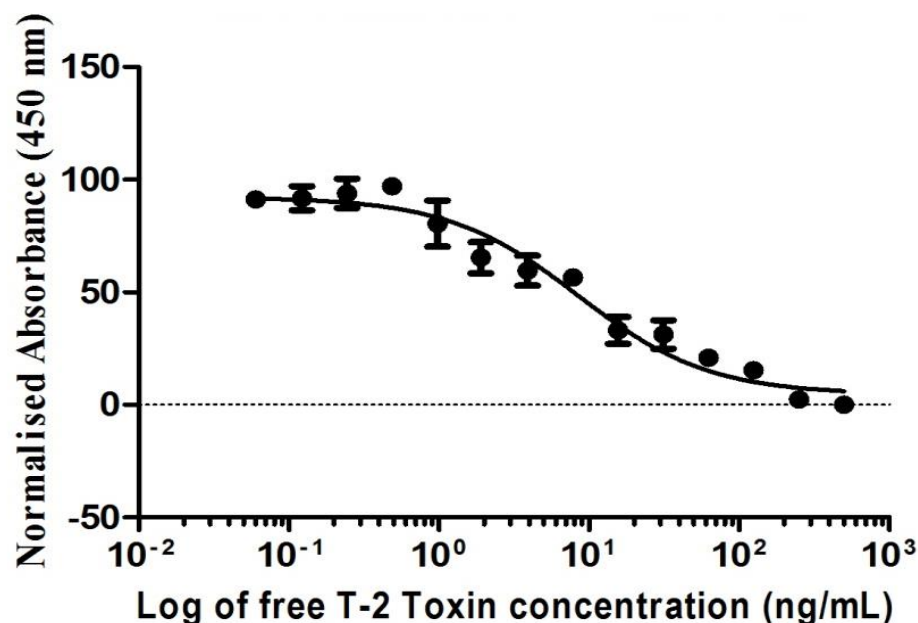


Figure 3.18: Indirect competitive inhibition ELISA with varying T-2 toxin-BSA and varying dilutions of free T-2 toxin against the commercial anti-T-2 toxin polyclonal antibody. T-2 toxin-BSA (10 $\mu\text{g/mL}$) was diluted with PBS and coated on an ELISA plate. Doubling dilutions of free T-2 toxin from 500 ng/mL down to 0 were prepared in PBS and allowed to incubate with a 1/500 dilution of anti-T-2 toxin commercial polyclonal antibody in PBST with 1% (w/v) Milk Marvel. A HRP labelled anti-rabbit secondary antibody diluted 1/10,000 in PBST with 1% (w/v) Milk Marvel was added, followed by TMB substrate. The reaction was stopped with 10% (v/v) HCl and absorbance was measured at 450 nm using a Tecan Safire™ 2 plate reader. Experiments were performed three times with three replicates and results averaged ($n = 3$). Errors bars represent the standard error of the mean (SEM) calculated by dividing the standard deviation by the square root of the n number using Graphpad Prism 5 software

3.3 Discussion

The need for specific and sensitive methods for detection of the T-2 toxin in cereals and crops is of great importance. This chapter focused on the development of recombinant anti-T-2 toxin scFv antibody fragments for integration in a 'point-of-site' mycotoxin detection system. Recombinant antibody engineering provides an effective way to generate specific antibody fragments for screening, diagnostic and therapeutic use. The development of recombinant antibody fragments which can be effectively incorporated in immunoassays for 'in-field' testing will provide a solution to laboratory-based mycotoxin analysis and help detect and monitor mycotoxins present in food. Commercially available ELISA kits and lateral flow devices (Randox, r-biopharm, Alltech, Neogen, Sigma-Aldrich, Eurofins Scientific and Vicam) are now being rapidly deployed by companies to permit 'on-site' testing of mycotoxins. The global market has been exhaustively investigated in the recent market analysis entitled 'Global Mycotoxin Testing Sales Market (Aflatoxins, Ochratoxins, Patulin, Fusarium toxins and Other toxin) Opportunity Analysis, Market Shares and Forecast 2017-2022' published by Global QYResearch and indicates the vast commercial interest and potential for the mycotoxin detection industry.

In this chapter, the generation of recombinant scFv antibody fragments was underpinned by the synthesis of functional mycotoxin-conjugates. T-2 toxin is a low molecular weight haptens and, therefore, conjugation to carrier proteins for screening (OVA and BSA) purposes was necessary. Conjugation was verified by indirect competitive inhibition ELISA and a decreasing response was produced by the commercial antibody when inhibited by a range of free T-2 toxin concentrations. Furthermore, the conjugate was deemed useful for the recombinant antibody screening processes when the absorbance '0' value was in excess of 1. Competitive inhibition ELISA using decreasing concentrations of T-2 toxin-OVA and T-2 toxin-BSA showed that the inhibited polyclonal antibody gave decreasing absorbance responses and indicated that the T-2 toxin-OVA (5, 2 and 1 $\mu\text{g/mL}$) and T-2 toxin-BSA (10 $\mu\text{g/mL}$) conjugate complexes delivered absorbance values in excess of 1.

The development of an anti-T-2 toxin scFv antibody fragment was undertaken, through cDNA synthesis, scFv library building, phage display and panning against T-2 toxin-OVA and T-2 toxin-BSA. The spleen and bone marrow are a rich source of antibody-producing

cells, therefore, previously isolated avian bone marrow and spleen RNA was successfully reversed transcribed into cDNA to provide a template for the amplification of variable antibody gene sequences. The V_H and V_L gene sequences were successfully amplified using sense and reverse primers which introduce identical overlap tail sequences that were successfully linked together to produce a complete scFv gene sequence construct using Splice by Overlap-Extension-PCR (SOE-PCR). The bone marrow and spleen SOE-PCR products and pComb3xSS phagemid vector were then restriction digested, ligated and electroporated into electrocompetent XL1-Blue *E. coli* cells. The resulting anti-T-2 toxin scFv library was 2.9×10^6 cfu/mL in size. The generated library size suggests the number of possible scFv clones that could potentially bind to T-2 toxin. Barbas *et al.* (2001) recommend a library size in excess of 1×10^7 cfu/mL, however, this is subject to the concentration and quality of DNA, as well as the efficiency of the electrocompetent cells used. Furthermore, previous work in this lab has yielded specific antibodies from scFv libraries $\times 10^5$ cfu/mL in size. Therefore, the library was subjected to panning to obtain an anti-T-2 toxin scFv antibody fragment.

Four rounds of panning were completed and enrichment for anti T-2 toxin and OVA scFv antibody fragments was evident following analysis of the panning process. T-2 toxin-OVA was used as a screening conjugate for panning and, therefore, a response against T-2 toxin-OVA and OVA was evident following polyclonal phage ELISA. A positive control, KLH, and a negative control, BSA, were also included to determine if panning and enrichment was successful. KLH was used as a protein carrier for the T-2 toxin immunogen and, therefore, the avian immune response produced a repertoire of antibodies against KLH, as well as, the T-2 toxin target during the immunisation period. Expectedly, the response decreased for KLH with successive rounds of panning as specific anti-KLH scFv (or non-specific anti-T2 scFv antibody fragments) were washed away. A low BSA response was also elicited as expected. These results suggested that enrichment was successfully achieved, however, whether enrichment for T-2 toxin, OVA or both had occurred was unclear.

Monoclonal ELISA involved growing *E. coli* cells infected with polyclonal phage from Pan 4 for soluble expression of individual clones from the anti-T-2 scFv library. Monoclonal ELISA indicated that the anti-T-2 scFv library had been enriched for OVA and not T-2 toxin, with each individual clone eliciting a higher response for OVA than T-2 toxin. To overcome the issue of enrichment for OVA, an OVA depletion step was

incorporated into the panning strategy and the panning strategy repeated (Ma, 2013). Following four rounds of panning, the depletion of OVA did not result in the enrichment of T-2 toxin-specific scFv antibody fragments. There is a possibility that 0.1% (w/v) OVA in PBS used for depletion may have saturated the anti-T-2 scFv displaying phage. Alternatively, the T-2 toxin-OVA conjugate may have undergone degradation and caused dissociation of the T-2 toxin from the immobilised OVA carrier protein. Stability is a major concern with conjugate construction and degradation can be a common issue due to temperature changes or solvent effects (Al-Warhi *et al.*, 2012). This would result in a lack of T-2 toxin availability for anti-T-2 toxin-specific scFv antibody fragments to successfully bind. Instead the OVA carrier protein would be available as a panning target and for subsequent polyclonal phage and monoclonal ELISA. Synthesis of a T-2 toxin-BSA conjugate eliminated the need for OVA depletion and offered a means to reduce selection of OVA binders present during polyclonal phage and monoclonal ELISA. Therefore, T-2 toxin specific phage were re-amplified from the un-panned polyclonal phage and subjected to phage display and a T-2 toxin-BSA panning strategy.

Five rounds of panning were completed and indicated the responses elicited for T-2 toxin-BSA, BSA and KLH were low for all rounds of panning. These results indicate that the anti-T-2 toxin phage-displaying scFv antibody fragments were not binding T-2 toxin significantly after repeating the panning and polyclonal phage ELISA experiments using T-2 toxin-BSA as the screening conjugate molecule. Furthermore, this supports the results produced during panning, polyclonal phage ELISA and monoclonal ELISA against T-2 toxin-OVA, where the phage displayed anti-T-2 toxin scFv antibody fragments bound to the OVA conjugate molecule, however, were not shown to specifically bind T-2 toxin. This suggests that the library does not contain phage-displaying scFv antibody fragments which are specific to T-2 toxin and capable of producing a high binding response when targeted to T-2 toxin. Experimentation was conducted to determine if the pComb3xSS vector contained the SOE-PCR product coding for the scFv fragment of interest, by using colony pick PCR. Colonies (15) were selected from LB agar plates (unpanned, pan1, pan 2 and pan 5) capable of selecting for cells producing bacterial colonies containing the pComb3xSS vector of interest. Colony pick PCR indicated that the SOE-PCR product was successfully amplified using specific SOE-PCR primers (specific for the insert of interest). The SOE-PCR product was present at ~750 bp in the majority (56/60) of all clones amplified and analysed by identification on agarose gel. Therefore, it was concluded that

the SOE-PCR product coding for the scFv antibody fragment was evident in the pComb3xSS vector, however, the resulting phage displayed scFv antibody fragments that were tested against T-2 toxin-OVA and T-2 toxin-BSA were not specific for T-2 toxin. The key to achieving specific antibodies lies in the generation of a good immune response which in-turn delivers quality RNA and cDNA from which the scFv library is constructed (Barbas *et al.*, 2001). If the integrity of the RNA or cDNA became compromised at any stage throughout the library generation process, then, this may have resulted in a lack of specificity in the RNA or cDNA used to generate the anti-T-2 toxin scFv library. Furthermore, a major determining factor in the quality of an antibody library is its complexity, which can be more simply described as the number of different antibodies present in the library. If the library is substantially complex the possibility of selecting an antibody with the required sensitivity and/or specificity is increased. The complexity of the library cannot exceed the number of transformants present after library ligation and transformation and, therefore, is defined by library size. The library size and, thus, complexity of the anti-T-2 toxin scFv library was limited to 2.9×10^6 cfu/mL, which is less than the recommended 10^7 library size. A lack of diversity and complexity may have been evident in the anti-T-2 toxin scFv library which resulted in the generation of only low specificity anti-T-2 toxin binders. The rate of antibody-displaying phage is also influenced by variations in the antibody sequence which the phage possess. As a consequence, phage which display different antibodies are produced at different rates (Barbas *et al.*, 2001). This suggests that if non-specific anti-T-2 toxin phage acquire the advantage of growing at a faster rate than specific anti-T-2 toxin phage, then, non-specific anti-T-2 toxin phage are more likely to propagate dominantly. Together, a loss in RNA or cDNA integrity, a lack of library complexity and the dominance of non-specific anti-T-2 toxin phage may have resulted in the overall generation and bias of non-specific anti-T-2 toxin scFv antibody fragment library.

In the absence of the a functional and specific anti-T-2 scFv recombinant fragment for the detection of T-2 toxin, a commercial polyclonal antibody fragment was investigated and characterised for its use as a detection molecule for T-2 toxin. The antibody proved successful for the detection of T-2 toxin in indirect ELISA and in indirect competitive inhibition ELISA yielding an IC₅₀ value of 8.5 ppb and a limit of detection of 5.8 ppb in this format. This antibody was deemed capable of specifically binding T-2 toxin and was

selected for use in Chapter 4 to develop a simple, rapid, sensitive and ‘point-of-site’ device for the detection of T-2 toxin.

Chapter Four

**The selection and characterisation of
recombinant antibody fragments for detection
of mycotoxins in a ‘point-of-site’ device**

4.1. Introduction

Detection and monitoring of mycotoxins is of great importance as ingestion of contaminated food or feed can have severe effects in humans and animals. Cases of acute aflatoxicosis can result in death. Chronic aflatoxicosis can cause cancer, immune suppression, and other pathological conditions, whilst exposure to zearalenone (ZEN) can result in decreased fertility, still-birth or deformities in animal off-spring (Bennett and Klich, 2003). As described in Chapter 3, the gold standard for analysis and assessment of mycotoxin-contaminated food and animal feed is traditionally by use of lab-based chromatography methods that are costly, both in terms of expense and time. Recombinant antibody fragments which can sensitively detect mycotoxins at EU legislative limits are essential for mycotoxin detection at the 'point-of-site.' Incorporation of such fragments into cost-effective biosensing platform enables the specific nature of the antibody interaction with its cognate target to deliver rapid and simple mycotoxin recognition. Furthermore, direct result-readout platforms, provide the resources for a viable monitoring process that can be immediately interpreted to prevent mycotoxin exposure in humans and animals.

This chapter focuses on the selection, expression, purification and characterisation of pre-existing recombinant Fab antibody fragment to detect aflatoxin B₁ (AFB₁) and scFv antibody fragments to detect aflatoxin B₂ (AFB₂) and ZEN. The overall aim of successfully selecting these recombinant antibody fragments is to provide specific mycotoxin-binders for inclusion in an MBio multiplex optical-planar waveguide biosensor device to detect mycotoxins in contaminated animal feed samples. To achieve this goal the antibodies must be capable of detecting the relevant mycotoxins at EU legislative limits. The anti-AFB₁ Fab, anti-AFB₂ scFv and anti-ZEN scFv antibody fragments were characterised by SDS-PAGE, Western blotting analysis and indirect checkerboard ELISA and tested in indirect competitive inhibition ELISA to determine their respective IC₅₀ value, limit of detection (LoD) and dynamic range. These factors were then analysed to indicate if the recombinant antibody fragments delivered the required sensitivity to detect their associated mycotoxin to EU legislative limits. The anti-AFB₂ and anti-ZEN scFv antibody fragments selected did not meet the stringent requirements of this research. However, the anti-AFB₁ Fab antibody fragment delivered an IC₅₀ value of 7.33 ng/mL and a LoD of 1.54 ng/mL. Therefore, the anti-AFB₁ Fab antibody fragment and the anti-T-2 toxin polyclonal antibody (Chapter 3)

exhibited functionality at the desired sensitivities and were successfully deployed to detect AFB₁ and T-2 toxin in Dried Distillers Grain with Solubles (DDGS) samples using the MBio detection system. Coupled with this platform, each antibody delivered limits of detection for AFB₁ (4.12 ng/mL) and T-2 toxin (5.08 ng/mL) in DDGS extract to below EU legislative limits. A ‘proof-of-concept’ study was also completed to demonstrate that both mycotoxins could be detected from a single contaminated DDGS sample in a multiplex format. These results show that the multiplex detection of AFB₁ and T-2 toxin using the anti-AFB₁ Fab antibody fragment and anti-T-2 toxin polyclonal antibody on the MBio detection system, provides a simple solution to ‘point-of-site’ mycotoxin testing, that could be easily effectuated for screening other mycotoxins or possibly multiple mycotoxins.

This chapter also discusses the process of chemically conjugating AFB₂ and ZEN to OVA carrier proteins to allow for selection of recombinant antibody fragments. The conjugation of AFB₂ and ZEN to OVA was tested and confirmed by indirect competitive inhibition ELISA.

4.2. Results

4.2.1. Expression, purification and characterisation of an anti-AFB₁ Fab antibody fragment

The pComb3xSS vector facilitates the purification of *E. coli* expressed antibody fragments by incorporation of a hexa-histidine (HIS6) tag fused to the N-terminal of the recombinant antibody fragment. Immobilized metal-affinity chromatography (IMAC) is a widely used method to purify recombinant proteins containing histidine residues. IMAC is based on the interactions between a transition metal ion (Co^{2+} , Ni^{2+} , Cu^{2+} , Zn^{2+}) immobilized on a matrix and specific amino acid side chains. Histidine is the amino acid that exhibits the strongest interaction with immobilized metal ion matrices, as electron donor groups on the histidine imidazole ring readily form co-ordination (dative covalent) bonds with the immobilized transition metal. Recombinant antibody fragments containing a HIS tag can, therefore, be retained on IMAC column matrices with relative ease. Following washing of the matrix material, bound antibody fragments can be easily eluted by adjusting either the pH of the column buffer or by adding free imidazole to the column buffer (Bornhurst and Falke, 2000).

Previously, an anti-AFB₁ Fab antibody fragment was developed by Dr. Sharon Stapleton (2007). This antibody was expressed and purified, as described in Sections 2.2.19 – 2.2.23. Briefly, the bacterial anti-AFB₁ clone was used to inoculate 10 mL of SB media supplemented with 50 µg/mL of carbenicillin and 1% (w/v) glucose and was incubated at 37°C overnight while shaking at 250 rpm. The following day, 2 mL (1% (v/v) cell density) of the overnight culture was sub-cultured into 200 mL of fresh SB_{GC} media and incubated at 37°C while shaking at 250 rpm until an OD₆₀₀ of 0.6 was reached, at which point the optimised concentration of isopropyl β-D-1-thiogalactopyranoside (IPTG) [0.1 mM] was added. The cultures were incubated overnight at the optimised temperature of 30°C and 220 rpm and the following day were subjected to freeze-thaw cycling and sonication at 40% amplitude to achieve cell lysis, as described in Section 2.2.20. Purification using IMAC (Ni^{+} -NTA) was completed, as described in Section 2.2.21. Following buffer exchange and concentration of the sample, a polishing step to remove contaminating proteins was completed using an AKTA FPLC system and a S75 (16/60) analytical gel filtration column (GE Healthcare), as described in Sections 2.2.22 - 2.2.23. The purified

anti-AFB₁ Fab antibody fragments were analysed by SDS-PAGE, Western blotting analysis, indirect ELISA and indirect competitive inhibition ELISA, as described in Sections 2.2.24 – 2.2.27.

4.2.2. SDS-PAGE and Western Blotting Analysis of an anti-AFB₁ Fab antibody fragment

SDS-PAGE is a universal method for separating proteins by electrophoresis based on the differential migration of denatured proteins due to their mass and charge, through a polyacrylamide gel. Following the fractionation of proteins in a polyacrylamide gel and their transference onto a nitrocellulose membrane, Western blotting is used to identify specific amino-acid sequences in proteins through the addition of a probing antibody specific for the appropriate epitope (i.e. a HA tag). The HA tag sequence within the recombinant antibodies is targeted by addition of a HRP labelled anti-HA antibody. This approach can be utilised to determine the presence and relative quantity of the antibody, the relative molecular weight of the antibody to a molecular weight ladder/marker and the efficiency of antibody purification (Blancher and Jones, 2000). Fab antibody fragments are approximately 50 kDa in size, consisting of a full light chain and half a heavy chain. During preparation for SDS-PAGE and Western blotting analysis the Fab antibody fragment is reduced into two approximately 25 kDa chains. A band at ~25 kDa can be seen in Figure 4.1 A.) representing the expected band for the anti-AFB₁ Fab antibody fragment following purification (eluted Fab) and protein concentration (concentrated Fab). To confirm that the band of interest was that of anti-AFB₁ Fab antibody fragment, Western blotting analyses probing specifically for the HA tag of anti-AFB₁ Fab antibody at ~28 kDa (Figure 4.1 B.)), and for the anti-AFB₁ Fab antibody human lambda light chain ~25 kDa (Figure 4.1 C.)), were completed. The anti-AFB₁ Fab antibody heavy chain can be seen at ~28 kDa in the eluted Fab and concentrated Fab samples in Figure 4.1 B.) indicating that the desired anti-AFB₁ Fab antibody heavy chain had been probed successfully. Additionally, the anti-AFB₁ Fab antibody human lambda light chain can be seen just below ~25 kDa in the concentrated Fab samples in Figure 4.1 C). This result indicates the desired anti-AFB₁ Fab antibody heavy and light chains were successfully detected through Western blotting analysis.

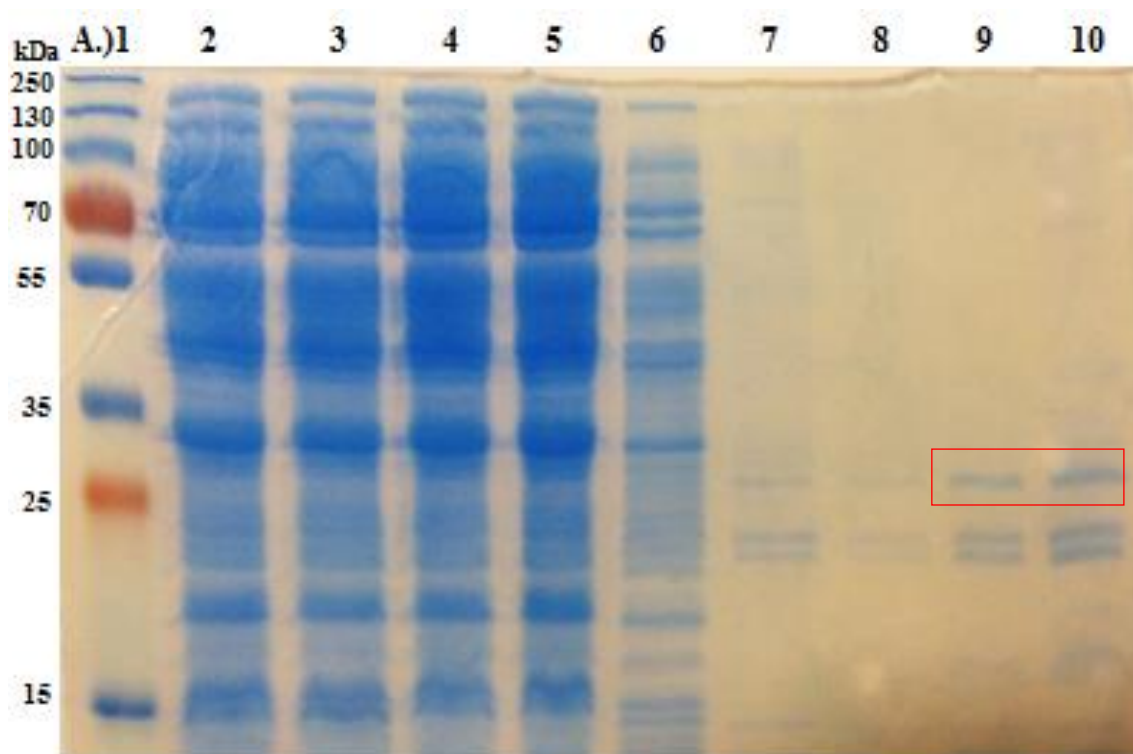


Figure 4.1: (A) SDS-PAGE analysis of IMAC purified anti-AFB₁ Fab antibody fragment. A 1 litre culture of *E. coli* was grown overnight and anti-AFB₁ Fab antibody fragments purified from lysate using IMAC. Samples were taken at all steps of the purification process, denatured and applied to a 12.5% (w/v) acrylamide gel. The proteins present in the samples were visualised by adding Instant Blue dye and the sizes of the respective proteins were assessed based on the inclusion of a standard protein ladder. The expected denatured Fab protein band is present at approximately 25 kDa. (Lane 1: Ladder; Lane 2: Filtered lysate; Lane 3: Flow-through 1; Lane 4: Flow-through 2; Lane 5: Flow-through 3; Lane 6: 40mM Imidazole wash; Lane 7: 40mM Imidazole wash; Lane 8: 50mM Imidazole wash; Lane 9: Eluted Fab; Lane 10: Concentrated Fab.

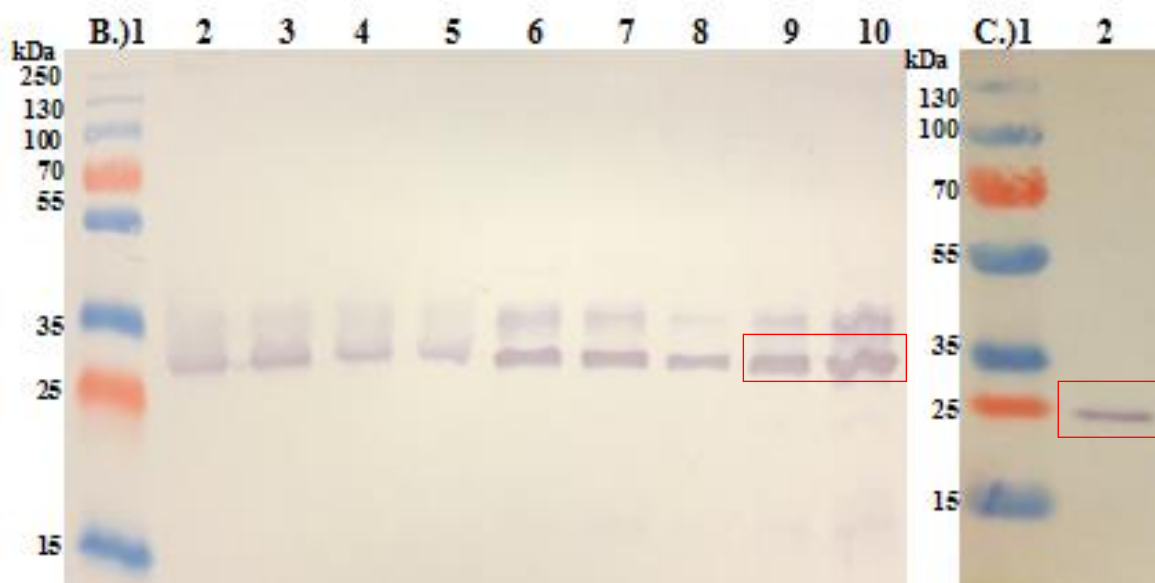


Figure 4.1: (B) Western blotting analysis of expressed and purified anti-AFB₁ Fab Heavy chain and (C) Light chain. Separated proteins were transferred from a 12.5% (w/v) acrylamide gel to a nitrocellulose membrane. The proteins present in the samples were visualised by adding 1/1,000 HRP-labelled anti-HA antibody (B) or 1/2,000 monoclonal mouse anti-human lambda light chain followed by a HRP-labelled anti-mouse secondary antibody diluted 1/20,000 in PBST with 1% (w/v) Milk Marvel (C). TMB substrate was added to develop a colour change and the respective proteins were assessed based on the inclusion of a standard protein ladder. ((B) Lane 1: Ladder, Lane 2: Filtered lysate, Lane 3: Flow-through 1, Lane 4: Flow-through 2, Lane 5: Flow-through 3, Lane 6: 40mM Imidazole wash, Lane 7: 40mM Imidazole wash, Lane 8: 50mM Imidazole wash, Lane 9: Eluted Fab, Lane 10: Concentrated Fab. ((C) Lane 1: Ladder, Lane 2: Concentrated Fab).

As indicated in Figure 4.1 A.), a small number of non-specific, contaminating protein bands can occur during the anti-AFB₁ Fab antibody fragment IMAC purification. To overcome this issue and ensure antibody product of high purity was available for assay use, further gel filtration chromatography was completed using an AKTA FPLC system and a S75 (16/60) analytical gel filtration column (GE Healthcare), as described in Section 2.2.23. In both the SDS-PAGE and Western blotting analysis completed for the IMAC-purified and eluted Fab (Figure 4.1 D.) and Figure 4.1 E.) lanes 2-8), there is non-reduced Fab antibody fragment evident at approximately 50 kDa, however, a contaminating band is also present at approximately 15 kDa. Following gel filtration only the desired Fab antibody fragment is apparent in the two fractions collected by the AKTA FPLC system (Figure 4.1 D.) and Figure 4.1 E.), lanes 9-10). IMAC purification coupled with gel

filtration ensured a highly pure anti-AFB₁ Fab antibody fragment for characterisation and assay development.

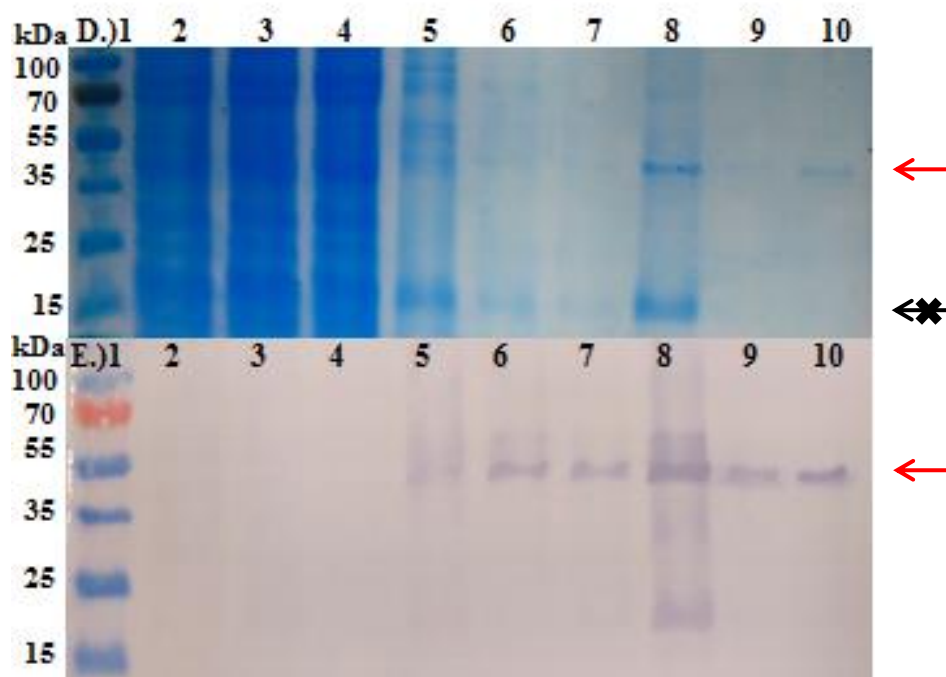


Figure 4.1: (D) SDS-PAGE and (E) Western blotting analysis of IMAC and gel filtration-purified anti-AFB₁ Fab antibody fragment. Separated proteins were transferred from a 12.5% (w/v) acrylamide gel to a nitrocellulose membrane. The proteins present in the samples were visualised by adding 1/1,000 HRP-labelled anti-HA antibody in PBST with 1% (w/v) Milk Marvel (E). TMB substrate was added to develop a colour change and the respective proteins were assessed based on the inclusion of a standard protein ladder. ((D and E) Lane 1: Ladder, Lane 2: Unfiltered lysate, Lane 3: Filtered lysate, Lane 4: Flow-through 3, Lane 5: 40mM Imidazole wash, Lane 6: 50mM Imidazole wash, Lane 7: IMAC-eluted Fab, Lane 8: Concentrated Fab, Lane 9: Gel filtration-eluted Fab fraction 1, Lane 10: Gel filtration-eluted Fab fraction 2).

4.2.3. Indirect checkerboard ELISA using varying concentrations of anti-AFB₁ Fab and AFB₁-BSA coating concentrations

The purified anti-AFB₁ Fab antibody fragment was tested in an indirect checkerboard ELISA to determine the correct coating concentration of AFB₁-BSA and working concentration of anti-AFB₁ Fab antibody fragment. AFB₁-BSA coating concentrations (1, 5 and 10 µg/mL) enabled the successful binding of anti-AFB₁ Fab antibody with both 5 µg/mL and 10 µg/mL coatings of AFB₁-BSA indicating an effective antibody titre of ~1/10,000. Results from Figure 4.2 indicate a coating of 5 µg/mL of AFB₁-BSA and a

1/2,000 dilution of the anti-AFB₁ Fab antibody fragment were suitable concentrations for future anti-AFB₁ Fab antibody fragment characterisation experiments. A negative control of 4% (w/v) BSA was coated to ensure the anti-AFB₁ Fab antibody fragment was not binding to the carrier protein.

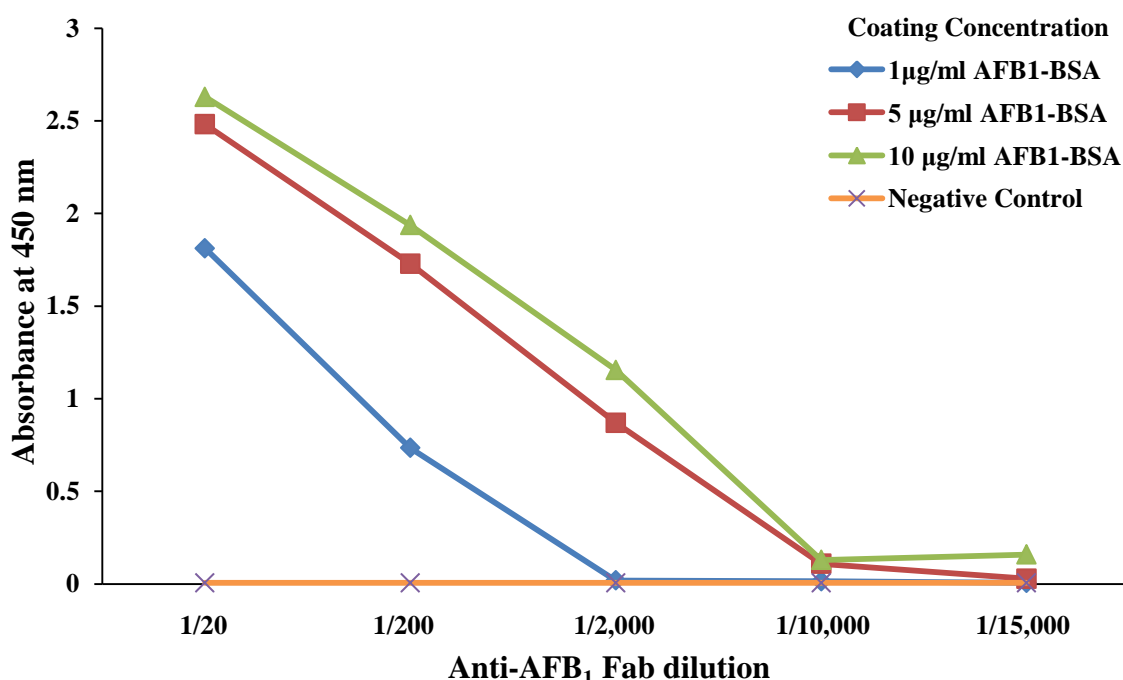


Figure 4.2: Indirect checkerboard ELISA with varying dilutions of AFB₁-BSA and anti-AFB₁ Fab antibody fragment. AFB₁-BSA was diluted to 1, 5 and 10 µg/mL with PBS and used to coat an ELISA plate. BSA (4% (w/v)) was used to coat the ELISA plate as a negative control. Purified anti-AFB₁ Fab antibody diluted at 1/20, 1/200, 1/2,000, 1/10,000 and 1/15,000 in PBST with 1% (w/v) Milk Marvel was added to the plate. A HRP-labelled anti-HA secondary antibody diluted 1/1,000 in PBST with 1% (w/v) Milk Marvel was added to detect the anti-AFB₁ Fab antibody followed by TMB. The reaction was stopped with 10% (v/v) HCl and absorbance was measured at 450 nm using a Tecan Safire™ 2 plate reader. Experiments were performed with three replicates and results averaged (n = 1).

4.2.4. Indirect competitive inhibition ELISA using anti-AFB₁ Fab and varying concentrations of free AFB₁ and AFB₁-BSA coating concentrations

Following a checkerboard ELISA the anti-AFB₁ Fab antibody fragment was tested in an indirect competitive inhibition ELISA to determine an IC₅₀, limit of detection value and

dynamic range, as described in Section 2.2.30. Indirect competitive inhibition ELISA, using anti-AFB₁ Fab against AFB₁-BSA and varying concentrations of free AFB₁ was repeated three times and using GraphPad Prism 5 software, normalized absorbance was plotted against a range of free AFB₁ concentration to determine the IC₅₀ value of the antibody. The IC₅₀ value is the free toxin concentration corresponding with the half maximum absorbance value was determined from Figure 4.3 and serves as a measure of the effectiveness of free AFB₁ toxin in inhibiting the specific binding interaction of anti-AFB₁ Fab antibody fragments with immobilized AFB₁-BSA on an ELISA plate. The IC₅₀ value was calculated at 7.33 ng/mL using Graphpad Prism 5 software. The limit of detection was calculated using the competitive inhibition ELISA format to test 20 blank replicates and 20 low concentration analyte replicates, according to the equations described by Armbruster and Pry (2008) and Tang *et al.* (2013). The limit of detection was determined as 1.54 ng/mL. These results indicated that the anti-AFB₁ Fab antibody fragment was functioning to below stringent E.U. legislative limits for AFB₁ in this assay format and was a suitable candidate for use in the MBio multiplex mycotoxin detection system. The dynamic range of the AFB₁ indirect competitive inhibition ELISA was determined based on the IC₁₀ – IC₉₀ of the assay and was calculated as 1 – 54 ng/mL.

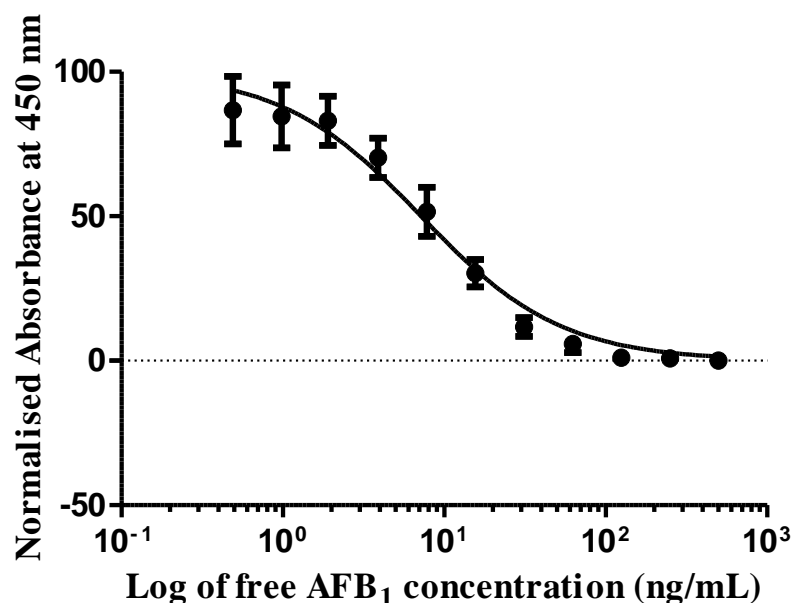


Figure 4.3: Indirect competitive inhibition ELISA with varying dilutions of AFB₁-BSA and free AFB₁ against a 1/2000 dilution of anti-AFB₁ Fab antibody fragment. AFB₁-BSA (5 µg/mL) was diluted with PBS and coated on an ELISA plate. Doubling dilutions of free AFB₁ from 1 µg/mL down to 0 were prepared in PBST with 5% (v/v) methanol and allowed to incubate with a 1/2,000 dilution of anti-AFB₁ Fab in PBST with 1% (w/v) Milk Marvel. A HRP-labelled anti-HA secondary antibody diluted 1/1,000 in PBST with 1% (w/v) Milk Marvel was added, followed by TMB substrate. The reaction was stopped with 10% (v/v) HCl and absorbance was measured at 450 nm using a Tecan Safire™ 2 plate reader. Experiments were performed three times with three replicates and the results averaged ($n = 3$). Errors bars represent the standard error of the mean (SEM) calculated by dividing the standard deviation by the square root of the n number using Graphpad Prism 5 software.

4.2.5. Evaluation criteria of AFB₂ conjugates

In order to screen and select previously generated anti-AFB₂ scFv antibody fragments AFB₂-BSA conjugates had to be synthesised. To assess the integrity of the mycotoxin-conjugates synthesised ‘in-house,’ indirect competitive inhibition ELISA was completed. This technique was used to determine if AFB₂ was successfully conjugated to the carrier protein Ovalbumin (OVA) and to ensure their usefulness for screening recombinant antibody fragments. In accordance with Sanders (2014), mycotoxin-conjugates were considered functional for screening protocols if the absorbance ‘0’ (no competitor toxin) value exceeded 1 and if decreasing absorbance values were obtained in the presence of increasing standard mycotoxin concentrations. The indirect competitive inhibition ELISA

was completed, as described in Section 2.2.27, and involved coating varying concentrations of the mycotoxin-conjugate on a Nunc MaxiSorp® flat-bottom 96 well plate and incubating a range of free mycotoxin concentrations with the relevant cognate antibodies. The cognate antibody bound the free mycotoxin in each sample and with increasing concentrations of free mycotoxin, the antibody was inhibited differentially from binding the immobilised mycotoxin-conjugate (e.g. a high concentration of free mycotoxin saturated the cognate antibody preventing it from binding to the immobilised mycotoxin-conjugate, whilst, a low concentration of free mycotoxin did not saturate the cognate antibody and the remaining antibody was available to bind the immobilised mycotoxin-conjugate). A HRP-labelled secondary antibody was added, developed with 3,3',5,5'-Tetramethylbenzidine (TMB) and the absorbance read at 450 nm using a Tecan Safire™ 2 plate reader.

The response produced by the antibody binding to the immobilised mycotoxin-conjugate was inversely proportional to the concentration of free mycotoxin used to inhibit the cognate antibody. A decreasing response could only be elicited if the mycotoxin was directly conjugated to the carrier protein and immobilised on the plate.

4.2.5.1 Evaluation of AFB₂-OVA

Evaluation of the AFB₂-OVA conjugate was completed through the use of indirect competitive inhibition ELISA using a commercial monoclonal antibody against AFB₁ which exhibits 76% cross reactivity with AFB₂. Therefore, as commercial antibodies against AFB₂ were not readily available, the anti-AFB₁ monoclonal antibody which was capable of binding to AFB₂ was selected to investigate if successful AFB₂-OVA conjugation had been achieved. A range of free inhibitor AFB₂ and immobilised AFB₂-OVA concentrations were used to indicate if an absorbance '0' (no competitor toxin) value in excess of 1 and, if a decreasing absorbance response could be achieved. This occurs when the free AFB₂ binds, and, reduces availability of the anti-AFB₁ monoclonal antibody for immobilised AFB₂-OVA interaction. The anti-AFB₁ monoclonal antibody was incubated with increasing concentrations of free AFB₂ toxin (0 - 50 ng/mL) and was then applied to a plate coated with a range of decreasing concentrations of AFB₂-OVA conjugate (15, 6 and 3 µg/mL). The absorbance results in Figure 4.4 indicate that when 15, 6 and 3 µg/mL of AFB₂-OVA were immobilised, the absorbance '0' (no competitor toxin)

value gave a much higher response (~4) than 1. Furthermore, a similar decreasing response was elicited by the inhibited monoclonal antibody when applied to all the concentrations of immobilised AFB₂-OVA conjugate. A difference in the absorbance responses would be expected based on the decreasing concentrations of AFB₂-OVA used to coat the plate. The similar response delivered at each AFB₂-OVA concentration may be explained by the concentration of antibody or conjugate used in the evaluation. As the antibody has 76% cross-reactivity with AFB₂, a high concentration of antibody was selected (1/200 dilution) to ensure a response could be achieved. However, at this concentration the antibody may have saturated the response. A lower concentration of antibody, would have resulted in more inhibited antibody and therefore, the reduced availability of free antibody, would have led to decreased antibody binding to the coated AFB₂-OVA conjugate and a decreased absorbance response across the varying coating concentrations of AFB₂-OVA. Alternatively, lowering the concentration of AFB₂-OVA coated on the plate to concentrations below 3 µg/mL may have exhibited the same decrease in the absorbance results. Though a difference in absorbance response was not evident between the varying AFB₂-OVA coating concentrations, an absorbance '0' (no competitor toxin) value in excess of 1 and a decreasing absorbance response with increased free AFB₂ concentrations was achieved. This indicated that AFB₂ was successfully conjugated to its protein carrier and was functional for screening purposes. A coating concentration maximum of 3 µg/mL was deemed acceptable for future anti-AFB₂ scFv antibody fragment screening experiments. The total protein concentration of AFB₂-OVA (2.9 mg/mL) was calculated using the Pierce™ BCA Protein Assay Kit, as described by the manufacturer's guidelines (Section 2.2.4).

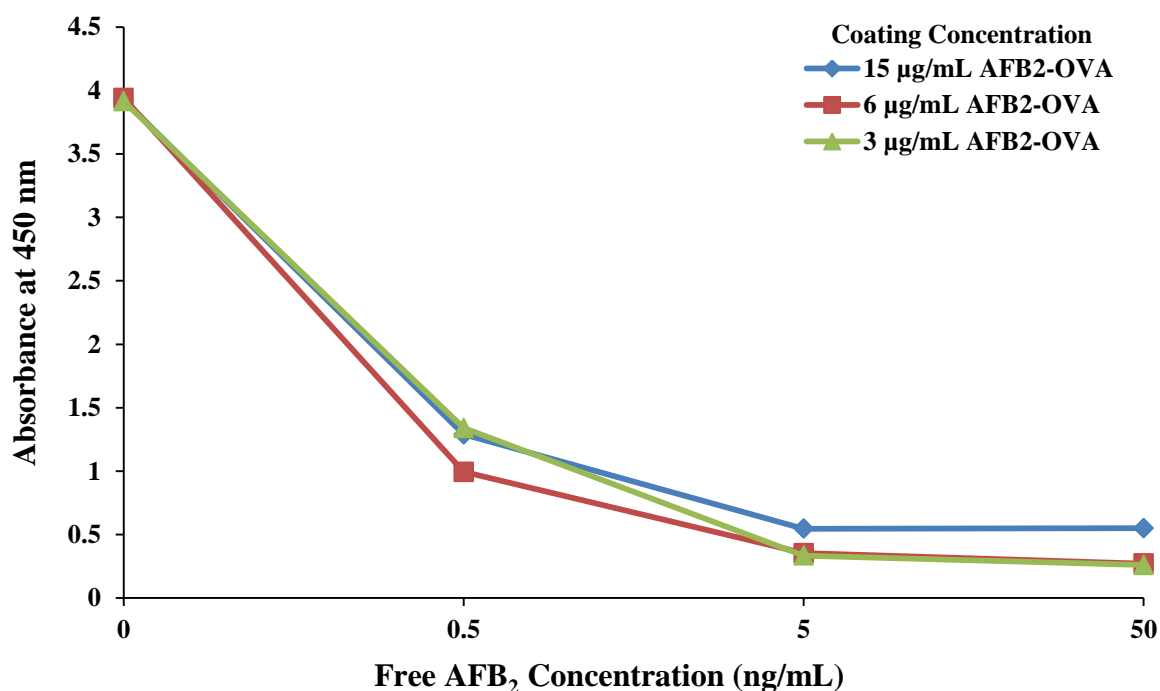


Figure 4.4: Competitive Inhibition ELISA with varying dilutions of AFB₂-OVA and free AFB₂ toxin against a 1/200 dilution of monoclonal antibody (76% CR with AFB₂). AFB₂-OVA (2.9 mg/mL) was diluted to 15, 6, and 3 µg/mL with PBS. Free AFB₂ (0, 0.5, 5 and 50 ng/mL) was prepared in PBST with 5% (v/v) methanol and allowed to incubate with a 1/200 dilution of mouse anti-AFB₁ monoclonal antibody with 76% cross reactivity to AFB₂ in PBST with 1% (w/v) Milk Marvel. A HRP-labelled anti-mouse secondary antibody diluted 1/20,000 in PBST with 1% (w/v) Milk Marvel was added, followed by TMB substrate. The reaction was stopped with 10% (v/v) HCl and absorbance was measured at 450nm using a Tecan Safire™ 2 plate reader. Experiments were performed with three replicates and results averaged (n = 1).

4.2.6. Monoclonal ELISA selection of anti-AFB₂ scFv antibody fragments

Monoclonal ELISA was completed to select specific anti-AFB₂ scFv expressing clones from an anti-AFB₂ scFv library previously generated and panned by Dr. Soujanya Ratna Edupuganti (2013). Anti-AFB₂ scFv-expressing clones (384) were selected from master plates, as described in Section 2.2.15. Briefly, each clone was used to inoculate 150 µL of SB media supplemented with 50 µg/mL of carbenicillin and 1% (w/v) glucose in 96 deep well plates and was then incubated at 37° C overnight while shaking at 250 rpm. The following day, 30 µL of the overnight culture was sub-cultured into 370 µL of fresh SB_{GC} media and incubated at 37°C while shaking at 220 rpm for 5 hours, at which point IPTG [0.1mM] was added. The cultures were then incubated overnight at the optimised

concentration of 30°C and 220 rpm and the following day were centrifuged at 3220g (Eppendorf 5810 R, Rotor A-4-62) for 40 minutes, pellet re-suspended in equilibration buffer [50 mM NaH₂PO₄, 300 mM NaCl, 10 mM imidazole, pH 7.5] and subjected to freeze-thawing cycles for cell lysis, as described in Section 2.2.20.1. The cultures were then centrifuged at 3220g (Eppendorf 5810 R, Rotor A-4-62) for 40 minutes and re-suspended 1:2 in PBST with 1% (w/v) Milk Marvel. The lysates were applied to a Nunc MaxiSorp® flat-bottom 96 well plate coated with 100 µL per well of a 1/1,000 dilution of AFB₂-OVA (3 µg/mL). Following washing, a HRP-labelled anti-HA secondary antibody was added followed by TMB substrate. The results in Figure 4.5 indicate numerous anti-AFB₂ clones elicited high responses against AFB₂. Therefore, an absorbance ‘cut-off’ point of 0.3 was determined and the 5 highest responding clones were selected for 100 mL (small-scale) expression studies, as described in Section 2.2.19.

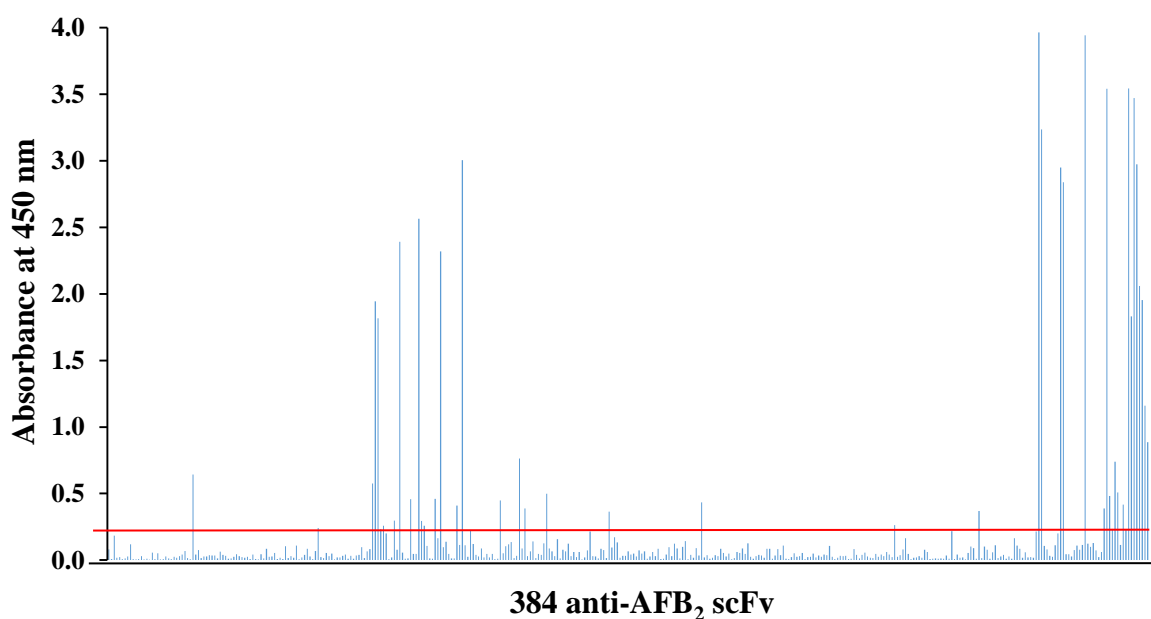


Figure 4.5: Anti-AFB₂ monoclonal ELISA of 384 anti-AFB₂ scFv-expressing clones. The lysate of clones expressing scFv antibody fragments were screened against 3 µg/mL of AFB₂-OVA diluted in PBS and coated on ELISA plates. A HRP-labelled anti-HA secondary antibody diluted 1/1,000 in PBST with 1% (w/v) Milk Marvel was added followed by TMB substrate. The reaction was stopped with 10% (v/v) HCl and absorbance was measured at 450 nm using a Tecan Safire™ 2 plate reader. The red line represents a ‘cut-off’ point of 0.3 and the 8 binders with the highest level of absorbance were selected for further analysis. Experiments were performed once (n = 1).

4.2.7. Expression, purification and indirect ELISA with varying dilutions of anti-AFB₂ scFv antibody fragments

Small-scale expression studies (100 mL), as described in Section 2.2.19, indicate if the clones can solubly express the anti-AFB₂ scFv for purification purposes. Purification using IMAC (Ni⁺-NTA) was completed, as described in Section 2.2.21. Following buffer exchange and concentration of the sample, the scFv antibody fragments expressed by each clone were applied neat, and at 1/100 and 1/1,000 dilutions in PBS to a plate coated with a 1/1,000 dilution of AFB₂-OVA (1 µg/mL). Clones 1, 2, 4, 5 and 7 expressed scFv antibody fragments that bound most successfully to AFB₂-OVA at all scFv concentrations, as shown in Figure 4.6. A negative control of 4% (w/v) OVA indicated no scFv binding to the carrier protein and that scFv binding was specifically to AFB₂. These clones were applied to SDS-PAGE and Western blotting analysis to investigate purity and if the expressed scFvs could be specifically probed for by HA-tagging.

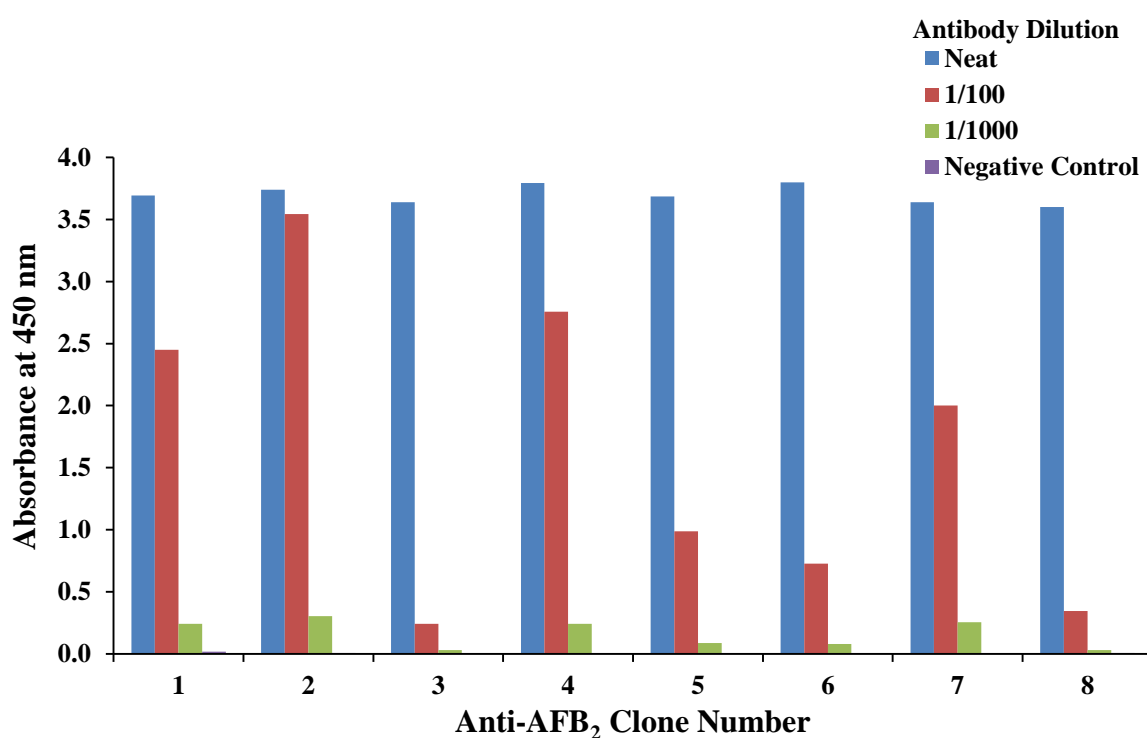


Figure 4.6: Indirect ELISA of 8 anti-AFB₂ scFv-producing clones neat, diluted 1/100 and 1/1,000. Anti-AFB₂ scFv antibody fragments purified using IMAC were tested against 1 µg/mL of AFB₂-OVA diluted in PBS and a negative control (4% (w/v) OVA) coated on ELISA plates. A HRP-labelled anti-HA secondary antibody diluted 1/1,000 in PBST with 1% Milk Marvel was added, followed by TMB substrate. The reaction was stopped with 10% (v/v) HCl and absorbance was measured at 450 nm using a Tecan Safire™ 2 plate reader. Experiments were performed with three replicates and results averaged (n = 1).

4.2.8. SDS-PAGE and Western blotting analysis of anti-AFB₂ scFv antibody fragments

The purified scFv products expressed by clones 1, 2, 4, 5 and 7 were analysed by SDS-PAGE and Western blotting analysis, as described in Section 2.2.24 and 2.2.25, respectively. ScFv antibody fragments are approximately 25 kDa in size, consisting of variable regions of the heavy (V_H) and light chains (V_L). Strong bands for clone 1, 2, and 7 at ~25 kDa can be seen in Figure 4.7 (A). However, Western blotting analysis was necessary to probe for the HA-tag which is incorporated into the scFv antibody fragment for specific detection. The anti-AFB₂ scFv antibody fragment can be seen at ~25 kDa in Figure 4.7 (B) indicating the desired anti-AFB₂ scFv antibody fragment had been probed for successfully in clones 1, 3, 4 and 7. From the SDS-PAGE and Western blotting analysis clone 1 appeared to have expressed the greatest and purest yield of anti-AFB₂ scFv antibody fragments. This clone was, therefore, tested in indirect ELISA, as described in Section 2.2.26.

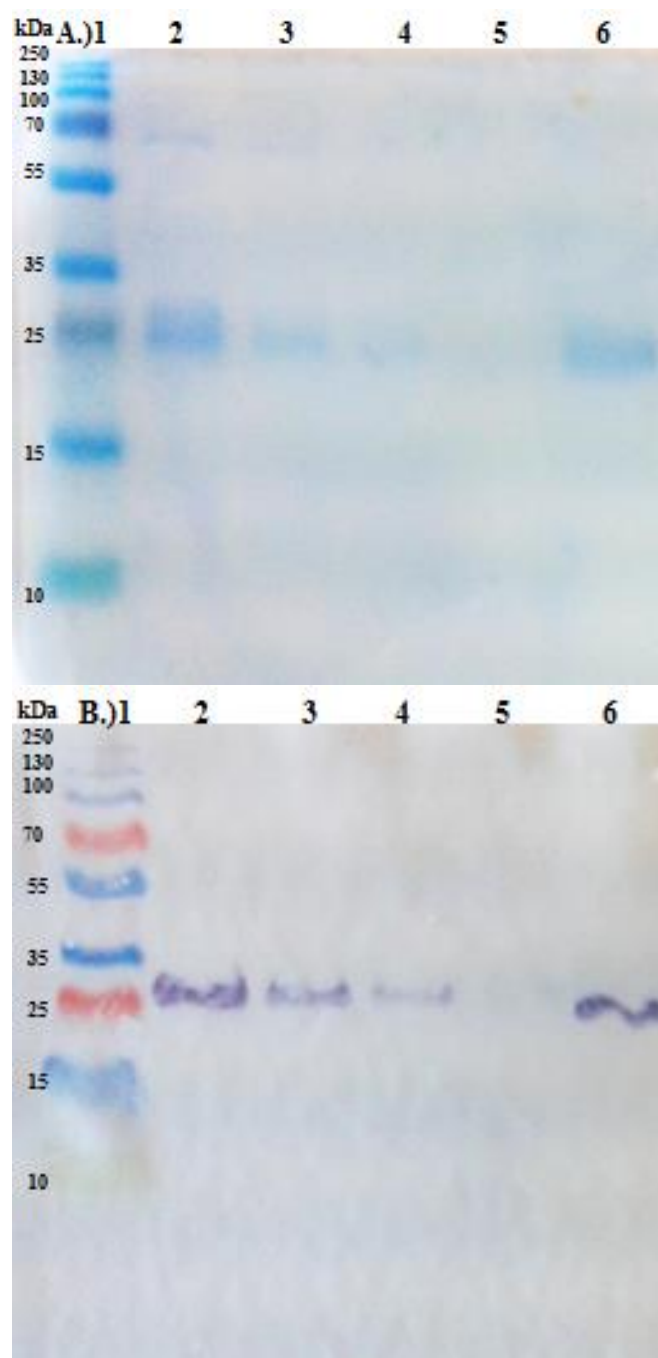


Figure 4.7: (A) SDS-PAGE and (B) Western blotting analysis of 5 expressed and IMAC-purified anti-AFB₂ scFv-producing clones. Samples were taken at all steps of the IMAC purification process, denatured and applied to a 12.5% acrylamide gel for separation based on charge and mass. (A) The proteins present in the samples were visualised by adding Instant Blue dye. (B) Proteins were transferred to nitrocellulose membrane and anti-AFB₂ scFvs probed with 1/1,000 HRP-labelled anti-HA antibody and TMB substrate. The size of the respective proteins was assessed based on the inclusion of a standard protein ladder (Pageruler Plus Prestained Protein Ladder). The expected denatured scFv protein band is present at approximately 25kDa. SDS-PAGE ((A) Lane 1: Ladder, Lane 2: Clone 1, Lane 3: Clone 3, Lane 4: Clone 4, Lane 5: Clone 5 and Lane 6: Clone 7). Western Blotting (B) Lane 1: Ladder, Lane 2: Clone 1, Lane 3: Clone 3, Lane 4: Clone 4, Lane 5: Clone 5 and Lane 6: Clone 7).

4.2.9. Indirect ELISA of a selected anti-AFB₁ scFv antibody fragment with varying concentrations of AFB₂-OVA

The results in Figure 4.7, indicate the anti-AFB₂ scFv antibody fragment expressed and purified from clone 1 produced a good titre of approximately 1/20,000 when tested in indirect ELISA against decreasing concentrations of AFB₂-OVA, shown in Figure 4.8. The selected anti-AFB₂ scFv antibody fragment was applied to indirect competitive inhibition ELISA to determine its IC₅₀ value, LoD and dynamic range, as described in Section 2.2.30.

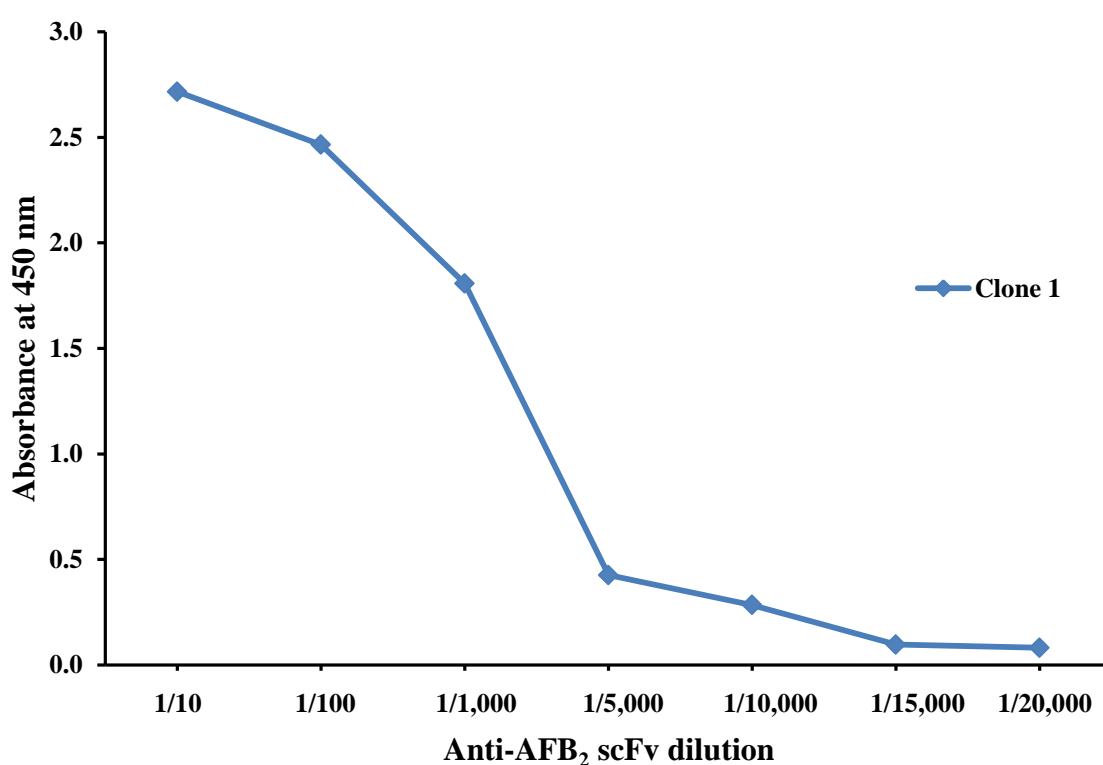


Figure 4.8: Indirect ELISA of AFB₂-OVA and selected anti-AFB₂ scFv antibody fragment at varying dilutions. AFB₂-OVA was in PBS (3 µg/mL) and used to coat an ELISA plate. The selected clone was diluted 1/10, 1/100, 1/1000, 1/5000, 1/10,000, 1/15,000 and 1/20,000 in PBST with 1% (w/v) Milk Marvel and applied to the ELISA plate. A HRP-labelled anti-HA secondary antibody diluted 1/1,000 in PBST with 1% (w/v) Milk Marvel was added, followed by TMB substrate. The reaction was stopped with 10% (v/v) HCl and absorbance was measured at 450 nm using a Tecan Safire™ 2 plate reader. Experiments were performed with three replicates and results averaged (n = 1).

4.2.10. Indirect competitive inhibition ELISA using anti-AFB₂ scFv antibody fragment and varying concentrations of free AFB₂ and AFB₂-OVA coating concentrations

The indirect competitive inhibition ELISA was repeated three times and Graphpad prism used to plot normalised absorbance against free AFB₂ concentrations mixed with anti-AFB₂ scFv antibody in a 1/500 dilution to determine the IC₅₀ value of the antibody. The IC₅₀ value was determined from Figure 4.9 representing, the free toxin concentration corresponding with the half maximum absorbance value and serves as a measure of the effectiveness of free AFB₂ toxin in inhibiting the specific biological interaction of anti-AFB₂ scFv antibody fragments with immobilized AFB₂-OVA on an ELISA plate. The IC₅₀ value was calculated at (2 µg/mL). The limit of detection was calculated at 2.35 µg/mL, as previously discussed in Section 4.2.2, using the formulae described by Armbruster and Fry (2008) and Tang *et al.* (2013). This indicated that though the anti-AFB₂ scFv antibody fragment was capable of binding to AFB₂ the level of sensitivity offered by the antibody was not deemed sufficient for further use in the detection of AFB₂ or future AFB₂ studies. Methods including site-directed mutations that affect the CDR of the antibody and light chain shuffling can be employed to overcome limited sensitivity, however, this was not feasible within the time-constraints of this project.

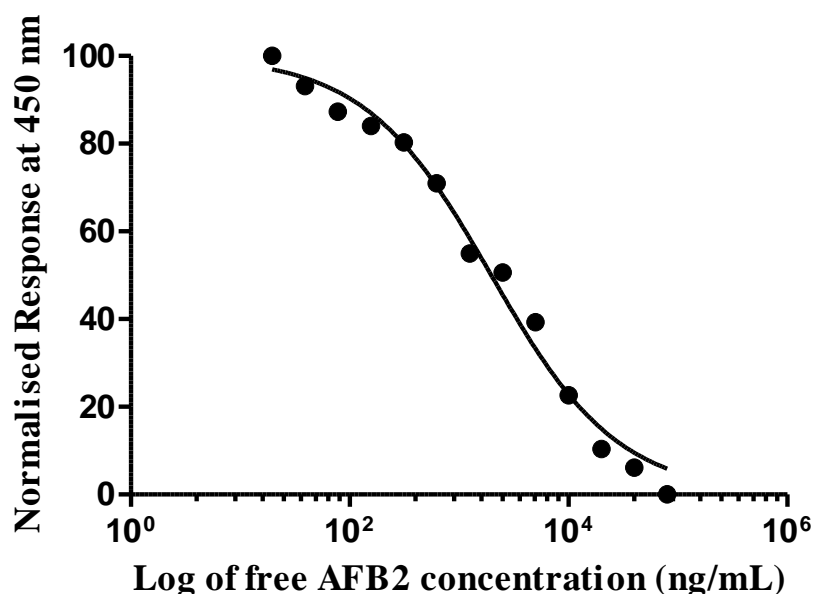


Figure 4.9: Indirect competitive inhibition ELISA with AFB₂-OVA and varying dilutions of free AFB₂ against the anti-AFB₂ scFv antibody fragment. AFB₂-OVA (3 µg/mL) was diluted in PBS (3 µg/mL) and coated on an ELISA plate. Doubling dilutions of free AFB₂ from 8 µg/mL down to 0 were prepared in PBST with 5% (v/v) methanol and allowed to incubate with a 1/500 dilution of anti-AFB₂ scFv antibody fragment (0.44 µg/mL) in PBST with 1% (w/v) Milk Marvel. A HRP-labelled anti-HA secondary antibody diluted 1/1,000 in PBST with 1% (w/v) Milk Marvel was added, followed by TMB substrate. The reaction was stopped with 10% (v/v) HCl and absorbance was measured at 450 nm using a Tecan Safire™ 2 plate reader. Experiments were performed with three replicates and results averaged (n = 1).

4.2.11. Evaluation criteria of ZEN conjugates

In order to screen and select previously generated anti-ZEN scFv antibody fragments ZEN-OVA conjugates had to be synthesised, as described in Section 2.2.3. To assess the integrity of the mycotoxin-conjugates synthesised ‘in-house,’ indirect competitive inhibition ELISA and evaluation was completed, as previously described in Section 4.3.5.

4.2.11.1 Evaluation of ZEN-OVA conjugate

Evaluation of the ZEN-OVA conjugate was completed through the use of indirect competitive inhibition ELISA using an anti-ZEN monoclonal antibody gifted from University Ghent, Belgium. The antibody was incubated with increasing concentrations of

free ZEN toxin (0-50 ng/mL) and was then applied to a plate coated with decreasing concentrations of ZEN-OVA conjugate (6, 3 and 1 µg/mL). A range of free inhibitor ZEN and immobilised ZEN-OVA concentrations were used to indicate if an absorbance '0' (no competitor toxin) value in excess of 1 and a decreasing absorbance response could be achieved. This occurs when the free ZEN binds, and, reduces availability of the anti-ZEN monoclonal antibody for immobilised ZEN-OVA interaction. The absorbance results in Figure 4.10 indicate an inverse response was elicited by the inhibited anti-ZEN monoclonal antibody which decreased when applied to the immobilised ZEN-OVA at all concentrations. The result also showed that when 6, 3 and 1 µg/mL of ZEN-OVA were immobilised, the absorbance '0' (no competitor toxin) value gave a much higher response (~3) than 1. This indicated that ZEN was successfully conjugated to its protein carrier and was functional for screening purposes at a concentration of 6, 3 and 1 µg/mL. The total protein concentration of ZEN-OVA (3.1 mg/mL) was calculated using the Pierce™ BCA Protein Assay Kit, as described by the manufacturer's guidelines (Section 2.2.4).

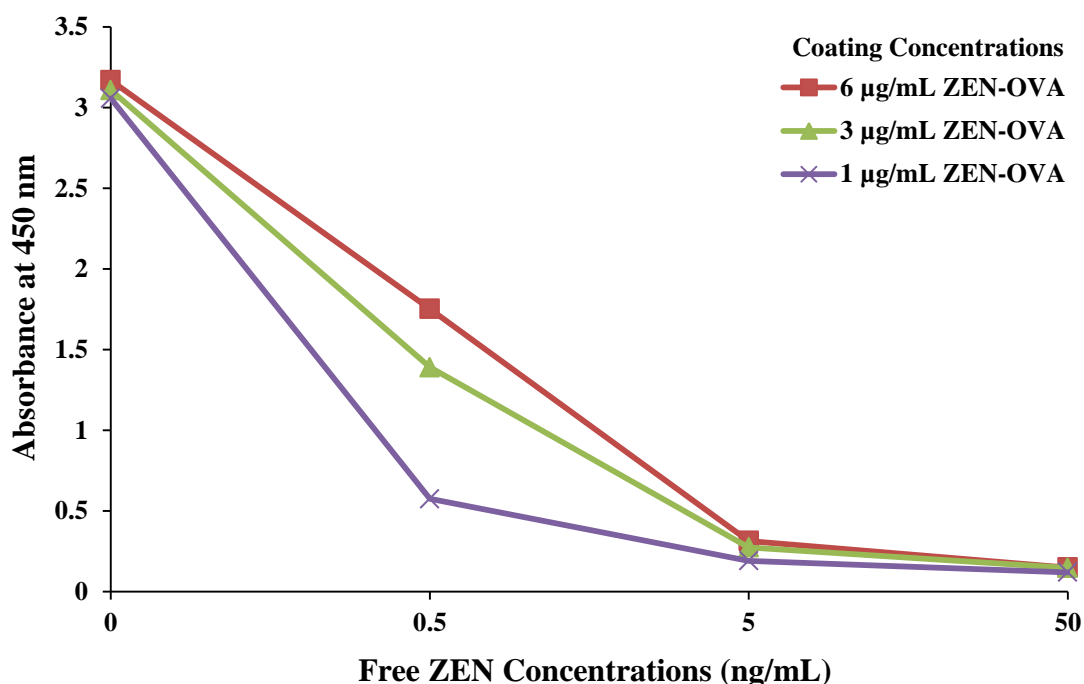


Figure 4.10: Competitive inhibition ELISA with varying dilutions of ZEN-OVA and free ZEN toxin against a 1/500 dilution of anti-ZEN antibody. ZEN-OVA (3.1 mg/mL) was diluted to 6, 3, and 1 µg/mL with PBS. Free ZEN (0, 0.5, 5 and 50 ng/mL) of was prepared in PBST with 5% (v/v) methanol and allowed to incubate with a 1/500 dilution of anti-ZEN monoclonal antibody in PBST with 1% (w/v) Milk Marvel. The mixed samples were applied to the ZEN-OVA coated plate. A HRP-labelled anti-mouse secondary antibody diluted 1/20,000 in PBST with 1% (w/v) Milk Marvel was added, followed by TMB. The reaction was stopped with 10% (v/v) HCl and absorbance was measured at 450 nm using a Tecan Safire™ 2 plate reader. Experiments were performed with three replicates and results averaged (n = 1).

4.2.12. Monoclonal ELISA selection of anti-ZEN scFv antibody fragments

Monoclonal ELISA was completed to select specific anti-ZEN scFv-expressing clones from an anti-ZEN scFv library previously built and panned by Dr. Soujanya Ratna Edupuganti (2013). Anti-ZEN scFv-expressing clones (288) were selected from masterplates, as described in Section 2.2.15. Briefly, each clone was used to inoculate 150 µL of SB media supplemented with 50 µg/mL of carbenicillin and 1% (w/v) glucose in 96 deep well plates and these were incubated at 37° C overnight while shaking at 250 rpm. The following day, 30 µL of the overnight culture was sub-cultured into 370 µL of fresh SB_{GC} media and incubated at 37° C while shaking at 220 rpm for 5 hours, at which point the IPTG [0.1mM] was added. The cultures were incubated overnight at the optimised temperature of 30° C while shaking at 220 rpm and the following day were centrifuged at

3220g (Eppendorf 5810 R, Rotor A-4-62) for 40 minutes, pellet re-suspended in equilibration buffer [50 mM NaH₂PO₄, 300 mM NaCl, 10 mM imidazole, pH 7.5] and subjected to freeze-thawing cycles for cell lysis, as described in Section 2.2.20.1. The cultures were centrifuged at 3220g (Eppendorf 5810 R, Rotor A-4-62) for 40 minutes. The pellet was re-suspended 1:2 in PBST with 1% (w/v) Milk Marvel. The lysates were applied to a Nunc MaxiSorp® flat-bottom 96 well plate coated with 100 µL of 1 µg/mL ZEN-OVA. Following washing three times with PBS and three times with PBST with 1% (w/v) Milk Marvel, a HRP-labelled anti-HA secondary antibody was added followed by TMB substrate. The results in Figure 4.11 indicate numerous anti-ZEN clones elicited high responses against ZEN. Therefore, an absorbance cut off point of 0.3 was determined and the 5 highest responding clones were selected for expression and purification studies and testing in indirect ELISA.

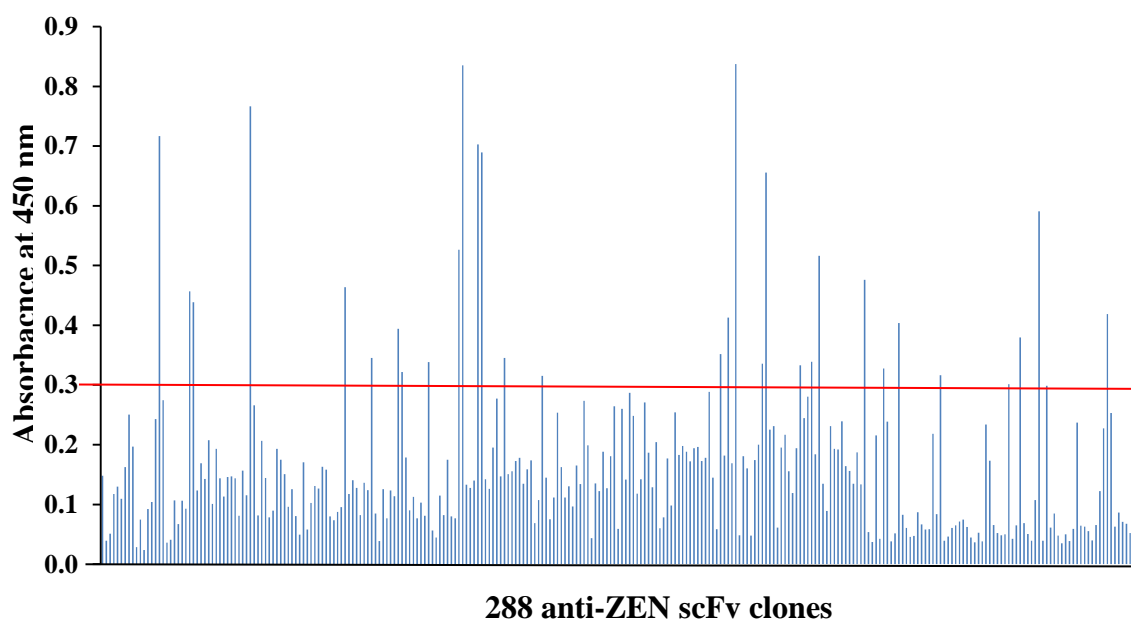


Figure 4.11: Anti-ZEN monoclonal ELISA of 288 anti-ZEN scFv-expressing clones. Anti-ZEN scFv-rich lysate was tested against 1 µg/mL of ZEN-OVA diluted in PBS and coated on ELISA plates. A HRP-labelled anti-HA secondary antibody diluted 1/1,000 in PBST with 1% (w/v) Milk Marvel was added followed by TMB substrate. The reaction was stopped with 10% (v/v) HCl and absorbance was measured at 450 nm using a Tecan Safire™ 2 plate reader. The red line represents a cut-off point of 0.3 and the 5 binders with the highest level of absorbance were selected for further analysis. Experiments were performed once (n = 1).

4.2.13. Expression, purification and indirect ELISA with varying dilutions of anti-ZEN scFv antibody fragments

Small-scale expression studies (100 mL), as described in Section 2.2.19, indicate if the clones can solubly express the anti-ZEN scFv for purification purposes. Purification using IMAC (Ni-NTA) was completed, as described in Section 2.2.21. Following buffer exchange and concentration of the sample, the scFv antibody fragments from clones 4, 14, 15, 21, 26 were diluted 1/10, 1/100, 1/1,000, 1/5,000 and 1/10,000 in PBS and tested in indirect ELISA, as described in Section 2.2.26. Clones 4, 14, 15, 21 and 26 were shown to express scFvs that bound successfully to ZEN-OVA at all antibody dilutions in Figure 4.12. However, clone 4 offered the highest absorbance reading across all dilutions and the greatest titre (~1/1,200). SDS-PAGE and Western blotting analysis were conducted to further characterise the anti-ZEN scFv antibody fragments.

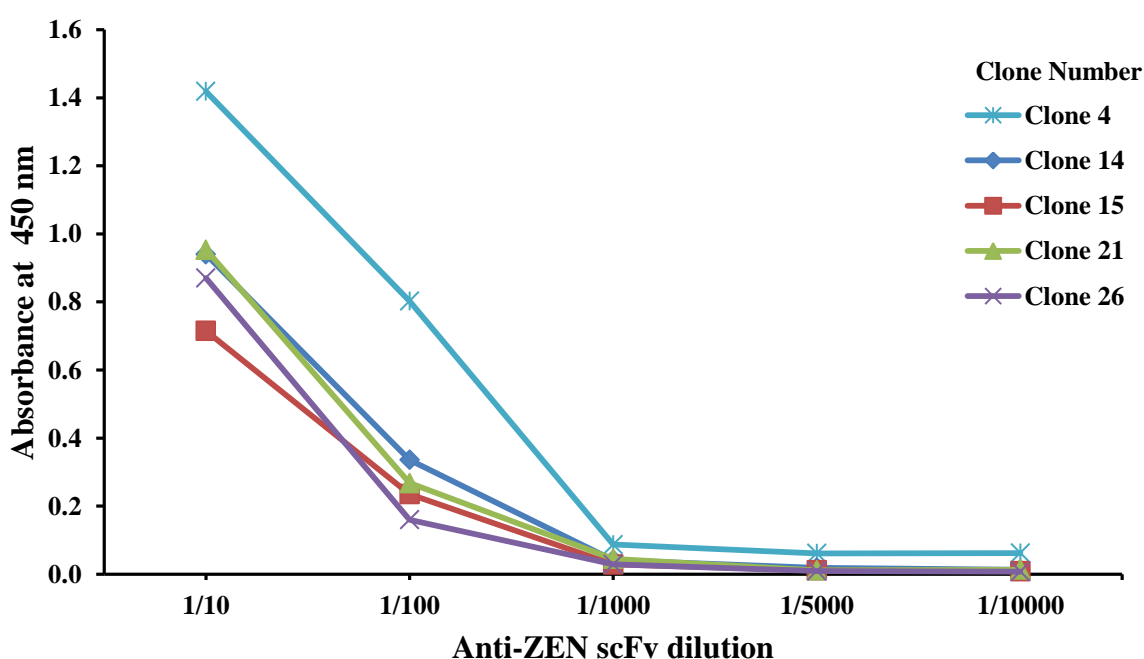


Figure 4.12: Indirect ELISA of ZEN-OVA and varying dilutions of anti-ZEN-expressing clones at varying dilutions. ZEN-OVA was diluted in PBS (3 µg/mL) and used to coat an ELISA plate. Each clone was diluted 1/10, 1/100, 1/1,000, 1/5,000 and 1/10,000 in PBST with 1% (w/v) Milk Marvel and applied to the ELISA plate. A HRP-labelled anti-HA secondary antibody diluted 1/1,000 in PBST with 1% (w/v) Milk Marvel was added, followed by TMB. The reaction was stopped with 10% (v/v) HCl and absorbance was measured at 450nm using a Tecan Safire™ 2 plate reader. Experiments were performed with three replicates and results averaged (n = 1).

4.2.14. SDS-PAGE and Western blotting analysis of anti-ZEN scFv antibody fragments

The purified scFv products expressed by Clone 4, 14, 15, 21 and 26 were analysed by SDS-PAGE and Western blotting analysis, as described in Sections 2.2.24 and 2.2.25. ScFv antibody fragments are approximately 25 kDa in size, consisting of variable regions of the heavy (V_H) and light chains (V_L). Bands at ~25 kDa can be seen in Figure 4.12 (A) and (C) representing the expected sized band of the anti-ZEN scFv antibody fragments in clones 4 and 21. Weaker bands can also be seen at this size for clones 15 and 26, whilst clone 14 appears very faintly. To determine that the bands present were that of anti-ZEN scFv antibody fragments, Western blotting analysis probing specifically for the HA tag of anti-AFB₂ scFv antibody fragment can be seen in Figure 4.13 (B) and (D). The nitrocellulose membrane was probed with HRP-labelled anti-HA antibody to detect the HA tag of anti-ZEN scFv antibody fragment. The anti-ZEN scFv antibody fragment can be seen at ~25 kDa indicating the desired anti-ZEN scFv antibody fragments were successfully detected.

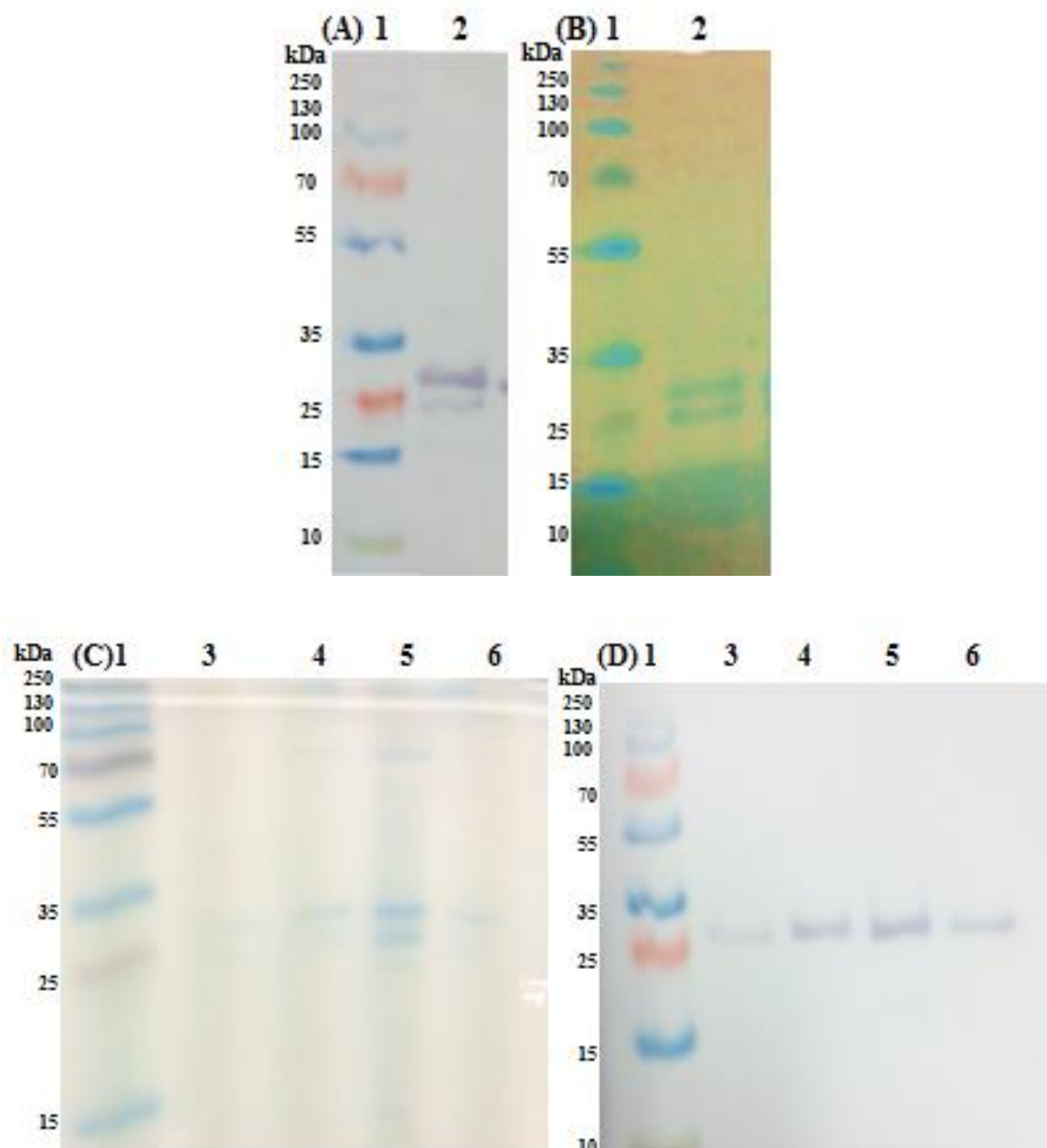


Figure 4.13: SDS-PAGE and Western blotting analysis of expressed and IMAC-purified anti-ZEN scFv-producing clones. SDS-PAGE (A) and Western blotting (B) analysis of clone 4. SDS-PAGE (C) and Western blotting (D) analysis of clones 14, 15, 21 and 26. Samples were taken at all steps of the IMAC purification process, denatured and applied to a 12.5% (w/v) acrylamide gel for separation based on charge and mass. The proteins present in the samples were visualised by adding Instant Blue dye. Proteins were transferred to nitrocellulose and anti-ZEN scFvs probed with a 1/1,000 HRP-labelled anti-HA antibody, followed by TMB substrate. The size of the respective proteins was assessed based on the inclusion of a standard protein ladder (Pageruler Plus Prestained Protein Ladder). The expected denatured scFv protein band is present at approximately 25 kDa. (A) Lane 1: Ladder; Lane 2: Clone 4; (B) Lane 1: Ladder; Lane 2: Clone 4; (C) Lane 1: Ladder; Lane 3: Clone 14; Lane 4: Clone 15; Lane 5: Clone 21; Lane 6: Clone 26; (D) Lane 1: Ladder; Lane 3: Clone 14; Lane 4: Clone 15; Lane 5: Clone 21; Lane 6: Clone 26).

4.2.15. Indirect checkerboard ELISA using varying concentrations of anti-ZEN scFv antibody fragments and ZEN-OVA coating concentrations

From the SDS-PAGE and Western blotting analysis clone 4 and clone 21 have expressed the greatest and purest yield of anti-ZEN scFv antibody fragments and, therefore, were selected for large-scale (1 litre) expression, as described in Section 2.2.19 and IMAC purification. Following this indirect checkerboard ELISA was completed to determine the optimal anti-ZEN scFv antibody fragment dilution of each clone and the optimal ZEN-OVA coating concentration for use in indirect competitive inhibition ELISA. Results shown in Figure 4.14 and Figure 4.15 indicate that the purified anti-ZEN scFv antibody fragments produced by clone 14 and clone 21, respectively, at multiple dilutions were not eliciting a response across a range of ZEN-OVA coating concentrations. This suggested there was an issue with both clones ability to bind ZEN. Previously completed indirect ELISA in Figure 4.13 using small- scale expression of these clones indicated that the scFv antibody fragments were binding their target and provided a titre of approximately 1/1,000. It was noted that clone 14 and clone 21 used for the indirect checkerboard ELISA were expressed from a large-scale (1 L) bacterial culture. Therefore, this factor may be related to the decrease in antibody specificity and activity. It was noted during large-scale expression that maintaining bacterial growth in overnight subcultures was not always possible, therefore, toxicity to the bacterial host may have been a problem. Toxicity is typically induced when the desired recombinant antibody fragment elicits a detrimental effect resulting in slower growth rate, low cell density and cell death. Conversely, the desired recombinant antibody fragment may provoke toxicity to the host which results in the incorrect functioning of the expression vector whilst the host still maintains viability. The recombinant anti-ZEN antibody fragment may have been having a toxic effect on the bacterial host environment, given that cell death was evident in some cultures and repeated attempts at culturing yielded low levels of non-functioning anti-ZEN scFv antibody fragments. As these antibodies were not eliciting the ability to bind their target, it was decided to exclude them from inclusion in future ZEN and mycotoxin studies.

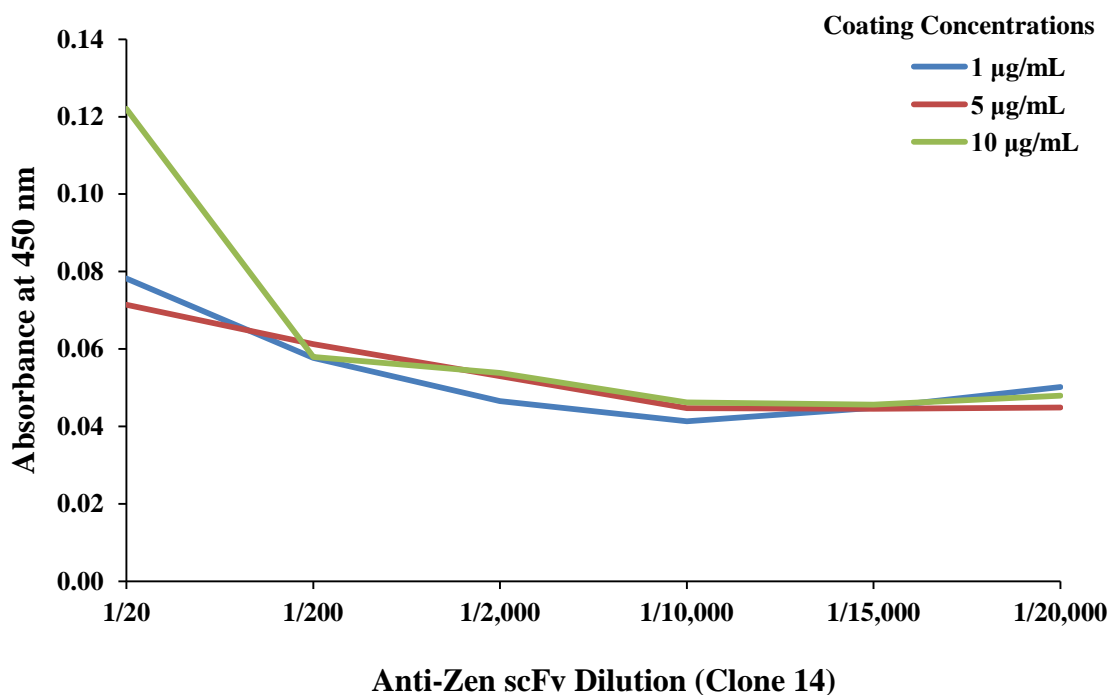


Figure 4.14: Indirect checkerboard ELISA of Clone 14 anti-ZEN scFv antibody fragment at varying dilutions against a range of ZEN-OVA coating concentrations. ZEN-OVA was diluted to 1, 5 and 10 µg/mL with PBS and used to coat an ELISA plate. Purified anti-ZEN scFv antibody fragment diluted at 1/20, 1/200, 1/2,000, 1/10,000, 1/15,000 and 1/20,000 in PBST with 1% (w/v) Milk Marvel was added to the plate. A HRP-labelled anti-HA secondary antibody diluted 1/1,000 in PBST with 1% (w/v) Milk Marvel was added to detect the anti-ZEN scFv antibody fragment followed by TMB. The reaction was stopped with 10% (v/v) HCl and absorbance was measured at 450 nm using a Tecan Safire™ 2 plate reader. Experiments were performed with three replicates and results averaged (n = 1).

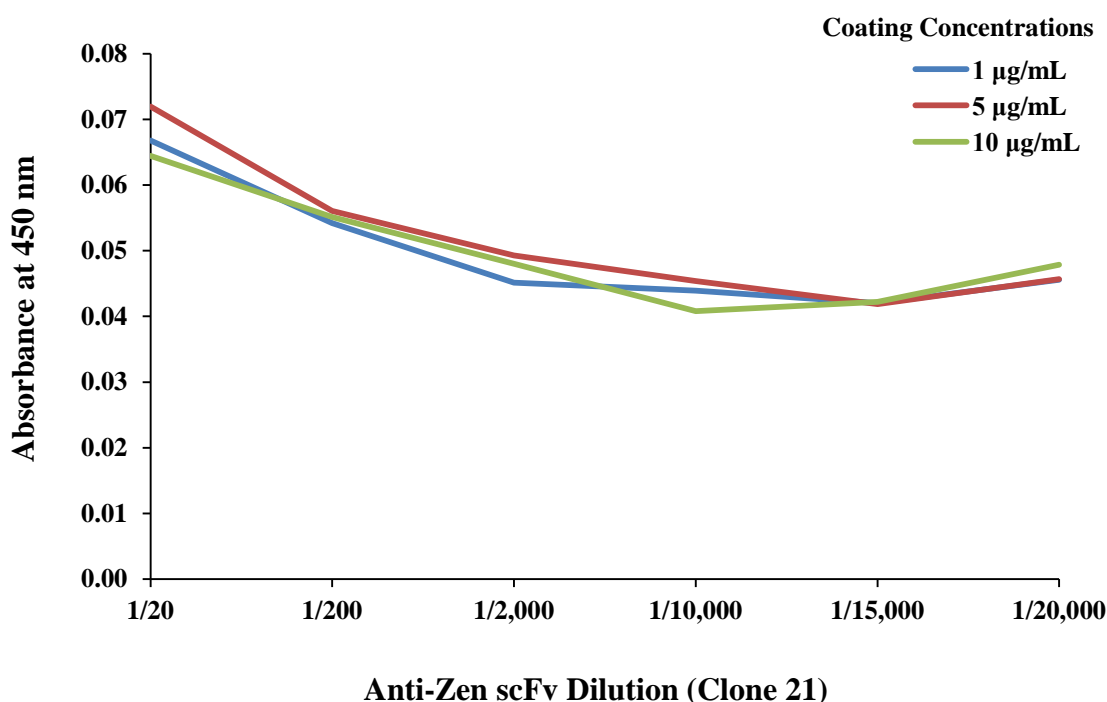


Figure 4.15: Indirect checkerboard ELISA of Clone 21 anti-ZEN scFv antibody fragment at varying dilutions against a range of ZEN-OVA coating concentrations. ZEN-OVA was diluted to 1, 5 and 10 µg/mL with PBS and used to coat an ELISA plate. Purified anti-ZEN scFv antibody fragment diluted at 1/20, 1/200, 1/2,000, 1/10,000, 1/15,000 and 1/20,000 in PBST with 1% (w/v) Milk Marvel was added to the plate. A HRP-labelled anti-HA secondary antibody diluted 1/1,000 in PBST with 1% (w/v) Milk Marvel was added to detect the anti-ZEN scFv antibody fragment followed by TMB. The reaction was stopped with 10% (v/v) HCl and absorbance was measured at 450 nm using a Tecan Safire™ 2 plate reader. Experiments were performed with three replicates and results averaged (n = 1).

4.2.16. MBio Testing and Analysis of AFB₁ in PBS

The MBio detection system provides a multiplex platform for the detection of multiple mycotoxins in a sample. The anti-AFB₁ Fab antibody fragment was tested in an indirect competitive inhibition assay to produce a standard curve and determine an IC₅₀ and limit of detection value, as described in Section 2.2.29. Indirect competitive inhibition assay on the MBio detection system was completed by incubating the anti-AFB₁ Fab with varying concentrations of free AFB₁ in PBS and testing against 50 µg/mL of AFB₁-BSA immobilised on the cartridge. GraphPad Prism 5 software was used to plot the normalized fluorescence against the range of free AFB₁ concentrations (Figure 4.16) and to determine the IC₅₀ value of the antibody in this assay. The IC₅₀ value was calculated at 0.51 ng/mL using Graphpad Prism 5 software. The limit of detection was calculated using the

competitive inhibition format, according to Armbruster and Pry (2008) and Tang *et al.* (2013) at 0.03 ng/mL. These results indicated that the anti-AFB₁ Fab antibody fragment was functioning to below stringent E.U. legislative limits for AFB₁ using the MBio multiplex mycotoxin detection system. The dynamic range of the AFB₁ MBio indirect competitive inhibition assay was determined based on the IC₁₀ – IC₉₀ of the assay and was calculated as 0.04 – 7.5 ng/mL.

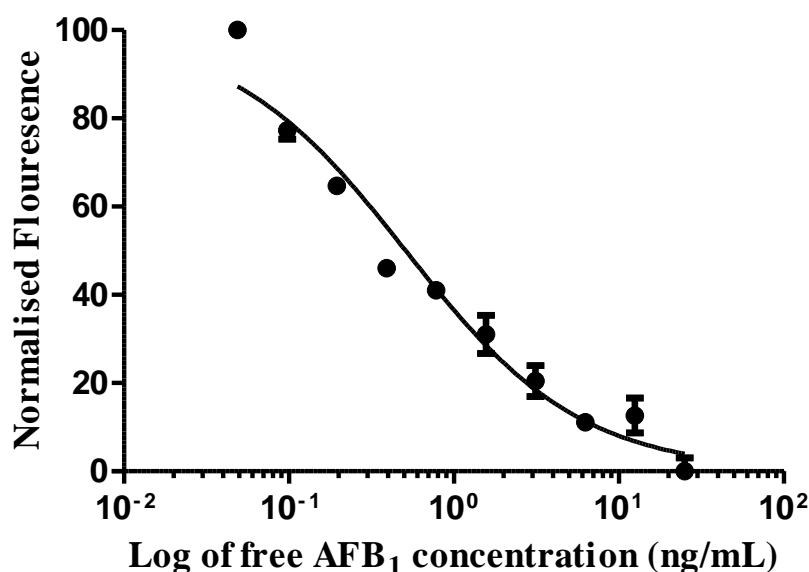


Figure 4.16: MBio Indirect Competitive Inhibition Assay with anti-AFB₁ Fab antibody fragment against free AFB₁ in PBS and immobilised AFB₁-BSA (50 µg/mL). AFB₁-BSA was previously spotted on an MBio Cartridge. Doubling dilutions of free AFB₁ from 50 ng/mL down to zero were prepared in PBS and allowed to incubate with 14 µg/mL anti-AFB₁ Fab in PBS. A 1/250 dilution of goat anti-mouse IgG (H+L) secondary antibody labelled with Alexa Fluor 647, in PBS was added for detection. The fluorescence was measured at 647 nm using the MBio detection platform. Experiments were performed twice with two replicates and the results averaged (n = 2). Errors bars represent the standard error of the mean (SEM) calculated by dividing the standard deviation by the square root of the n number using Graphpad Prism 5 software.

4.2.17. MBio Testing and Analysis of T-2 Toxin in PBS

The anti-T-2 toxin polyclonal antibody was tested in an indirect competitive inhibition assay to produce a standard curve and determine an IC₅₀ and limit of detection value, as described in Section 2.2.29. Indirect competitive inhibition assay on the MBio detection

system was completed by incubating the anti-T-2 toxin antibody fragment with varying concentrations of free T-2 toxin in PBS and testing against 50 µg/mL of T-2 toxin-BSA immobilised on the cartridge. GraphPad Prism 5 software was used to plot the normalized fluorescence against the range of free T-2 toxin concentrations (Figure 4.17) and to determine the IC₅₀ value of the antibody in this assay. The IC₅₀ value was calculated at 0.9 ng/mL using Graphpad Prism 5 software. The limit of detection was calculated at 0.51 ng/mL using the competitive inhibition format, according to Armbruster and Pry (2008) and Tang *et al.* (2013). These results indicated that the anti-T-2 toxin polyclonal antibody was functioning to below stringent E.U. legislative limits for T-2 toxin using the MBio multiplex mycotoxin detection system. The dynamic range of the T-2 toxin MBio indirect competitive inhibition assay was determined based on the IC₁₀ – IC₉₀ of the assay and was calculated as 0.08 – 10 ng/mL.

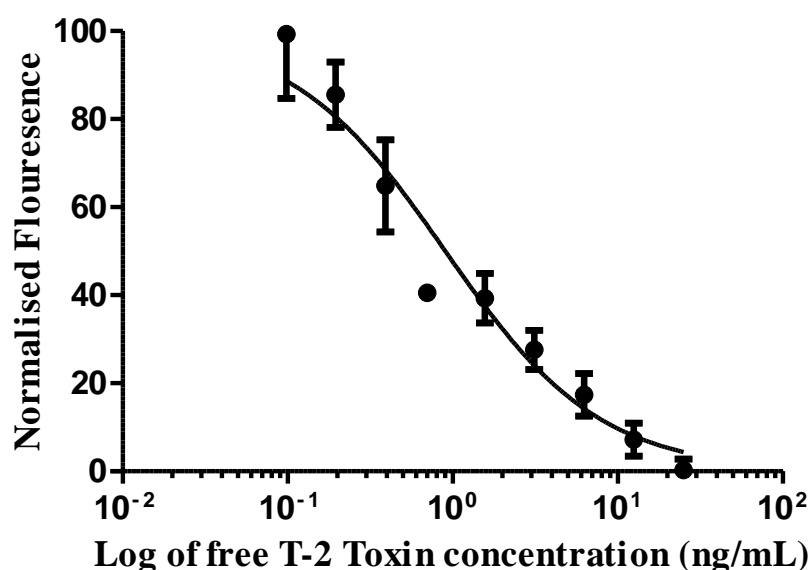


Figure 4.17: MBio Indirect Competitive Inhibition Assay with anti-T-2 toxin polyclonal antibody fragment against free T-2 toxin in PBS and immobilised T-2 toxin-BSA (50 µg/mL). T-2 toxin-BSA was previously spotted on an MBio Cartridge. Doubling dilutions of free T-2 toxin from 25 ng/mL down to zero were prepared in PBS and allowed to incubate with 1/500 dilution of anti-T-2 toxin polyclonal antibody in PBS. A 1/250 dilution of goat anti-rabbit IgG (H+L) secondary antibody labelled with Alexa Fluor 647, in PBS was added for detection. The fluorescence was measured at 647 nm using the MBio detection platform. Experiments were performed twice with two replicates and the results averaged (n = 2). Errors bars represent the standard error of the mean (SEM) calculated by dividing the standard deviation by the square root of the n number using Graphpad Prism 5 software.

The values outlined in Table 4.1 suggest that the anti-AFB₁ Fab antibody fragment and the T-2 toxin polyclonal antibody are capable of functioning well in PBS in the MBio detection system. Consequently, the antibodies were applied to the generation of standard curves for AFB₁ and T-2 toxin in DDGS samples and for analysis of spiked DDGS sample. Furthermore, comparison with ELISA methods for AFB₁ and T-2 toxin detection indicate increased IC₅₀ value, LoD and dynamic range sensitivities (Table 4.1) with use of the MBio assay for mycotoxin detection.

Table 4.1: ELISA and MBio assay results for AFB₁ and T-2 Toxin spiked PBS standard curve

Test		IC ₅₀ value (ng/mL)	Limit of Detection (ng/mL)	Dynamic Range (ng/mL)
ELISA	AFB₁	7.33	1.54	1 - 54
	T-2 Toxin	8.5	5.8	0.3 - 327
MBio	AFB₁	0.51	0.03	0.035 – 7.5
	T-2 Toxin	0.9	0.51	0.08 – 10

4.2.18. MBio Testing and Analysis of AFB₁ spiked in DDGS extract

The MBio detection system was utilised to investigate the detection of AFB₁ and T-2 toxin in contaminated DDGS samples. The anti-AFB₁ Fab antibody fragment was used in an indirect competitive inhibition assay, as described in Section 2.2.29 to produce a standard curve and determine the concentration of AFB₁ extracted from a contaminated DDGS sample. Extraction of contaminated DDGS and blank DDGS samples were completed with 80:20% (v/v) water:methanol solution, as described in Section 2.2.33. Indirect competitive inhibition assay on the MBio detection system was completed by incubating the anti-AFB₁ Fab with varying concentrations of free AFB₁ (50 – 0.39 ng/mL) in blank DDGS extract against 50 µg/mL of AFB₁-BSA immobilised on the cartridge. GraphPad Prism 5 software was used to plot the normalized fluorescence against the range of free AFB₁ concentrations (Figure 4.18) and to determine the IC₅₀ value of the antibody in this assay. The IC₅₀ value was calculated at 10.15 ng/mL using Graphpad Prism 5 software. The limit of detection was calculated using the competitive inhibition assay format to test 3 blank replicates and 3

low concentration analyte replicates, according to the equations described by Armbruster and Pry (2008) and Tang *et al.* (2013). The limit of detection was determined as 4.12 ng/mL. DDGS blank extracts were then spiked with 5 ng/mL of AFB₁ and tested on the MBio device to determine recovery and delivered a 112% recovery. These results indicated that the anti-AFB₁ Fab antibody fragment was functioning to below stringent E.U. legislative limits for AFB₁ in feed using the MBio multiplex mycotoxin detection system. The dynamic range of the AFB₁ MBio indirect competitive inhibition assay in spiked DDGS samples was determined based on the IC₁₀ – IC₉₀ of the assay and was calculated as 2.1 – 48.82 ng/mL.

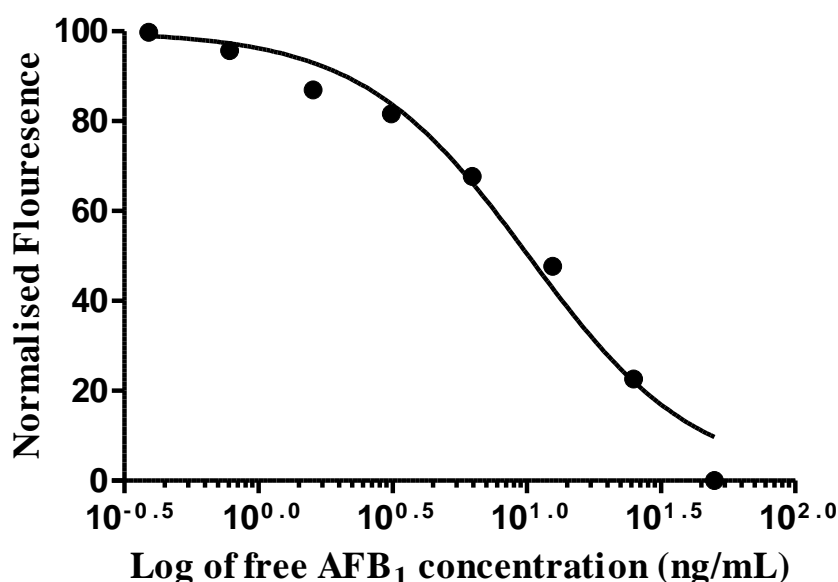


Figure 4.18: MBio Indirect Competitive Inhibition Assay with anti-AFB₁ Fab antibody fragment against free AFB₁ in DDGS extract and immobilised AFB₁-BSA (50 µg/mL). AFB₁-BSA was previously spotted on an MBio Cartridge. Doubling dilutions of free AFB₁ from 50 ng/mL down to 0 were prepared in blank DDGS extract and allowed to incubate with 14 µg/mL anti-AFB₁ Fab in PBS. A 1/250 dilution of goat anti-mouse IgG (H+L) secondary antibody labelled with Alexa Fluor 647, in PBS was added for detection. The fluorescence was measured at 647 nm using the MBio detection platform. Experiments were performed with two replicates and results averaged (n = 1).

4.2.19. MBio Testing and Analysis of T-2 toxin spiked in DDGS extract

The anti-T-2 toxin polyclonal antibody was used in an indirect competitive inhibition assay to produce a standard curve and determine the concentration of T-2 toxin extracted from a contaminated DDGS sample. Extraction of contaminated DDGS and blank DDGS samples were completed with 80:20% (v/v) water:methanol solution, as described in Section 2.2.33. Indirect competitive inhibition assay on the MBio detection system was completed, as described in Section 2.2.29 by incubating the anti-T-2 toxin polyclonal antibody with varying concentrations of free T-2 toxin (25 – 0.39 ng/mL) in blank DDGS extract against 50 µg/mL of T-2 toxin immobilised on the cartridge. GraphPad Prism 5 software was used to plot the normalized fluorescence against a range of known, free T-2 toxin concentrations (Figure 4.19) and to determine the IC₅₀ value of the antibody in this assay. The IC₅₀ value was calculated at 12.2 ng/mL using Graphpad Prism 5 software. The limit of detection was calculated using the competitive inhibition assay format to test 3 blank replicates and 3 low concentration analyte replicates, according to the equations described by Armbruster and Pry (2008) and Tang *et al.* (2013). The limit of detection was determined as 5.08 ng/mL. DDGS blank samples were then spiked with 10 ng/mL of T-2 toxin and tested on the MBio device to determine recovery and delivered a 120% recovery. These results indicated that the anti-T-2 polyclonal antibody was functioning to below stringent E.U. legislative limits for T-2 toxin using the MBio multiplex mycotoxin detection system. The dynamic range of the T-2 MBio indirect competitive inhibition assay in spiked DDGS samples was determined based on the IC₁₀ – IC₉₀ of the assay and was calculated as 0.6 – 11.9 ng/mL.

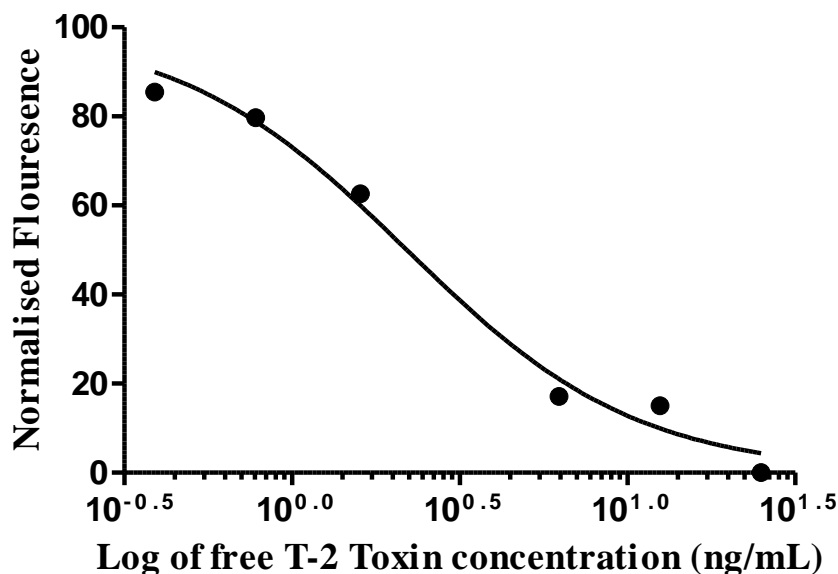


Figure 4.19: MBio Indirect Competitive Inhibition Assay with anti-T-2 toxin polyclonal antibody against free T-2 toxin in DDGS extract and immobilised T-2 toxin-BSA (50 µg/mL). T-2 toxin-BSA was previously spotted on an MBio Cartridge. Doubling dilutions of free T-2 toxin from 25 ng/mL down to 0 were prepared in blank DDGs extract and allowed to incubate with 1/250 dilution of anti-T-2 toxin polyclonal antibody in PBS. A 1/250 dilution of goat anti-rabbit IgG (H+L) secondary antibody labelled with Alexa Fluor 647, in PBS was added for detection. The fluorescence was measured at 647 nm using the MBio detection platform. Experiments were performed with two replicates and results averaged (n = 1).

The values outlined in Table 4.2 suggest that the anti-AFB₁ Fab antibody fragment and the T-2 toxin polyclonal antibody are capable of functioning well in DDGS extracts in the MBio detection system. Consequently, the antibodies were applied to a ‘proof-of-concept’ study for simultaneous detection of AFB₁ and T-2 toxin in a contaminated DDGS sample.

Table 4.2: MBio assay results for AFB₁ and T-2 Toxin spiked DDGS standard curve and spiked extract tests

	IC ₅₀ value (ng/mL)	Limit of Detection (ng/mL)	Dynamic Range (ng/mL)	Spiked Recovery (%)
AFB₁	10.15	4.12	2.1 – 48.82	112
T-2 Toxin	12.2	5.08	0.6 – 11.9	120

4.2.20. MBio Multiplex Testing and Analysis of AFB₁ and T-2 toxin in Contaminated DDGS samples

The anti-AFB₁ Fab antibody fragment and anti-T-2 toxin polyclonal antibody were used in a ‘proof-of-concept’ experiment to determine if AFB₁ and T-2 toxin could be detected simultaneously from a contaminated DDGS sample in a multiplex approach. Extraction of AFB₁ and T-2 toxin from contaminated DDGS was completed simultaneously with 80% (v/v) water:methanol solution, as described in Section 2.2.33. Indirect competitive inhibition assay on the MBio detection system was completed, as described in Section 2.2.29.1 by incubating the anti-AFB₁ Fab and the anti-T-2 toxin polyclonal antibody with the AFB₁ and T-2 toxin-contaminated DDGS extract and testing against 50 µg/mL of AFB₁-BSA and T-2 toxin immobilised on the cartridge. The unknown concentrations of AFB₁ and T-2 toxin were extrapolated using GraphPad Prism 5 software from the standard curves described in Section 4.2.20 for AFB₁ and described in Section 4.2.21 for T-2 toxin. The test was completed twice on two separate cartridges and results are presented in Table 4.3.

AFB₁ was successfully detected at 12.1 ng/mL and 10.3 ng/mL calculable as 16.1 µg/kg and 13.7 µg/kg respectively and giving an average recovery of 98% recovery in comparison with UPLC-MS/MS methods. The coefficient of variance (CV%) was calculated as 11%. T-2 toxin was detected at 7.09 ng/mL and 5.08 ng/mL calculable as 9.5 µg/kg and 6.7 µg/kg and giving an average recovery of 69% in comparison with UPLC-MS/MS methods. The CV% was calculated as 24%.

Table 4.3: Multiplex analysis of DDGS sample to test AFB₁ and T-2 toxin concentration

Reference Sample		MBio Assay Performance (<i>n</i> = 2)		
AFB ₁ (µg/mL)	AFB ₁ (µg/mL)	Recovery (%)	CV (%)	
15.2	16.1	106	10.6	
	13.7	90	12	
Average	14.9	98	11	
T-2 Toxin (µg/mL)	T-2 Toxin (µg/mL)	Recovery (%)	CV (%)	
11.8	9.45	80	20	
	6.70	57	28	
Average	8.1	69	24	

These results show that the anti-AFB₁ Fab antibody fragment and the anti-T-2 toxin polyclonal antibody in conjunction with the MBio detection system can deliver a simple, ‘point-of-site’ detection platform that delivers detection at EU legislative limits for T-2 toxin and AFB₁. The simultaneous detection of both mycotoxins also provides a ‘proof-of-concept’ for the multiplex detection of mycotoxins and suggests other mycotoxins or multiple mycotoxins could be detected using this assay format. This would be greatly beneficial for multi-mycotoxin analysis directly in the field, allowing users including farmers and millers to determine if, and what, mycotoxins are affecting their products and feeds.

4.3 Discussion

Due to the severe effects caused by mycotoxin exposure in humans and animals, foods and animal feeds must be monitored to detect the presence of harmful contaminants. Food safety is a global concern with many Government bodies and regulatory authorities establishing mycotoxin limits in numerous food and feed commodities. To ensure the regulatory limits are adhered to, suitable detection system must be available to identify and quantify mycotoxins occurring in the food supply chain. Despite the vast utilization of chromatography and mass spectrometry methods in mycotoxin analysis, farmers, millers, customs, and small industrial producers need rapid, easy, high-throughput, and preferably portable screening methods and devices (Arola *et al.*, 2016). The purpose of this chapter was to obtain specific antibody fragments against target mycotoxins, for incorporation in an MBio multiplex optical-planar waveguide biosensor device capable of detecting mycotoxins in Dried Distillers Grain with Solubles (DDGS) animal feed to EU legislative levels. In this study the selection, expression, purification and characterisation of anti-AFB₁ Fab, anti-AFB₂ scFv and anti-ZEN scFv antibody fragments was presented. As previously highlighted, recombinant antibody fragments which can be integrated in simple immunoassays for ‘point-of-site’ testing, can provide a solution to laboratory-based mycotoxin analysis.

In this work a previously isolated HIS tagged anti-AFB₁ Fab antibody fragment was successfully expressed in *E. coli* and purified by IMAC followed by size exclusion chromatography. SDS-PAGE and Western blotting analysis confirmed the expression and purity of the Fab antibody fragment. Both the heavy and light chains of the fragment were evident at approximately 25 kDa following denaturation. The Fab was then tested in indirect ELISA and indirect competitive inhibition ELISA. These experiments indicated that the anti-AFB₁ Fab antibody fragment had an IC₅₀ value of 7.33 ng/mL. The LoD was calculated at 1.7 ng/mL. Therefore, the anti-AFB₁ Fab antibody fragment was very sensitive and could detect AFB₁ down to the EU maximal allowable levels of 2 - 4 ppb in foods for direct consumption and, was suitable for further testing within the MBio multiplex optical-planar waveguide biosensor system.

To enable the selection, screening and ELISA-based testing of the anti-AFB₂ scFv and anti-ZEN scFv antibody fragments, the synthesis of functional mycotoxin-conjugates was

necessary. Competitive inhibition ELISA using decreasing concentrations of AFB₂-OVA and ZEN-OVA showed that the inhibited antibodies gave decreasing absorbance responses and indicated that the AFB₂-OVA (15, 6 and 3 µg/mL) and ZEN-OVA (6, 3 and 1 µg/mL) conjugate complexes delivered absorbance values in excess of 1. This indicated that AFB₂ and ZEN had been successfully coupled to OVA and that the conjugates could be used for screening and selection of anti-AFB₂ and anti-ZEN scFv antibody fragments.

Following the successful synthesis of AFB₂-OVA and ZEN-OVA, screening of previously constructed murine anti-AFB₂ and anti-ZEN scFv libraries were undertaken. Clones from the anti-AFB₂ (384) and anti-ZEN (288) scFv libraries were successfully evaluated by monoclonal ELISA, SDS-PAGE, Western blotting analysis and indirect ELISA to select sensitive AFB₂ and ZEN binders. An anti-AFB₂ scFv was selected and applied to indirect competitive inhibition ELISA and delivered an IC₅₀ value of 2.35 µg/mL and a limit of detection of 2 µg/mL using methods described by Armbruster and Pry and Tang *et al.* AFB₂ is tested for within the current EU legislation, as part of ‘total aflatoxin’ maximal levels, which are set out at 5-10 ppb. Therefore, the selected anti-AFB₂ scFv antibody fragment was not deemed to have the required sensitivity for detection at EU levels and was not selected for further analysis on the MBio detection system. Several approaches can be taken to increase recombinant antibody specificity. The binding pocket of a scFv antibody fragment and its antigen can be optimised to deliver increased binding and affinity using specific structure driven mutations that affect the CDR of the antibody. However, this process relies on X-ray crystallography data to provide insights on the binding interaction (Thakkar *et al.*, 2014), the collection of which data was not feasible within this study. Light chain shuffling can be employed to obtain improved combinations of V_H and V_L chain pairings and circumvent limited affinity maturation. Previous work by Fitzgerald involving the amplification of un-panned light chains and panned heavy chains of the target library increased the sensitivity of a halofuginone-specific scFv antibody with limits of detection of 30 ng/mL to limits as low as 80 pg/ml (Fitzgerald, 2011). This method is limited by the need for the un-panned light chain of the necessary library which had been previously completed and was not available for use. Alternatively, higher affinity mutant scFvs may be more easily generated by site-directed mutagenesis. In this process the importable variable regions or residues critical to binding activity are identified from sequence analysis and custom designed oligonucleotide primers are utilised to confer a desired mutation to the vector of interest allowing mutants with higher affinity to be

created (Ahmad *et al.*, 2012). In particular, alanine scanning is a technique used to determine the contribution of a specific residue to the stability or function of given protein and can also be used to determine whether the side chain of a specific residue plays a significant role in binding or bioactivity. Single amino-acid substitutions can then be incorporated into the CDR regions using specifically designed site-specific primers. The site-directed mutagenesis can then be performed using PCR amplification and splice by overlap-extension reactions to produce a fully mutated scFv antibody fragment (Morrison and Weiss, 2001; Moreira *et al.*, 2007). Therefore, though the selected anti-AFB₂ scFv antibody fragment did not achieve the required level of specificity, it provides an excellent scaffold for future mutagenic studies to enhance affinity and achieve sensitivities suitable for inclusion in the proposed multiplex optical-planar waveguide biosensor device for AFB₂ detection.

Anti-ZEN scFv antibody fragments from small-scale expression (100 mL cultures) and purification of each clone were successful, however, scaling-up of the expression process had to be completed to provide sufficient quantity of scFv antibody for use in indirect competitive inhibition ELISA and potentially for use in the MBio detection system. This process had a detrimental effect on the anti-ZEN scFv antibody fragments. Following the expression of the scFvs in 1 litre cultures, the antibodies expression rate and ability to perform in indirect ELISA was lost. As the anti-ZEN scFv antibody fragments were no longer functioning as desired, these antibody fragments were not selected for further analysis in the MBio detection system. Expression of scFv antibody fragments can be subject to the formation of unstable aggregates that can be degraded by the cell, however issues are typically symptomatic of cytoplasmic expression where disulphide bonds cannot be formed in the reducing environment (Guglielmi and Martineau, 2009). The anti-ZEN scFv antibody fragments were targeted to the oxidising environment of the periplasm to avoid such problems. It was noted that there was difficulty in maintaining bacterial growth when expressing the scFv antibody fragment therefore, toxicity to the host may have been a problem. Toxicity may arise when the expressed recombinant antibody fragment performs an unnecessary and detrimental function in the host cell. This function hinders the normal proliferation and homeostasis of the bacteria and the visible result is slower growth rate, low cell density, and cell death. Alternatively, if the recombinant antibody fragment is toxic to the cell, genetic reorganization of the expression vector leading to loss of activity may occur, however, the host may survive and eventually take over the culture.

This may have been evident for the anti-ZEN scFv antibody fragments as though cell death was evident in some cultures, repeated attempts at culturing yielded low levels of anti-ZEN scFv antibody fragments. Furthermore, point mutations, deletions, insertions, or rearrangement may explain low activity of a purified recombinant protein and ascertain to the unsuccessful application of the anti-ZEN scFv antibody fragments in indirect checkerboard ELISA. Protein inactivity can also occur due to incomplete folding were the protein adopts a stable soluble conformation but the exact architecture of the active site is still unsuitable for activity. Incorrect disulfide bond formation can also induce inactivity (Rosano and Ceccarelli, 2014). Some *E. coli* mutants (e.g. C41(DE3) and C43(DE3)) have been shown to withstand the expression of toxic proteins (Miroux and Walker, 1996). Alternatively other approaches in garnering successful expression of recombinant antibody fragments have included, co-expression of molecular chaperones and folding modulators (e.g. *skp* and osmotically inducible protein Y), re-folding using detergent or additives and expression in alternative host systems (Ahmed *et al.* 2012; Wang *et al.* 2013). The selected anti-ZEN scFv antibody fragment could be optimised for expression by undertaking these approaches.

The anti-AFB₁ Fab antibody fragment and the anti-T-2 polyclonal antibody (Chapter 3) were integrated with the MBio detection system for analysis of AFB₁ and T-2 toxin in PBS and DDGS. Initial testing using AFB₁ and T-2 toxin diluted in PBS was completed to ensure the MBio system and required antibodies were functioning. This testing indicated that the MBio system in conjunction with the anti-T-2 toxin polyclonal antibody could deliver increased sensitivity when compared to previous ELISA testing. The IC₅₀ and LoD values decreased from 8.5 to 0.9 ng/mL and 5.8 to 0.51 ng/mL, respectively. This increase in sensitivity was also demonstrated for AFB₁ detection using the MBio system and the anti-AFB₁ Fab antibody fragment, with the IC₅₀ and LoD values decreasing from 7.33 to 0.51 ng/mL and 1.54 to 0.03 ng/mL, respectively when compared to ELISA testing. Following the successful detection of AFB₁ and T-2 toxin and the increased sensitivity delivered by MBio detection, solvent extraction of both mycotoxins from contaminated Dried Distillers Grains with Solubles (DDGS) samples was undertaken for MBio testing.

An aqueous-based method (80:20% (v/v) water:methanol) was selected for simultaneous extraction of AFB₁ and T-2 toxin, which proved apt for direct extract-testing on the MBio detection system. Together, the anti-AFB₁ Fab antibody fragment and the anti-T-2 toxin polyclonal antibody delivered a limit of detection of 4.12 ng/mL and 5.08 ng/mL for their

respective targets in the MBio assay. These limits of detection meet current EU maximal limits for AFB₁ and T-2 toxin in feed for animals at 20 ppb and 25 ppb, respectively. Furthermore, the antibodies were coupled with the MBio detection system in a ‘proof-of-concept’ multiplex mycotoxin detection approach. AFB₁ was successfully detected in 2 separate tests at 12.1 ng/mL and 10.3 ng/mL (16.1 µg/kg and 13.7 µg/kg) representing an average recovery of 98% in comparison with UPLC-MS/MS methods, whilst T-2 toxin was detected at 7.09 ng/mL and 5.08 ng/mL (9.5 µg/kg and 6.7 µg/kg) and represented an average recovery of 69%. The coefficients of variance for detection of AFB₁ and T-2 toxin in contaminated DDGS samples were 11% and 24%, respectively.

These results show that the anti-AFB₁ Fab antibody fragment and the anti-T-2 toxin polyclonal antibody in conjunction with the MBio detection system can deliver a simple, ‘point-of-site’ detection platform that delivers detection at EU legislative limits for T-2 toxin and AFB₁. The anti-AFB₁ Fab antibody fragment delivered a limit of detection of 4.12 ng/mL and a dynamic range of 2.1 – 48.82 ng/mL for detection of AFB₁ in DDGS samples. The anti-T-2 toxin polyclonal antibody delivered a limit of detection of 5.08 ng/mL and a dynamic range of 0.6 – 11.9 ng/mL for detection of T-2 toxin in DDGS samples. The simultaneous detection of AFB₁ at a recovery of 98% and T-2 toxin at 69% compared to UPLC-MS/MS methods, was established. Intra-day assay with an $n=2$ was completed as only limited cartridges were available for testing. An $n=3$ and inter-day assaying would provide a more robust validation of the functionality of the assay. The ability to test both mycotoxins provides a ‘proof-of-concept’ for the multiplex detection of mycotoxins and suggests other mycotoxins or multiple mycotoxins could be detected using this assay format. Though full validation of the extraction process and MBio analysis would be necessary, the described detection method would be greatly beneficial for simple, multi-mycotoxin analysis directly in the field, allowing users including farmers and millers to determine if, and what, mycotoxins are affecting their products and feeds.

Chapter 5

The investigation of AFB₁ and anti-AFB₁ Fab effects on HepG2 hepatocellular carcinoma cells

5.1 Introduction

Hepatocellular carcinoma (HCC) is the most well-known primary liver malignancy worldwide and with occurrence growing at an alarming rate, HCC represents a public concern globally (Hamid *et al.*, 2013). Epidemiological research suggests that contamination of food with aflatoxin B₁ (AFB₁) is a major risk factor for human liver cancer and that regions with high AFB₁ exposure coincide with regions of high HCC prevalence (Montalto *et al.*, 2002). Accordingly, there is a prominent geographical incidence of HCC, with the greatest burden evident in developing countries, where over 80% of cases occur (Ferlay *et al.*, 2010). Furthermore, approximately 500 million of the poorest people in sub-Saharan Africa, Latin America, and Asia are exposed to mycotoxins at levels that substantially escalate mortality and morbidity (Alberts *et al.*, 2017). AFB₁-associated HCC is a preventable cancer. Therefore, complete understanding of the AFB₁ mechanism of action and identification of its high-risk sources are necessary to reduce the incidence of AFB₁-induced HCC (Montalto *et al.*, 2002). AFB₁ is a potent, genotoxic hepato-carcinogen shown to induce liver cancer following metabolism by cytochrome P450 to a reactive AFB₁-8-9-epoxide, which in-turn binds to DNA forming AFB₁-N7-Gua and promotes mutational effects in the *P53* tumor suppressor gene at the codon 249. However, further research has suggested that AFB₁ may affect a range of signalling pathways resulting in diverse cellular effects.

Ubagai *et al.* (2010) and Ma *et al.* (2012) have demonstrated that AFB₁ exerts an influence on hepatocellular carcinoma cell lines via the Insulin-like Growth Factor (IGF) pathway. AFB₁ (50 ng/mL) was shown to modulate the Insulin-like Growth Factor-2 (IGF-2)-dependent signalling axis. IGF-2 induces proliferation and differentiation in many cell types and it is mediated via Insulin-like Growth Factor-1 receptor (IGF-1R) (Ubagai *et al.*, 2010). Ma *et al.* (2012) found that IGF-1R inhibition or Insulin Receptor Substrate-2 (IRS-2) knockdown suppressed hepatoma cell migration following exposure to AFB₁ (2.5 μ M = 780.7 ng/mL). IRS-2 is activated by a signalling cascade following IGF-2 or IGF-1 binding to the IGF-1R. After IGF-1/2 ligand binding, the β subunit of IGF-1R undergoes conformational change which causes auto-phosphorylation of its own tyrosine kinase domain and the full activation of IGF-1R. IGF-1R induces anti-apoptosis mechanisms and increases tumour cell mobility. Oncogenes including Src kinase and Akt kinase were both shown to stimulate the gene expression of IGF-1R, indicating its importance in

carcinogenesis (Wu and Zhu, 2011). The overexpression of IGF-1R and IGF-2R are characteristics of malignant transformation and the growth of tumours (Scharf and Braulke, 2003), hence the ability to interact with, and, inhibit the IGF-1R axis may provide a platform to reduce AFB₁-induced HCC.

In addition to the IGF pathway, type 1 Interferon (IFN) signalling has been described as a mediator of AFB₁-associated HCC by Narkwa *et al.* (2017). The IFN pathway, involved in innate immunity, restricts viral infections and up-regulates tumour suppressor activities and pro-apoptotic pathways via activation of the JAK-STAT-ISRE pathway. The research by Narkwa *et al.* showed that AFB₁ (10 μ M = 3122.8 ng/mL) inhibited the IFN signalling pathway in HepG2 cells by suppressing the transcript levels of *JAK1*, *STAT1* and *OAS3* and the accumulation of STAT1 protein (responsible for the suppression of tumour development by inducing apoptosis and also tumour angiogenesis inhibition). Therefore, the inhibition of the IFN pathway by AFB₁-induced suppression of STAT1 and consequential down-regulation of genes which are required to promote apoptosis, inhibit cell proliferation and angiogenesis, suggests a novel mechanism by which AFB₁ may induce hepatocellular carcinoma in humans.

Furthermore, AFB₁ can negatively regulate the Wnt/ β -Catenin signalling pathway in human hepatoma cells. β -catenin is a component of the Wnt/ β -catenin signalling pathway known to play an important role in cell differentiation, proliferation, apoptosis, metastasis and tumorigenesis. MicroRNAs (miR) are vital in modulating gene expression in various diseases including cancers and cardiovascular disorders. miR-33a regulates receptor-interacting protein 140 (RIP140) in inflammatory cytokine production and following hepatoma cell-exposure to 10 μ g/mL of AFB₁, miR-33a was upregulated, resulting in a decrease in β -catenin expression. Consequently, the downstream genes (C-myc and cyclin D1) of β -catenin in the Wnt/ β -catenin pathway were also down-regulated (Zhu *et al.*, 2015). This research also described a novel mode of action by AFB₁ in HCC, mediated by miRNA.

Therefore, it is evident that AFB₁ induces its hepatocellular carcinogenic effects in a varied and complex manner. The research outlined here, describes AFB₁ exposures at relatively high doses. Although the high doses detailed in previous research are relevant to reveal the AFB₁-driven carcinogenic consequences of exposure, the aim of the research described in this chapter was to determine the effects of relatively low doses of AFB₁ on HepG2

carcinoma cells. In addition to this, it was hypothesised that the anti-AFB₁ Fab antibody fragment may be able to exert an effect on HepG2 cells given its ability to bind the toxin (even at very low concentrations) or alternatively that the anti-AFB₁ Fab antibody fragment could bind and inhibit AFB₁, and, inhibit its effects on HepG2 cells. It was considered that the complementary binding domains (CDRs) of the Fab antibody fragment which are highly specific for AFB₁, may be complementary to ligands on the HepG2 cells which interact with, and are affected by AFB₁ to induce carcinogenesis.

The findings in this chapter suggest that low doses of AFB₁ (0.01 and 0.1 ng/mL) have an inhibitory effect on HepG2 cancer cell migration and proliferation predominantly after 24 hours and which return to normal levels after 72 hours. Furthermore, it was shown that 48 hours of exposure was necessary for low doses of AFB₁ to significantly increase IL-8 expression. The inhibitory effects of AFB₁ on HepG2 cancer cells is evident following 24 hours of exposure, however, further exposure for 48 hours is necessary to induce IL-8 expression. After 72 hours of AFB₁ exposure, the HepG2 cells returned to normal levels of cellular migration, proliferation and IL-8 expression.

The results of anti-AFB₁ Fab antibody fragment (0.14 µM) treatment revealed its function as a potent inhibitor of HepG2 cell migration and proliferation. This is the first report of a highly specific recombinant Fab antibody fragment (nominally reacting specifically with a mycotoxin) acting as an inhibitor of cancer cell migration and inhibition, possibly by means of interaction with a common HepG2 cell ligand, to that specifically for the HCC promoter, AFB₁. However, additional investigations would be necessary to determine the exact mechanism of anti-AFB₁ Fab antibody fragment action.

5.2 Results

5.2.1 The effects of AFB₁ dosing and anti-AFB₁ Fab antibody fragment treatment on HepG2 cell migration

The *in vitro* scratch assay, also commonly referred to as scratch-wound or wound-healing assay, is a simple, reproducible, well-developed assay commonly used to measure basic cell migration parameters, principally speed of movement. The steps involve introducing a scratch in a cell monolayer and capturing images at defined time-frames of cell migration across the wound space, until the scratch is closed. The images are then compared to investigate the migration rate of the cells (Liang *et al.*, 2007; Cory 2011). The scratch assay was completed, as described in Section 2.2.40. Briefly, HepG2 cells were plated at 5×10^5 cells/mL in a 6-well cell culture plate and grown to confluence for 24 hours at 37°C in a 5% CO₂ humidified atmosphere. A 1 mm scrape was placed through the middle of the confluent monolayer of cells using a 200 µL pipette tip, followed by washing with 2 mL of PBS solution twice and the addition of 2 mL of fresh media. The effects of AFB₁ dosing and anti-AFB₁ Fab antibody fragment treatment on HepG2 cells were investigated by adding AFB₁ doses (0.01 and 0.1 ng/mL) for various time-frames (24, 48, 72 and 96 hours) or anti-AFB₁ Fab antibody fragment (0.14 µM) treatment for various time-frames (24, 48, 72 and 96 hours). Previous research completed by Loftus *et al.* (2016) revealed that picogram concentrations of multiple mycotoxins can significantly affect viability and cytokine modulation of J774A.1 murine macrophage, whilst Bruneau *et al* (2012) indicated that 0.1 and 0.01 ng/mL concentrations of AFB₁ can modulate cytokine secretion and cell surface marker expression in the same cell line. Therefore, the research in this chapter investigated the effects of 0.1 and 0.01 ng/mL of AFB₁ on HepG2 cells. Literature indicates that a wide range of antibody concentrations are frequently applied in research to determine treatment effects in HCC cell lines. Ma *et al.* (2017) investigated the use of 2.5 – 640 nM (0.375 - 9.6 µg/mL) of anti-CD24 monoclonal antibody, G7mAb and a G7mAb-DOX antibody-drug conjugate on Huh-7 human hepatoma cell line. Another study reported treating Huh-7 cells with 2, 5 and 10 µg/ml of anti-CD47 mAb antibody and subjected them to invasion and migration assays (Lo *et al.*, 2015). Xiao *et al.* (2015) examined the effects of an anti-CD47 mAb400 at concentrations of 1.1 µg/mL, 3.3 µg/mL and 10 µg/mL on HepG2 cells. The selected concentration of 0.14 µM (0.7 µg/mL) of anti-AFB₁ Fab antibody fragment

treatment was based on knowledge of its binding capacity at low concentrations. A high-affinity monoclonal antibody specific for the native form of glypcian-3 (GPC3) was generated by Phung *et al.*, (2012) and tested in Hep3B, HepG2 and Huh-7 cells. The YP7 anti-GPC3 mAb was not shown to have effects on cell proliferation in concentrations ranging from 0.1 to 2.5 μ M. The original hypothesis was that the Fab fragment could mop up available AFB₁ and thus modulate its activity. Therefore, 0.14 μ M of anti-AFB₁ Fab antibody fragment treatment was administered to determine if the AFB₁-specific Fab could effectively perform this function and to check if it could itself exert any effects on HepG2 cells at a low concentration.

5.2.1.1 The effects of AFB₁ exposure on HepG2 cell migration

A single scratch was applied per test to monolayers of HepG2 cells plated on tissue culture 6 well plates, as described in Section 2.2.40. Fresh media and AFB₁ doses (0.01 and 0.1 ng/mL) were added to the plates every 24 hours for 72 hours and HepG2 cell migration was monitored and imaged every 24 hours using an OPTIKA XDS-2FL inverted HBO Fluorescence Microscope. The percent coverage of cells was analysed using RStudio software and a program designed by Ivan McGuire. To determine the effects of migration on the HepG2 cells, an image of the original cell monolayer prior to administration of the scratch was analysed using the RStudio software and taken as 100 % of cell coverage. The subsequent images of the scratched or dosed cell layer were analysed using the RStudio software and the percentage coverage calculated relative to the original monolayer. The results in Figure 5.1 show that after 24 hours of 0.01 and 0.1 ng/mL AFB₁ exposure there was a reduction in the migration of HepG2 cells compared to untreated cells alone and the vehicle control. Both concentrations of AFB₁ reduced migration to a similar level after 24 hours of exposure. Table 5.1 indicates that the HepG2 cells (+ vehicle) migrated by 42 % in the 24 hours following administration of the scratch, however, the cells migrated by only 25 and 34 % when dosed with 0.01 and 0.1 ng/mL of AFB₁, respectively. After 48 hours of AFB₁ exposure, the HepG2 cells fully migrated to close the scratch and remained fully migrated after 72 hours. These results indicated that both concentrations of AFB₁ affect HepG2 migration for the initial 24 hours before the cells migrate to levels of untreated cells alone and cells treated with the vehicle control. These findings are in contrast to pro-HepG2 migration effects reported by Ma *et al.*, (2012), however, that report cites the use of

higher concentrations of AFB₁ (2.5 µM = 780.7 ng/mL). AFB₁ is a potent hepatocellular carcinogen (IARC, 2002) and Ma *et al.* have shown that at high doses, the mycotoxin stimulates HepG2 cell migration which is in agreement with cancer-progression mechanisms. Furthermore, AFB₁ was shown to stimulate hepatoma cell migration through the Insulin-like Growth Factor (IGF) pathway and previous research by Ubagai *et al.* (2010) supports this theory. This was achieved by blocking the IGF-1R or by Insulin Receptor Substrate-2 (IRS-2) knockdown to suppress hepatoma cell migration. Therefore, the relatively low doses of AFB₁ (0.01 and 0.1 ng/mL) may be exerting an inhibitory effect on HepG2 cell migration via the IGF pathway, however, IGF pathway-specific investigations would be necessary to determine the exact impact of low AFB₁ doses on signalling.

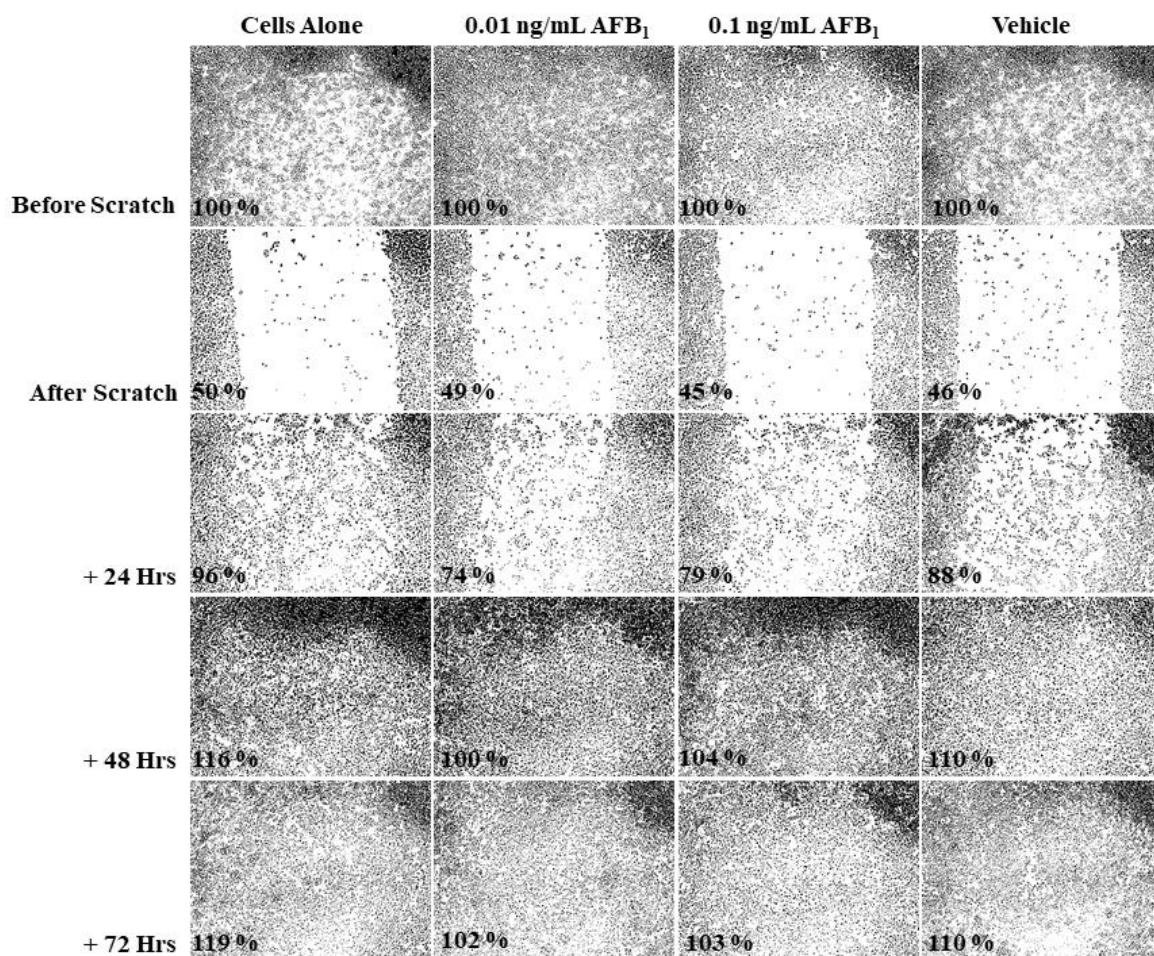


Figure 5.1: Scratch assays to analyse the effects of AFB₁ on HepG2 cell migration. HepG2 (0.5×10^6 cells/mL) cells were plated in complete DMEM in a tissue culture 6 well plate and a scratch applied. The cells were exposed to AFB₁ (in methanol and complete DMEM) diluted to a final concentration of 0.01 ng/mL and 0.1 ng/mL when added to complete DMEM on the plate for 24, 48 and 72 hours. A vehicle control of methanol in DMEM diluted to a final concentration of 0.05 % (v/v) when added to complete DMEM on the plate was also incubated with HepG2 cells. The percentage of cell coverage was analysed using RStudio software and a custom-built programme. Scratches were performed once per test and control condition (n = 1).

Table 5.1: Analysis of AFB₁ exposure on HepG2 cell migration

Scratch	Cells Alone	Cells + 0.01 ng/mL AFB ₁	Cells + 0.1 ng/mL AFB ₁	Cells + Vehicle
Before	100 %	100 %	100 %	100 %
After	50 %	49 %	45 %	46 %
+ 24 hrs	96 % + 46 %	74 % + 25 %	79 % + 34 %	88 % + 42 %
+ 48 hrs	116 % + 20 %	100 % + 26 %	104 % + 25 %	110 % + 22 %
+ 72 hrs	119 % + 3 %	102 % + 2 %	103 % - 1 %	110 % 0 %
Cell Coverage % Cell Migration %				

HepG2 (0.5×10^6 cells/mL) cells were plated in complete DMEM in a tissue culture 6 well plate and a scratch applied. Cells alone were grown in the absence of AFB₁ exposure. Cells were exposed to AFB₁ (in methanol and complete DMEM) diluted to a final concentration of 0.01 ng/mL and 0.1 ng/mL when added to complete DMEM on the plate for 24, 48 and 72 hours. A vehicle control of methanol in DMEM diluted to a final concentration of 0.05 % (v/v) when added to complete DMEM on the plate was also incubated with HepG2 cells. Cell monolayers for each test were imaged prior to the scratch being applied and a coverage value generated using RStudio software. The coverage value for the cell monolayer before the scratch was applied for each test (Before) was designated as 100 % cell coverage. The subsequent images of the scratched cell layers for each test (After, + 24 hrs, + 48 hrs and + 72 hrs) after the scratches were applied, were imaged and a coverage value generated using the RStudio software. The cell coverage percent (black) of each test after the scratch was applied (After, + 24 hrs, + 48 hrs and + 72 hrs) was calculated by dividing the RStudio generated coverage value of for each test by, the RStudio generated coverage value of the cell monolayer before the scratch was applied and multiplying by 100. The cell migration percent (red) across the scratch was calculated by observing the percentage increase or decrease in cell coverage percent for each test (After, + 24 hrs AFB₁, + 48 hrs AFB₁ and + 72 hrs AFB₁) at 24 hourly intervals.

5.2.1.2 The effects of anti-AFB₁ Fab antibody fragment on HepG2 cell migration

A single scratch was applied per test to monolayers of HepG2 cells plated on tissue culture 6 well plates. Fresh media and anti-AFB₁ Fab antibody fragment treatments (0.14 μ M) were added to the plates every 24 hours and HepG2 cell migration was monitored every 24 hours using an OPTIKA XDS-2FL inverted HBO Fluorescence Microscope. The percent coverage of cells was analysed using RStudio software, as described in Section 5.2.1.1. The results in Figure 5.2 show that after 24 hours of anti-AFB₁ Fab antibody fragment treatment there was a reduction in the migration of HepG2 cells compared to untreated cells alone and the vehicle control. Table 5.3 indicates that the HepG2 cells (+ vehicle) migrated by 36 % in the 24 hours following administration of the scratch, however, the cells migrated by only 13 % when treated with the anti-AFB₁ Fab antibody fragment alone. Further treatment with the Fab resulted in decreased HepG2 migration after 48, 72 and 96 hours and only reached 92 % total cell coverage, whilst HepG2 cells (+ vehicle) alone fully

migrated at 104 % cell coverage. These results indicate that the anti-AFB₁ Fab antibody fragment can reduce HepG2 cell migration for over 96 hours.

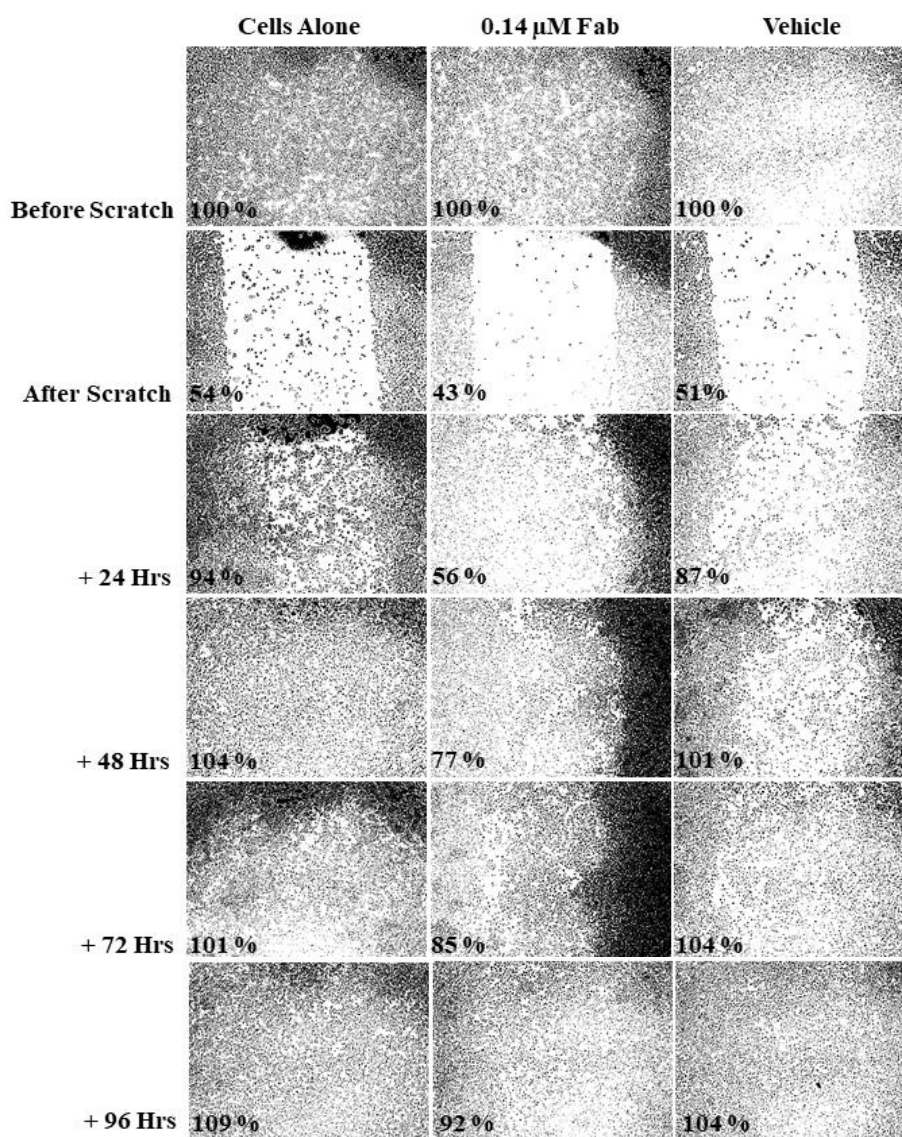


Figure 5.2: Scratch assays to analyse the effects of anti-AFB₁ Fab antibody fragment on HepG2 cell migration. HepG2 (0.5×10^6 cells/mL) cells were plated in complete DMEM in a tissue culture 6 well plate and a scratch applied. The cells were treated with anti-AFB₁ Fab antibody fragment (in Dulbecco's PBS) diluted to a final concentration of 0.14 μ M when added to complete DMEM on the plate for 24, 48, 72 and 96 hours. A vehicle control of Dulbecco's PBS diluted to a final concentration of 0.01% (v/v) when added to complete DMEM on the plate was also incubated with HepG2 cells. The percentage of cell coverage was analysed using RStudio software and a custom-built programme. Scratches were performed once per test and control condition (n = 1).

Table 5.2: Analysis of anti-AFB₁ Fab antibody fragment effects on HepG2 cell migration

Scratch	Cell Alone	Cells + 0.14 μ M Fab	Cells + Vehicle
Before	100 %	100 %	100 %
After	54 %	43 %	51 %
+ 24 hrs	94 % + 40 %	56 % + 13 %	87 % + 36 %
+ 48 hrs	104 % + 10 %	77 % + 21 %	101 % + 14 %
+ 72 hrs	101 % - 3 %	85 % + 8 %	104 % + 3 %
+ 96 hrs	109 % + 8 %	92 % + 7 %	104 % 0 %
Cell Coverage %Cell Migration %			

HepG2 (0.5×10^6 cells/mL) cells were plated in complete DMEM in a tissue culture 6 well plate and a scratch applied. Cells alone were grown in the absence of anti-AFB₁ Fab antibody fragment treatment. Cells were exposed to anti-AFB₁ Fab antibody fragment (in Dulbecco's PBS) diluted to a final concentration of 0.14 μ M when added to complete DMEM on the plate for 24, 48 and 72 hours. A vehicle control of Dulbecco's PBS diluted to a final concentration of 0.01% (v/v) when added to complete DMEM on the plate was also incubated with HepG2 cells. Cell monolayers for each test were imaged prior to the scratch being applied and a coverage value generated using RStudio software. The coverage value for the cell monolayer before the scratch was applied for each test (Before) was designated as 100 % cell coverage. The subsequent images of the cell layers for each test (After, + 24 hrs, + 48 hrs, + 72 hrs and + 92 hrs) after the scratches were applied, were imaged and a coverage value generated using the RStudio software. The cell coverage percent (black) of each test after the scratch was applied (After, + 24 hrs, + 48 hrs, + 72 hrs and + 92 hrs) was calculated by dividing the RStudio generated coverage value for each test by, the RStudio generated coverage value of the cell monolayer before the scratch being applied and multiplying by 100. The cell migration percent (red) across the scratch was calculated by observing the percentage increase or decrease in cell coverage percent for each test (After, + 24 hrs, + 48 hrs, + 72 hrs and + 92 hrs) at 24 hourly intervals.

5.2.1.3 The effects of anti-AFB₁ Fab antibody fragment treatment on HepG2 and THLE-2 cell migration

The scratch assays were completed, as described in Section 2.2.40. Briefly, HepG2 cells (0.5×10^6 cells/mL) and THLE-2 cells (0.25×10^6 cells/mL) were added to a tissue culture 6 well plate and grown to confluence for 24 hours 37°C in a 5% CO₂ humidified atmosphere. A single 1 mm scrape per test, was placed through the middle of the confluent monolayer of cells using a 200 μ L pipette tip, followed by washing with 2 mL of PBS twice and addition of 2 mL of fresh media. The HepG2 and THLE-2 cells were treated with the anti-AFB₁ Fab antibody fragment (0.14 μ M) and anti-EpCAM monoclonal antibody (0.14 μ M) every 24 hours and HepG2 and THLE-2 cell migration was monitored using an OPTIKA XDS-2FL inverted HBO Fluorescence Microscope. EpCAM is a cell surface glycoprotein, approximately 40 kDa in size and is highly expressed in epithelial

cancers, such as hepatocellular carcinoma, and at lower levels in normal, simple epithelia. EpCAM has been implicated in a diversity of processes including cell migration, proliferation, cell-cell adhesion, differentiation and cell signalling (Schnell *et al.*, 2013). Therefore, an anti-EpCAM monoclonal antibody was included as a control to determine if binding to a cell surface receptor or ligand had an effect on cellular migration.

The percentage coverage of cells was analysed using RStudio software, as described in Section 5.2.1.1. The results in Figure 5.3 show that after 24 hours of anti-AFB₁ Fab antibody fragment treatment there was a reduction in the migration of HepG2 cells compared to untreated cells alone and the vehicle control. Anti-EpCAM monoclonal antibody was added to cells to determine if the binding of this antibody to EpCAM receptors, known to be located on the surface of HepG2 cells, could affect cell migration. The results show that a reduction in HepG2 cell migration was evident after 24 hours of anti-EpCAM monoclonal antibody treatment. Table 5.3 indicates that the HepG2 cells (+ vehicle) migrated by 33 % in the 24 hours following administration of the scratch, however, the cells migrated by only 16 % when treated with either the anti-AFB₁ Fab antibody fragment or the anti-EpCAM monoclonal antibody. Further treatment with the Fab resulted in the decreased migration of HepG2 cells for up 144 hours, until 100% cell coverage was achieved. In contrast, treatment with the anti-EpCAM monoclonal antibody only reduced migration for the initial 24 hours until 111 % cell coverage was reached after 48 hours. These results indicate that the binding of the anti-EpCAM monoclonal antibody to the HepG2 cell did impact cellular migration for the initial 24 hours of treatment. The results suggest that the anti-AFB₁ Fab antibody fragment may be functioning by interacting directly with the HepG2 cells to moderate migration at a decreased rate. THLE-2 cells were treated with the anti-AFB₁ Fab antibody fragment and the anti-EpCAM monoclonal antibody to indicate if the antibodies had an effect on normal liver cells. This was completed to investigate if the effect of reduced migration was limited to the carcinoma HepG2 cell line or evident for normal liver epithelial cells.

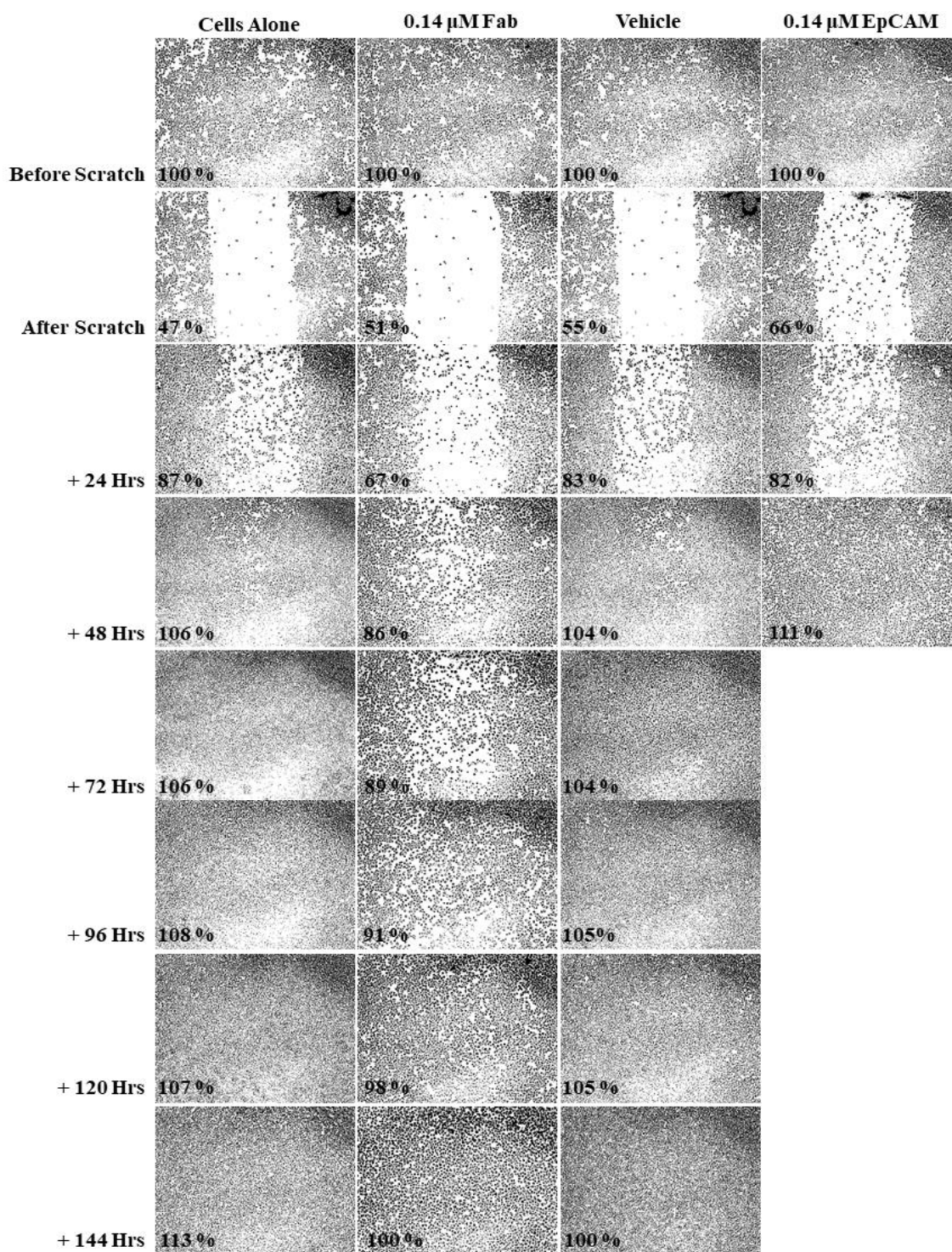


Figure 5.3: Scratch assays to analyse the effects of the anti-AFB₁ Fab antibody fragment and anti-EpCAM monoclonal antibody on HepG2 cell migration. HepG2 (0.5×10^6 cells/mL) cells were plated in complete DMEM in a tissue culture 6 well plate and a scratch applied. The cells were treated with anti-AFB₁ Fab antibody fragment (in Dulbecco's PBS) diluted to a final concentration of 0.14 μ M when added to complete DMEM on the plate for 24, 48, 72, 96, 120 and 144 hours. The cells were also treated with anti-EpCAM monoclonal antibody diluted to a final concentration of 0.14 μ M when added to complete DMEM on the plate for 24 and 48 hours. A vehicle control of Dulbecco's PBS diluted to a final concentration of 0.01% (v/v) when added to complete DMEM on the

plate was also incubated with HepG2 cells. The percentage of cell coverage was analysed using RStudio software and a custom-built programme. Scratches were performed once per test and control condition (n = 1).

Table 5.3: Analysis of anti-AFB₁ Fab antibody fragment and anti-EpCAM monoclonal antibody effects on HepG2 cell migration

Scratch	Cells Alone		Cells + Fab (0.14 μ M)		Cells + Vehicle		Cells + EpCAM (0.14 μ M)	
Before	100 %		100 %		100 %		100 %	
After	47 %		51 %		50 %		66 %	
+ 24 hrs	84 %	+ 37 %	67 %	+ 16 %	83 %	+ 33 %	82 %	+ 16 %
+ 48 hrs	106 %	+ 22 %	86 %	+ 19 %	104 %	+ 21 %	111 %	+ 29 %
+ 72 hrs	106 %	0 %	89 %	+ 3 %	104 %	0 %	-	-
+ 96 hrs	108 %	+ 2 %	91 %	+ 2 %	105 %	+ 1 %	-	-
+ 120 hrs	107 %	- 1 %	98 %	+ 7 %	105 %	0 %	-	-
+ 144 hrs	113 %	+ 8 %	100 %	+ 2 %	100 %	- 5 %	-	-
Cell Coverage %Cell Migration %								

HepG2 (0.5×10^6 cells/mL) cells were plated in complete DMEM in a tissue culture 6 well plate and a scratch applied. Cells alone were grown in the absence of anti-AFB₁ Fab antibody fragment treatment. Cells were exposed to anti-AFB₁ Fab antibody fragment (in Dulbecco's PBS) diluted to a final concentration of 0.14 μ M when added to complete DMEM on the plate for 24, 48, 72, 96, 120 and 144 hours. Cells were also exposed to anti-EpCAM monoclonal antibody diluted to a final concentration of 0.14 μ M when added to complete DMEM on the plate for 24 and 48 hours. A vehicle control of Dulbecco's PBS diluted to a final concentration of 0.01% (v/v) when added to complete DMEM on the plate was also incubated with HepG2 cells. Cell monolayers for each test were imaged prior to the scratch being applied and a coverage value generated using RStudio software. The coverage value for the cell monolayer before the scratch was applied for each test (Before) was designated as 100 % cell coverage. The subsequent images of the cell layers for each test (After, + 24 hrs, + 48 hrs, + 72 hrs, + 92 hrs, +102 hrs and + 144 hrs) after the scratches were applied, were imaged and a coverage value generated using the RStudio software. The cell coverage percent (black) of each test after the scratch was applied (After, + 24 hrs, + 48 hrs, + 72 hrs, + 92 hrs, +102 hrs and + 144 hrs) was calculated by dividing the RStudio generated coverage value for each test by, the RStudio generated coverage value of the cell monolayer before the scratch being applied and multiplying by 100. The cell migration percent (red) across the scratch was calculated by observing the percentage increase or decrease in cell coverage percent for each test (After, + 24 hrs, + 48 hrs, + 72 hrs, + 92 hrs, +102 hrs and + 144 hrs) at 24 hourly intervals.

A single scratch was applied per test to monolayers of THLE-2 cells plated on tissue culture 6 well plates. Fresh media, anti-AFB₁ Fab antibody fragment treatments (0.14 μ M) and anti-EpCAM monoclonal antibody (0.14 μ M) were added to the plate every 24 hours and HepG2 cell migration was monitored using an OPTIKA XDS-2FL inverted HBO Fluorescence Microscope. The percent coverage of cells was analysed using RStudio

software, as described above in Section 5.2.1.1. The results in Figure 5.4 show that 96 hours of anti-AFB₁ Fab antibody fragment treatment had very little effect in the migration of THLE-2 cells compared to untreated cells alone and the vehicle control. Anti-EpCAM monoclonal antibody was added to cells to determine if the binding of this antibody to the limited number of EpCAM receptors known to be located on the surface of THLE-2 cells, could affect cell migration. The results show that a reduction in THLE-2 cell migration was evident after 24 hours of anti-EpCAM monoclonal antibody treatment. Table 5.4 indicates that the THLE-2 cells (+ vehicle) migrate by 18 % in the 24 hours following administration of the scratch, however, the cells migrate by 20 % and 6 % when treated with the anti-AFB₁ Fab antibody fragment and anti-EpCAM monoclonal antibody, respectively. Further treatment with the Fab resulted in a relatively normal migration of the THLE-2 cells compared to cells alone and the vehicle control, resulting in 100% cell coverage after 96 hours. Similarly, treatment with the anti-EpCAM antibody only reduced migration for the initial 24 hours and reached 101 % cell coverage also after 96 hours. The results here and from Figure 5.4, indicate anti-EpCAM monoclonal antibody-binding to the THLE-2 cells (and HepG2 cells) exerts an effect in reducing cell migration for the first 24 hours of treatment. Additionally, the results suggest that the anti-AFB₁ Fab antibody fragment is capable of interacting with a HepG2 cell-specific ligand to exert an effect in reducing cell migration, however, the same effect is not evident with normal liver epithelial, THLE-2 cells. THLE-2 cells may not have a suitable binding site for interaction with the anti-AFB₁ Fab antibody fragment. Alternatively, cancerous cells often demonstrate up-regulation or over-expression of cell surface markers or receptors which may be in more abundance on HepG2 cells and available for interaction with the Fab fragment. These results show that the anti-AFB₁ Fab antibody fragment is interacting with the HepG2 carcinoma cells in a manner which can specifically reduce HepG2 cancer cell migration.


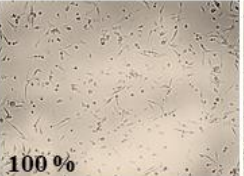
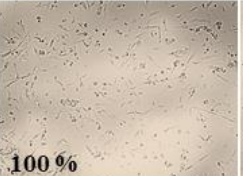
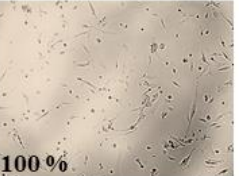
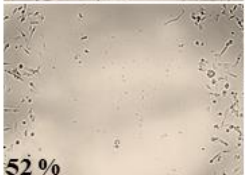

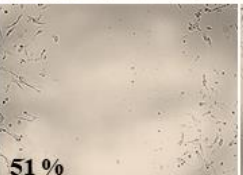












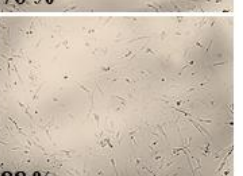




	Cells Alone	0.14 μ M Fab	Vehicle	0.14 μ M EpCAM
Before Scratch	 100 %	 100 %	 100 %	 100 %
After Scratch	 52 %	 50 %	 51 %	 60 %
+ 24 Hrs	 68 %	 70 %	 69 %	 66 %
+ 48 Hrs	 70 %	 74 %	 72 %	 70 %
+ 72 Hrs	 82 %	 81 %	 78 %	 88 %
+ 96 Hrs	 103 %	 100 %	 106 %	 101 %

Figure 5.4: Scratch assays to analyse the effects of the anti-AFB₁ Fab antibody fragment and anti-EpCAM monoclonal antibody on THLE-2 cell migration. THLE-2 (0.25×10^6 cells/mL) cells were plated in complete LHC-8 medium in a tissue culture 6 well plate and a scratch applied. The cells were treated with anti-AFB₁ Fab antibody fragment (in Dulbecco's PBS) diluted to a final concentration of 0.14 μ M when added to complete LHC-8 medium on the plate for 24, 48, 72 and 96 hours. The cells were also treated with anti-EpCAM monoclonal antibody diluted to a final concentration of 0.14 μ M when added to complete LHC-8 medium on the plate for 24, 48, 72 and 96 hours. A vehicle control of Dulbecco's PBS diluted to a final concentration of 0.01% (v/v) when added to complete LHC-8 medium on the plate was also incubated with THLE-2 cells. The percentage of cell coverage was analysed using RStudio software and a custom-built programme. Scratches were performed once per test and control condition (n = 1).

Table 5.4: Analysis of anti-AFB₁ Fab antibody fragment and anti-EpCAM monoclonal antibody effects on THLE-2 cell migration

Scratch	Cells Alone	Cells + Fab (0.14 μ M)	Cells + Vehicle	Cells + α -EpCAM (0.14 μ M)
Before	100 %	100 %	100 %	106 %
After	52 %	50 %	51 %	60 %
+ 24 hrs	68 % + 16 %	70 % + 20 %	69 % + 18 %	66 % + 6 %
+ 48 hrs	70 % + 8 %	74 % + 4 %	72 % + 3 %	70 % + 4 %
+ 72 hrs	82 % + 12 %	81 % + 7 %	78 % + 6 %	88 % + 18 %
+ 96 hrs	103 % + 21 %	100 % + 19 %	106 % + 28 %	101 % + 13 %
% Coverage % Migration				

THLE-2 (0.25×10^6 cells/mL) cells were plated in complete LHC-8 medium in a tissue culture 6 well plate and a scratch applied. Cells alone were grown in the absence of anti-AFB₁ Fab antibody fragment treatment. Cells were exposed to anti-AFB₁ Fab antibody fragment (in Dulbecco's PBS) diluted to a final concentration of 0.14 μ M when added to complete LHC-8 medium on the plate for 24, 48, 72 and 96 hours. Cells were also exposed to anti-EpCAM monoclonal antibody diluted to a final concentration of 0.14 μ M when added to complete LHC-8 medium on the plate for 24, 48, 72 and 96 hours. A vehicle control of Dulbecco's PBS diluted to a final concentration of 0.01% (v/v) when added to complete LHC-8 medium on the plate was also incubated with THLE-2 cells. Cell monolayers for each test were imaged before the scratch was applied and a coverage value generated using RStudio software. The coverage value for the cell monolayer before the scratch was applied for each test (Before) was designated as 100 % cell coverage. The subsequent images of the cell layers for each test (After, + 24 hrs, + 48 hrs, + 72 hrs and + 92 hrs) after the scratches were applied, were imaged and a coverage value generated using the RStudio software. The cell coverage percent (black) of each test after the scratch was applied (After, + 24 hrs, + 48 hrs, + 72 hrs and + 92 hrs) was calculated by dividing the RStudio generated coverage value for each test by, the RStudio generated coverage value of the cell monolayer before the scratch being applied and multiplying by 100. The cell migration percent (red) across the scratch was calculated by observing the percentage increase or decrease in cell coverage percent for each test (After, + 24 hrs, + 48 hrs, + 72 hrs and + 92 hrs) at 24 hourly intervals.

5.2.2 The effects of AFB₁ dosing combined with anti-AFB₁ Fab antibody fragment treatment on HepG2 cell proliferation

Cell-based assays are often used for screening compounds to evaluate consequential effects on cell proliferation, cytotoxicity and cell death. Tetrazolium compounds including MTT (3-(4,5-dimethylthiazol-2-yl)-2,5-diphenyltetrazolium bromide) are frequently used to detect viable cells. MTT is positively charged and readily penetrates viable eukaryotic cells. Viable cells with active metabolism convert MTT into a purple coloured formazan product (presumably directly proportional to the number of viable cells). When cells die, the ability to convert MTT into formazan is lost, therefore, colour formation serves as

marker of the viable cells. It is important to note that MTT reduction represents viable cell metabolism and not specifically cell cytotoxicity or cell death (Riss *et al.*, 2013). The TACS® MTT Cell Proliferation Assay was completed according to the manufacturer's guidelines and as described in Section 2.2.41. Briefly, HepG2 (5×10^5 cells/mL) were plated in 100 μ L of appropriate culture medium in a flat-bottomed 96 well culture plate (and a control of media alone) in triplicate for 1 hour at 37°C in a 5% CO₂ humidified atmosphere. The effects of AFB₁ dosing and anti-AFB₁ Fab antibody fragment treatment on HepG2 cells was investigated by adding AFB₁ doses (0.01 and 0.1 ng/mL) for various time-frames (24, 48 and 72 hours) and/or anti-AFB₁ Fab antibody fragment (0.14 μ M) treatment for various time-frames (24, 48 and 72 hours). To complete the proliferation assay 10 μ L of MTT reagent was added to each well and incubated at 37°C in a 5% CO₂ humidified atmosphere for 2 hours. Detergent reagent (100 μ L) was added to each well and incubated at room temperature for 24 hours. These experiments were conducted to determine the effects of AFB₁ and the anti-AFB₁ Fab antibody fragment on HepG2 cell proliferation. Statistical analysis of data was completed using GraphPad Prism version 5 (GraphPad, La Jolla, CA, USA.). Significance was evaluated by 1-way ANOVA analysis and the Newman-Keuls Multiple Comparison Test with $P < 0.05^*$; $P < 0.01^{**}$ and $P < 0.001^{***}$.

5.2.2.1 The effects of AFB₁ dosing on HepG2 cell proliferation

HepG2 cells were plated on sterile 96-well culture plates. Fresh media and AFB₁ doses (0.01 and 0.1 ng/mL) were added to the plates every 24 hours for 72 hours and HepG2 cell proliferation was tested every 24 hours. The results in Figure 5.5 indicate that after 24 hours of exposure with both concentrations of AFB₁, a significant reduction in HepG2 proliferation (**$P < 0.05$**) compared to cells (+ vehicle) was observed. Proliferation was only significantly affected for the initial 24 hours of exposure and at 48 and 72 hours the HepG2 cells recovered to normal proliferation levels. This result indicates that at these concentrations of AFB₁, the HepG2 cells are impacted for the initial 24 hours of exposure, before the cells return to normal levels of proliferation and the effects of AFB₁ are attenuated. These results complement the findings shown in Section 5.2.1, which indicate that the migration of the HepG2 cells was reduced for the initial 24 hours with 0.01 and 0.1 ng/mL of AFB₁ exposure. These results are in contrast to studies completed by Ma *et al.*

and Ubagai *et al.* which indicated HepG2 cell growth or proliferation was stimulated when exposed to high concentrations of AFB₁. Ma *et al.* showed that HepG2 cells dosed with 0.32 – 0.64 μ M (100 – 200 ng/mL) of AFB₁ stimulated growth in a dose dependent manner. Similarly, Ubagai *et al.*, demonstrated that HepG2 cells exposed to 50 ng/mL of AFB₁ reached cell numbers 2-fold more than those of controls. Overall, the results presented here indicate that 0.01 and 0.1 ng/mL of AFB₁ can reduce HepG2 cell migration and proliferation.

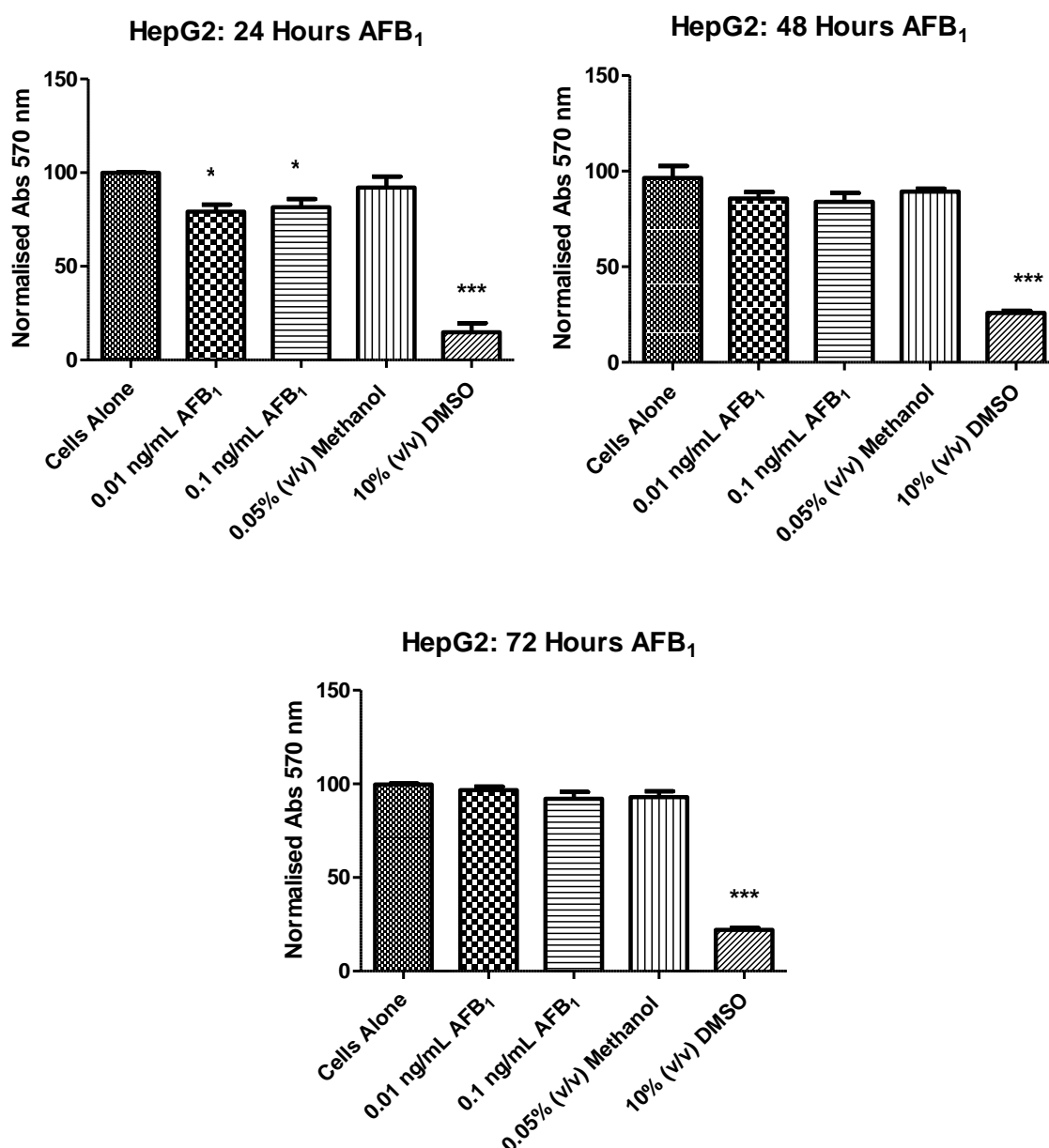


Figure 5.5: MTT proliferation assay to analyse the effects of AFB₁ on the HepG2 cell proliferation. HepG2 (5×10^5 cells/mL) cells were plated in biological triplicate in complete DMEM ($n = 3$). The cells were exposed to AFB₁ (in methanol and complete DMEM) diluted to a final concentration of 0.01 and 0.1 ng/mL when added to complete DMEM on the plate for 24, 48 or 72 hours. A vehicle control of methanol in complete DMEM diluted to a final concentration of 0.05 % (v/v) when added to complete DMEM on the plate was also incubated with HepG2 cells. 10% (v/v) DMSO in complete DMEM was included as a positive control for inhibited proliferation. Statistical analysis of data was completed using GraphPad Prism version 5 (GraphPad, La Jolla, CA, USA.). Significance was evaluated by 1-way ANOVA analysis and the Newman-Keuls Multiple Comparison Test with $P < 0.05^*$; $P < 0.01^{**}$ and $P < 0.001^{***}$. Errors bars represent the standard error of the mean (SEM) calculated by dividing the standard deviation by the square root of the n number.

5.2.2.2 The effects of AFB₁ dosing and anti-AFB₁ Fab antibody fragment treatment on HepG2 cell proliferation

HepG2 cells plated on sterile 96-well culture plates. Fresh media and AFB₁ doses (0.01 and 0.1 ng/mL) were added to the plates for 72 hours, followed by fresh media and anti-AFB₁ Fab antibody fragment treatment (0.14 µM) for 24 hours and HepG2 cell proliferation was tested. The results in Figure 5.6 indicate that after 24 hours of exposure with all concentrations of AFB₁, followed by 24 hours of treatment with the anti-AFB₁ Fab antibody fragment, a significant reduction in HepG2 proliferation (**P<0.05**) compared to cells (+ vehicles) was observed. Proliferation was reduced to a greater significance following dosing for 48 hours (**P<0.01**) and 72 hours (**P<0.001**) at both concentrations of AFB₁ and subsequent treatment for 24 hours with the anti-AFB₁ Fab antibody fragment treatment. This suggests that extended cellular exposure to AFB₁, increases the sensitivity of the cells to anti-AFB₁ Fab antibody fragment resulting in the further decrease in proliferation. A control with HepG2 cells in the absence of AFB₁ and treated with the anti-AFB₁ Fab antibody fragment indicated a significant reduction in HepG2 proliferation (**P<0.05, <0.01 and 0.001**) over the 72 hours. These results indicate that the anti-AFB₁ Fab antibody fragment is capable of exerting a strong effect in reducing HepG2 proliferation without the presence of AFB₁. The results here and the findings from Section 5.2.1 indicate that the anti-AFB₁ Fab antibody fragment is capable of interacting with the HepG2 cells to reduce migration, and, that this interaction also has a potent effect in reducing HepG2 proliferation.

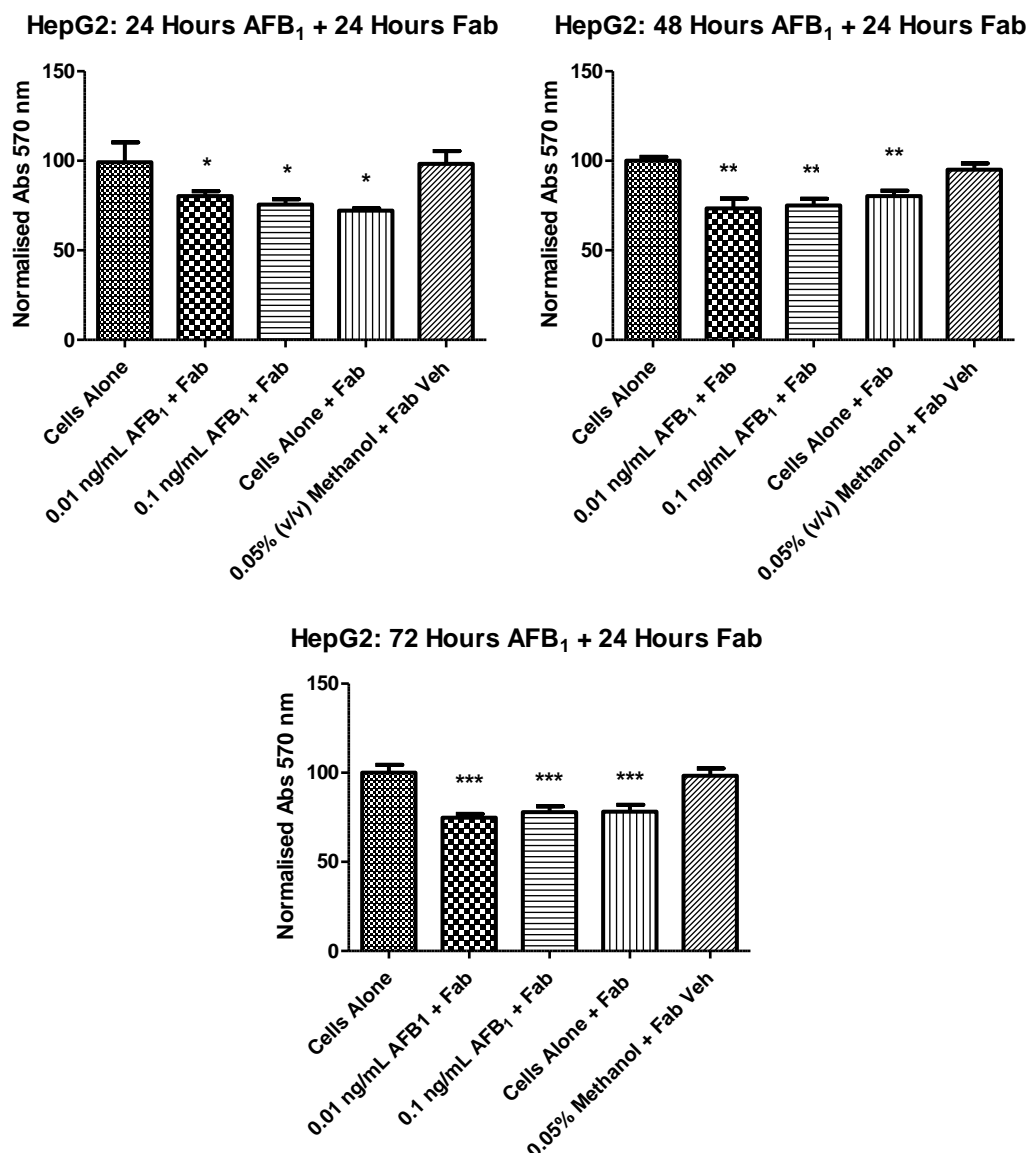


Figure 5.6: MTT proliferation assay to analyse the effects of AFB₁ and anti-AFB₁ Fab antibody fragment treatment on the HepG2 cell proliferation. HepG2 (5×10^5 cells/mL) cells were plated in biological triplicate in complete DMEM ($n = 3$). The cells were exposed to AFB₁ (in methanol and Dulbecco's PBS) diluted to a final concentration of 0.01 and 0.1 ng/mL when added to complete DMEM on the plate for 24, 48 or 72 hours. The cells were then treated with anti-AFB₁ Fab antibody fragment (in Dulbecco's PBS) diluted to a final concentration of 0.14 μ M when added to complete DMEM on the plate for 24 hours. A vehicle control of Dulbecco's PBS diluted to a final concentration of 0.01 % (v/v) and methanol diluted to a final concentration of 0.05 % (v/v) when added to complete DMEM on the plate was also incubated with HepG2 cells. Statistical analysis of data was completed using GraphPad Prism version 5 (GraphPad, La Jolla, CA, USA.). Significance was evaluated by 1-way ANOVA analysis and the Newman-Keuls Multiple Comparison Test with $P < 0.05^*$; $P < 0.01^{**}$ and $P < 0.001^{***}$. Errors bars represent the standard error of the mean (SEM) calculated by dividing the standard deviation by the square root of the n number.

5.2.2.3 The combined effects of AFB₁ anti-AFB₁ Fab antibody fragment treatments on HepG2 cell proliferation

HepG2 cells were plated on sterile 96-well culture plates. AFB₁ (0.5 ng/mL) and anti-AFB₁ Fab antibody fragment (0.14 μ M) were added directly to the plate together or pre-treated together for 15 minutes before being added to the plate and HepG2 cell proliferation was tested after 24 hours. The results in Figure 5.7 indicate that after 24 hours of the direct addition of AFB₁ and anti-AFB₁ Fab antibody fragment, a significant reduction in HepG2 proliferation (**P<0.05**) compared to cells (+ vehicles) was observed. However, proliferation was reduced to a greater significance (**P<0.01**) following exposure to AFB₁ and the anti-AFB₁ Fab antibody fragment which were pre-treated together for 15 minutes prior to addition to the cells. This indicates that together AFB₁ and the Fab have a potent effect in reducing HepG2 cell proliferation. Due to the low dose of AFB₁ (0.5 ng/mL) and the excess of anti-AFB₁ Fab antibody fragment (0.14 μ M) used for this experiment, there would be a significant amount of free Fab available for interaction with the HepG2 cells. The pre-treatment of the Fab with the limited dose of AFB₁ induced the most significant effect in reducing HepG2 cell proliferation. This suggests a combinatorial or synergistic effect of both on the HepG2 together, possibly via the same signalling pathway or across a combination of signalling pathways. Due to the evident HepG2 proliferation-inhibitory effects demonstrated by the AFB₁ Fab antibody fragment, an anti-AFB₁ scFv-dimer (from which the anti-AFB₁ Fab antibody fragment was developed) was expressed and purified and a commercial anti-AFB₁ monoclonal and polyclonal antibody selected to investigate their impact on HepG2 proliferation. As these antibodies are specific for AFB₁, this study was completed to identify if all AFB₁ antibody-formats could interact with, and, affect HepG2 cells or whether a specific antibody domain was responsible for the HepG2 interaction and subsequent effects.

HepG2: 24 Hours Combined AFB₁ and Fab

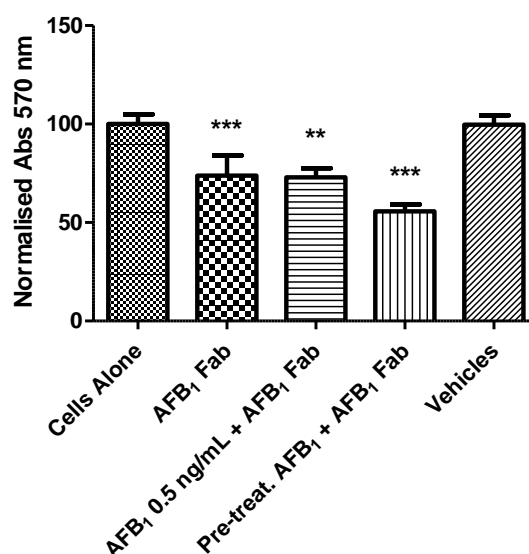


Figure 5.7: MTT proliferation assay to analyse the effects of AFB₁ and the anti-AFB₁ Fab antibody fragment on HepG2 cell proliferation. HepG2 (5×10^5 cells/mL) cells were plated in biological triplicate in complete DMEM ($n = 3$). The cells were exposed to AFB₁ (in methanol and complete DMEM) diluted to a final concentration of 0.5 ng/mL when added to complete DMEM on the plate and anti-AFB₁ Fab antibody fragment (in Dulbecco's PBS) diluted to a final concentration of 0.14 μ M when added to complete DMEM on the plate for 24 hours. The anti-AFB₁ Fab antibody fragment and AFB₁ were also pre-treated together for 15 minutes before being added to plate to a final concentration of 0.14 μ M and 0.5 ng/mL in complete DMEM, respectively. A vehicle control of Dulbecco's PBS diluted to a final concentration of 0.01 % (v/v) and methanol diluted to a final concentration of 0.05 % (v/v) when added to complete DMEM on the plate was also incubated with HepG2 cells. Statistical analysis of data was completed using GraphPad Prism version 5 (GraphPad, La Jolla, CA, USA.). Significance was evaluated by 1-way ANOVA analysis and the Newman-Keuls Multiple Comparison Test with $P < 0.05^*$; $P < 0.01^{**}$ and $P < 0.001^{***}$. Errors bars represent the standard error of the mean (SEM) calculated by dividing the standard deviation by the square root of the n number.

5.2.2.4 SDS-PAGE and Western blotting analysis of anti-AFB₁ scFv-dimer antibody fragment

The pAK500 vector facilitates the purification of *E. coli* expressed antibody fragments by incorporation of a hexa-histidine (HIS5) tag fused to the N-terminal of the recombinant antibody fragment. Immobilized metal-affinity chromatography (IMAC) was used to purify the recombinant antibody protein containing these histidine residues. Previously, an anti-AFB₁ scFv-dimer antibody fragment was developed by Dr. Lynsey Dunne (2002). This antibody was expressed and purified, as described in Sections 2.2.19 – 2.2.22. Briefly,

the bacterial anti-AFB₁ scFv-dimer clone was used to inoculate 10 mL of SB media supplemented with 25 µg/mL of chloramphenicol and 1% (w/v) glucose and was incubated at 37°C overnight while shaking at 250 rpm. The following day, 2 mL (1% (v/v) cell density) of the overnight culture was sub-cultured into 200 mL of fresh SB media supplemented with 25 µg/mL of chloramphenicol and 1% (w/v) glucose and incubated at 37°C while shaking at 250 rpm until an OD₆₀₀ of 0.6 was reached, at which point the optimised concentration of isopropyl β-D-1-thiogalactopyranoside (IPTG) [0.1 mM] was added. The cultures were incubated overnight at the optimised temperature of 30°C and 220 rpm and the following day were subjected to periplasmic osmotic shock and sonication at 40% amplitude to achieve cell lysis, as described in Section 2.2.20.2. Purification using IMAC (Ni⁺-NTA) was completed, as described in Section 2.2.21, followed by buffer exchange and concentration of the scFv-dimer, as described in Sections 2.2.22. The purified anti-AFB₁ scFv-dimer antibody fragment was analysed by SDS-PAGE and Western blotting analysis, as described in Sections 2.2.24 – 2.2.25. The pAK500 vector contains a single chain double helix (dHLX) which represents amphipathic helices used for dimerization of scFv fragments. Anti-AFB₁ scFv-dimer antibody fragment are approximately 60 kDa in size, consisting of two variable regions of the heavy chain (V_H) and two variable regions of the light chain (V_L) linked via a double helix (Dunne, 2002). A band at ~30 kDa representing the cleaved dimeric scFv, consisting of a monomeric scFv attached to a portion of the double helix, can be seen in Figure 5.8 (A.). Western blotting analysis was necessary to probe for the HIS5-tag which is incorporated into the scFv-dimer antibody fragment for purification and specific detection. The anti-AFB₁ scFv-dimer antibody fragment can be seen at ~30 kDa in Figure 5.8 (B.) indicating the desired anti-AFB₁ scFv-dimer antibody fragment was successfully expressed. The purified anti-AFB₁ scFv-dimer antibody fragment was then used to investigate its effects on HepG2 cell proliferation.

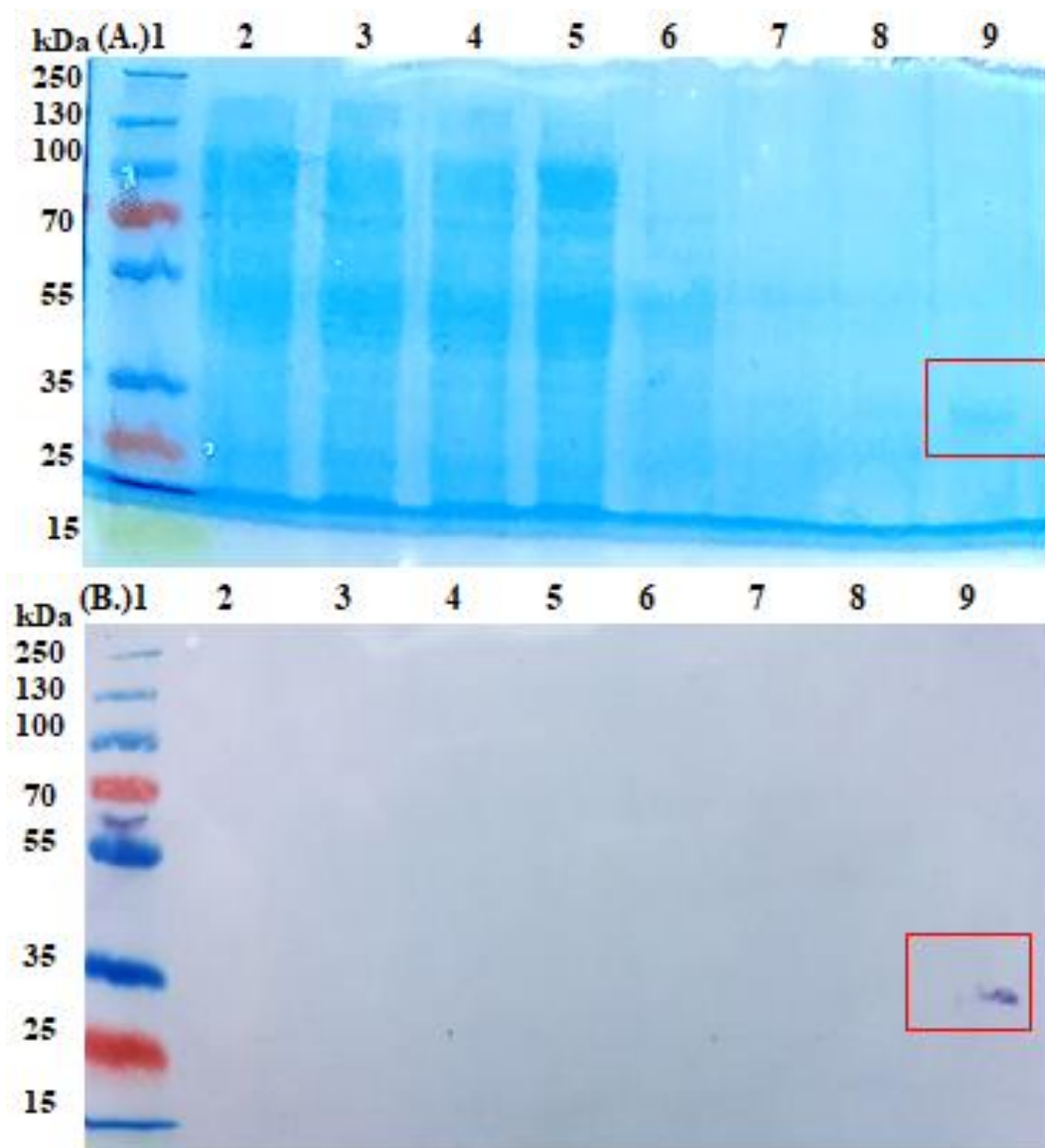


Figure 5.8: (A.) SDS-PAGE and (B.) Western blotting analysis of IMAC purified anti-AFB₁ scFv-dimer antibody fragment. A 1 litre culture of *E. coli* was grown overnight and anti-AFB₁ Fab antibody fragments purified from lysate using IMAC. Samples were taken at all steps of the purification process, denatured and applied to a 12.5% (w/v) acrylamide gel. The proteins present in the samples were visualised by adding Instant Blue dye and the sizes of the respective proteins were assessed based on the inclusion of a standard protein ladder. The expected denatured scFv-dimer antibody fragment band is present at approximately 30 kDa. (Lane 1: Ladder; Lane 2: Unfiltered lysate; Lane 3: Filtered Lysate; Lane 4: Flow-through 2; Lane 5: Flow-through 3; Lane 6: 20 mM Imidazole wash; Lane 7: 20 mM Imidazole wash; Lane 8: Eluted scFv-dimer; Lane 9: Concentrated scFv-dimer).

5.2.2.5 The effects of varying anti-AFB₁ antibody-format treatments on HepG2 cell proliferation

The TACS® MTT Cell Proliferation Assay was completed according to the manufacturer's guidelines and as described in Section 2.2.41. Briefly, HepG2 cells (5×10^5 cells/mL) were plated in 100 μ L of appropriate culture medium in a flat-bottomed 96 well culture plate for 1 hour at 37°C in a 5% CO₂ humidified atmosphere. The anti-AFB₁ Fab antibody fragment, anti-AFB₁ scFv-dimer antibody fragment, commercial anti-AFB₁ monoclonal antibody and anti-AFB₁ polyclonal antibody (0.14 μ M) were added to the HepG2 cells for 24 hours. The results in Figure 5.9 indicate that the anti-AFB₁ Fab antibody fragment had a significant effect in reducing HepG2 cell proliferation (**P<0.01**) compared to cells (+ vehicle). The anti-AFB₁ scFv-dimer antibody fragment also significantly reduced HepG2 cell proliferation but to a greater extent (**P<0.001**). The greater inhibitory effect was most likely due to the double scFv present in the dimer structure. In contrast, both the commercial monoclonal and polyclonal antibodies did not have an effect in decreasing HepG2 proliferation. These results suggest that the shared scFv structure and function of the anti-AFB₁ Fab and scFv-dimer was responsible for the reduced HepG2 proliferation. Both recombinant antibody fragments are specific for AFB₁, opposed to the HepG2 cells. Further scrutiny was necessary to investigate which domain of the scFv region of each recombinant fragment was responsible for the HepG2 interaction and reduction in proliferation. Accordingly, another recombinant Fab antibody fragment (anti-Morphine-3-Glucuronide (M3G)) was examined and aligned with the anti-AFB₁ Fab antibody fragment using a Blast Protein Alignment tool. This was completed to determine if the Fab fragments contained shared sequences in their scFv region which could be used to further identify the specific HepG2-interacting domains.

HepG2: 24 Hours Anti-AFB₁ Antibody Formats

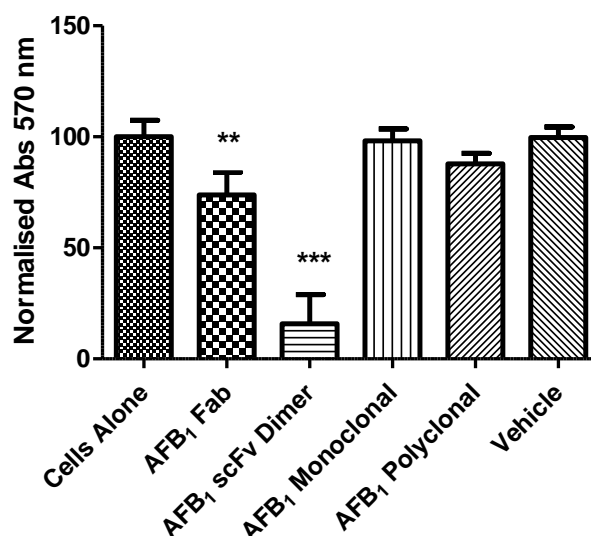


Figure 5.9: MTT proliferation assay to analyse the effects of anti-AFB₁ antibody-formats on HepG2 cell proliferation. HepG2 (5×10^5 cells/mL) cells were plated in biological triplicate in complete DMEM ($n = 3$). The cells were then treated with anti-AFB₁ Fab antibody fragment, anti-AFB₁ scFv-dimer antibody fragment, commercial anti-AFB₁ monoclonal antibody or commercial anti-AFB₁ polyclonal antibody (in Dulbecco's PBS) diluted to a final concentration of $0.14 \mu\text{M}$ when added to complete DMEM on the plate for 24 hours. A vehicle control of Dulbecco's PBS diluted to a final concentration of 0.01 % (v/v) when added to complete DMEM on the plate was also incubated with HepG2 cells. Statistical analysis of data was completed using GraphPad Prism version 5 (GraphPad, La Jolla, CA, USA.). Significance was evaluated by 1-way ANOVA analysis and the Newman-Keuls Multiple Comparison Test with $P < 0.05^*$; $P < 0.01^{**}$ and $P < 0.001^{***}$. Error bars represent the standard error of the mean (SEM) calculated by dividing the standard deviation by the square root of the n number.

5.2.2.6 The effects of antibody fragment CDR sequences on HepG2 cell proliferation

The pComb3xSS vector containing the anti-AFB₁ Fab antibody fragment was grown overnight in 10 mL of SB media supplemented with $50 \mu\text{g/mL}$ of carbenicillin and 1% (w/v) glucose and was incubated at 37°C overnight while shaking at 250 rpm. The following day the culture was centrifuged at $3,220g$ (Eppendorf 5810 R, Rotor A-4-62) at 4°C for 40 minutes. The supernatant was discarded and the plasmid was purified using the Nucleospin plasmid prep kit, as per the manufacturer's guidelines. Sequence analysis was carried out by Source Bioscience Ltd., Dublin, Ireland. The DNA sequence was translated using the ExPASy translate tool and aligned to the anti-Morphine-3-Glucuronide (M3G) Fab (Townsend, 2009) and the anti-AFB₁ scFv-dimer antibody fragments (Dunne, 2002)

using the Blast Protein Alignment tool. Complementarity-determining regions (CDRs) were identified using Kabat rules (Kabat *et al.*, 1991). The results in Figure 5.10 indicate that the anti-AFB₁ Fab and the anti-AFB₁ scFv-dimer have the same sequence as expected. Therefore, the effect elicited by both antibody fragments on HepG2 proliferation can be attributed to their shared scFv binding regions. The light chain of the anti-M3G antibody fragment has 98 % identity with both anti-AFB₁ antibody fragment light chain sequences, differing by only 2 bases. However, the heavy chains are shown to have only 60 %, with little sequence similarity occurring in the relevant binding regions of the heavy chain CDRs. This analysis suggests that the shared light chain sequences of the anti-AFB₁ Fab and the anti-M3G Fab antibody fragment, which contains three CDRs involved in target binding, may be able to interact with, and, affect HepG2 cell proliferation. Therefore, the anti-M3G Fab was expressed and purified to investigate its effect on HepG2 proliferation.

(A.)				
			CDR 1	CDR 2
AFB ₁ Fab	Light	AVVTQESALTTSPGETVTTLTCRSSTGAVTTSNYANWVQEKPDHLFTGLIGGTNNRAPGVP		
AFB ₁ scFv	Light	AVVTQESALTTSPGETVTTLTCRSSTGAVTTSNYANWVQEKPDHLFTGLIGGTNNRAPGVP		
M3G Fab	Light	AVVTQESALTTSPGETVTTLTCRSSTGAVTTSNYANWVQEKPDHLFTGLIGGTNNRAPGVP		
Consensus	Region	AVVTQESALTTSPGETVTTLTCRSSTGAVTTSNYANWVQEKPDHLFTGLIGGTNNRAPGVP		
			CDR 3	
AFB ₁ Fab	Light	ARFSGSLIGDKAALTITGAQTEDEAIYFCALWYSNHVVFVGGGKTLTVLGQPK		
AFB ₁ scFv	Light	ARFSGSLIGDKAALTITGAQTEDEAIYFCALWYSNHVVFVGGGKTLTVLGQPK		
M3G Fab	Light	ARFSGSLIGDKAALTITGAQTEDEAIYFCVWYSNHLVFGGGKTLTVLGQPK		
Consensus	Region	ARFSGSLIGDKAALTITGAQTEDEAIYFC LWYSNH VFVGGGKTLTVLGQPK		
Identities 110/122 = 98%			Positives 110/122 = 98%	Gaps 0/112 = 0%
(B.)				
			CDR 1	CDR 2
AFB ₁ Fab	Heavy	SGPELVPRPGASVKMSCKSSGYSFTSYWLHWVKQRPQGLEWIGAIYPGNSDTRYNQKFKG		
AFB ₁ scFv	Heavy	SGPELVPRPGASVKMSCKSSGYSFTSYWLHWVKQRPQGLEWIGAIYPGNSDTRYNQKFKG		
M3G Fab	Heavy	SGAELMKPGASVKISCKATGYTFSRYWIEWVKQRPQHGLEWIGEILPGSGSTKYNEKFKG		
Consensus	Region	SG EL++PGASVK+SCK++GY+F+ YW+ WVKQRPQ GLEWIG I PG+ T+YN+KFKG		
			CDR 3	
AFB ₁ Fab	Heavy	KVKLTAVTSASTAYMETELSSLTNEDSAVYYCTRGEAYRYGGIWFAYWGQGLTVTVSAAS		
AFB ₁ scFv	Heavy	KVKLTAVTSASTAYMETELSSLTNEDSAVYYCTRGEAYRYGGIWFAYWGQGLTVTVSAAS		
M3G Fab	Heavy	RATFTADTSSNTVYM--QLSSLTSEDSAVYHCAWSQVHV-----MDYWGQGTTVTVSSAS		
Consensus	Region	+ TA TS++T YM +LSSLT+EDSAVY+C R + YWGQGTVTVS+AS		
Identities 73/121 = 60%			Positives 92/121 = 76%	Gaps 7/112 = 5%

Figure 5.10: Anti-AFB₁ Fab, anti-AFB₁ scFv-dimer and anti-M3G antibody fragment sequence analysis. The amino acid sequences aligned using the Blast Protein Alignment tool. The light and heavy chain complementarity determining regions (CDRs) were defined according to Kabat *et al.* (1991) and are highlighted in yellow. (A.) The light chain variable regions of the three antibodies were found to be 98 % identical with the exception of two amino acids. (B.) The heavy chain variable regions were found to be only 60% identical and lacked similarity in the CDRs.

5.2.2.7 SDS-PAGE and Western blotting analysis of anti-M3G Fab antibody fragment

The pCom3xSS vector facilitates the purification of *E. coli* expressed antibody fragments by incorporation of a hexa-histidine (HIS6) tag fused to the N-terminal of the recombinant antibody fragment. Immobilized metal-affinity chromatography (IMAC) was used to purify the recombinant antibody protein containing these histidine residues. Previously, an anti-M3G Fab antibody fragment was developed by Dr. Sue Townsend (2009). This

antibody fragment was expressed and purified from a pComb3x vector, as described in Sections 2.2.19 – 2.2.22. Briefly, the bacterial anti-M3G Fab clone was used to inoculate 10 mL of SB media supplemented with 50 µg/mL of carbenicillin and 1% (w/v) glucose and was incubated at 37°C overnight while shaking at 250 rpm. The following day, 2 mL (1% (v/v) cell density) of the overnight culture was sub-cultured into 200 mL of fresh SB_{GC} media and incubated at 37°C while shaking at 250 rpm until an OD₆₀₀ of 0.6 was reached, at which point the optimised concentration of isopropyl β-D-1-thiogalactopyranoside (IPTG) [0.1 mM] was added. The cultures were incubated overnight at the optimised temperature of 30°C and 220 rpm and the following day were subjected to freeze-thaw cycling and sonication at 40% amplitude to achieve cell lysis, as described in Section 2.2.20. Purification using IMAC (Ni⁺-NTA) was completed, as described in Section 2.2.21, followed by buffer exchange and concentration, as described in Section 2.2.22. The purified anti-M3G Fab antibody fragment was analysed by SDS-PAGE and Western blotting analysis, as described in Sections 2.2.24 – 2.2.25. Fab antibody fragments are approximately 50 kDa in size, consisting of a full light chain and half a heavy chain. A band at ~50 kDa can be seen in Figure 5.11 (A.) representing the expected band for the anti-M3G Fab antibody fragment following purification. To confirm that the band of interest was that of anti-M3G Fab antibody fragment, Western blotting analysis probing specifically for the HA tag of anti-M3G Fab antibody fragment at ~50 kDa was completed. The anti-M3G Fab antibody heavy chain can be seen at ~50 kDa in Figure 5.11 (B.). This result indicates the desired anti-AFB₁ M3G antibody fragment had been successfully purified and, therefore, was used to investigate its effects on HepG2 cell proliferation.

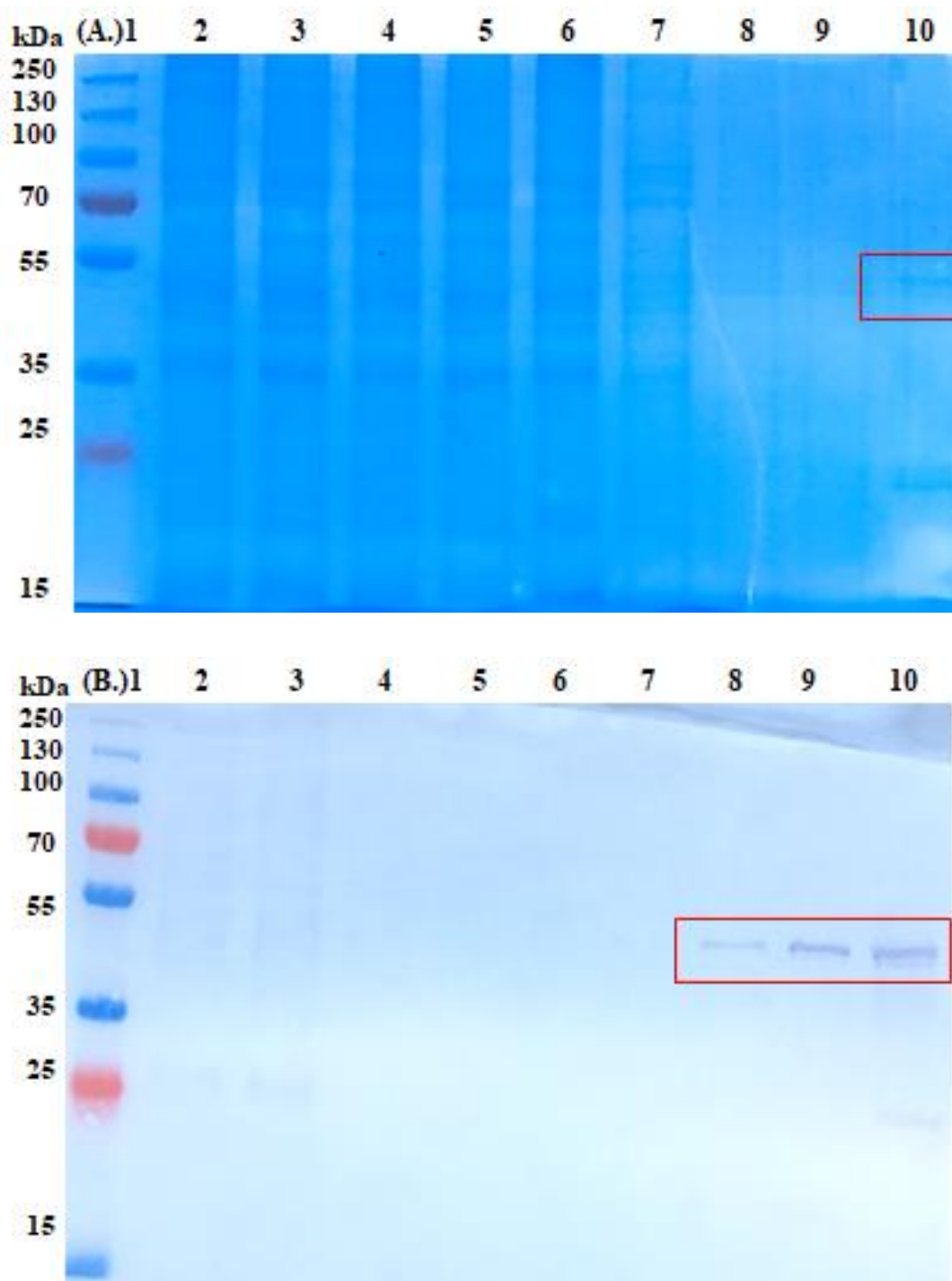


Figure 5.11: (A.) SDS-PAGE and (B.) Western blotting analysis of IMAC purified anti-M3G Fab antibody fragment. A 1 litre culture of *E. coli* was grown overnight and anti-AFB₁ Fab antibody fragments purified from lysate using IMAC. Samples were taken at all steps of the purification process, denatured and applied to a 12.5% (w/v) acrylamide gel. The proteins present in the samples were visualised by adding Instant Blue dye and the sizes of the respective proteins were assessed based on the inclusion of a standard protein ladder. The expected denatured Fab antibody fragment band is present at approximately 30 kDa. (Lane 1: Ladder; Lane 2: Unfiltered lysate; Lane 3: Filtered Lysate; Lane 4: Flow-through 1; Lane 5: Flow-through 2; Lane 6: Flow-through 3; Lane 7: 40 mM Imidazole wash; Lane 8: 40 mM Imidazole wash; Lane 9: Eluted Fab; Lane 10: Concentrated Fab).

5.2.2.8 The effects of anti-AFB₁ and anti-M3G Fab antibody fragment treatments on HepG2 cell proliferation

The TACS® MTT Cell Proliferation Assay was completed according to the manufacturer's guidelines and as described in Section 2.2.41. Briefly, HepG2 cells (5×10^5 cells/mL) were plated in 100 μ L of appropriate culture medium in a flat-bottomed 96 well culture plate for 1 hour at 37°C in a 5% CO₂ humidified atmosphere. The effects of the anti-AFB₁ Fab antibody fragment treatment and anti-M3G Fab antibody were investigated by adding both Fab antibody fragments (0.14 μ M) to the HepG2 cells for 24 hours. The results in Figure 5.12 indicate that the anti-AFB₁ Fab antibody fragment has a significant effect in reducing HepG2 cell proliferation (**P<0.001**) compared to cells (+ vehicle). Similarly, the anti-M3G Fab antibody fragment also has a significant effect in reducing HepG2 cell proliferation (**P<0.001**). Therefore, it can be hypothesised that the similarity evident in their structure is responsible for the similar effect both Fab antibody fragments are exerting in reducing HepG2 proliferation.

Previously, competitive inhibition ELISAs were completed (Section 4.2.1) to characterise the anti-AFB₁ Fab antibody fragment and determined that 1 μ g/mL of free AFB₁ could effectively inhibit and eliminate anti-AFB₁ antibody fragment (0.14 μ M) binding to the AFB₁-BSA coated. Therefore, inhibitory AFB₁ was added to the anti-AFB₁ antibody fragment for 1 hour to effectively bind and theoretically inhibit it from exerting an effect on HepG2 proliferation. The results in Figure 5.12 show that under these conditions there was no significant reduction in HepG2 proliferation. In contrast, the addition of inhibitory AFB₁ was not shown to have an inhibitory effect on the anti-M3G Fab antibody fragment, as HepG2 proliferation was significantly reduced to the same extent as when the free AFB₁ was absent (**P<0.001**). The anti-M3G Fab antibody fragment is not specific for AFB₁, therefore, it would not be anticipated that binding and inhibition should occur. Sequence analysis of the anti-M3G Fab antibody fragment, as described in Section 5.2.2.7, indicated that the heavy chain differed from that of the anti-AFB₁ Fab antibody fragment. Typically the CDR3 of the heavy chain is largely responsible for specific binding to an antigen. Accordingly, the CDR3 is specific for M3G and not AFB₁, therefore the anti-M3G Fab antibody fragment was not interacting with the inhibitory AFB₁, and was free to bind and interact with the HepG2 cells. In contrast, the anti-AFB₁ Fab antibody fragment was bound by the inhibitory AFB₁ and the relevant binding domains were not available to interact

with the HepG2 cells. It is difficult to ascertain which HepG2 receptor or ligand is subject to the anti-AFB₁ Fab antibody fragment interaction. Given the known interactions that occur between AFB₁ and the IGF pathway, it may be possible that the Fab is exerting an effect via the same signalling pathway, sequence analysis comparisons are completed in Section 5.2.2.10 to determine similarity between both, however, further experimentation would be necessary to confirm this theory. Alternatively, HepG2 cell receptors specifically involved in cellular migration and proliferation would seem likely to be the relevant interacting partners for the anti-AFB₁ Fab antibody fragment given the inhibitory impact it exerts on these cellular functions.

HepG2: 24 Hours Fab Antibody Fragments

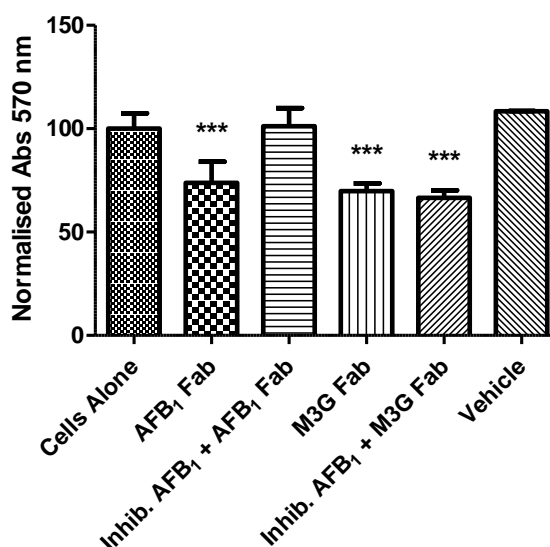


Figure 5.12: MTT proliferation assay to analyse the effects of Fab antibody fragments on HepG2 cell proliferation. HepG2 (5×10^5 cells/mL) cells were plated in biological triplicate in complete DMEM ($n = 3$). The cells were then treated with anti-AFB₁ Fab antibody fragment or anti-M3G Fab antibody fragment (in Dulbecco's PBS) diluted to a final concentration of $0.14 \mu\text{M}$ when added to complete DMEM on the plate for 24 hours. Additionally, an inhibitory concentration of AFB₁ ($1 \mu\text{g/mL}$) to block anti-AFB₁ Fab antibody fragment binding was added to HepG2 cells with $0.14 \mu\text{M}$ anti-AFB₁ Fab and the anti-M3G Fab antibody fragments and HepG2 cell proliferation was tested. A vehicle control of Dulbecco's PBS diluted to a final concentration of 0.01% (v/v) and methanol diluted to a final concentration of 0.05% (v/v) when added to complete DMEM on the plate was also incubated with HepG2 cells. Statistical analysis of data was completed using GraphPad Prism version 5 (GraphPad, La Jolla, CA, USA.). Significance was evaluated by 1-way ANOVA analysis and the Newman-Keuls Multiple Comparison Test with $P < 0.05^*$; $P < 0.01^{**}$ and $P < 0.001^{***}$. Errors bars represent the standard error of the mean (SEM) calculated by dividing the standard deviation by the square root of the n number.

5.2.2.9 The effects of varying anti-AFB₁ antibody-format treatments on THLE-2 cell proliferation

The TACS® MTT Cell Proliferation Assay was completed according to the manufacturer's guidelines and as described in Section 2.2.41. Briefly, THLE-2 cells (2.5×10^5 cells/mL) were plated in 100 μ L of appropriate culture medium in a flat-bottomed 96 well culture plate for 1 hour at 37°C in a 5% CO₂ humidified atmosphere. The anti-AFB₁ Fab antibody fragment, anti-AFB₁ scFv-dimer antibody fragment, commercial anti-AFB₁ monoclonal antibody and anti-AFB₁ polyclonal antibody (0.14 μ M) were added to the THLE-2 cells for 24 hours. The results in Figure 5.13 indicate that the anti-AFB₁ antibody-formats did not have a significant effect in reducing THLE-2 cell proliferation. This result suggests that the THLE-2 cells do not have a relevant ligand or pathway for any of the anti-AFB₁ antibody formats to target and induce an effect on THLE-2 proliferation. Alternatively, as cancerous cells over-express certain surface markers, it may be possible that the THLE-2 cells may not have the relevant ligand over-expressed on their surface and available for the inhibitory-interaction evident in HepG2 cells. The THLE-2 cells effectively function as a negative control in comparison with the results described in Section 5.2.2.4, to show that the anti-AFB₁ Fab and scFv-dimer antibody fragment-formats specifically reduced proliferation in HepG2 cells.

THLE-2: 24 Hours Anti AFB₁ Antibody Formats

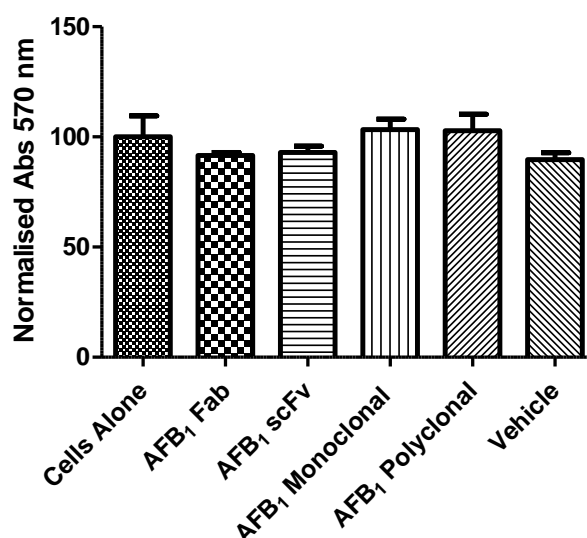


Figure 5.13: MTT proliferation assay to analyse the effects of anti-AFB₁ antibody-formats on THLE-2 cell proliferation. THLE-2 (2.5×10^5 cells/mL) cells were plated in biological triplicate in complete LHC-8 medium ($n = 3$). The cells were then treated with anti-AFB₁ Fab antibody fragment, anti-AFB₁ scFv-dimer antibody fragment, commercial anti-AFB₁ monoclonal antibody or commercial anti-AFB₁ polyclonal antibody (in Dulbecco's PBS) diluted to a final concentration of $0.14 \mu\text{M}$ when added to complete LHC-8 medium on the plate for 24 hours. A vehicle control of Dulbecco's PBS diluted to a final concentration of 0.01 % (v/v) when added to complete LHC-8 medium on the plate was also incubated with HepG2 cells. Statistical analysis of data was completed using GraphPad Prism version 5 (GraphPad, La Jolla, CA, USA.). Significance was evaluated by 1-way ANOVA analysis and the Newman-Keuls Multiple Comparison Test with $P < 0.05^*$; $P < 0.01^{**}$ and $P < 0.001^{***}$. Errors bars represent the standard error of the mean (SEM) calculated by dividing the standard deviation by the square root of the n number.

5.2.2.10 Sequence analysis of anti-AFB₁ fab antibody fragment and IGF-1R

Sequence analysis was carried out by Source Bioscience Ltd., Dublin, Ireland. The DNA sequence was translated using the Expsy translate tool and aligned to IGF-1R obtained from the Uniport website. The results in Figure 5.14 indicate that the anti-AFB₁ Fab antibody fragment and IGF-1R have sequence similarity evident in the CDR3 region of the light chain. The CDR3 region in antibodies is vital for binding interactions, therefore, it may be possible that the anti-AFB₁ Fab antibody fragment could exert an effect on the HepG2 cells via interactions at this region in IGF-1R. However, further investigations would be necessary to determine the true mechanism of interaction.

AFB ₁ Fab Light Chain	YSNHWVFG
IGF-1R	YSDVWSFG
Consensus Region	YS+ W FG

Identities 5/8 = 63% Positives 6/8 = 75% Gaps 0/8 = 0%

Figure 5.14: Anti-AFB₁ Fab antibody fragment and IGF-1R sequence analysis. The amino acid sequences were aligned using the Blast Protein Alignment tool.

5.2.3 The effects of AFB₁ dosing combined with anti-AFB₁ Fab antibody fragment treatment on HepG2 cell cytokine expression

Cytokines participate in the induction and effector phases of all immune and inflammatory responses. Measurement of cytokine expression has yielded useful information on the pathologic process in different disease, in the monitoring of disease progression and/or inflammation. The detection of secreted cytokine protein is the most commonly used method of analysis. Secreted proteins represent biologically relevant moieties and the detection of such provides the closest possible manifestation of what the cells are responding to. Secreted protein is typically measured by ELISA (Kelso, 1998; Sullivan *et al.*, 2000). IL-8 is a critical inflammatory mediator, specifically functioning in the recruitment of neutrophils, although it is also responsible for the chemotactic migration and activation of monocytes, lymphocytes, basophils and eosinophils at sites of inflammation. Following binding to CXCR1 or CXCR2, intracellular signalling cascades result in the activation of MAPK signalling and alter gene expression to promote cell survival, proliferation and inflammation. Furthermore, IL-8 signalling *via* MAPK and phosphatidylinositol-3 kinase (PI3K) induces the expression of adhesion molecules (integrins) necessary for chemotaxis. Therefore, IL-8 mediates the recruitment and activation of neutrophils by complex signalling mechanisms and extracellular adhesion molecules (Turner *et al.*, 2014). Cytokine testing for IL-8 was completed using R&D duoset ELISA incomplete Kits according to the manufacturer's guidelines and as described in Section 2.2.42. Briefly, HepG2 (20 x 10⁵ cells/mL) were plated in 100 µL of appropriate culture medium in a flat-bottomed 96 well culture plate in triplicate for 1 hour at 37°C in a 5% CO₂ humidified atmosphere. The effects of AFB₁ dosing and anti-AFB₁ Fab antibody fragment treatment on HepG2 cells was investigated by adding a range of AFB₁ doses

(0.01 and 0.1 ng/mL) for various time-frames (24, 48 and 72 hours) and/or anti-AFB₁ Fab antibody fragment (0.14 μ M) treatment for various time-frames (24, 48 and 72 hours). Supernatants were collected and tested in an IL-8 cytokine ELISA. The appropriate concentration of relevant capture antibody was coated on a Nunc MaxiSorp® flat-bottom 96 well plate, was used to capture the relevant cytokine present in the HepG2 supernatants. The appropriate concentration of relevant detection antibody was added following by Streptavidin-HRP to detect the presence of the cytokine of interest. These experiments were conducted to determine the effects of AFB₁ and the anti-AFB₁ Fab antibody fragment on HepG2 cell IL-8 expression. Statistical analysis of data was completed using GraphPad Prism version 5 (GraphPad, La Jolla, CA, USA.). Significance was evaluated by 1-way ANOVA analysis and the Newman-Keuls Multiple Comparison Test with $P < 0.05^*$; $P < 0.01^{**}$ and $P < 0.001^{***}$.

5.2.3.1 The effects of AFB₁ dosing on HepG2 cell IL-8 cytokine expression

HepG2 cells were plated on sterile 96-well culture plates. Fresh media and AFB₁ doses (0.01 and 0.1 ng/mL) were added to the plates every 24 hours for 72 hours and HepG2 cell IL-8 cytokine expression was tested every 24 hours. The results in Figure 5.15 indicate that after 24 hours of exposure with all concentrations of AFB₁, no significant change in the expression of IL-8 by HepG2 cells compared to cells (+ vehicle) was observed. A significant increase in IL-8 expression ($P < 0.01$) was seen after 48 hours of 0.01 and 0.1 ng/mL of AFB₁ exposure. It was established by using a best fit polynomial curve that after 48 hours, cells (+ vehicle) expressed 328.65 pg/mL of IL-8, cells exposed to 0.01 ng/mL of AFB₁ expressed 375.07 pg/mL and cells exposed to 0.1 ng/mL of AFB₁ expressed 428.72 pg/mL. After 72 hours of AFB₁ exposure, IL-8 expression returns to similar levels as the cells alone and cells treated with the vehicle. This result indicates that at these low concentrations of AFB₁, the expression of IL-8 is not initially impacted, however, after 48 hours of exposure IL-8 is expressed to significant levels before the effects of AFB₁ are attenuated and return to normal levels of expression after 72 hours. The findings in Section 5.2.1 and 5.2.2 indicate that AFB₁ exposure results in decreased HepG2 migration and proliferation after 24 hours, before returning to normal levels after 48 hours. Together, this profile suggest that HepG2 proliferation and migration are initially impacted, followed by an increase in IL-8 expression after 48 hours to help recover normal proliferation and

migration. Subsequent to HepG2 recovery, IL-8 expression levels return to normal levels after 72 hours.

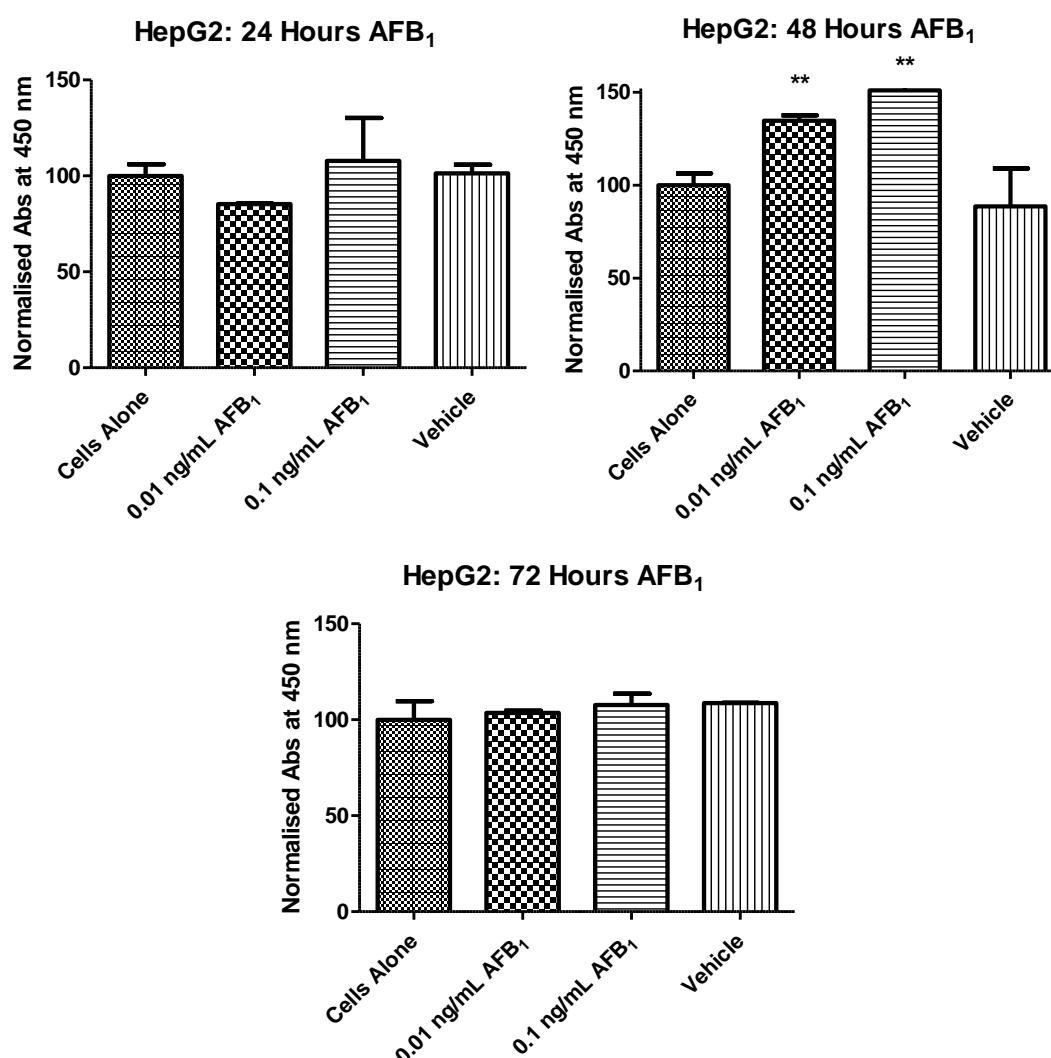


Figure 5.15: IL-8 cytokine assay to analyse the effects of AFB₁ on the HepG2 cell cytokine expression. HepG2 (20×10^5 cells/mL) cells were plated in biological triplicate in complete DMEM ($n = 3$). The cells were exposed to AFB₁ (in methanol and complete DMEM) diluted to a final concentration of 0.01 and 0.1 ng/mL when added to complete DMEM on the plate for 24, 48 or 72 hours. A vehicle control of methanol in complete DMEM diluted to a final concentration of 0.05 % (v/v) when added to complete DMEM on the plate was also incubated with HepG2 cells. Statistical analysis of data was completed using GraphPad Prism version 5 (GraphPad, La Jolla, CA, USA.). Significance was evaluated by 1-way ANOVA analysis and the Newman-Keuls Multiple Comparison Test with $P < 0.05^*$; $P < 0.01^{**}$ and $P < 0.001^{***}$. Errors bars represent the standard error of the mean (SEM) calculated by dividing the standard deviation by the square root of the n number.

5.2.3.2 The effects of anti-AFB₁ Fab antibody fragment treatment on HepG2 cell IL-8 cytokine expression

HepG2 cells were plated on sterile 96-well culture plates. Fresh media and anti-AFB₁ antibody fragment treatments (0.14 µM) was added to the plates every 24 hours for 72 hours and HepG2 cell IL-8 cytokine expression was tested every 24 hours. The results in Figure 5.16 indicate that after treatment of cells for 24 and 48 hours anti-AFB₁ Fab antibody fragment a significant increase (**P < 0.001**) in the expression of IL-8 by HepG2 cells compared to cells (+ vehicle) was observed. It was established by using a best fit polynomial curve that after 24 hours, cells (+ vehicle) expressed 76.72 pg/mL of IL-8 and cells exposed to anti-AFB₁ Fab antibody fragment expressed 680.30 pg/mL of IL-8 whilst after 48 hours, cells (+ vehicle) expressed 77.55 pg/mL of IL-8 and cells exposed to anti-AFB₁ Fab antibody fragment expressed 868.39 pg/mL of IL-8. The very significant increase in expressed IL-8 may be due to the significant effect the anti-AFB₁ Fab antibody fragment has in attenuating HepG2 migration and proliferation, as described in Section 5.2.1 and 5.2.2, resulting in the stimulation of a pro-inflammatory response from the HepG2 cells. However, after 72 hours of anti-AFB₁ Fab antibody fragment treatment IL-8 expression returned to normal levels. These results indicate that the anti-AFB₁ Fab antibody fragment can elicit a significant increase in HepG2-cell IL-8 expression during the first 48 hours of exposure, causing acute IL-8 secretion. Research indicates that anti-cancer drugs can increase IL-8 secretion. A study completed by Park *et al.* (2014) showed that anti-cancer drugs upregulated both secretion of IL-8 and expression of IL-8 receptor in hepatoma cells. Furthermore, their research indicated IL-8 positively correlated with expression of drug resistance genes in human hepatoma cells and HCC tissues, and that silencing of IL-8 reduced tumourigenicity of hepatoma cells. Therefore, IL-8 is correlated with poor chemotherapeutic responses. Accordingly, though the anti-AFB₁ Fab antibody fragment may have positive effects in inhibiting HepG2 cell migration and proliferation, it also elicits the secretion of high levels of IL-8. The inhibition of IL-8 expression and secretion offers another therapeutic target which may be useful in the treatment of HCC.

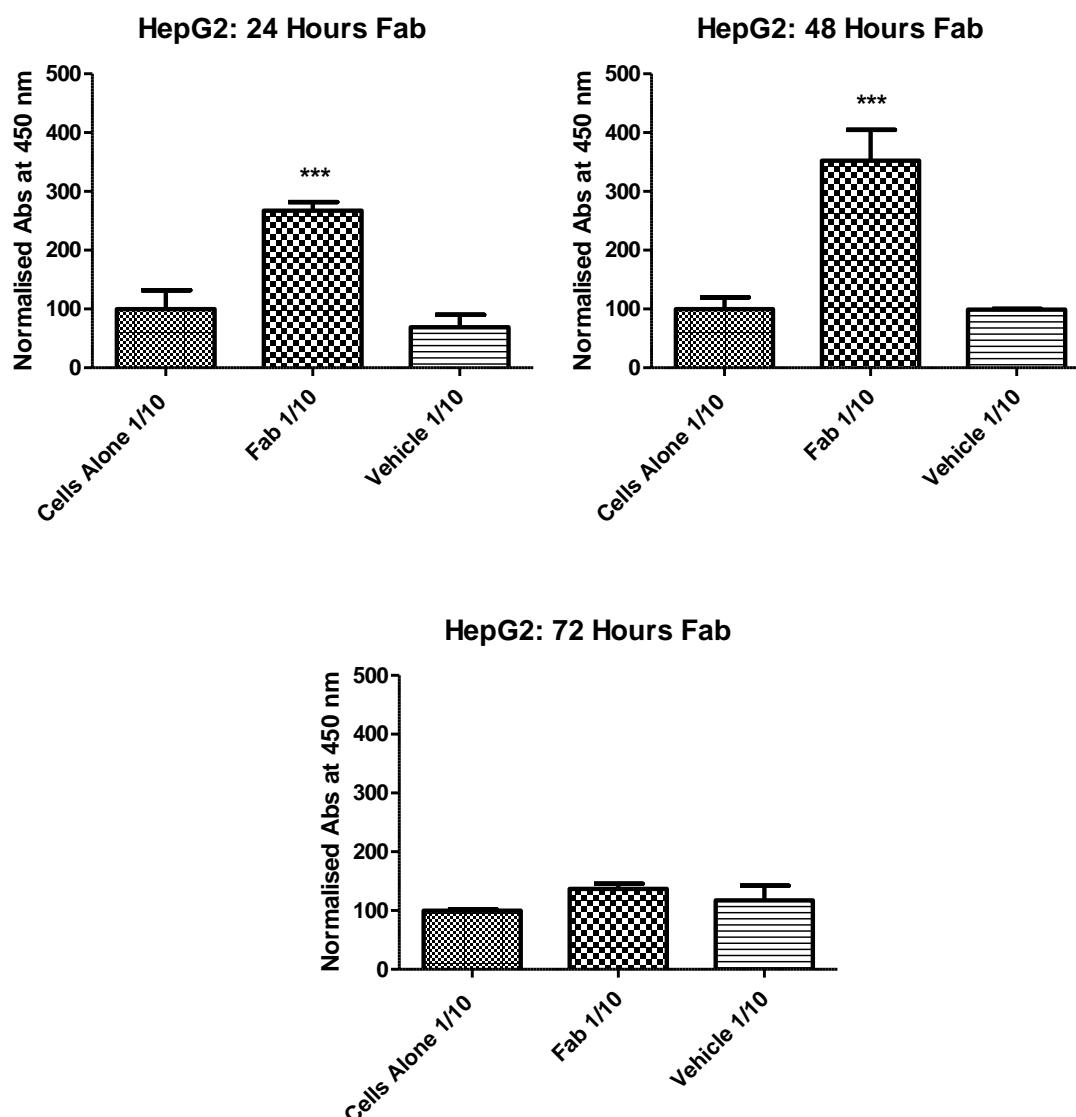


Figure 5.16: IL-8 cytokine assay to analyse the effects of anti-AFB₁ Fab antibody fragment on HepG2 cell cytokine expression. HepG2 (20×10^5 cells/mL) cells were plated in biological triplicate in complete DMEM ($n = 3$). The cells were treated with anti-AFB₁ Fab antibody fragment (in Dulbecco's PBS) diluted to a final concentration of 0.14 μ M when added to complete DMEM on the plate for 24, 48 and 72 hours. A vehicle control of Dulbecco's PBS diluted to a final concentration of 0.01% (v/v) when added to complete DMEM on the plate was also incubated with HepG2 cells. Statistical analysis of data was completed using GraphPad Prism version 5 (GraphPad, La Jolla, CA, USA.). Significance was evaluated by 1-way ANOVA analysis and the Newman-Keuls Multiple Comparison Test with $P < 0.05^*$; $P < 0.01^{**}$ and $P < 0.001^{***}$. Errors bars represent the standard error of the mean (SEM) calculated by dividing the standard deviation by the square root of the n number.

5.2.3.3 The effects of AFB₁ dosing and anti-AFB₁ Fab antibody fragment treatment on HepG2 cell IL-8 cytokine expression

HepG2 cells were plated on sterile 96-well culture plates. Fresh media, various concentrations of AFB₁ (0.01 and 0.1 ng/mL) and anti-AFB₁ antibody fragment treatments (0.14 μ M) was added to the plates every 24 and 48 hours and HepG2 cell IL-8 cytokine expression was tested. The results in Figure 5.17 indicate that after 24 hours of AFB₁ exposure and 24 hours of anti-AFB₁ Fab antibody fragment treatment a significant increase (**P < 0.001**) in the expression of IL-8 by HepG2 cells compared to cells (+ vehicle) was observed. It was established by using a best fit polynomial curve that after 24 hours, cells (+ vehicle) expressed 425.76 pg/mL of IL-8, cells exposed to 0.01 ng/mL of AFB₁ and anti-AFB₁ Fab antibody fragment expressed 2,039.14 pg/mL of IL-8 and cells exposed to 0.1 ng/mL of AFB₁ and anti-AFB₁ Fab antibody fragment expressed 2,056.46 pg/mL of IL-8. Furthermore, after 48 hours of AFB₁ exposure and 48 hours of anti-AFB₁ Fab antibody fragment treatment a significant increase (**P < 0.001**) in the expression of IL-8 was still evident. After 48 hours, cells (+ vehicle) expressed 329.18 pg/mL of IL-8, cells exposed to 0.01 ng/mL of AFB₁ and anti-AFB₁ Fab antibody fragment expressed 890.91 pg/mL of IL-8 and cells exposed to 0.1 ng/mL of AFB₁ and anti-AFB₁ Fab antibody fragment expressed 756.18 pg/mL of IL-8. The results described in Section 5.2.3.1 indicated that AFB₁ exposure for 24 hours did not impact HepG2 IL-8 expression, however, the results described in Section 5.2.3.2 indicated that the anti-AFB₁ antibody fragment could significantly increase IL-8 expression. Therefore, the increase in IL-8 expression after 24 hours of AFB₁ exposure and 24 hours of anti-AFB₁ antibody fragment treatment, is most likely due to the latter treatment. Furthermore, the IL-8 increase is similar to that already seen for anti-AFB₁ antibody fragment treatment after 24 hours. After 48 hours of either AFB₁ exposure (0.01 and 0.1 ng/mL) (**P < 0.05**) or after 48 hours of anti-AFB₁ Fab antibody fragment treatment (**P < 0.001**) significant increases in IL-8 expression were evident. Consequently, after 48 hours of AFB₁ exposure, followed with 48 hours of anti-AFB₁ Fab antibody fragment treatment, a significant increase in IL-8 expression was elicited. These results support the theory suggested in Sections 5.2.1 and 5.2.2, that AFB₁ and anti-AFB₁ Fab antibody fragment function in combination of a synergistic manner, exerting an increased effect on IL-8 secretion from HepG2 cells.

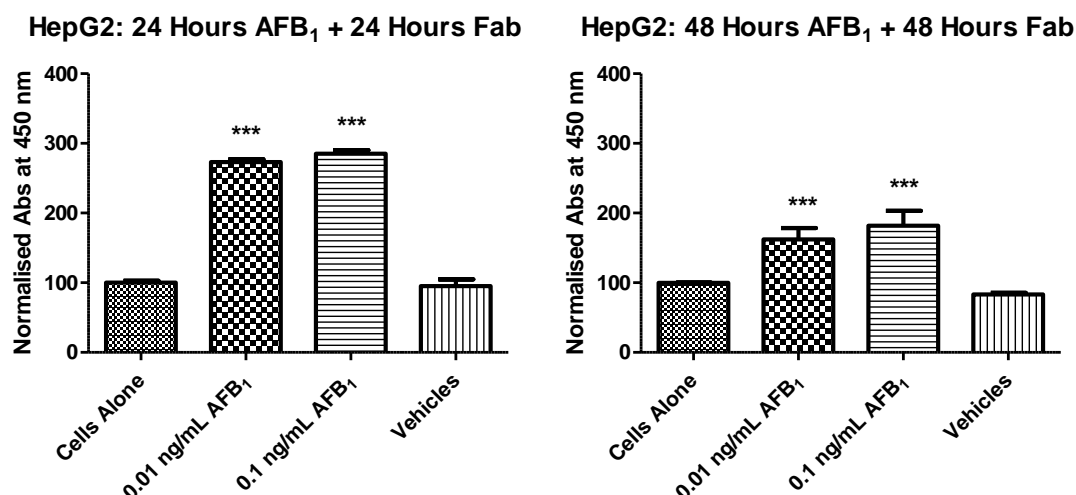


Figure 5.17: IL-8 cytokine assay to analyse the effects of AFB₁ and anti-AFB₁ Fab antibody fragment treatment on the HepG2 cell cytokine expression. HepG2 (20×10^5 cells/mL) cells were plated in biological triplicate in complete DMEM ($n = 3$). The cells were exposed to AFB₁ (in methanol and complete DMEM) diluted to a final concentration of 0.01 and 0.1 ng/mL when added to complete DMEM on the plate for 24 or 48 hours. The cells were then treated with anti-AFB₁ Fab antibody fragment (in Dulbecco's PBS) diluted to a final concentration of 0.14 μ M when added to complete DMEM on the plate for 24 or 48 hours. A vehicle control of Dulbecco's PBS diluted to a final concentration of 0.01 % (v/v) and methanol diluted to a final concentration of 0.05 % (v/v) when added to complete DMEM on the plate was also incubated with HepG2 cells. Statistical analysis of data was completed using GraphPad Prism version 5 (GraphPad, La Jolla, CA, USA.). Significance was evaluated by 1-way ANOVA analysis and the Newman-Keuls Multiple Comparison Test with $P < 0.05^*$; $P < 0.01^{**}$ and $P < 0.001^{***}$. Errors bars represent the standard error of the mean (SEM) calculated by dividing the standard deviation by the square root of the n number.

5.3 Discussion

Hepatocellular carcinoma (HCC) is the fifth most common cancer in men and the seventh in women worldwide. However, due to poor prognosis, HCC is the third leading cause of cancer-related mortality. Aflatoxin B₁ (AFB₁), now considered a ubiquitous food-contaminant in developing countries, demonstrates a positive association between exposure and development of hepatocellular carcinoma HCC (Kew, 2003; Khlangwiset and Wu, 2010). Consequently, the geographical incidence of HCC is evident in developing countries, where over 80% of cases present (Ferlay *et al.*, 2010). The carcinogenic effect of AFB₁ exposure is attributed to AFB₁ metabolism by cytochrome P450 enzymes which convert the mycotoxin to an unstable, reactive AFB₁-8-9-epoxide. The epoxide acts a mutagen, reacting with the N7 position of guanine in DNA to generate an AFB₁-N7-Gua intermediate which have been proven to cause HCC in humans. Liver tumour tissues with high AFB₁ exposure have been shown to develop a specific mutation at codon 249 in P53 tumour suppressing gene resulting in a G to T transversion (AGG to AGT). However, the exact mechanism and pathway by which AFB₁ exerts its hepatocellular carcinogenic effect appears to have further complexities. Studies by Ubagai *et al.* (2010) demonstrated that AFB₁ stimulated expression of Insulin-like Growth Factor-2 (IGF-2) and Insulin-like Growth Factor-1 Receptor (IGF-1R). Furthermore, research by Lee *et al.* (2000) indicated that mutation of codon 249 in the P53 gene can increase IGF-2 transcription, inferring that the AFB₁-induced mutation of the P53 gene may be responsible for IGF-2 stimulation. The IGF system is known to transduce diverse effects in cellular metabolism, proliferation, development and survival, however, further scrutiny also implicates it has a role in human cancer progression and tumourigenesis (Siddle, 2011). Ma *et al.* (2012) conducted further investigations into the impact of AFB₁ exposure on the IGF pathway. Their work revealed that IGF-1R inhibition or Insulin Receptor Substrate-2 (IRS-2) knockdown, suppressed AFB₁-induced hepatoma cell migration. Ubagai *et al.* and Ma *et al.* demonstrated that the IGF axis is vitally important in understanding the effects of AFB₁ on hepatocellular carcinoma cells.

It was noted that previous studies to investigate AFB₁ effects in-vitro, typically used relatively high doses of AFB₁ (up to 10 µM). Therefore, the research in this chapter focused on the effects of low doses of AFB₁ (0.01 and 0.1 ng/mL) on HepG2 liver carcinoma cells. AFB₁-dosed HepG2 cells were examined in terms of cellular migration,

proliferation and expression of the cytokine IL-8. The results of scratch assays, as described in Section 5.2.1.1 indicated that HepG2 cells exposed to 0.01 and 0.1 ng/mL of AFB₁ resulted in a decrease in cellular migration after 24 hours compared to cells (+ vehicle). After 48 hours of exposure, the scratch closed and remained fully migrated after 72 hours of exposure. The findings from proliferation assays, as described in Section 5.2.2.1, suggested that HepG2 cells exposed to 0.01 and 0.1 ng/mL of AFB₁ decreased cellular proliferation significantly ($P < 0.05$) after 24 hours compared to cells (+ vehicle) and returned to normal proliferation levels at 48 and 72 hours. Finally, the results in Section 5.2.3.1 showed that HepG2 cell expression of IL-8 was not affected by exposure to 0.01 and 0.1 ng/mL of AFB₁ after 24 hours compared to cells alone. However, after 48 hours of exposure, the cells significantly increased IL-8 secretion ($P < 0.01$), before returning to normal expression levels after 72 hours. Together, these results indicate that after 24 hours of exposure to low doses of AFB₁ HepG2 migration and proliferation were inhibited. Interesting, it is only after 48 hours of AFB₁ exposure that HepG2 cell IL-8 secretion is significantly increased. The significance for both doses of AFB₁ is the same ($P < 0.01$), however, a greater increase in IL-8 expression is evident following exposure to 0.1 ng/mL of AFB₁, implying that slightly more IL-8 is produced in response to the higher concentration of AFB₁. IL-8 serves as a major chemoattractant for neutrophils and is also involved in a signalling cascade to promote cell survival, proliferation and inflammation. These results suggest that at both low doses of AFB₁ an inhibitory effect on HepG2 cell migration and proliferation for the initial 24 hours of exposure is evident, however, after 48 hours of exposure, IL-8 secretion is significantly increased followed by the return of HepG2 cell migration, proliferation and IL-8 expression to normal levels after 72 hours.

Research conducted by Kooijman *et al.* (2003) determined that IGF-1R stimulates IL-8 mRNA expression and IL-8 secretion in the leukemic cell line HL-60. Further studies were carried out by Zhao *et al.* (2011) on neurotensin, a gastrointestinal neuropeptide that modulates intestinal inflammation and healing by binding to neurotensin receptor-1. One of the roles of neurotensin in inflammation was demonstrated in a model of colitis induced by *Clostridium difficile* toxin A and involved NF- κ B-dependent IL-8 expression. Zhao *et al.* showed that inhibition of IGF-1R activation by either its specific antagonist AG1024 or siRNA against IGF-1 significantly reduced neurotensin-induced IL-8 expression and NF- κ B-dependent reporter gene expression in human colonic epithelial cells. Together, these studies suggest that activation or stimulation of IGF-1R can result in IL-8 expression. The

previous research conducted by Ubagai *et al.*, indicated that AFB₁ stimulated IGF-1R, therefore, this interaction may be responsible for the induction of IL-8 expression in HepG2 cells. The research described in this chapter indicated that low doses of AFB₁ (0.01 ng/mL and 0.1 ng/mL) caused a significant inhibitory effect on HepG2 cell migration and proliferation after 24 hours of AFB₁ exposure, yet stimulated expression of IL-8 and the recovery of the HepG2 cells after 72 hours of exposure. These results build on previous research to suggest that AFB₁ may interact with IGF-1R, and possibly, subsequently upregulate IL-8 secretion in HepG2 cells. Further experimentation would be required to determine if this theory was accurate. A similar approach adapted to that of Zhao *et al.* to block HepG2 cell IGF-1R activation by its antagonist AG1024 or by siRNA inhibition against IGF-1R, followed by exposure to 0.01 and 0.1 ng/mL of AFB₁ and subsequent testing by scratch, proliferation and IL-8 cytokine expression assay would determine if the inhibitory effect of low doses of AFB₁ on HepG2 cells was IGF-1R specific. This method would also signify whether IL-8 expression was upregulated by IGF-1R stimulation in HepG2 cells and give a greater understanding of AFB₁ toxicity. Given that over-expression of IL-8 is potently linked to cancer tumourigenesis, this finding could indicate a previously unreported mode of action by which AFB₁ stimulates IL-8 expression and HepG2 cell survival.

Previous studies reveal AFB₁ stimulates different signalling pathways and indicate that the AFB₁ mode of action is indeed very complex. As more research is accomplished, the complete mechanistic effect of AFB₁ may be elucidated. It seems likely, that further signalling pathways responsible for pro-cancer cellular characteristics (for example VEGF, TNF- α , NF-K β) could also be impacted by AFB₁ exposure. The cross-talk of signalling pathways extends the function of individual pathway signalling and results in a more complex regulatory network and is exemplified by the Wnt/ β -catenin pathway components that mediate inflammatory and immune responses through interaction with NF- κ B, or mutually the NF- κ B influence on the Wnt/ β -catenin signalling pathway (Ma and Hottiger, 2016). Therefore, ultimately cross-talk between signalling pathways may be intensified and responsible for the complexities and potency of AFB₁ toxicity.

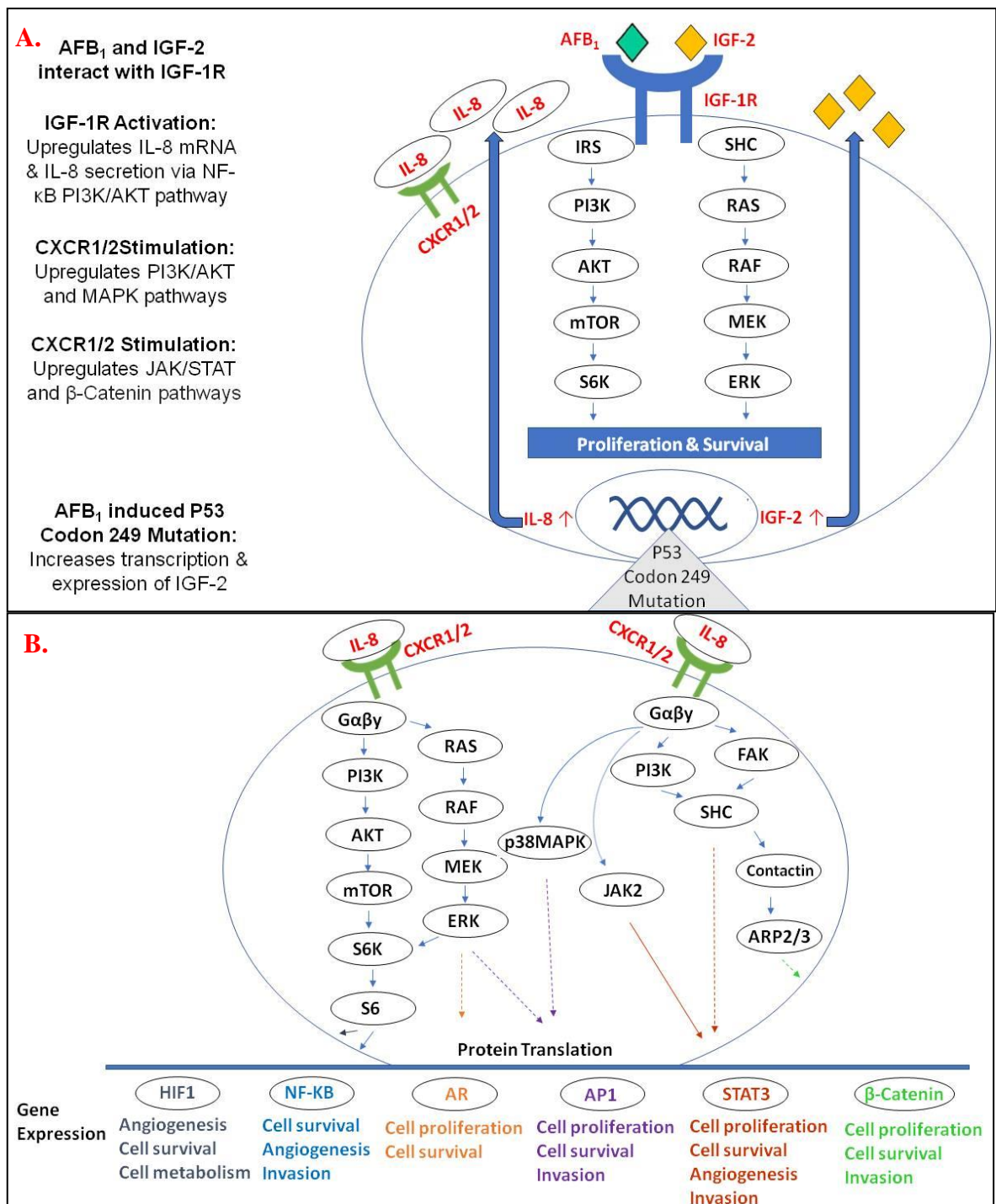


Figure 5.18: Proposed AFB₁-IGF-1R interaction and mode of action in HepG2 cells.
A.) AFB₁ and IGF-2 can interact with IGF-1R. Activation of IGF-1R upregulates levels of IL-8 mRNA and IL-8 secretion via the NF- κ B PI3K/AKT signalling pathway. Furthermore, mutations in the P53 codon 249 can increase the transcription and expression of IGF-2. Increased IGF-2 can additionally interact via IGF-1R further stimulating IL-8 up-regulation. **B.)** Increased levels of IL-8 are then available for target ligand (CXCR1/2) binding which in-turn up-regulates the PI3K/AKT, JAK/STAT and β -Catenin pathways which promote cell survival, proliferation and invasion.

In addition to examining the effects of low doses of AFB₁, experiments were conducted to determine if the anti-AFB₁ Fab antibody fragment could exert an effect on the HepG2 cells. It was initially theorised that perhaps the anti-AFB₁ Fab antibody fragment could exert an effect on HepG2 cells. Accordingly, anti-AFB₁ Fab antibody fragment-treated HepG2 cells were examined in terms of cellular migration, proliferation and expression of the cytokine IL-8. The results described in Section 5.2.1.2 indicated that the anti-AFB₁ Fab antibody fragment could reduce HepG2 cell migration for over 96 hours, compared to cells (+ vehicle). As the anti-AFB₁ Fab antibody fragment was functioning in the absence of its cognate antigen (AFB₁), further investigation was undertaken to determine which region of the antibody was exerting an effect on HepG2 proliferation. The results in Section 5.2.2.5 indicated that following the addition of (0.14 µM) an anti-AFB₁- Fab, scFv-dimer, monoclonal and polyclonal antibody, only the anti-AFB₁ Fab (P<0.05) and scFv-dimer (P<0.001) caused a significant decrease in HepG2 proliferation. The more significant decrease in proliferation exerted by the scFv-dimer was attributed to its double-scFv binding fragments. These results indicated that the shared scFv domain of the anti-AFB₁ Fab and scFv-dimer was responsible for the interaction with, and, inhibitory effect on HepG2 cell proliferation. This effect was also specific to the HepG2 cells, as the same experiment was conducted on normal liver THLE-2 cells, as described in Section 5.2.2.9, and no significant effect on proliferation was elicited. To further elucidate the binding domain of the anti-AFB₁ antibody fragments, sequence analysis was completed, as described in Section 5.2.2.6. These results revealed that an anti-M3G Fab antibody fragment light chain had 98 % homology with the light chains of the both anti-AFB₁ antibody fragments. Consequently, experiments were conducted to indicate if the anti-M3G Fab antibody fragment could exert a similar effect on the HepG2 cells. The results in Section 5.2.2.8 revealed that both the anti-AFB₁ and anti-M3G Fab antibody fragment significantly reduced HepG2 proliferation after 24 hours of treatment (P<0.001). Both fragments were then treated with an inhibitory dose (Section 4.2.1) of AFB₁. It was hypothesised that the inhibitory dose of AFB₁ would bind and fully inhibit the anti-AFB₁ Fab antibody fragment due to cognate specificity, whilst, an inhibitory dose of AFB₁ would not interact with, and, impact anti-M3G Fab antibody fragment-binding. The results supported this theory, with the inhibited anti-AFB₁ Fab antibody fragment losing its ability to reduce HepG2 cell proliferation, however, the inhibitory dose of AFB₁ did not affect the anti-M3G Fab antibody fragment, with the treatment resulting in a consistent, significant

decrease in HepG2 cell proliferation ($P < 0.001$). Together these results indicated that the anti-AFB₁ Fab antibody fragment was exerting its effect on HepG2 cells via its ability to interact with the cells, and also, that this interaction was via the shared light chain sequence evident in all three recombinant antibody fragments tested. This can be concluded due to the 98 % homology seen across the three sequences, as well as, by the understanding that the CDR3 found in the heavy chain of recombinant fragments is typically responsible for antigen-specific binding and interactions. The anti-AFB₁ Fab antibody fragment-heavy chain CDR3 was specific for the inhibitory dose of AFB₁ and accordingly became bound and inhibited from binding to the HepG2 cells. Given that the anti-M3G Fab antibody fragment has a different heavy chain CDR3 sequence to the anti-AFB₁ Fab antibody fragment-heavy chain CDR3 it was not capable of binding and becoming inhibited by the inhibitory dose of AFB₁. Therefore, the differences in the important binding regions of both Fabs CDRs resulted in their different function when exposed to inhibitory AFB₁. Accordingly, their shared ability to interact with, and, reduce proliferation of HepG2 cells must be attributed to their shared light-chain sequence. Sequence analysis, as described in Section 5.2.2.10, also indicated similarity between the anti-AFB₁ Fab antibody fragment light chain and IGF-R1 suggested this may be the region of interaction between both players. However, an investigation of current literature has not identified any reports of non-ligand-specific recombinant antibody fragments interacting with, and, affecting cancerous cells. Therefore, much further experimentation would be necessary to determine the exact mechanism or signalling pathway by which the anti-AFB₁ Fab antibody fragment is exerting its inhibitory effect.

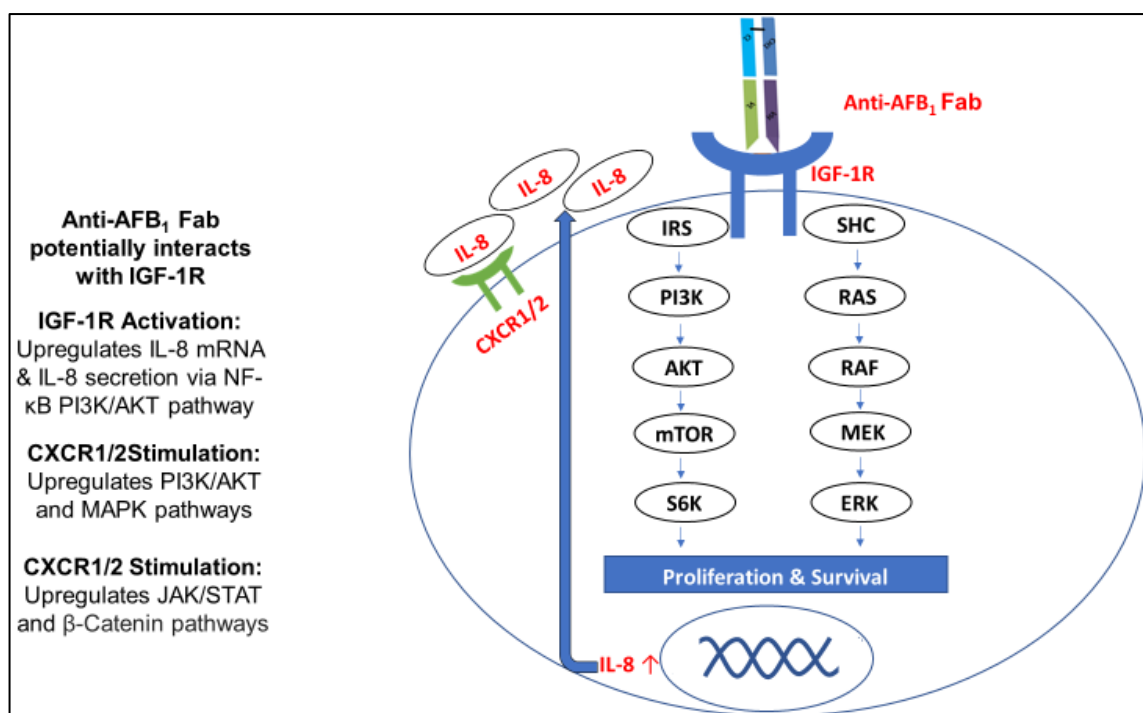


Figure 5.19: Proposed Anti-AFB₁ Fab antibody fragment-IGF-1R interaction and mode of action in HepG2 cells. This research suggests that the anti-AFB₁ Fab antibody fragment may interact with IGF-1R. Activation of IGF-1R upregulates levels of IL-8 mRNA and IL-8 secretion via the NF-κB PI3K/AKT signalling pathway. Increased levels of IL-8 are then available for target ligand (CXCR1/2) binding which in-turn upregulates the PI3K/AKT, JAK/STAT and β-Catenin pathways which promote cell survival, proliferation and invasion as illustrated in Figure 5.18.

Finally, this chapter focused on the combined effects of AFB₁ (0.01 and 0.1 ng/mL) exposure and anti-AFB₁ Fab antibody fragment treatment on HepG2 proliferation and IL-8 expression. The results described in Section 5.2.2.2 showed that after 24 hours of AFB₁ exposure, followed by 24 hours of treatment with the anti-AFB₁ Fab antibody fragment, a significant reduction in HepG2 proliferation ($P < 0.05$) compared to cells (+ vehicle) was observed. However, proliferation was reduced to a greater significance ($P < 0.01$) after 48 hours and 72 hours ($P < 0.001$) of AFB₁ exposure and subsequent treatment for 24 hours with the anti-AFB₁ Fab antibody fragment. A control of the anti-AFB₁ Fab antibody fragment was added to cells grown for 24, 48, and 72 hours without AFB₁ and exhibited the same significance in reduced proliferation ($P < 0.05$, 0.01, 0.001). This indicated that the Fab was having an inhibitory effect on the hepatocellular carcinoma cells in the absence of the AFB₁. Furthermore, hepatocellular carcinoma cells were shown to recover after 24 hours of AFB₁ dosage therefore, the decrease in proliferation can be attributed to the anti-

AFB₁ Fab antibody fragment treatment. These results also showed that when HepG2 cells were treated with the anti-AFB₁ Fab antibody fragment, IL-8 expression was significantly increased ($P < 0.001$) compared to cells (+ vehicle). Furthermore, when AFB₁ exposure (24 or 48 hours) was followed by anti-AFB₁ Fab antibody fragment treatment (24 or 48 hours), IL-8 expression was again significantly increased ($P < 0.001$). The increased expression of IL-8 following exposure to the anti-AFB₁ Fab antibody fragment further supports the theory that AFB₁ and the anti-AFB₁ Fab antibody fragment are exerting an inhibitory effect which up-regulates the release of IL-8 following decreased migration and proliferation. Further investigation with THLE-2 cells would be necessary to determine if IL-8 secretion was affected by anti-AFB₁ Fab antibody treatment. This would indicate if the increased expression of IL-8 following anti-AFB₁ Fab antibody fragment treatment is specific to hepatocellular carcinoma cells or ubiquitous in nature.

Overall, the findings of this chapter are complex but consistent. The effects of low doses of AFB₁ (0.01 and 0.1 ng/mL) are most significant in terms of decreased HepG2 cell migration and proliferation after 24 hours of exposure, however, after 48 hours significant increases in IL-8 expression are evident. HepG2 cells return to normal migration, proliferation and IL-8 secretion levels at 48 hours and maintain normal profiles at 72 hours. Additionally, this research shows that treating HepG2 cells with the anti-AFB₁ Fab antibody fragment can also significantly reduce cellular migration and proliferation. Through sequence analysis it was determined that the light chain of the recombinant antibody fragment, possibly via the CDR3 region, was responsible for this inhibitory interaction. The anti-AFB₁ Fab antibody fragment also increased IL-8 expression whether in treatment alone or following AFB₁ exposure. The exact mechanism or signalling pathway by which the anti-AFB₁ Fab antibody fragment functions requires further investigation. However, these results indicate a novel effect for the Fab, and, also the first report of a recombinant antibody fragment exerting an inhibitory effect on hepatocellular carcinoma cells. Significant further work would be necessary to fully elucidate the precise mechanisms involved. This research suggests there is potential for the development of recombinant antibody fragments that are specific to external stimulants that induce pro-cancerous effects via specific ligands (and pathways), which in-turn can also be influenced by the recombinant antibody fragment.

Conclusions

6.1. Overall Conclusions

Mycotoxins are toxic contaminants propagated by fungal species and are a concern due to their occurrence in globally consumed foods and feed. In 1998, The Food and Agriculture Organization (FAO) reported that at least 25% of the world's food crops were contaminated with mycotoxins (Boutrif and Canet, 1998) and drew attention globally to the mycotoxin problem. Studies carried out in the first quarter of 2017, by the company Biomin indicated 80% of 3715 finished feed and raw commodity samples collected from 54 countries were found to contain mycotoxins (Biomin, 2017) and demonstrated the magnitude of the mycotoxin problem today. These toxic contaminants have huge implications for food safety due to their ability to elicit acute and chronic effects. Chronic exposure stimulates mutagenic and carcinogenic effects in humans and animals (Milićević *et al.*, 2010). In particular, aflatoxin B₁ (AFB₁) is a potent carcinogen and a major risk factor for human hepatocellular carcinoma. Montalto *et al.* (2002) reported that regions with high AFB₁ exposure coincide with regions of high HCC prevalence and that the greatest HCC burden is evident in developing countries, where over 80% of cases occur (Ferlay *et al.*, 2010). Furthermore, approximately 4.5 - 5 billion of the poorest people in developing regions including sub-Saharan Africa, Asia and Latin America are exposed to mycotoxins at levels that are reported to significantly increase mortality and morbidity (Alberts *et al.*, 2017). The potential for human exposure is increased when there is a lack of regulatory systems for monitoring and controlling aflatoxin contamination (Liu and Wu, 2010; Wu *et al.*, 2011). Global efforts in food safety are being made to control and minimise the risk of mycotoxin-contamination. Consequently, mycotoxin detection and analysis is now considered one of the most important areas for food quality improvement. The European Union (EU) has established stringent legislative levels for mycotoxins in foods and feed to protect humans and animals from mycotoxin exposure. Accordingly, there is a real need for sensitive detection methods which can quantify the level of mycotoxins evident in samples to determine safe food. The aim of this research was to develop and incorporate recombinant antibody fragments for the detection of mycotoxins in a 'point-of-site,' optical-planar waveguide detection system capable of meeting requirements set-out by EU and establish a 'proof-of-concept' format for multiplex testing.

The detection system used for mycotoxin analysis was composed of a simple optical-planar waveguide cartridge-construct spotted with mycotoxin-conjugates in a competitive

inhibition format, coupled with a light-weight optical reader platform for rapid result read-out. The strategies employed in this research involved the generation, development and characterisation of recombinant antibody fragments for the competitive inhibition format. An anti-AFB₁ Fab antibody fragment was successfully expressed and purified for this purpose. Experimentation was conducted to generate an anti-T-2 toxin scFv antibody fragment, however, this was not successful and an anti-T-2 toxin polyclonal antibody was selected for use instead. Further investigation into the development of the mycotoxin conjugate used for screening methods may have aided the selection of a specific anti-T-2 toxin recombinant antibody. The chemistry employed to conjugate the mycotoxin to the screening protein could be optimised to include a less stringent approach like that described by Arola *et al.*, (2016). This method involves the addition of diphosgene in dry dioxan in the presence of pyridine as a catalyst to produce toxin linker for further protein conjugation. The removal of the unstable hemisuccinate intermediate introduced during conjugation could potentially overcome the stability issues that can be associated with mycotoxin-conjugates. Additionally, repetition of a full immunization schedule with an optimally designed mycotoxin conjugate and monitoring antibody titre could potentially yield an improved antibody response from the host animal and a greater diversity of genetic material for amplification and generation of the anti-T-2 toxin recombinant antibody. An indirect competitive inhibition assay format was used to produce standard curves for AFB₁ and T-2 toxin, by incubating the anti-AFB₁ Fab with varying concentrations of free AFB₁ (50 – 0.39 ng/mL) in blank Dried Distillers Grain with Solubles (DDGS) extract and adding to 50 µg/mL of AFB₁-BSA immobilised on the cartridge or by incubating the anti-T-2 toxin polyclonal antibody with varying concentrations of free T-2 toxin (25 – 0.39 ng/mL) in blank DDGS extract and adding to 50 µg/mL of T-2 toxin-BSA immobilised on the cartridge. The limit of detection was calculated according to the equations described by Armbruster and Pry (2008) and Tang *et al.* (2013) and by means of an inhibition assay format to test 3 blank replicates and 3 low concentration analyte replicates. The limit of detection was determined as 4.12 ng/mL for AFB₁ and 5.08 ng/mL for T-2 toxin in DDGS extract. These results provide detection levels below the EU legislative limits for AFB₁ and T-2 toxin in feed for animals at 20 ppb and 25 ppb, respectively. A dynamic range of 0.08 – 10 ng/mL for detection of AFB₁ in DDGS extract and 0.6 – 11.9 ng/mL for detection of T-2 toxin in DDGS extract was also determined.

Furthermore, a 'proof-of-concept' format for multiplex testing was established. An aqueous-based method (80:20 % (v/v) water:methanol) was used for simultaneous extraction of AFB₁ and T-2 toxin from contaminated DDGS samples. The anti-AFB₁ Fab antibody fragment, the anti-T-2 toxin polyclonal antibody and the contaminated DDGS extract were incubated together for 5 minutes before application to the optical-planar waveguide cartridge for competitive inhibition assay. In this process, both the antibody formats were able to simultaneously bind their cognate mycotoxin in the contaminated DDGS extract and the excess, unbound antibody formats were available to interact with the mycotoxin conjugates on the cartridge surface producing an inverse response, which was analysed to report the concentration of each mycotoxin present in the DDGS extract. AFB₁ was successfully detected at 12.1 ng/mL and 10.3 ng/mL which calculates as 16.1 µg/kg and 13.7 µg/kg, respectively and represents an average recovery of 98 % recovery. T-2 toxin was detected at 7.09 ng/mL and 5.08 ng/mL which calculates as 9.5 µg/kg and 6.7 µg/kg, respectively and represents an average recovery of 69 %. The percentage recoveries were calculated using the average mycotoxin concentration determined by the optical-planar waveguide detection system and the mycotoxin concentration determined by LC/MS-MS detection for the same contaminated DDGS samples, (completed by the Global Research Institutes in Health and Food Security, Queens University, Belfast). The coefficients of variance for detection of AFB₁ and T-2 toxin in contaminated DDGS samples were 11% and 24%, respectively. The ability to test both mycotoxins presents a 'proof-of-concept' for the multiplex detection of mycotoxins. This suggests other mycotoxins or multiple mycotoxins could be detected using this 'proof-of-concept' format. The detection system described in this research would be greatly beneficial for simple, 'point-of-site,' multi-mycotoxin analysis, allowing users, particularly farmers and millers, to determine the presence of mycotoxins in cereals and permit selection of safe food products.

Determining the presence of mycotoxins in our food is massively important for ensuring human and animal health. The potent effects of AFB₁ exposure are well established in terms of cancer causation. Therefore, investigations and understanding of mycotoxic effects and mechanisms in human health and cancer states are imperative to enable suitable interventions and treatments, in the eventuality that not all food commodities will be 'mycotoxin-free'. This research focused on determining the effects of AFB₁ on HepG2 human hepatoma cells. Experiments were conducted to determine the effects of relatively

low doses of AFB₁ on HepG2 cell migration, proliferation and IL-8 cytokine responses. It was hypothesized that the anti-AFB₁ Fab antibody fragment which sensitively binds AFB₁, could possess a binding region capable of interacting with the AFB₁-cognate ligand on HepG2 cells. Therefore, HepG2 cells were also treated with the anti-AFB₁ Fab antibody fragment and the cellular migration, proliferation and IL-8 profiles examined. These experiments were completed to offer further understanding of AFB₁ effects in HCC, and to determine if the anti-AFB₁ Fab antibody fragment could interact with, and, affect HepG2 cellular functions.

Previous studies to investigate AFB₁ effects on hepatocellular cancer cells *in vitro*, typically apply relatively high doses of AFB₁ (up to 10 μ M). This research demonstrated the effects of low doses of AFB₁ (0.01 and 0.1 ng/mL) on HepG2 cells and established that the most significant impacts are seen after 24 hours of exposure in terms of inhibited cellular migration and proliferation, coupled with significant increases in IL-8 expression after 48 hours of exposure. HepG2 cells return to normal migration, proliferation and IL-8 secretion levels after 72 hours. These results show that low concentrations of AFB₁ can have a positive outcome in reducing HepG2 cell proliferation and migration for 24 hours before IL-8 secretion is increased and the cells return to normal levels of activity. Investigations to determine the effects of anti-AFB₁ Fab antibody fragment treatment on HepG2 cells found that the Fab was interacting with cells, and could also potentially inhibit cellular migration and proliferation to a significant level. Analysis of shared DNA sequences between various recombinant (anti-AFB₁ scFv-dimer, anti-AFB₁ Fab and anti-M3G Fab) antibody fragments implied that the light chain was responsible for this inhibitory interaction. Further sequence analysis suggested that the interaction may be mediated via the CDR3 region of the light chain and IGF-1R, however, significant research would be necessary to demonstrate the exact mode of action by which the anti-AFB₁ Fab antibody fragment interacts with HepG2 cells. Exposure to AFB₁ and treatment with anti-AFB₁ Fab antibody fragment revealed that initial exposure to AFB₁ amplified the effect of the anti-AFB₁ Fab antibody fragment in reducing HepG2 cell proliferation. The anti-AFB₁ Fab antibody fragment also significantly increased IL-8 expression whether in treatment alone or following AFB₁ exposure. These findings allude to a combinatorial or synergistic effect of AFB₁ exposure and anti-AFB₁ Fab antibody fragment treatment on HepG2 cells. Further experimentation would be required to conclude whether the co-exposure of both AFB₁ and the Fab impacts HepG2 cells via the same signalling pathway or by combination

of different signalling pathway cascades. Overall, the anti-AFB₁ Fab antibody fragment has been shown to significantly inhibit HepG2 cells, with or in the absence of AFB₁ exposure. These results describe the first recombinant Fab antibody fragment interacting with, and, having an inhibitory effect on hepatocellular carcinoma cell migration and proliferation.

The findings from this research indicate that the anti-AFB₁ Fab antibody fragment and anti-T-2 toxin polyclonal antibody can be incorporated into an MBio detection system for the successful detection of AFB₁ and T-2 toxin in contaminated cereal samples. Together this system provides a sensitive method which could be utilised for simple 'point-of-site' mycotoxin detection. The application of this device and such systems allows for increased detection, monitoring and analysis of mycotoxin contamination and enables a greater understanding of mycotoxin prevalence and occurrence. This is necessary to ensure procurement of safe, uncontaminated food and feed, but also, to provide data to support in-depth studies on mycotoxin physiological effects experienced by people living in regions of prevalence. Together, mycotoxin occurrence data and epidemiology studies from relevant areas of prevalence will provide a complete insight into the global mycotoxin problem. Therefore, this research also examined the effects of low levels of AFB₁ exposure in hepatocellular carcinoma cells and normal liver cells to better understand the mycotoxic impact on these physiological conditions. The results determined that very low doses of AFB₁ can reduce hepatocellular carcinoma cell migration, proliferation and increase IL-8 secretion. This profile suggests that AFB₁ exerts an inhibitory effect on hepatocellular carcinoma cells which is modulated by IL-8 expression. Previous research has indicated that AFB₁ interaction with the IGF axis is important and the results described in this research provide a possible link in AFB₁-IGF-1R receptor binding resulting in up-regulation of IL-8 secretion by numerous contributory pathways. The anti-AFB₁ Fab antibody fragment exhibited similar effects in hepatocellular carcinoma cells and possibly functions via the IGF-1R pathway to up-regulate IL-8 secretion. Future work incorporating a comparison of hepatocellular carcinoma cells with normal liver cell IL-8 secretion following anti-AFB₁ Fab antibody treatment would be necessary to determine if IL-8 secretion was modulated by anti-AFB₁ Fab antibody fragment interaction specifically with the IGF-1R receptor. Normal liver cells have low levels of IGF-1R receptor and were not inhibited in terms of migration or proliferation by anti-AFB₁ Fab antibody fragment treatment, therefore, low levels of IL-8 secretion would be expected from the normal liver

cells provided if the anti-AFB₁ Fab antibody fragment was functioning via the IGF-1R receptor. Accessing the IL-8 secretion levels from the normal liver cells would provide more insight on the anti-AFB₁ Fab antibody fragments possible interaction via the IGF-1R pathway. A range of studies could be implemented to investigate how the anti-AFB₁ Fab antibody fragment and hepatocellular carcinoma cell interact, however, a high through-put method which can examine a range of hepatocellular ligands and receptors would offer the greatest understanding of potential interactions. This can be achieved by acquiring a selection of overly-expressed receptors in hepatocellular carcinoma and testing these in a binding study with the anti-AFB₁ Fab antibody fragment. Surface Plasmon Resonance instruments, for example, the Biacore 4000 would provide the high through-put capabilities for immobilisation of multiple receptors on a chip, over which the anti-AFB₁ Fab antibody fragment can be passed. Interactions and binding is monitored by the technology and determines which receptors are being bound and more specifically the affinity of the binding action. This study would determine if the anti-AFB₁ Fab antibody fragment was interacting with hepatocellular cells via the IGF-1R receptor as hypothesised.

Overall, the inhibitory effect of the anti-AFB₁ Fab antibody fragment represents a very interesting result which suggests that the Fab treatment can reduce hepatocellular cancer cell migration and proliferation and additional investigations should be conducted to investigate the Fabs potential as a therapeutic resource for reducing hepatocellular carcinoma progression.

Bibliography

- AHMAD, Z.A.**, YEAP, S.K., ALI, A.M., HO, W.Y., ALITHEEN, N.B.M. and HAMID, M., 2012. ScFv antibody: principles and clinical application. *Clinical and Developmental Immunology*, **2012**, 1-15.
- ALBERTS, J.**, LILLY, M., RHEEDER, J., BURGER, H., SHEPHARD, G. and GELDERBLUM, W., 2017. Technological and community-based methods to reduce mycotoxin exposure. *Food Control*, **73**, 101-109.
- ALTSHULER, E.P.**, SEREBRYANAYA, D.V. and KATRUKHA, A.G., 2010. Generation of recombinant antibodies and means for increasing their affinity. *Biochemistry (Moscow)*, **75**(13), 1584-1605.
- AL-WARHI, T.I.**, AL-HAZIMI, H.M.A. and EL-FAHAM, A., 2012. Recent developments in peptide coupling reagents. *Journal of Saudi Chemical Society*, **16**(2), 97-119.
- ANASTASSIADES, M.**, LEHOTAY, S.J., STAJNBAHER, D., and SCHENCK, F.J., 2003. Quick, Easy, Cheap, Effective, Rugged and Safe (QuEChERS) approach for the determination of pesticide residues. *Journal of AOAC International*, **86**(2), 412-431.
- ARBABI-GHAHROUDI, M.**, TANHA, J. and MACKENZIE, R., 2009. Isolation of monoclonal antibody fragments from phage display libraries. *Methods in Molecular Biology*, **502**, 341-364.
- ARMBRUSTER, D.A.** and PRY, T., 2008. Limit of blank, limit of detection and limit of quantitation. *Clinical Biochemist Reviews*, **29**(Supplement (i)), S49-S52.
- AROLA, H.**, TULLILA, A., KILJUNEN, H., CAMPBELL, K., SIITARI, H. and NEVANEN, T., 2016. Specific noncompetitive immunoassay for HT-2 mycotoxin detection. *Analytical Chemistry*, **88**(4), 2446-2452.
- BANADA, P.P.** and BHUNIA, A.K., 2008. Antibodies and immunoassays for detection of bacterial pathogens. in: M. ZOUIROB, S. ELWARY and A.P.F. TURNER, (eds), *Principles of Bacterial Detection: Biosensors, Recognition Receptors and Microsystems*. 567-602. New York, NY: Springer.
- BARBAS, C. F.**, BURTON, D. R., SCOTT, J. K. and SILVERMAN, G. J., 2001. Phage display: A laboratory manual. Cold Spring Harbor Laboratory Press, New York, USA.
- BELHASSEN, H.**, JIMÉNEZ-DÍAZ, I., ARREBOLA, J.P., GHALI, R., GHORBEL, H., OLEA, N. and HEDILI, A., 2015. Zearalenone and its metabolites in urine and breast cancer risk: A case-control study in Tunisia. *Chemosphere*, **12**(8), 1-6.
- BELOGLAZOVA, N.V.**, DEBOEVRE, M., GORYACHEVA, I.Y., WERBROUCK, S., GUO, Y. and DESAEGER, S., 2013. Immunochemical approach for zearalenone-4-glucoside determination. *Talanta*, **106**, 422-430.

- BELOGLAZOVA, N.V., SPERANSKAYA, E.S., WU, A., WANG, Z., SANDERS, M., GOFTMAN, V., ZHANG, D., GORYACHEVA, I.Y. and DE SAEGER, S., 2014.** Novel multiplex fluorescent immunoassays based on tricolored quantum dot nanolabels for mycotoxins determination. *Biosensors and Bioelectronics*, **62**, 59-65.
- BENNETT, J.W.** and KLICH, M., 2003. Mycotoxins. *Clinical Microbiology Reviews*, **16**(3), 497-516.
- BERTHILLER, F., CREWS, C., DALL'ASTA, C., DE SAEGER, S., HAESAERT, G., KARLOVSKY, P., OSWALD, I.P., SEEFELDER, W., SPEIJERS, G. and STROKA, J., 2013.** Masked mycotoxins: a review. *Molecular Nutrition & Food Research*, **57**(1), 165-186.
- BERTHILLER, F., SULYOK, M., KRSKA, R. and SCHUHMACHER, R., 2007.** Chromatographic methods for the simultaneous determination of mycotoxins and their conjugates in cereals. *International Journal of Food Microbiology*, **119**(1-2), 33-37.
- BEZERRA DA ROCHA, M.E., DA CHAGAS OLIVEIRA FREIRE, F., FEITOSA MAIA, F.E., FLORINDO GUEDES, M.I. and RONDINA, D., 2014.** Mycotoxins and their effects on human and animal health. *Food Control Volume*, **36**(1), 159-165.
- BIEHL, M.L., PRELUSKY, D.B., KORITZ, G.D., HARTIN, K.E., BUCK, W.B. and TRENHOLM, H.L., 1993.** Biliary excretion and enterohepatic cycling of zearalenone in immature pigs. *Toxicology and Applied Pharmacology*, **121**, 152-159.
- BIOMIN, 2017.** World Mycotoxin Survey - The Global Threat 2017 Q1. Biomin World Mycotoxin Survey. [Online] Available at: https://info.biomin.net/acton/attachment/14109/f-04f9/1/-/-/1-0009/1-0009:6b8e/REP_MTXsurvey_Quater1_2017_EN_0417_PKO.pdf [Accessed 20 October 2017].
- BLANCHER, C. and JONES, A., 2000.** SDS-PAGE and Western blotting techniques. in: S.A. BROOKS and U. SCHUMACHER, (eds), *Metastasis Research Protocols. Volume I: Analysis of Cells and Tissues*. Vol **57**, 145-162. 999 Riverview Dr Ste 208, Totowa, New Jersey, 07512: Humana Press.
- BORNHURST, J.A. and FALKE, J.J., 2000.** Purification of proteins using polyhistidine affinity tags. *Methods in Enzymology*, **326**, 245-254.
- BOUTRIF, E. and CANET, C., 1998.** Mycotoxin prevention and control: FAO programmes. *Revue de Médecine Vétérinaire*, **149**(6), 681-694.
- BROADWAY, N., 2012.** How to develop assays: 5 considerations and 8 fundamentals. *Materials and Methods* 2. [Online] Available at: <https://www.labome.com/method/How-to-Develop-Assays-5-Considerations-and-8-Fundamentals.html> [Accessed 09 June 2017].

BRUNEAU, J., STACK, E., O'KENNEDY, R. and LOSCHER, C.E., 2012. Aflatoxins B₁, B₂ and G₁ modulate cytokine secretion and cell surface marker expression in J774A.1 murine macrophages. *Toxicology in Vitro*, **26**(5), 686-693.

BURKIN, A.A., KONONENKO, G.P., SOBOLEVA, N.A. and ZOTOVA, E.V., 2000. Preparation of conjugated antigens based on zearalenine carboxymethyloxime and their use in enzyme immunoassay. *Applied Biochemistry and Microbiology*, **36**(3), 282-288.

BURKIN, A.A., KONONENKO, G.P. and SOBOLEVA, N.A., 2002. Group-specific antibodies against zearalenone and its metabolites and synthetic analogs. *Applied Biochemistry and Microbiology*, **38**(2), 169-176.

BUGUZI S., 2016. Tanzania: New questions on food poison. News. [Online] Available at: <http://allafrica.com/stories/201608020624.html> [Accessed 03 November 2016].

BYRNE, B., STACK, E., GILMARTIN, N. and O' KENNEDY, R.J., 2009. Antibody-based sensors: principles, problems and potential for detection of pathogens and associated toxins. *Sensors*, **9**(6), 4407-4445.

CAMMARATA, C.R., HUGHES, M.E. and OFNER, C.M., 2015. Carbodiimide induced cross-linking, ligand addition, and degradation in gelatin. *Molecular Pharmaceutics*, **12**(3), 783-793.

CAMPBELL, K., STEWART, L., DOUCETTE, G., FODEY, T., HAUGHEY, S., VILARIÑO, N., KAWATSU, K. and ELLIOTT, C., 2007. Assessment of specific binding proteins suitable for the detection of paralytic shellfish poisons using optical biosensor technology. *Analytical Chemistry*, **79**(15), 5906-5914.

CAPECE, D., FISCHIETTI, M., VERZELLA, D., GAGGIANO, A., CICCARELLI, G., TESSITORE, A., ZAZZERONI, F. AND ALESSE, E., 2013. The inflammatory microenvironment in hepatocellular carcinoma: a pivotal role for tumor-associated macrophages. *BioMed Research International*, **2013**, 1-15.

CCFAC (CODEX COMMITTEE ON FOOD ADDITIVES AND CONTAMINANTS), 2000. *Joint FAO/WHO Expert Committee on Food Additives: Position paper on zearalenone*. Codex Alimentarius Commission, Rome, Italy. Publication CCFAC **00/19**.

COMMISSION RECOMMENDATION (EC) No 1881/2006 of 19 December 2006 on setting maximal levels for certain contaminants in foodstuffs. *Official Journal European Communities*, **L364**, 5-24.

COMMISSION RECOMMENDATION (EC) No 2013/165/EU of 27 March 2013 on the presence of T-2 and HT-2 toxin in cereals and cereal products. *Official Journal European Communities*, **L91**, 12-14.

CONROY, P.J., HEARTY, S., LEONARD, P. and O' KENNEDY, R.J., 2009. Antibody production, design and use for biosensor-based applications. *Seminars in Cell & Developmental Biology*, **20**(1), 10-26.

- CORY, G.**, 2011. Scratch-wound assay. *Methods in Molecular Biology*, **769**, 25-30.
- COSGROVE, B.**, CHENG, C., PRITCHARD, J., STOLZ, D., LAUFFENBURGER, D. and GRIFFITH, L., 2008. An inducible autocrine cascade regulates rat hepatocyte proliferation and apoptosis responses to tumour necrosis factor- α . *Hepatology*, **48**(1), 276-288.
- COSKUN, U.**, BUKAN, N., SANCAK, B., GÜNEL, N., OZENIRLER, S., UNAL, A. and YUCEL, A., 2004. Serum hepatocyte growth factor and interleukin-6 levels can distinguish patients with primary or metastatic liver tumours from those with benign liver lesions. *Neoplasma*, **51**(3), 209-213.
- DUNNE, L.**, 2004. *The development of immunoassays for the detection of bovine brucellosis and aflatoxin B₁*. PhD thesis, Dublin City University, Glasnevin, Dublin 9, Ireland.
- DYCAICO, M.J.**, STUART, G.R., TOBAL, G.M., DEBOER, J.G., GLICKMAN, B.W. and PROVOST, G.S., 1999. Species-specific differences in hepatic mutant frequency and mutational spectrum among lambda/*lacI* transgenic rats and mice following exposure to aflatoxin B₁. *Carcinogenesis*, **17**(11), 2347-2356.
- EDUPUGANTI, S. R.**, 2013. *Development of immunoassays and immunoaffinity columns for the detection and isolation of mycotoxins*. PhD thesis, Dublin City University, Glasnevin, Dublin 9, Ireland.
- Edupuganti, S.R.**, Edupuganti, O.P., O’Kennedy, R., Defrancq, E. and Boullanger, S., 2013. Use of T-2 toxin-immobilized amine-activated beads as an efficient affinity purification matrix for the isolation of specific IgY. *Journal of Chromatography B*, 923-924, 98-101.
- FEINBERG, B.** and MCLAUGHLIN, C.S., 1989. Biochemical mechanism of action of trichothecene mycotoxins. in: V.R. BEASLEY (ed) *Trichothecene mycotoxins: pathophysiologic effects*, Vol I, 27-35. Boca Raton, Fla.: CRC Press.
- FERLAY, J.**, SHIN, H.R., BRAY, F., FORMAN, D., MATHERS, C. and PARKIN, D.M., 2010. Estimates of worldwide burden of cancer in 2008: GLOBOCAN 2008. *International Journal of Cancer*, **127**(12), 2893-2917.
- FITZGERALD, J.**, 2012. Rapid methods for the detection of anti-protozoan drug residues. PhD thesis, Dublin City University, Glasnevin, Dublin 9, Ireland.
- FRANCIS, D. M.** and PAGE, R., 2010. Strategies to optimize protein expression in *E. coli*. Current Protocols in Protein Science, **C5 Unit 5.24.**, 1-29.
- FRENZEL, A.**, HUST, M. and SCHRIRRMANN, T., 2013. Expression of recombinant antibodies. *Frontiers in Immunology*, **4**(217), 1-20.

- FRIEDMAN, M.** and **RASOOLY, R.**, 2013. Review of the inhibition of biological activities of food-related selected toxins by natural compounds. *Toxins*, **5**(4), 743-775.
- GALLUCCI, R.**, **SIMEONOVA, P.**, **TORIUMI, W.** and **LUSTER, M.**, 2000. TNF- α regulates transforming growth factor- α expression in regenerating murine liver and isolated hepatocytes. *The Journal of Immunology*, **164**(2), 872-878.
- GIBBS, J.**, 2001, Optimizing the immobilization of protein and other biomolecules ELISA technical bulletin – No 2 [Online] Available at: <http://csmedia2.corning.com/LifeSciences/media/pdf/elisa2.pdf> [Accessed 24 October 2015].
- GORELICK, N.J.**, 1990. Risk assessment for aflatoxin: I. Metabolism of aflatoxin B₁ by different species. *Risk Analysis*, **10**(4), 539-559.
- GORYACHEVA, I.Y.** and **DE SAEGER, S.**, 2011. Immunochemical methods for rapid mycotoxin detection in food and feed in: **DE SAEGER, S.** (ed) *Determining mycotoxins and mycotoxigenic fungi in food and feed*. Vol **203**, 135-167. Cambridge, UK: Woodhead.
- GROOPMAN, J.D.**, **KENSLER, T.W.** and **WILD, C.P.**, 2008. Protective interventions to prevent aflatoxin-induced carcinogenesis in developing countries. *Annual Review of Public Health*, **29**, 187-203.
- GUGLIELMI, L.** and **MARTINEAU, P.**, 2009. Expression of single-chain fv fragments in *E. coli* cytoplasm. *Methods in Molecular Biology*, **562**, 215-224.
- GLOBAL QYRESEARCH**, 2017. Global Mycotoxin Testing Sales Market (Aflatoxins, Ochratoxins, Patulin, Fusarium toxins and Other toxin) Opportunity Analysis, Market Shares and Forecast 2017-2022. [Online] Available at: <https://www.medgadget.com/2017/02/global-mycotoxin-testing-sales-market-aflatoxins-ochratoxins-patulin-fusarium-toxins-and-other-toxin-opportunity-analysis-market-shares-and-forecast-2017-2022-global-qyresearch.html>.
- HAMID, A.**, **TESFAMARIAM, I.**, **ZHANG, Y.** and **ZHANG, Z.** (2013). Aflatoxin B₁-induced hepatocellular carcinoma in developing countries: Geographical distribution, mechanism of action and prevention (Review). *Oncology Letters*. **5**(4), 1087-1092.
- HAMMERS, C.M.** and **STANLEY, J.R.**, 2014. Antibody phage display: technique and applications. *Journal of Investigative Dermatology*, **137**(e17), 1-5.
- HAN, K.N.**, **LI, C.A.** and **SEONG, G.H.**, 2013. Microfluidic chips for immunoassays. *Annual Review of Analytical Chemistry*, **6**, 119-141.
- HANLY, W.C.**, **ARTWOHL, J.E.** and **BENNETT, B.T.**, 1995. Review of polyclonal antibody production procedures in mammals and poultry. *Institute of Laboratory Animal Resources, Journals*, **37**(3), 93-118.

- HANNEMAN, S., COX, C., GREEN, K. and KANG, D., 2011.** Estimating intra- and inter-assay variability in salivary cortisol. *Biological Research For Nursing*, **13**(3), 243-250.
- HARTLEY, R., NESBITT, B. and O'KELLY, J., 1963.** Toxic metabolites of *Aspergillus flavus*. *Nature*, **198**, 1056-1058.
- HAYHURST, A., 2000.** Improved expression characteristics of single-chain Fv fragments when fused downstream of the *Escherichia coli* maltose-binding protein or upstream of a single immunoglobulin-constant domain. *Protein Expression and Purification*, **18**(1), 1-10.
- INTERNATIONAL AGENCY FOR RESEARCH ON CANCER (IARC), 2002.** Aflatoxin. *in*: IARC monograph evaluation of carcinogenic risk to humans. Some traditional herbal medicines, some mycotoxins, naphthalene and styrene, Vol **82**, 171-300. Lyon: IARC.
- ITOH, Y., JOH, T., TANIDA, S., SASAKI, M., KATAOKA, H., ITOH, K., OSHIMA, T., OGASAWARA, N., TOGAWA, S. and WADA, T., 2005.** IL-8 promotes cell proliferation and migration through metalloproteinase-cleavage proHB-EGF in human colon carcinoma cells. *Cytokine*. **29**(6), 275-282.
- JOFFE, A.Z. and YAGEN, B., 1978.** Intoxication produced by toxic fungi *Fusarium poae* and *F. sporotrichioides* on chicks. *Toxicon* **16**(3), 263-273.
- JOHNSEN, B. and HECHT, M., 1994.** Recombinant proteins can be isolated from *E.coli* cells by repeated cycles of freezing and thawing. *Bio/Technology*, **12**, 1357-1360.
- KABAT, E.A., WU, T.T., REID-MILLER, M., PERRY, H.M., GOTTESMAN, K.S. and FOELLER, C., 1991.** *Sequences of proteins of immunological interest, 5th edn.*, Public Services, NIH, Washington: US Department of Health and Human Services.
- KALANTARI, H. and MOOSAVI, M., 2010.** Review on T-2 Toxin. *Jundishapur Journal of Pharmaceutical Natural Products*, **5**(1), 26-38.
- KALLIOLIAS, G. and IVASHKIV, L., 2015.** TNF biology, pathogenic mechanisms and emerging therapeutic strategies. *Nature Reviews Rheumatology*, **12**(1), 49-62.
- KELSO, A., 1998.** Cytokines: principles and prospects. *Immunology and Cell Biology*, **76**(4), 300-317.
- KEW, M.C., 2003.** Synergistic interaction between aflatoxin B₁ and hepatitis B virus in hepatocarcinogenesis. *Liver International*, **23**(6), 405-409.
- KHLANGWISSET, P. and WU, F., 2010.** Health economic impacts and cost-effectiveness of aflatoxin reduction strategies in Africa: Case studies in biocontrol and postharvest interventions. *Food Additives & Contaminants: Part A, Chemistry, analysis, control, exposure & risk assessment*, **27**(4), 496-509.

- KIM, Y., BABNIGG, G., JEDRZEJCZAK, R., ESCHENFELDT, W.H., LI, H., MALTSEVA, N., HATZOS-SKINTGES, C., GU, M., MAKOWSKA-GRZYSKA, M., WU, R., AN, H., CHHOR, G., and JOACHIMIAK, A., 2011.** High-throughput protein purification and quality assessment for crystallization. *Methods*, **55** (1), 12–28.
- KOHNO, H., YOSHIZAWA, T., FUKAGI, M., MIYOSHI, M., SAKAMOTO, C., HATA, N. and KAWAMURA, O., 2001.** Production and characterisation of monoclonal antibodies against 3, 4, 15-triacetylnivalenol and 3, 15-diacetyldeoxynivalenol. *Food and Agricultural Immunology*, **15**(3), 243-254.
- KOOLJMAN, R., COPPENS, A. and HOOGHE-PETERS, E., 2003.** IGF-I stimulates IL-8 production in the promyelocytic cell line HL-60 through activation of extracellular signal-regulated protein kinase. *Cellular Signalling*, **15**(12), 1091-1098.
- KRALJ CIGIĆ, I. and PROSEN, H., 2009.** An overview of conventional and emerging analytical methods for the determination of mycotoxins. *International Journal of Molecular Sciences*, **10**(1), 62-115.
- KRSKA, R. and MOLINELLI, A., 2006.** Mycotoxin analysis: state-of-the-art and future trends. *Analytical and Bioanalytical Chemistry*, **387**(1), 145-148.
- KUBO, F., UENO, S., HIWATASHI, K., SAKODA, M., KAWAIDA, K., NURUKI, K. and AIKOU, T., 2005.** Interleukin 8 in human hepatocellular carcinoma correlates with cancer cell invasion of vessels but not with tumour angiogenesis. *Annals of Surgical Oncology*, **12**(10), 800-807.
- LAPČÍK, O., ŠTURSA, J., KLEINOVÁ, T., VÍTKOVÁ, M., DVOŘÁKOVÁ, H., KLEJDUS, B. and MORAVCOVÁ, J., 2003.** Synthesis of hapten and conjugates of coumestrol and development of immunoassay. *Steroids*, **68**(14), 1147-1155.
- LE BLOND, J., 2013.** Germany tests milk in carcinogen scare. [Online] Available: <http://www.guardian.co.uk/world/2013/mar/03/germany-tests-milk-carcinogen-scare> [Accessed 04 October 2013].
- LEE, S., KIM, G. and MOON, J., 2013.** Performance improvement of the one-dot lateral flow immunoassay for aflatoxin B₁ by using a smartphone-based reading system. *Sensors*, **13**(4), 5109-5116.
- LEE, Y., LEE, S., DAS, G., PARK, U., PARK, S. and LEE, Y., 2000.** Activation of the insulin-like growth factor II transcription by aflatoxin B₁ induced p53 mutant 249 is caused by activation of transcription complexes; implications for a gain-of-function during the formation of hepatocellular carcinoma. *Oncogene*, **19**(33), 3717-3726.
- LEEMHUIS, S., STEIN, V., GRIFFITHS, A.D. and HOLLFELDER, F., 2005.** New genotype-phenotype linkages for directed evolution of functional proteins. *Current Opinion in Structural Biology*, **15**(4), 472-478.

- LI, H.**, MCGUIRE, T.C., MULLER-DOBLIES, U.U. and CRAWFORD, T.B., 2001. A simpler, more sensitive competitive inhibition enzyme-linked immunosorbent assay for detection of antibody to malignant catarrhal fever viruses. *Investigation Journal of Veterinary Diagnostic*, **13**, 361-364.
- LI, Y.**, WANG, Z., BEIER, R.C., SHEN, J., DE SMET, D., DE SAEGER, S. and ZHANG, S., 2011. T-2 Toxin, a trichothecene mycotoxin: review of toxicity, metabolism, and analytical methods. *Journal of Agricultural and Food Chemistry*, **59**(8), 3441-3453.
- LI, Y.**, ZHANG, J., MAO, X., WU, Y., LIU, G., SONG, L., LI, Y., YANG, J., YOU, Y. and CAO, X., 2016. High-sensitivity chemiluminescent immunoassay investigation and application for the detection of T-2 toxin and major metabolite HT-2 toxin. *Journal of the Science of Food and Agriculture*, **97**(3), 818-822.
- LIANG, C.**, PARK, A. and GUAN, J., 2007. *In vitro* scratch assay: a convenient and inexpensive method for analysis of cell migration *in vitro*. *Nature Protocols*, **2**(2), 329-333.
- LIPMAN, N.S.**, JACKSON, L.R., TRUDEL, L.J. and WEIS-GARCIA, F., 2005. Monoclonal versus polyclonal antibodies: distinguishing characteristics, applications, and information resources. *Institute of Laboratory Animal Resources, Journals*, **46**(3), 258-268.
- LIU, Y.** and WU, F., 2010. Global burden of aflatoxin-induced hepatocellular carcinoma: A risk assessment. *Environmental Health Perspectives*, **118**(6), 818-824.
- LO, J.**, LAU, E., SO, F., LU, P., CHAN, V., CHEUNG, V., CHING, R., CHENG, B., MA, M., NG, I. and LEE, T., 2015. Anti-CD47 antibody suppresses tumour growth and augments the effect of chemotherapy treatment in hepatocellular carcinoma. *Liver International*, **36**(5), 737-745.
- LOFTUS, J.**, KIJANKA, G., O'KENNEDY, R. and LOSCHER, C., 2016. Patulin, deoxynivalenol, zearalenone and T-2 toxin affect viability and modulate cytokine secretion in J774A.1 murine macrophages. *International Journal of Chemistry*, **8**(2), 22.
- LUEDDE, T.** and SCHWABE, R., 2011. NF- κ B in the liver-linking injury, fibrosis and hepatocellular carcinoma. *Nature Reviews Gastroenterology & Hepatology*, **8**(2), 108-118.
- MA, B.** and HOTTIGER, M., 2016. Crosstalk between Wnt/ β -Catenin and NF- κ B signalling pathway during inflammation. *Frontiers in Immunology*, **7**(378), 1-14.
- MA, H.**, 2013. *Targeted neurotherapeutics for chronic inflammatory pain*. PhD thesis, Dublin City University, Glasnevin, Dublin 9, Ireland.
- MA, Y.**, KONG, Q., HUA, H., LUO, T. and JIANG, Y., 2012. Aflatoxin B₁ up-regulates insulin receptor substrate 2 and stimulates hepatoma cell migration. *PLoS ONE*, **7**(10):e47961, 1-11.

- MA, Z.,** HE, H., SUN, F., XU, Y., HUANG, X., MA, Y., ZHAO, H., WANG, Y., WANG, M. and ZHANG, J., 2017. Selective targeted delivery of doxorubicin via conjugating to anti-CD24 antibody results in enhanced antitumor potency for hepatocellular carcinoma both *in vitro* and *in vivo*. *Journal of Cancer Research and Clinical Oncology*, **143**(10), 1929-1940.
- MADDEN, C.R.,** FINEGOLD, M.J. and SLAGLE, B.L., 2002. Altered DNA mutation spectrum in aflatoxin B₁-treated transgenic mice that express the hepatitis B virus protein. *Journal of Virology*, **76**(2), 11770-11774.
- MAEDA, S.,** KAMATA, H., LUO, J., LEFFERT, H. and KARIN, M., 2005. IKK β couples hepatocyte death to cytokine-driven compensatory proliferation that promotes chemical hepatocarcinogenesis. *Cell*, **121**(7), 977-990.
- MAGNUSSEN, A.** and PARSI, M., 2013. Aflatoxins, hepatocellular carcinoma and public health. *World Journal of Gastroenterology*, **19**(10), 1508-1512.
- MALEKINEJAD, H.,** MAAS-BAKKER, R. and FINK-GREMMELS, J., 2006. Species differences in the hepatic biotransformation of zearalenone. *The Veterinary Journal*, **172**(1), 96-102.
- MARAGOS, C.M.** and MCCORMICK, S.P., 2000. Monoclonal antibodies for the mycotoxins deoxynivalenol and 3-acetyl-deoxynivalenol. *Food and Agricultural Immunology*, **12**(3), 181-192.
- MARIN, S.,** RAMOS, A.J., CANO-SANCHO, G. and SANCHIS, V., 2013. Mycotoxins: Occurrence, toxicology, and exposure assessment. *Food and Chemical Toxicology*, **60**, 218-237.
- MARROQUÍN-CARDONA, A.G.,** JOHNSON, N.M., PHILLIPS, T.D. and HAYES, A.W., 2014. Mycotoxins in a changing global environment – A review. *Food and Chemical Toxicology*, **69**, 220-230.
- MCGLYNN, K.A.,** 2005. Epidemiology and natural history of hepatocellular carcinoma. *Best Practice & Research Clinical Gastroenterology*, **19**(1), 3-23.
- MILIĆEVIĆ, R.R.,** ŠKRINJAR, M. and BALTIĆ, B., 2010. Real and perceived risks for mycotoxin contamination in foods and feeds: Challenges for food safety control, *Toxins*, **2**(4), 572-591.
- MIROUX B.,** and WALKER J. E., 1996. Over-production of proteins in *Escherichia coli*: mutant hosts that allow synthesis of some membrane proteins and globular proteins at high levels. *Journal of Molecular Biology*, **260**, 289-298.
- MOLINELLI, A.,** GROSSALBER, K., FÜHRER, M., BAUMGARTNER, S., SULYOK, M. and KRŠKA, R., 2008. Development of qualitative and semiquantitative immunoassay-

based rapid strip tests for the detection of T-2 toxin in wheat and oat. *Journal of Agricultural and Food Chemistry*, **56**(8), 2589-2594.

MONTALTO, G., CERVELLO, M., GIANNITRAPANI, L., DANTONA, F., TERRANOVA, A. and CASTAGNETTA, L.A., 2002. Epidemiology, risk factors, and natural history of hepatocellular carcinoma. *Annals of the New York Academy of Sciences*, **963**, 13-20.

MORAN, K.L.M., FITZGERALD, J., MCPARTLIN, D.A., LOFTUS, J.H. and O'KENNEDY, R. 2016. Biosensor-Based Technologies for the Detection of Pathogens and Toxins in: Viviana Scognamiglio, V., Rea, G., Arduini, F. and Giuseppe Palleschi (eds) *Comprehensive Analytical Chemistry: Biosensors for Sustainable Food - New Opportunities and Technical Challenges*. Vol **74**, 93-20. Cambridge: Elsevier Inc.

MORAN, K.L.M., LEMASS, D. and O' KENNEDY R. 2018. Surface Plasmon Resonance-based Immunoassays: Approaches, Performance and Applications in: Paguio, J. (ed) *Handbook of Immunoassay Technologies: Approaches, Performances, and Applications*. Cambridge Elsevier Inc. Accepted by Elsevier for publication.

MORAN, K.L.M., LOFTUS, J.H., MURPHY, C., O' KENNEDY, R. 2018. Current and emerging technologies for the analysis of fungal and marine toxin contaminants in food. Submitted to CLC press for publication.

MOREIRA, I.S., FERNANDES, P.A. and RAMOS, M.J., 2007. Computational alanine scanning mutagenesis - An improved methodological approach. *Journal of Computational Chemistry*, **28**(3), 644-654.

MORRISON, K.L. and WEISS, G.A., 2001. Combinatorial alanine-scanning. *Current Opinion in Chemical Biology*, **5**, 302-307.

NAEHRER, K., 2014. Polar versus non-polar mycotoxins. [Online] Available at: <https://www.wattagnet.com/articles/20483-polar-versus-non-polar-mycotoxins> [Accessed 10 October 2015].

NAKAGAWA, H., MAEDA, S., YOSHIDA, H., TATEISHI, R., MASUZAKI, R., OHKI, T., HAYAKAWA, Y., KINOSHITA, H., YAMAKADO, M., KATO, N., SHIINA, S. and OMATA, M., 2009. Serum IL-6 levels and the risk for hepatocarcinogenesis in chronic hepatitis C patients: An analysis based on gender differences. *International Journal of Cancer*, **125**(10), 2264-2269.

NARKWA, P., BLACKBOURN, D. and MUTOCHELUH, M., 2017. Aflatoxin B₁ inhibits the type 1 interferon response pathway via STAT1 suggesting another mechanism of hepatocellular carcinoma. *Infectious Agents and Cancer*, **12**(17), 1-9.

NELSON, A.L., 2010. Antibody fragments hope and hype. *Monoclonal Antibodies (mAbs)*, **2**(1), 77-83.

- NING, Y.** and **LENZ, H.** (2012). Targeting IL-8 in colorectal cancer. *Expert Opinion on Therapeutic Targets*, **16**(5), 491-497.
- O' KENNEDY, R.J.,** TOWNSEND, S., DONOHOE, G., LEONARD, P., HEARTY, S. and BYRNE, B., 2010. Speedy, small, sensitive and specific. Reality or myth for future analytical methods. *Analytical Letters*, **43**(10), 1630-1648.
- O'REILLY, J.A.,** MORAN, K.L.M. AND O' KENNEDY, R.J. 2013. Antibody-based sensors for disease detection in: OZKAN-ARIKSOYSA, D. (ed) *Biosensors and their Applications in Healthcare*. 6-23. London: Future Science Ltd.
- OANCEA, S.** and **STOIA, M.**, 2008. Mycotoxins: a review of toxicology, analytical methods and health risks. *Acta Universitatis Cibiniensis Series E: Food Technology*, **XII**(1), 19-36.
- PANDE, J.,** SZEWCZYK, M.M. and GROVER, A.K., 2010. Phage display: Concept, innovations, applications and future. *Biotechnology Advances*, **28**(6), 849-858.
- PARK, S.,** HAN, J., KIM, J., YANG, M., KIM, Y., LIM, H., AN, S. and KIM, J., 2014. Interleukin-8 is related to poor chemotherapeutic response and tumourigenicity in hepatocellular carcinoma. *European Journal of Cancer*, **50**(2), 341-350.
- PESTKA, J.J.**, 2010. Deoxynivalenol: mechanisms of action, human exposure, and toxicological relevance. *Archives of Toxicology*, **84**, 663-679.
- PESTKA, J.J.,** ZHOU, H.R., MOON, Y. and CHUNG, Y.J., 2004. Cellular and molecular mechanisms for immune modulation by deoxynivalenol and other trichothecenes: unraveling a paradox. *Toxicology Letters*, **153**(1), 61-73.
- PHUNG, Y.,** GAO, W., MAN, Y., NAGATA, S. and HO, M., 2012. High-affinity monoclonal antibodies to cell surface tumor antigen glypican-3 generated through a combination of peptide immunization and flow cytometry screening. *Monoclonal Antibodies (mAbs)*, **4**(5), 592-599.
- PIKARSKY, E.,** PORAT, R., STEIN, I., ABRAMOVITCH, R., AMIT, S., KASEM, S., GUTKOVICH-PYEST, E., URIELI-SHOVAL, S., GALUN, E. and BEN-NERIAH, Y., 2004. NF- κ B functions as a tumour promoter in inflammation-associated cancer. *Nature*, **431**(7007), 461-466.
- QI, H.,** LU, H., QIU, H.J., PETRENKO, V. and LIU, A., 2012. Phagemid vectors for phage display: Properties, characteristics and construction. *Journal of Molecular Biology*, **417**(3), 129-143.
- RAHMANI, A.,** JINAP, S. and SOLEIMANY, F., 2009. Qualitative and quantitative analysis of mycotoxins. *Comprehensive Reviews in Food Science and Food Safety*, **8**(3), 202-251.

REED, G., LYNN, F. and MEADE, B., 2002. Use of coefficient of variation in assessing variability of quantitative assays. *Clinical and Vaccine Immunology*, **9**(6), 1235-1239.

REN, Y., TUNG-PING POON, R., TSUI, H., CHEN, W., LI, Z., LAU, C., YU, W. and FAN, S., 2003. Interleukin-8 serum levels in patients with hepatocellular carcinoma. *Clinical Cancer Research*, **9**(16), 5996-6001.

RICHARD, J.L., 2007. Some major mycotoxins and their mycotoxicoses - An overview. *International Journal of Food Microbiology*, **119**(1-2), 3-10.

RISS, T., MORAVEC, R., NILES, A., DUELLMAN, S., BENINK, H., WORZELLA, T. and MINOR, L., 2017. Cell viability assays *in*: SITTAMPALAM, G.S., COUSSENS, N.P., BRIMACOMBE, K., *et al.* (ed) *Assay guidance manual*. 1-31. U.S. National Library of Medicine 8600 Rockville Pike, Bethesda MD, 20894 USA: National Centre for Biotechnology Information.

RODGERS, A., VAUGHAN, P., PRENTICE, T., EDEJER, T.T., EVANS, D. and LOWE, J., 2002. Reducing Risks, Promoting Healthy Life. *in*: The World Health Report. Geneva: World Health Organisation.

ROSANO, G. and CECCARELLI, E., 2014. Recombinant protein expression in *Escherichia coli*: advances and challenges. *Frontiers in Microbiology*, **5**(172), 1-17.

ROUET, R., LOWE, D., DUDGEON, K., ROOME, B., SCHOFIELD, P., LANGLEY, D., ANDREWS, J., WHITFIELD, P., JERMUTUS, L. and CHRIST, D., 2012. Expression of high-affinity human antibody fragments in Bacteria. *Nature Protocols*, **7**, 364-373.

RYCHLIK, M., HUMPF, H.U., MARKO, D., DÄNICKE, S., MALLY, A., BERTHILLER, F., KLAFFKE, H. and LORENZ, N., 2014. Proposal of a comprehensive definition of modified and other forms of mycotoxins including “masked” mycotoxins. *Mycotoxin Research*, **30**(4), 197-205.

RYSCHICH, E., LIZDENIS, P., ITTRICH, C., BENNER, A., STAHL, S., HAMANN, A., STAHL, S., HAMANN, A., SCHMIDT, J., KNOLLE, P., ARNOLD, B., HÄMMERLING, G. AND GANSS, R., 2006. Molecular fingerprinting and autocrine growth regulation of endothelial cells in a murine model of hepatocellular carcinoma. *Cancer Research*, **66**(1), 198-211.

SACHDEVA, M., 2015. Immunology of hepatocellular carcinoma. *World Journal of Hepatology*, **7**(17), 2080-2090.

SANDERS, M. 2014. *Bio-analytical detection strategies for deoxynivalenol in wheat dust*, PhD Thesis, Ghent University, St. Pietersnieuwstraat 33, 9000 Gent, Belgium.

SANDERS, M., GUO, Y., IYER, A., GARCÍA, Y.R., GALVITA, A., HEYERICK, A., DEFORCE, D., RISSEEUW, M.D., VAN CALENBERGH, S., BRACKE, M., EREMIN, S., MADDER, A. and DE SAEGER, S., 2014. An immunogen synthesis strategy for the development of specific anti-deoxynivalenol monoclonal antibodies. *Food Additives &*

Contaminants: Part A, Chemistry, analysis, control, exposure & risk assessment, **31**(10), 1751-1759.

SANTOS, R.R., SCHOEVERS, E.J., ROELEN, B.A.J. and FINK-GREMMELS, J., 2013. Mycotoxins and female reproduction: *in-vitro* approaches. *World Mycotoxin Journal*, **6**(3), 245-253.

SCHARF, J. and BRAULKE, T., 2003. The role of the IGF axis in hepatocarcinogenesis. *Hormone and Metabolic Research*, **35**(11/12), 685-693.

SCHNELL, U., CIRULLI, V. and GIEPMANS, B., 2013. EpCAM: structure and function in health and disease. *Biochimica et Biophysica Acta (BBA) - Biomembranes*, **1828**(8), 1989-2001.

SCHUNK, M.K. and MACALLUM, G.E., 2005. applications and optimization of immunization procedures. *Institute of Laboratory Animal Resources, Journals*, **46**(3), 241-257.

SEBAUGH, J.L., 2011. Guidelines for accurate EC50/IC50 estimation. *Pharmaceutical Statistics*, **10**(2), 128-134.

SHEEDY, C., MACKENZIE, C.R. and HALL, C., 2007. Isolation and affinity maturation of hapten-specific antibodies *Biotechnology Advances*, **25**(4), 333-352.

SIDDLE, K., 2011. Signalling by insulin and IGF receptors: supporting acts and new players. *Journal of Molecular Endocrinology*, **47**(1), R1-R10.

SMELA, M.E., 2002. The aflatoxin B₁ formamidopyrimidine adduct plays a major role in causing the types of mutations observed in human hepatocellular carcinoma. *Proceedings of the National Academy of Sciences (PNAS)*, **99**(10), 6655-6660.

SMITH, G.P., 1985. Filamentous fusion phage: novel expression vectors that display cloned antigens on the virion surface. *Science*, **228**(4705), 1315-1317.

SOBROVA, P., VOJTECH ADAM, V., VASATKOVA, A., BEKLOVA, M., ZEMAN, L. and KIZEK, R., 2010. Deoxynivalenol and its toxicity. *Interdisciplinary Toxicology*, **3**(3), 94-99.

SOTOMAYOR, R.E., SAHU, S., WASHINGTON, M., HINTON, D.M. and CHOU, M., 1999. Temporal patterns of DNA adduct formation and glutathione S-transferase activity in the testes of rats fed aflatoxin B₁: a comparison with patterns in the liver. *Environmental and Molecular Mutagenesis*, **33**(4), 293-302.

STAPLETON, S., 2007. *Novel antibody-based assays for disease and food contaminant detection*. PhD thesis, Dublin City University, Glasnevin, Dublin 9, Ireland.

STECHER, G., JARUKAMJORN, K., ZABORSKI, P., BAKRY, R., HUCK, C. and BONN, G., 2007. Evaluation of extraction methods for the simultaneous analysis of simple and macrocyclic trichothecenes. *Talanta*, **73**(2), 251-257.

STILLS, H.F., 2005. Adjuvants and antibody production: Dispelling the myths associated with Freund's complete and other adjuvants. *Institute for Laboratory Animal Research Journal*, **46**(3), 280-293.

SULLIVAN, K., CUTILLI, J., PILIERO, L., GHAVIMI-ALAGHA, D., STARR, S., CAMPBELL, D. and DOUGLAS, S., 2000. Measurement of cytokine secretion, intracellular protein expression, and mRNA in resting and stimulated peripheral blood mononuclear cells. *Clinical and Vaccine Immunology*, **7**(6), 920-924.

TANG, Y.P., ZHAO, S.Q., WU, Y.S., ZHOU, J.W. and LI, MING, 2013. A direct competitive inhibition time-resolved fluoroimmunoassay for the detection of unconjugated estriol in serum of pregnant women. *Analytical Methods*, **5**, 4068–4073.

TARRATS, N., MOLES, A., MORALES, A., GARCÍA-RUIZ, C., FERNÁNDEZ-CHECA, J. and MARÍ, M., 2011. Critical role of tumour necrosis factor receptor 1, but not 2, in hepatic stellate cell proliferation, extracellular matrix remodelling, and liver fibrogenesis. *Hepatology*, **54**(1), 319-327.

THAKKAR, S., NANAWARE-KHARADE, N., CELIKE, R., PETERSON, E.C. and VARUGHESE, K.I., 2014. Affinity improvement of a therapeutic antibody to methamphetamine and amphetamine through structure-based antibody engineering. *Scientific Reports*, **4**(3673), 1-8.

THE NATIONAL COMMITTEE FOR CLINICAL LABORATORY STANDARDS, 2004. Protocols for determination of limit of detection and limit of quantification; Approved Guideline. NCCLS document **EP17-A**. 940 West Valley Road, Suite 1400, Wayne, Pennsylvania 19087-1898 USA: NCCLS.

THERMO SCIENTIFIC (PIERCE), 2010. *Antibody production and purification technical handbook*. Version 2. USA.

THOUVENOT, D. and MORFIN, R.F. 1983. Radioimmunoassay for zearalenone and zearalanol in human serum: production, properties, and use of porcine antibodies. *Applied and Environmental Microbiology*, **45**(1), 16-23.

TOWBIN, H., STAEBELIN, T. and GORDON, J. 1979. Electrophoretic transfer of proteins from polyacrylamide gels to nitrocellulose sheets: Procedure and some applications. *Proceedings of the National Academy of Sciences (PNAS)*, **76**(9), 4350-4354.

TOWNSEND, D.M. and TEW, K.D., 2003. The role of glutathione-S-transferase in anti-cancer drug resistance. *Oncogene*, **22**, 7369-7375.

TOWNSEND, S., 2009. *Genetic engineering of antibody fragments for the detection of illicit drugs*. PhD thesis, Dublin City University, Glasnevin, Dublin 9, Ireland.

- TURNER, M., NEDJAI, B., HURST, T. and PENNINGTON, D., 2014.** Cytokines and chemokines: At the crossroads of cell signalling and inflammatory disease. *Biochimica et Biophysica Acta (BBA) - Molecular Cell Research*, **1843**(11), 2563-2582.
- TURNER, N.W., SUBRAHMANYAM, S. and PILETSKY, S.A., 2009.** Analytical methods for determination of mycotoxins: A review. *Analytica Chimica Acta*, **632**(2), 168-180.
- UBAGAI, T., KIKUCHI, T., FUKUSATO, T. and ONO, Y., 2010.** Aflatoxin B₁ modulates the insulin-like growth factor-2 dependent signalling axis. *Toxicology in Vitro*, **24**(3), 783-789.
- UNITED NATIONS, 2013.** Department of Economic and Social Affairs/Population Division World population prospects: The 2012 revision, Vol I: Comprehensive Tables, 1-118. **ST/ESA/SER.A/336**, New York: United Nations.
- URRY, W.H., WEHRMEISTER, H.L., HODGE, E.B. and HIDY, P.H., 1966.** The structure of zearalenone *Tetrahedron Letters*, **27**, 3109-3114.
- VARDON, P., 2003.** Potential economic costs of mycotoxins in the United States *in: Mycotoxins: Risks in plants, animal and human systems*, Task Force Report No. **139**, 136-142. Ames, Iowa, USA: Council for Agricultural Science and Technology.
- VILARINO, N., LOUZAO, M.C., VIEYTES, M.R. and BOTANA, L.M., 2010.** Biological methods for marine toxin detection. *Analytical and Bioanalytical Chemistry*, **397**(5), 1673-1681.
- VILLERS, P., 2014.** Aflatoxins and safe storage. *Frontiers in Microbiology*, **5**(158), 1-6.
- WANG, J., DUAN, S., ZHANG, Y. and WANG, S., 2010.** Enzyme-linked immunosorbent assay for the detection of T-2 toxin in cereals and feedstuffs. *Microchimica Acta*, **169**(1-2), 137-144.
- WANG, R., XIANG, S., FENG, Y., SRINIVAS, S., ZHANG, Y., LIN, M. and WANG, S., 2013.** Engineering production of functional scFv antibody in *E. coli* by co-expressing the molecule chaperone Skp. *Frontiers in Cellular and Infection Microbiology*, **3**(72), 1-9.
- WANG, X., LU, X. and CHEN, J., 2014.** Development of biosensor technologies for analysis of environmental contaminants. *Trends in Environmental Analytical Chemistry*, **2**, 25-32.
- WAUGH, D. and WILSON, C., 2008.** The Interleukin-8 pathway in cancer. *Clinical Cancer Research*, **14**(21), 6735-6741.
- WHEELHOUSE, N., CHAN, Y., GILLIES, S., CALDWELL, H., ROSS, J., HARRISON, D. and PROST, S., 2003.** TNF- α induced DNA damage in primary murine hepatocytes. *International Journal of Molecular Medicine*. **12**(6), 889-894.

- WILLIAMS, J.H.**, PHILLIPS, T.D., JOLLY, P.E., STILES, J.K., JOLLY, C.M. and AGGARWAL, D., 2004. Human aflatoxicosis in developing countries: a review of toxicology, exposure, potential health consequences, and interventions. *American Journal of Clinical Nutrition*, **80**(5), 1106-1122.
- WU, F.**, NARROD, C., TIONGCO, M. and LIU, Y., 2011. The health economics of aflatoxins: Global burden of disease. Working paper **4**, 1-20. Washington D.C.: International Food Policy Research Institute.
- WU, H.C.** and SANTELLA, R., 2012. The role of aflatoxins in hepatocellular carcinoma. *Hepatitis Monthly*, **12**(10 HCC): e7238, 1-9.
- WU, J.** and ZHU, A., 2011. Targeting insulin-like growth factor axis in hepatocellular carcinoma. *Journal of Hematology & Oncology*, **4**(30), 1-11.
- WU, K.**, KRYCZEK, I., CHEN, L., ZOU, W. and WELLING, T., 2009. Kupffer cell suppression of CD8⁺ T cells in human hepatocellular carcinoma is mediated by B7-H1/Programmed Death-1 interactions. *Cancer Research*, **69**(20), 8067-8075.
- XIAO, Z.**, CHUNG, H., BANAN, B., MANNING, P., OTT, K., LIN, S., CAPOCCIA, B., SUBRAMANIAN, V., HIEBSCH, R., UPADHYA, G., MOHANAKUMAR, T., FRAZIER, W., LIN, Y. and CHAPMAN, W., 2015. Antibody mediated therapy targeting CD47 inhibits tumour progression of hepatocellular carcinoma. *Cancer Letters*, **360**(2), 302-309.
- XU, Y.**, HE, Z., HE, Q., QIU, Y., CHEN, B., CHEN, J. and LIU, X., 2014. Use of cloneable peptide-mbp fusion protein as a mimetic coating antigen in the standardized immunoassay for mycotoxin ochratoxin A. *Journal of Agricultural and Food Chemistry*, **62**(35), 8830-8836.
- YAZDANPANAHI, H.**, 2011. Mycotoxins: Analytical challenges. *Iranian Journal of Pharmaceutical Research*, **10**, 653-654.
- YENI, F.**, ACAR, S., POLAT, Ö.G., SOYER, Y. and ALPAS, H., 2014. Rapid and standardized methods for detection of foodborne pathogens and mycotoxins on fresh produce. *Food Control*, **40**, 359-367.
- ZAIN, M.E.**, 2011. Impact of mycotoxins on humans and animals. *Journal of Saudi Chemical Society*, **15**(4), 129-144.
- ZENG, X.**, SHEN, Z. and MERNAUGH, R., 2012. Recombinant antibodies and their use in biosensors. *Analytical and Bioanalytical Chemistry*, **402**(10), 3027-3038.
- ZHANG, Z.**, WANG, D., LI, J., ZHANG, Q. and LI, P., 2015. Monoclonal antibody-europium conjugate-based lateral flow time-resolved fluoroimmunoassay for quantitative determination of T-2 toxin in cereals and feed. *Analytical Methods*, **7**(6), 2822-2829.

ZHAO, D., BAKIRTZI, K., ZHAN, Y., ZENG, H., KOON, H. and POTHOUidakis, C., 2011. Insulin-like growth factor-1 receptor transactivation modulates the inflammatory and proliferative responses of neurotensin in human colonic epithelial cells. *Journal of Biological Chemistry*, **286**(8), 6092-6099.

ZHU, L., GAO, J., HUANG, K., LUO, Y., ZHANG, B. and XU, W., 2015. MiR-34a screened by miRNA profiling negatively regulates Wnt/ β -catenin signalling pathway in aflatoxin B₁ induced hepatotoxicity. *Scientific Reports*, **5**(16732), 1-13.

ZINEDINE, A., SORIANO, J.M., MOLTÓ, J.C. and MAÑES, J., 2007. Review on the toxicity, occurrence, metabolism, detoxification, regulations and intake of zearalenone: an oestrogenic mycotoxin. *Food and Chemical Toxicology*, **45**(1), 1-18.

Appendices

Appendix A

Faculty of Science and Health

Biological Safety Committee

Application Form – Class 2 and above Biological Agents

Proposal to undertake Hazard Group / Class 2 (and above) Biological Research

This is a standardised BSC full committee application form for all biological work (planned or underway) which falls into the following categories:

- Hazard group (biohazard level) 2 or above.
- Research involving primary human tissue, primary tumour or primary blood/plasma/serum.
- Research involving prion material.
- Research involving pathogenic/disease causing microbes.

This Notification Form **MUST** be accompanied by a (a) Biological Agent Risk Assessment and (b) Standard Operating Procedure Document for each associated risk. Completed documentation will be reviewed by the Biological Safety Committee, DCU.

- **Hazard Group / Class 2 activity relates to the use of biological agents that can cause human disease and might be a hazard to employees.**
- **Hazard Group / Class 3 activity relates to the use of biological agents that can cause severe human disease and presents a serious hazard to employees and which may present a risk of spreading to the community.**
- **Hazard Group / Class 4 activity relates to the use of biological agents that causes severe human disease and is a serious hazard to employees and which may present a high risk of spreading to the community.**

Project title	The treatment of THLE2/3 normal human liver cells with AFB1 to determine the cellular processes associated with hepatocellular carcinoma.
Date of application	19/10/2016
Research group / principal investigator	Applied Biochemistry Group – Prof. Richard O’ Kennedy National Institute for Cellular Biology (NICB) – Dr. Niall Barron
Name of applicant	Kara Moran
Contact phone number & e-mail	Ex 5580 Kara.moran24@mail.dcu.ie
Proposed duration and location of work	The proposed duration of the project will be 6 months. Culturing of THLE2/3 normal human liver cells will be completed in the NICB (Room GG22 in Lab GG21). Testing/assays on these cells will be completed in the School of Biotechnology (X273a).
Indicate if work will be undertaken by the following:-	Postgraduate student – Kara Moran Post doctorate researcher – Caroline Murphy

staff, postgraduate students, undergraduate students and/or other (please specify the breakdown of work among the team where relevant)	
Provide a brief description of work to be undertaken (approx 150 words)	<p>AFB1 can cause heritable genetic damage, may act as a teratogen and it is a known potent hepatocarcinogen. A novel <i>in-vitro</i> study will test AFB1 treatment in THLE2/3 normal liver cells to determine the effects of AFB1 on cell viability, apoptosis and growth. In addition DNA-binding protein (adducts) testing will be completed to examine DNA adduct intracellular pathways, processes and signalling which are important in hepatocellular cancer development. If significant effects are determined, a recombinant AFB1 Fab antibody will also be administered following AFB1 treatment and the same tests completed to determine if a positive therapeutic effect can be elicited.</p>

For work involving Genetically-Modified Organisms (GMO) or Genetically-Modified Microorganisms (GMM)	
Will this project involve the use of genetically-modified organisms (GMOs) or microorganisms (GMMs)	<p>The THLE2/3 normal human liver cells are not specifically a GMO, however, they harbour a GM retroviral vector. Normal human liver cells are difficult to propagate for long-term cell cultures, therefore, normal human liver epithelial cells have been transformed by infection with a retroviral vector containing a SV40 large T antigen for immortalisation.</p> <p>No genetic modifications will be applied to or completed in this work.</p>
If yes, have you included in your application a copy of the Environmental Protection Agency (EPA) GMO licence application, including a biological agent risk assessment(s) and standard operating procedure(s)?	The necessary EPA risk assessment template was drafted and submitted to the EPA.
Specify the relevant GMO licence number (where granted)	261
Identify the vectors, genes, cell lines and organisms to be used/developed	<p>THLE2/3 normal human liver cells used for the study will be purchased directly from ATCC already transfected and ready for propagation and are constructed as follows. A BglI-HpaI fragment of the SV40 viral DNA (nucleotides 5235-2666) is inserted into a pzipNeoSVX retroviral vector. The amphotropic packaging cell line, PA317, is</p>

	transfected with the retroviral vector. The transfected PA317 cells are then used to infect the primary liver tissue cell cultures for immortalisation.
--	---

For work involving Biological Hazards	
Has a written biological agent risk assessment been conducted for this?	Yes
Identity of the hazard/toxin/organism in use/to be used	<p>THLE2/3 normal human liver cells are a Biosafety level 2 Biological Reagent and appropriate safety procedures should be used with this material. The cells are derived from primary normal human liver epithelial cells which have proven difficult to support in long-term cell culture. The cells are immortalised by expression of the large T antigen of the SV40 virus. The cells contain the BglI-HpaI fragment of the SV40 viral DNA (nucleotides 5235-2666 and lack an early promoter and polyadenylation site) inserted in a pzipNeoSVX retroviral vector. SV40 (a DNA virus with the potential to cause tumors in animals) cannot be produced as only the T antigen is expressed and not the whole viral genome (Harris <i>et al</i>, 1998). The virus particles are ‘infectious’ for only one cycle, therefore, cells will not be capable of propagation in the event of a containment breach. The retrovirus lacks the necessary genes for recurrent infectivity. Generation of replication competent retroviruses (RCR) in target cells or tissues is the primary risk associated with the use of retroviral vectors. The retroviral genomes expressed are fully integrated into the target genome, therefore, no replication competent viruses can be produced (Mosier, 2004). The transfected packaging cell line, PA317 (not known to cause disease in healthy humans) is then used to infect the primary liver tissue cell cultures. PA317 cells are frequently used to stably infect and immortalize many cell types (Harris <i>et al</i>, 1998; Miller, 2002).</p> <p>The generated THLE2/3 liver cells express phenotypic characteristics of normal adult epithelial cells. Human pathogenicity has not been studied, however, THLE2/3 cells are non-tumorigenic when injected into athymic nude mice, have near-diploid karyotypes and do not express alpha-fetoprotein (Pfeifer <i>et al.</i>, 1993; ATCC Product Sheet, 2013).</p> <p>AFB1 is a chemical agent (CAS number: 1162-65-8) produced by <i>Aspergillus flavus</i> and <i>Aspergillus paraciticus</i> fungal species. AFB1, a Group 1 liver</p>

	<p>carcinogen, may cause heritable genetic damage and may be teratogenic. AFB1 consists of a difurofuran ring system that is fused to a substituted coumarin moiety, with a methoxy group attached at the corresponding benzene ring. Consumed aflatoxins are converted to aflatoxin derivatives in the liver. AFB1 is known to be oxidized by the mixed function oxygenases of the liver cytochrome P-450 system present in the microsomal fraction of liver extracts. This oxidation results in an AFB1-8,9-epoxide (major product). This reactive epoxide preferentially attacks certain guanine residues in double-stranded DNA, giving rise to AFB₁-N7-Gua, a large adduct which can induce mutations in pivotal genes and drive carcinogenic effects in animals and humans. Furthermore, AFB₁-N7-Gua adducts can result in GC to TA transversions. Liver tumor tissues with high AFB₁ exposure have been shown to develop a specific mutation at codon 249 in the P53 tumor suppressing gene resulting in a G to T transversion (AGG to AGT). Therefore, the inactivation of P53 tumor suppressor gene may be a key driver in primary hepatocellular carcinoma. Significantly, the specific mutation in codon 249 of the P53 gene has been referred to as the first example of a 'carcinogen-specific' biomarker that is fixed in tumor tissue (Bennett and Klich, 2003; Wu and Santella, 2012).</p>
<p>Based on your biological agent risk assessment, briefly indicate reasoning for categorising this work as Hazard Group 2 / Class 2 and above</p>	<p>THLE2/3 normal human liver cells are transfected with a retroviral vector containing a SV40 large T antigen and results in their categorisation as a Biosafety Level Group 2 risk. Hazardous include: percutaneous injury, ingestion and mucous membrane exposure.</p>
<p>Based on your biological agent risk assessment, briefly outline the measures to be utilised to control and minimise risks?</p>	<p>Culturing THLE2/3 normal liver cells in NICB Facility</p> <ul style="list-style-type: none"> • These cells will be cultured in a facility (NICB) tailored for Biosafety Level 2 cell lines. A Class II biological safety cabinet will be used to ensure user safety, containment of the cells and maintain absolute isolation. • These cells will be cultured in the NICB, collected in a sealed falcon tube, placed in a sealed un-contaminated container and carried carefully to the School of Biotechnology for treatment with AFB1 and assay/testing as outlined. The contained THLE2/3 cells will be placed into the container whilst wearing gloves. These gloves will be removed and a fresh, un-contaminated glove will be donned to carry the container to the School of Biotechnology

	<p>abiding by the ‘one-glove-rule’. A spare fresh, un-contaminated glove will be carried on the person also. On arrival to the School of Biotechnology, the worn glove will be disposed of and fresh, uncontaminated gloves will be donned for experiments.</p> <ul style="list-style-type: none"> • PPE will include lab coats, gloves and safety glasses. • The research users of the cell line are experienced in cell culture having completed a Masters (Kara Moran) and PhD (Caroline Murphy) based on <i>in-vitro</i> studies. In the event that an additional researcher may be required for this research, an individual competent in cell culturing techniques and practices will be selected and adequate training and undertaken to meet the S.O.P.s for Safe Handling of Class 2 Biological Agent requirements. • Researchers involved are trained in Good Laboratory Practice and will be fully competent in the processes/procedures of Biosafety Level 2 lab work, employing approved SOPs for work and ancillary activities such as cleaning and waste decontamination/disposal under the guidance of S.O.P.s for Safe Handling of Class 2 Biological Agents (NICB). • Researchers will be approved by specialist researchers who have vast experience in Biosafety level 2 procedures and signed off for Biosafety level 2 research under the Class 2 Biological Agent Training Sign-Off form (NICB). • A ‘buddy-system’ will be established between the researchers to ensure the cells are adequately maintained and controlled at all times. • Sharps usage will be avoided by not using pipette tips during THLE2/3 cell culturing procedures to avoid self-inoculation. Where assays/testing is to be completed and pipette tips may be necessary, 2 pairs of gloves will be donned for greater protection against percutaneous injury. • In the event of a spillage, only the immediate lab area is likely to be exposed and considerable care will be taken to ensure the cells are fully contained within this area. The spill treatment protocol outline in the S.O.P.s for Safe Handling of Class 2 Biological Agents (NICB) will be adhered to as follows. If there is a spill of Class 2 biological agent
--	---

	<p>inside of the Class II biological safety cabinet:</p> <p>The grill design of the Class II biological safety cabinet means that spills will normally be contained within the cabinet. To clean spills within the cabinet, first drop a lint-free wipe on the area to restrict its' spread. Spray a large volume of 1% (v/v) Virkon over the contaminate area and wait 5 minutes. Carefully transfer the 'lint-free' wipe to the virus waste autoclave bag in the hood and clean the surface of the Class II biological safety cabinet as usual.</p> <p>If there is a spill of Class 2 biological agent outside of the Class II biological safety cabinet:</p> <ol style="list-style-type: none"> Do not panic. Take a second to assess the situation and the nature of the spill, ensuring that it has not contacted shoes or clothing/labcoat. If spills contact clothing, remove the items and treat as described in section v). Do not walk around the laboratory before ensuring the spill did not contact shoes. Determine areas contacted by the spill. Place a small amount of A-tork/Lint-free wipe on the spill (this will prevent spread when subsequent Virkon is applied to the area). Pour Virkon on the spill and surrounding areas. Allow to stand for 15 min before transferring the A-tork to an autoclave bag. Carefully soak up Virkon and wash the area twice with 70% (v/v) Ethanol. Rinse with water and dry the area well. For larger spills (volumes being moved outside of the Class II biological safety cabinet should never exceed 20 mL at any one time so this should not be necessary) sprinkle powdered Virkon on the spill to inactivate it and continue as outlined above. <ul style="list-style-type: none"> A maximum volume of 1×10^7/100 μL of THLE2/3 cells will be cultured in T75 cell culture flasks for assay-based tests. <p>AFB1</p> <p>AFB1 is strictly used as per Aflatoxin handling SOP, revised June 2016.</p>
--	---

	<ul style="list-style-type: none"> • AFB1 users will be added to the carcinogen user list which is maintained for 10 years after use is completed. • AFB1 stocks are prepared in a clearly labelled designated fume-hood for toxin use assigned to toxin users only in the prep lab x271a segregated from the common lab area. • AFB1 stocks are stored in a locked fridge-freezer and the key only made available to relevant aflatoxin users. • All assays/tests are completed in a clearly labelled designated fume hood used exclusively for toxin research assigned toxin users. • PPE includes protective safety glasses, lab coats and 2 pairs of gloves. • All AFB1 waste is decontaminated as per Aflatoxin handling SOP, revised June 2016, by the addition of 10-12% (v/v) sodium hypochlorite, pH adjustment to 8 and addition of acetone. The decontaminated liquid AFB1 waste is disposed of with excess running water. Decontaminated solid waste and sharps are added to cytotoxic bins, removed to the School of Biotechnology waste disposal, logged appropriately and collected by a licensed disposal company (SRCL). • AFB1 spillages are treated as per Aflatoxin handling SOP, revised June 2016, and will be handled directly by Kara Moran who has experience dealing with aflatoxins. • Validation of aflatoxin liquid waste decontamination will be confirmed by testing for absence of fluorescence using a UV spectrophotometer. This will be executed using a Tecan Infinite c200 spectrophotometer at a wavelength of 360/440 nm (excitation/emission) for aflatoxin B1 as per Aflatoxin handling SOP, revised June 2016. • AFB1 can cause heritable genetic damage and may act as a teratogen. Therefore, researchers who may be pregnant/planning pregnancy should inform their supervisor and have a health and safety audit completed. Pregnant researchers should not partake in research activities involving AFB1. Researchers who are breast-feeding should also not complete research involving AFB1. • The equipment used in this research (i.e. the autoclave for decontamination, the Class II
--	---

	biological safety cabinet and fume hood) are validated on a yearly basis by established contractors.
Have you included in your application a copy of any HSA notification, where relevant? http://hsa.ie/eng/Topics/Business_Licensing_and_Notification_Requirements/Biological_Agents	n/a
Have you attached a copy of Hazardous Substance Assessment Forms (HSAF) for each chemical selected for use?	THLE2/3 normal liver cells – Yes AFB1 – Yes
Is dedicated equipment to be utilised?	THLE2/3 normal liver cells - NICB, GG22 in lab GG21: Class II biological safety cabinet, centrifuges, CO2 incubator. AFB1 - School of Biotechnology, X271a, X273a: Class II biological safety cabinet, incubator, fume hood. The listed equipment items are dedicated solely to the use and isolation of mycotoxins. The research users are fully trained and experienced in the use of the necessary equipment.
Where is material to be stored?	THLE2/3 normal liver cells will be cultured and stored in the NICB facility (GG22 in lab GG21), specifically designed with facilities for the culturing, containment and storage of biosafety level II cell lines. AFB1 stocks will be stored in a locked fridge/freezer with the key only accessible by assigned toxin users in X271a prep lab.
Clearly specify the steps to be taken when transporting material to/from the identified place(s) of work within DCU	THLE2/3 normal liver cells will be cultured in the NICB, collected in a sealed falcon tube, placed in a sealed container and carried carefully to the School of Biotechnology for treatment with AFB1 and assay/testing as outlined.
Will material be moved outside of DCU? If so, specify control measures to be implemented	No
Based on your biological agent risk assessment, briefly outline the waste management strategies to be employed here	THLE2/3 normal liver cells - All liquid and solid waste will be destroyed by autoclave cycling at 122°C, 15psi for 30 minutes and liquid disposed of down the sink, as per S.O.P.s for Safe Handling of Class 2 Biological Agents (NICB) , SOP W1 The Management of Biohazard Waste Disposal in the School of Biotechnology (Issue 3, Revised 08/12/2015) and SOP W3 The Management of Biohazard Waste Disposal in the School of Biotechnology - Disposal of Class 1 and Class 2 GMM waste (Issue 1, Issued 08/12/2015) in the School of Biotechnology Safety Statement. A SB-WRS-4 Biohazard Waste Management Application for Waste Disposal (Issue 3,

	<p>Issued 10/05/2015) will also be completed to track waste disposal.</p> <p>AFB1 - All AFB1 waste is decontaminated by the addition of 10-12% sodium hypochlorite, pH adjusted to 8 and with addition of acetone as per Aflatoxin handling SOP, revised June 2016. The decontaminated liquid AFB1 waste is disposed of with excess running water following validation of aflatoxin decomposition. Solid waste materials and decontaminated sharps are added to purple cytotoxic bins as per SOP W4 Disposal of Contaminated Sharps - UN Yellow Sharps Boxes (Issue 1, Revised 15/01/2016). The bins are labelled with the lab room number, extension phone number, PI name and as 'decontaminated toxin waste.' These are then removed to the School of Biotechnology waste disposal, logged in the appropriate folders and collected by a licensed disposal company (SRCL).</p> <p>Tests/Assays – All assay testing liquids, solids and sharps will be decontaminated for THLE2/3 by autoclave cycling at 122°C, 15psi for 30 minutes. Aflatoxins in liquid waste will then be decontaminated as outlined above and as per Aflatoxin handling SOP, revised June 2016, by addition of 10-12% sodium hypochlorite, pH adjusted to 8 and addition of acetone. Decontaminated liquid waste will be disposed of down the sink following validation of decomposition of AFB1. Autoclaved solids and sharps waste will be placed in purple cytotoxic bins and collected by a licensed disposal company (SRCL).</p> <p>A SB-WRS-4 Biohazard Waste Management Application for Waste Disposal (Issue 3, Issued 10/05/2015) will also be completed to track waste disposal (~1 L/month of waste expected).</p>
Has a SOP for waste management been appended?	<p>Yes – Aflatoxin handling SOP, revised June 2016.</p> <p>SOP W1 The Management of Biohazard Waste Disposal in the School of Biotechnology (Issue 3, Revised 08/12/2015).</p> <p>SOP W3 The Management of Biohazard Waste Disposal in the School of Biotechnology - Disposal of Class 1 and Class 2 GMM waste (Issue 1, issued 08/12/2015).</p> <p>SOP W4 Disposal of Contaminated Sharps - UN Yellow Sharps Boxes (Issue 1, revised 15/01/2016).</p> <p>SB-WRS-4 Biohazard Waste Management Application for Waste Disposal (Issue 3, issued 10/05/2015).</p> <p>S.O.P.s for Safe Handling of Class 2</p>

	Biological Agents (NICB)
--	---------------------------------

Applicant Signature	<i>Kara Moran</i>
Principal Investigator Signature	<i>Richard O' Kennedy</i>
Date	19/10/2016

To be submitted to grace.hickey@dcu.ie and bio.safety@dcu.ie

REFERENCES:

Bennett, J.W. and Klich, M. 2003. Mycotoxins. *Clinical Microbiology Reviews*, **16**(3), pp. 497-516.

Wu, H.C. and Santella, R. 2012. The role of aflatoxins in hepatocellular carcinoma. *Hepatitis Monthly*, 12(10 HCC): e7238, pp. 1-9.

ATCC, 2013. *THLE2 (ATCC® CRL2706™) Product Sheet* [Online]. Available from <file:///C:/Users/Kara/Desktop/CRL-2706.pdf> [Accessed 26 June 2016].

D. Miller, 2002. PA317 Retrovirus Packaging Cells, *Molecular Therapy*, 6(5), pp. 572-575 [Online]. Available from http://www.nature.com/mt/journal/v6/n5/pdf/mt2002216a.pdf?origin=publication_detail [Accessed 27 June 2016].

Harris, C.C., Cole, K.H., Lechner, J.F. and Reddel, R. The United States Of America As Represented By The Department Of Health And Human Services, 1998. *Human liver epithelial cell lines*, US5759765 A.

Biological Agent Risk Assessment

Project Title: The treatment of THLE2/3 normal human liver cells with AFB1 to determine the cellular processes associated with hepatocellular carcinoma.	
Name of applicant:	Kara Moran Postgraduate - PhD Researcher – Applied Biochemistry Group
Email address and extension number:	Kara.moran24@mail.dcu.ie Ex. 5580
Name of principal investigator:	Prof. Richard O' Kennedy – Applied Biochemistry Group Dr. Niall Barron – National Institute for Cellular Biotechnology (NICB)
School / research centre:	School of Biotechnology NICB

Number of researchers directly involved in activity:	2. Kara Moran, Caroline Murphy		
Date:	19/10/2016		
Hazard / Context			
Project background and purpose:	<p>AFB1 can cause heritable genetic damage, may act as a teratogen, and it is a known potent hepatocarcinogen. A novel <i>in-vitro</i> study will test AFB1 treatment in THLE2/3 normal liver cells to determine the effects of AFB1 on cell viability, apoptosis and growth. In addition DNA-binding protein (adducts) testing will be completed to examine DNA adduct intracellular pathways, processes and signalling which are important in hepatocellular cancer development. If significant effects are determined, a recombinant AFB1 Fab antibody will also be administered following AFB1 treatment and the same tests completed to determine if a positive therapeutic effect can be elicited.</p>		
Will your project involve the use of genetically-modified organisms (GMOs) or microorganisms (GMMs)?	<p>The proposed THLE2/3 normal human liver cells are not specifically a GMO, however, they harbour a GM retroviral vector. No genetic modifications will be completed on these cells.</p>		
Where will the work be performed?	<p>School of Biotechnology, X271a, X273a NICB, GG22 in lab GG21</p>		
Provide a list of the equipment that will be used.	<p>Class II biological safety cabinet, centrifuges, CO₂ incubator, incubator, fume hood. The equipment used in this research is validated on a yearly basis by established contractors.</p>		
Reasons Considered a Hazard			
Hazard	Biological Agent: Hazard Group	GMO / GMM: Class <i>[If Applicable]</i>	Risk
Biological Agent(s) THLE2/3 normal human liver cells transformed with SV40 large T antigen inserted in a pzipNeoSVX retroviral vector (1x10 ⁷ cells/100 µL required for assay based testing)	2	2	Low
AFB1 (0.1 ng/mL – 1 µg/mL, minimum volumes for assay based testing)	n/a	n/a	Medium - High
Hazardous Procedures / Activities	<p>THLE2/3 normal human liver cells are Biosafety level 2 biological agents and appropriate safety procedures should be used with this material as agents infectious for humans are most likely to arise from cells of human or primate origin (HSE, 2005). The cells are derived from primary normal human liver epithelial cells which have proven difficult to support in long-term cell culture. The cells are immortalised by expression of the large T antigen of the SV40 virus. The cells contain the BglI-HpaI fragment of the SV40 viral DNA (nucleotides 5235-2666 and lack an early promoter and polyadenylation site) inserted in a pzipNeoSVX retroviral vector, used to transfect the PA317 packaging cell line which is subsequently used to infect the primary liver</p>		

	<p>tissue cells for immortalisation. SV40 (a DNA virus with the potential to cause tumors in animals) cannot be produced as only the T antigen is expressed and not the whole viral genome (Harris, 1998). The virus particles are 'infectious' for only one replication cycle indicating the replication of THLE2/3 and their spread is a low risk if not fully contained (or if spillage occurs). The retrovirus lacks the necessary genes for recurrent infectivity. Generation of replication competent retroviruses (RCR) in target cells or tissues is the primary risk associated with the use of retroviral vectors. The retroviral genomes expressed are fully integrated into the target (packaging cell) genome, therefore, no replication competent viruses can be produced (Mosier, 2004).</p> <p>In the past ten years, there have been no reports of RCR positive results in samples of vector lots that were used for clinical studies. This is due to improvements in vector production systems designed to reduce the chance of RCR generation. Retroviral vectors are designed to avoid RCR generation by employing the following criteria a) reduction of homology between vector and helper sequences b) reduction in homology between vector/helper sequences and cellular DNA c) division of helper sequences to more than one expression cassette to increase the number of recombination events required to generate RCR and d) inclusion of other changes in the vector sequences such as introduction of stop codons into an open reading frame to prevent retroviral proteins from being expressed preventing generation of RCR.</p> <p>The transfected packaging cell line, PA317 (not known to cause disease in healthy humans), is then used to infect the primary liver tissue cell cultures. PA317 cells are frequently used to stably infect and immortalize many cell types (Harris <i>et al.</i>, 1998; Miller, 2002). The generated THLE2/3 liver cells express phenotypic characteristics of normal adult epithelial cells. Human pathogenicity has not been studied, however, THLE2/3 cells are non-tumorigenic when injected into athymic nude mice, have near-diploid karyotypes and do not express alpha-fetoprotein (Pfeifer <i>et al.</i>, 1993; ATCC Product Sheet, 2013) The described cell line is deemed a biosafety level 2 biological reagent due to the presence of a retrovirus containing a SV40 large T antigen, however, retroviral vectors have become standard tools in cell biology (Mosier, 2004), and under appropriate containment Level 2 procedures are reasoned to present a low risk.</p> <p>The THLE2/3 normal liver cells must be treated as a Biosafety level 2 biological reagent and suitable controls put in place for the safe culturing and use of these cells to avoid the potential (low) risk of exposure. Hazards include percutaneous injury, ingestion and mucous membrane exposure. Under the Containment Level 2 procedures and SOPs put in place it is deemed that this low risk will be acceptable.</p> <p>AFB1 is a chemical agent (CAS number: 1162-65-8) produced by <i>Aspergillus flavus</i> and <i>Aspergillus paraciticus</i> fungal species. A metabolised form of AFB1, AFB1-8,9-epoxide (major product) acts as reactive epoxide preferentially attacking certain guanine residues in double-stranded DNA, giving rise to AFB₁-N7-Gua. This can induce mutations in pivotal genes and drive carcinogenic effects in animals and humans. AFB1 will be used to treat THLE2/3 cells to determine the effects of AFB1 on cell viability, apoptosis and growth. In addition DNA-binding protein (adducts) testing will be completed to examine DNA adduct intracellular pathways, processes and signalling which are important in hepatocellular cancer development. AFB1 is a Group 1 liver carcinogen, may cause heritable genetic damage and may be teratogenic.</p> <p>The most hazardous procedures/activities involved in this work will include:</p> <ul style="list-style-type: none"> • Culturing THLE2/3 cells • Destruction and disposal of the THLE2/3 cells correctly
--	--

	<ul style="list-style-type: none"> • Transporting THLE2/3 cells from the NICB to the School of Biotechnology • Completing subsequent assay-based tests which include the use of the THLE2/3 cells and AFB1 • Disposal of decontaminated AFB1-treated THLE2/3 cells and associated solid/liquid waste materials correctly <p>To avoid the risk of percutaneous injury by sharps and exposure to THLE2/3 cells, culturing will be completed in the absence of pipette tips. Culturing will be completed in a Class II biological safety cabinet to avoid exposure to the user in the NICB 'purpose-designed' for the culture of biohazardous material.</p> <p>AFB1 for the treatment of the THLE2/3 cells will be prepared carefully using the necessary precautions in a fume hood designated for toxin use by assigned toxin users located in X271a prep room and when AFB1 is used to treat the THLE2/3 cells directly within a Class II biological safety cabinet designated for toxin use only by assigned users, located in x273a to protect the user from both the THLE2/3 cells and AFB1. Where assays/testing is to be completed and pipette tips may be necessary, 2 pairs of gloves will be donned for greater protection against percutaneous injury.</p> <p>The disposal risk of AFB1 is controlled by decontamination of all contaminated reagents and materials with 10%-12% sodium hypochlorite, pH adjustment to 8 and addition of acetone. The decontaminated liquid AFB1 waste is disposed of with excess running water following validation of AFB1 decomposition. Decontaminated solid waste and sharps are added to cytotoxic bins, removed to the School of Biotechnology waste disposal, logged appropriately and collected by a licensed disposal company (SRCL).</p>
Persons at Risk	Potential Injury / Loss**
<p>Persons at risk (research staff /cleaners /emergency responders etc.). Immediate research staff. AFB1 can cause heritable genetic damage and may act as a teratogen. Therefore, researchers who may be pregnant/planning pregnancy should inform their supervisor and have a health and safety audit completed. Pregnant researchers should not par-take in research activities involving AFB1. Breast-feeding researchers should not par-take in research activities involving AFB1. The risk of exposure to other researchers/cleaners is minimised by maintaining and storing toxic materials under lock and key. All equipment used is labelled clearly with warnings. Toxin work is completed in a specifically designated fume-hood and Class II biological safety cabinet used (only for toxin work) located in X271a and x273a by assigned toxin users.</p>	<p>THLE2/3 cells: Exposure of .the cells to the user. Hazards include percutaneous injury, ingestion and mucous membrane exposure. AFB1: Exposure to the user by inhalation, skin or mucous membrane. Hazards include liver carcinogen, heritable genetic damage agents, teratogen.</p>
<p>Medical conditions which can be adversely affected by exposure to agent.</p>	<p>Researchers whom are pregnant/planning pregnancy/breast feeding should not engage in AFB1 work. Researchers who are pregnant/planning pregnancy should report to their supervisor for health and safety audit.</p>

Current Controls / Precautions
<p>THLE2/3 normal human liver cells:</p> <p>These cells present a low risk due to the containment controls that will be implemented with their use. The transformed human liver epithelial cells are considered a biosafety level II hazard due to the presence of a retroviral vector containing SV40 large T antigen for immortalisation. These cells are used to study metabolism and toxicity and have been shown to be non-tumorigenic.</p> <p>Specific controls will be implemented to reduce the risk of THLE2/3 cell use and ensure containment level 2 is observed at all times:</p> <ul style="list-style-type: none"> • Cells will be grown in closed tissue culture vessels inside controlled-environment incubators in a dedicated cell culture suite (GG22 in lab GG21) with Class C air handling, in a building purpose designed for the culture of biohazardous material (NICB). • Manipulations (i.e. splitting cells, washing cells etc.) will be performed in a Class II biological safety cabinet. • Only the immediate lab area is likely to be exposed and considerable care will be taken to ensure the cells are fully contained within the containment area. • Researchers involved are trained in Good Laboratory Practice and will be fully competent in the processes/procedures of Biosafety Level 2 lab work, employing approved SOPs for work and ancillary activities such as cleaning, spillages, waste decontamination/disposal and emergency response procedures under the guidance of S.O.P.s for Safe Handling of Class 2 Biological Agents (NICB). • Researchers will be approved by specialist researchers who have vast experience in Biosafety level 2 procedures and signed off for Biosafety level 2 research under the Class 2 Biological Agent Training Sign-Off form (NICB). • PPE will include protective lab coats, safety glasses and gloves. • All liquid and solid waste will be destroyed by autoclave cycling at 122°C, 15psi for 30 minutes.
<p>AFB1:</p> <p>A number of mould species from the genus <i>Aspergillus</i> produce fungal metabolites called aflatoxins. Aflatoxins are an example of DNA damaging agents that effect the liver and can lead to hepatocellular carcinoma.</p> <ul style="list-style-type: none"> • AFB1 is strictly used as per Aflatoxin handling SOP, revised June 2016 attached. • AFB1 is a teratogen and pregnant researchers should not par-take in research activities involving AFB1. • AFB1 stocks are prepared in a clearly labelled fume-hood designated to assigned toxin users only, in a prep lab (X271a) segregated from the common lab area. • AFB1 stocks are stored in a locked fridge-freezer and the key only made available to relevant toxin users. • All assays/tests are completed in a clearly labelled fume-hood designated to assigned toxin users only or a Class II biological safety cabinet designated to assigned toxin users only. • PPE includes protective lab coats, safety glasses and 2 pairs of gloves. • The disposal risk of AFB1 is controlled by decontamination of all contaminated reagents and materials with 10%-12% sodium hypochlorite, pH adjustment to 8 and addition of acetone. The decontaminated liquid AFB1 waste is disposed of with excess running water following validation of aflatoxin decomposition. Decontaminated solid waste and sharps are added to cytotoxic bins, removed to the School of Biotechnology waste disposal, logged appropriately and collected by a licensed disposal company (SRCL).
Risk Matrix
<ul style="list-style-type: none"> • Taking account of the current controls/precautions listed above, use the Risk Matrix shown below to categorise the Likelihood of a hazardous event happening and the potential Severity of resulting harm. • Low risk activities are identified as being <i>Trivial or Acceptable (Green)</i>. • Medium risk activities are identified as being <i>Medium (Orange)</i>. • High risk activities are identified as being <i>Substantial or Intolerable (Red)</i>.

Severity → ↓ Likelihood	Slightly Harmful	Harmful	Very Harmful
Unlikely	Trivial	Acceptable	Medium
Likely	Acceptable	Medium	Substantial
Very Likely	Medium	Substantial	Intolerable

Agent Name/ Hazardous Procedure	Potential Injury/loss (see ** above)	Severity Rating	Likelihood Rating	Risk Rating
THLE2/3 normal human liver cells	Percutaneous injury, ingestion and mucous membrane exposure	Harmful	Unlikely	Acceptable
AFB1	DNA damaging agent, liver carcinogen	Very Harmful	Unlikely	Medium
Processes – Movement of cells	Ingestion and mucous membrane exposure	Harmful	Unlikely	Acceptable
Tests/Assays	Percutaneous injury, ingestion and mucous membrane exposure, DNA damaging agents, liver carcinogen	Very Harmful	Unlikely	Medium
All Risks acceptable?	Yes	Risk Assessment Date		

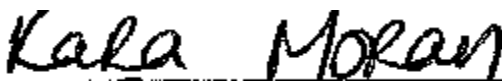
Actions:

- If ANY risk rating is **Intolerable or Substantial**: Cease/do not commence activity until further controls are implemented.
- If ANY risk rating is **Medium**: Consult Biological Safety Advisor.
- If ALL risk ratings are **Trivial / Acceptable**: No further controls required.
- For **Medium / Intolerable or Substantial Risks**: Please address further control measures to be implemented to reduce the residual risk (see below).

***Further Control Measures To Be Implemented for each Substantial/Intolerable Risk Identified**

<p>THLE2/3 normal liver cells:</p> <p>The research will be completed by culturing the THLE2/3 normal liver cells in room GG22 in lab GG21 in the NICB facility tailored for Biosafety Level 2 cell lines. Cells will be grown in closed tissue culture vessels inside controlled-environment incubators in dedicated cell cultures suites with Class C air handling, in a building purpose designed for the culture of biohazardous material (NICB) A Class II biological safety cabinet will be used to ensure user safety and containment of the cells in accordance with S.I. No. 572 of 2013 which outlines the need for containment level 2 for a group 2 biological agents and “where handling materials in respect of which there exists uncertainties about the presence of a biological agent which may cause human disease, but which laboratories do not have as their aim working with a biological agent including cultivating or concentrating a biological agent.” The Class II</p>	Date: 19/10/2016
--	------------------

<p>biological safety cabinet avoids user exposure and maintains THLE2/3 cell isolation by use of a front access opening with carefully maintained inward airflow, HEPA-filtered, vertical, unidirectional airflow within the work area and HEPA-filtered exhaust air to the room or exhaust to a facility exhaust system. To avoid the risk of percutaneous injury by sharps and exposure to THLE2/3 cells, culturing will be completed in the absence of sharps i.e. pipette tips. THLE2/3 cells will be destroyed by autoclave cycling at 122°C, 15psi for 30 minutes and disposed of down the sink.</p> <p>The THLE2/3 cells (cultured in the NICB) will be used for AFB1 treatment and assay based tests in the School of Biotechnology. Accordingly the cultured THLE2/3 cells will be collected and transferred to a sealed falcon tube, placed within a sealed container which will be carried carefully to the School of Biotechnology. The contained THLE2/3 cells will be placed into the container whilst wearing gloves. These gloves will be removed and a fresh, un-contaminated glove will be donned to carry the container to the School of Biotechnology abiding by the 'one glove rule'. A spare fresh, un-contaminated glove will be carried on the person also. On arrival to the School of Biotechnology, the worn glove will be disposed of and fresh, uncontaminated gloves will be donned for experiments.</p> <p>.</p> <p>AFB1: The THLE2 cells will be maintained and cultured in the appropriately contained facility (NICB) for Biosafety level 2 cell lines. Any treatment of the cells with AFB1 will be completed in the School of Biotechnology following careful carriage of the cells within a sealed falcon in a suitable, sealed container to the building. The cells will be transported always to the School of Biotechnology and never AFB1 to the culturing facility (NICB). AFB1 handling and decontamination will be completed as previously described in Aflatoxin handling SOP, revised June 2016.</p> <p>Tests/Assays:</p> <ul style="list-style-type: none"> • AFB1 used for assays with cells (i.e. proposed THLE2/3 cells) is prepared and contained in an assigned toxin user-only designated Class II biological safety cabinet to protect the user against both AFB1 and the THLE2/3 cells. • Where assays/testing is to be completed and pipette tips may be necessary, 2 pairs of gloves will be donned for greater protection against percutaneous injury from both THLE2/3 cells and AFB1. • All assay testing liquids, solids and sharps will be treated by autoclave cycling at 122°C, 15psi for 30 minutes to destroy THLE2/3 cells. Aflatoxins in liquid waste will then be decontaminated, as outlined previously and as per Aflatoxin handling SOP, revised June 2016, by addition of 10-12% sodium hypochlorite pH adjusted to 8 and addition of acetone. Decontaminated liquid waste will be disposed of down the sink following validation of decomposition of AFB1. Autoclaved solids and sharps waste will be placed in purple cytotoxic bins and collected by a licensed disposal company (SRCL). • A SB-WRS-4 Biohazard Waste Management Application for Waste Disposal (Issue 3, Issued 10/05/2015) will also be completed to track waste disposal. 			
Residual Risk Ratings <i>(when above measures* have been implemented)</i>	Severity Rating	Likelihood Rating	Residual Risk Rating
AFB1	Harmful	Unlikely	Acceptable

Tests/Assays	Harmful	Unlikely	Acceptable
All Residual risks acceptable?	Yes	Residual Risk Assessment Date	
Signature of Biological Safety Advisor			
Signature of Applicant			

FDA, 2010. *Briefing Document — Testing for Replication Competent Retrovirus (RCR)/Lentivirus (RCL) in Retroviral and Lentiviral Vector Based Gene Therapy Products — Revisiting Current FDA Recommendations* [Online]. Available from <http://www.fda.gov/downloads/AdvisoryCommittees/CommitteesMeetingMaterials/BloodVaccinesandOtherBiologics/CellularTissueandGeneTherapiesAdvisoryCommittee/UCM232592.pdf> [Accessed 26 June 2016].

Bennett, J.W. and Klich, M. 2003. Mycotoxins. *Clinical Microbiology Reviews*, 16(3), pp. 497-516.

Wu, H.C. and Santella, R. 2012. The role of aflatoxins in hepatocellular carcinoma. *Hepatitis Monthly*, 12(10 HCC): e7238, pp. 1-9.

ATCC, 2013. *THLE2 (ATCC® CRL2706™) Product Sheet* [Online]. Available from <file:///C:/Users/Kara/Desktop/CRL-2706.pdf> [Accessed 26 June 2016].

D. Miller, 2002. PA317 Retrovirus Packaging Cells, *Molecular Therapy*, 6(5), pp. 572-575 [Online]. Available from http://www.nature.com/mt/journal/v6/n5/pdf/mt2002216a.pdf?origin=publication_detail [Accessed 27 June 2016].

Harris, C.C., Cole, K.H., Lechner, J.F. and Reddel, R. The United States Of America As Represented By The Department Of Health And Human Services, 1998. *Human liver epithelial cell lines*, US5759765 A.

Safety, health and welfare at work (biological agents) regulations 2013. S.I. No. 572 of 2013. Dublin: Statutory Office. Available from http://www.hsa.ie/eng/Legislation/New_Legislation/Biological%20Agents%20Regulations%202013.pdf [Accessed 13 July 2016].

Biological agents: Managing the risks in laboratories and healthcare premises 2005. Norwich: Statutory Office. Available from <http://www.hse.gov.uk/biosafety/biologagents.pdf> [Accessed on 13 July 2016].



Faculty of Science & Health

Biological Safety Committee Approval Form

(Submission of Information on GMO & Biological Hazard)

Date of Approval
Submission on behalf of
Affiliated School/ Centre

8th November 2016
Kara Moran/ Prof. Richard O'Kennedy
School of Biotechnology

Project Title:

The treatment of THLE2/3 normal human liver cells with AFB1 to determine the cellular processes associated with hepatocellular carcinoma.

Decision

On behalf of the Biological Safety Committee, I hereby confirm approval for the project titled above. All amendments and additional information requested from Kara Moran/ Prof. Richard O'Kennedy have been completed and the relevant forms updated. Notification to the EPA in the form of an amendment to an existing license is necessary before commencing project.

A handwritten signature in black ink, reading 'Michael Burke', is written over a horizontal line.

Michael Burke
Chair of the Biological Safety Committee

EPA Register of Genetically Modified Organisms (GMOs)

Users in Ireland

Name and address of user:	Dr Niall Barron National Institute for Cellular Biotechnology Dublin City University Glasnevin Dublin 9
Location or postal address of the premises to which a record, notification or amended notification relates:	National Institute for Cellular Biotechnology Dublin City University Glasnevin Dublin 9
GMO register No.	G0261-01
Description of each genetically modified organism involved:	1. Adenovirus type 5 with E1A and E1B deletions and lentiviral vectors will be propagated on HEK 293 cells and used to deliver genes of interest to various cell lines. 2. Transfection of normal human liver cell line (Transformed Human Liver Epithelial THLE2/3 cells) with gammaretroviral vector containing SV40 large T antigen for immortalisation. Class 2 GMM
Purpose of the contained use:	1. The aim of this work is to determine how certain proteins, either viral in origin or cellular proteins, whose expression is induced by infection with Herpes Simplex Virus, Kaposi's Sarcoma-associated Herpes Virus or Vaccinia Virus, function to stimulate the cells protein synthesis machinery when expressed alone in cells. 2. The aim of this work is to immortalise the Transforming Human Liver Epithelial (THLE2/3) cell line for study of initiation and progression of toxicology and to provide an excellent model for assessing liver cell metabolism.
Date of receipt of a record, notification or amended notification:	05/Oct/2007 Notification received under Article 18(2), additional Class 2 GMM to a premises already registered (GMO Register No: 224) 29/Jan/2008 2007 annual report received. No changes to register. 13/Mar/2009 2008 annual report received. No changes to GMO register entry, RA or containment measures applied. 06/May/2010 2009 annual report received. No changes to GMO register entry, RA or containment measures applied. 14/Mar/2011 2010 Annual Report received. No changes in GMO Register entry, RA or containment measures applied. 22/Mar/2012 2011 Annual Report received. Due to departure of Dr Derek Walsh

	<p>from DCU, this register is transferred into the sole name of Dr. Niall Barron. No changes to RA or containment measures applied.</p> <p>28/Mar/2013 2012 Annual Report received. No changes to GMO Register entry, RA or containment measures applied.</p> <p>28/Mar/2014 2013 Annual Report received. No changes to GMO Register entry, RA or containment measures applied.</p> <p>14/May/2015 2014 Annual Report received. No changes to GMO Register entry, RA or containment measures applied.</p> <p>31/Mar/2016 2015 Annual Report received. No changes to GMO Register entry, RA or containment measures applied.</p> <p>17/Nov/2016 Risk Assessment submitted in respect of a Class 2 GMM (belonging to Group VI (ssRNA-RT) family of retroviridae similar to lentivirus (already notified) (see 2 above).</p>
Date and nature of any information provided under article 30(3):	
Date of any request by the Agency under article 10 or 25:	<p>10/Oct/2007 Additional information requested</p>
Date of any response from the user to any request by the Agency under article 10 or 25:	<p>12/Oct/2007 Additional information received</p>
Date of publication of a notice pursuant to article 20 or 21:	
Date of withdrawal of a notification or an amended notification:	
Date and nature of the decision by the Agency on a notification or an amended notification:	<p>17/Oct/2007 Consent Conditions granted</p>
Date and outcome of any review referred to in article 10 or carried out under article 10 or 29	

Appendix B

Extractions of AFB₁ from Dried Distillers Grain with Solubles

Extraction methods were investigated to determine if AFB₁ and T-2 toxin could be a) successfully isolated from Dried Distillers Grain with Solubles (DDGS) and b) if an aqueous based solution could be successfully employed for this purpose. This process was necessary to provide samples which could be tested on the MBio detection platform using the anti-AFB₁ Fab antibody fragment and the anti-T-2 toxin polyclonal antibody analysed in this research for this purpose. Four approaches were examined, as described in Sections 2.2.31 – 2.2.33 for the extraction of AFB₁ from contaminated DDGS samples and also for the extraction of blank DDGS samples (known to be free of AFB₁) to produce a DDGS representative matrix (Table App.1). AFB₁ is characterised by its intrinsic fluorescent nature and therefore, the fluorescent intensity of each DDGS extract was determined directly by the Tecan with excitation at 594 nm and emission at 633 nm (Figure App.1). The relevant blank DDGS samples were then subtracted from their counter-part AFB₁ contaminated DDGS samples, to establish which extract delivered the greatest quantity of extracted AFB₁ represented in Figure App.2 and indicated the optimal extracted process. Following the selection of a successful AFB₁ extraction method, the selected approach was applied for the extraction of T-2 toxin from contaminated DDGS samples to ensure both mycotoxins were obtainable using the one selected extraction process. The results of the T-2 toxin extraction are shown in Figure App.3.

Table App.1: Extraction conditions for DDGS samples

Extraction 1 & 1B Conditions	Extraction 2 & 2B Conditions	Extraction 3 & 3B Conditions	Extraction 4 & 4B Conditions
1 g sample	1 g sample	1 g sample	1 g sample
Add 5 mL 2% (v/v) formic acid in water.	3 mL 20% (v/v) methanol in water	Add 0.5 g NaCl + 0.2 g MgSO ₄ H ₂ O	Add 0.5 g NaCl + 0.2 g MgSO ₄ H ₂ O
Add 0.05g NaCl + 2g MgSO ₄ H ₂ O.	Shake 10 minutes	Add 6 mL acetonitrile + 2 mL methanol + 2 mL water	Add 6 mL acetonitrile + 2 mL methanol + 2 mL water
Centrifuge at 3,220g (Eppendorf 5810 R, Rotor A-4-62) at 4°C for 5 minutes.	Centrifuge at 3,220g (Eppendorf 5810 R, Rotor A-4-62) at 4°C for 20 minutes.	Shake at 300 rpm at room temperature overnight.	Shake at 300 rpm at room temperature overnight
Collect upper organic phase. Add 0.3g MgSO ₄ H ₂ O.	Filter and collect sample	Centrifuge at 3,220g (Eppendorf 5810 R, Rotor A-4-62) at 4°C for 10 minutes.	Centrifuge at 3,220g (Eppendorf 5810 R, Rotor A-4-62) at 4°C for 10 minutes.
Centrifuge at 3,220g (Eppendorf 5810 R, Rotor A-4-62) at 4°C for 1 minute.		Collect sample under Nitrogen flow & filter	Collect sample under Nitrogen flow, re-suspend in PBS & filter
Collect sample under Nitrogen flow & re-suspend in PBS			

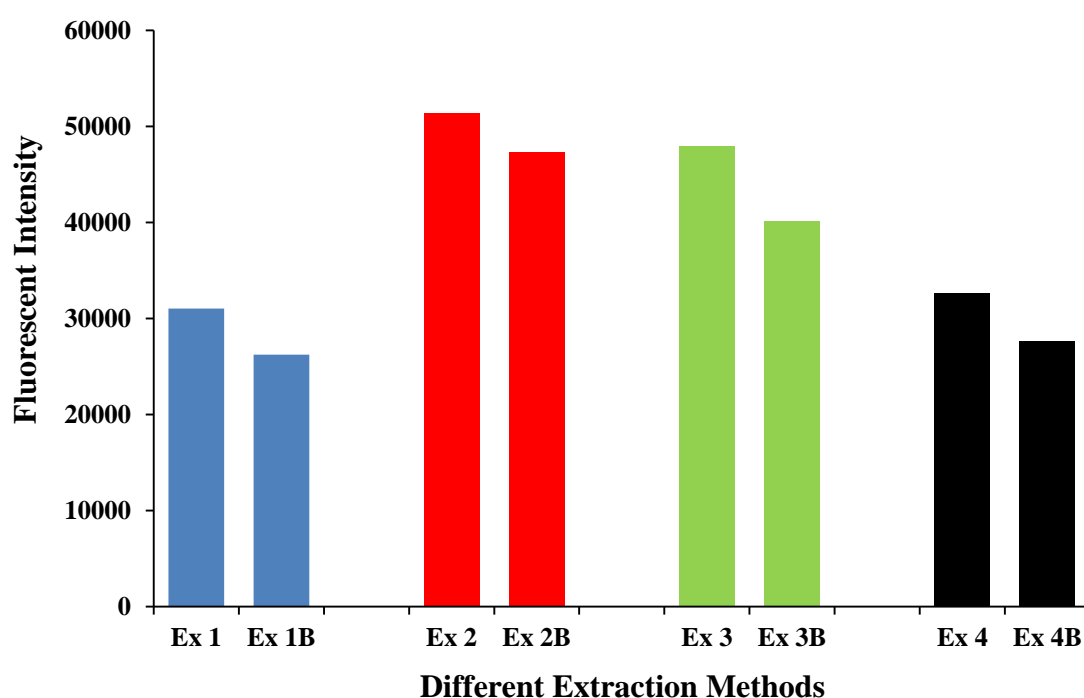


Figure App.1: Four extraction methods (Ex 1 - 4) used to extract AFB₁ from contaminated Dry Distillers Grain with Solubles (DDGS) samples. The same extraction processes were applied to blank DDGS (Ex 1B, Ex 2B, Ex 3B and Ex 4B). The same AFB₁ contaminated DDGS sample and blank DDGS sample was used each for all extraction methods. The fluorescent intensity was higher in all AFB₁ contaminated DDGS samples than their blank counterparts, indicating that AFB₁ has been successfully extracted in these samples.

Figure App.1 indicates that AFB₁ was successfully extracted using each extraction method (Ex 1, Ex 2, Ex 3 and Ex 4). The fluorescent intensity elicited by these extracts are greater than their blank counter-parts (Ex 1B, Ex 2B, Ex 3B and Ex 4B) indicating that the increased fluorescence is as a result of the extracted AFB₁.

To determine which extraction delivered the greatest yield of AFB₁, the relevant blank DDGS samples were subtracted from their counter-part AFB₁ contaminated DDGS samples. Figure App.2 shows that extraction method 3, gave the highest fluorescent intensity relative to its blank, suggesting this method isolated the highest yield of AFB₁. However, extraction method 2 which was completed with an aqueous-based solvent solution (80:20% (v/v) water:methanol) gave the second highest fluorescent intensity relative to its blank signifying that this method was suitable and effective for the extraction of AFB₁ from DDGS samples. Extraction method 1 and 4 also indicated increased fluorescent responses relative to their blanks implying that AFB₁-extraction was successfully achieved using these approaches. In particular, extraction method 2, which permitted the aqueous-based extraction of AFB₁ compared to the other solvent-based extraction methods was important for future use in the MBio multiplex detection system. The results indicated that extraction method 2 would provide a more suitable extraction process that avoids high percentage solvent-use that could affect the immunoassay format of the MBio multiplex detection system. However, the extraction method 2 had to be assessed to determine its effectiveness for the extraction of T-2 toxin from DDGS samples, to permit multiplex analysis of both AFB₁ and T-2 toxin from the same sample following this procedure.

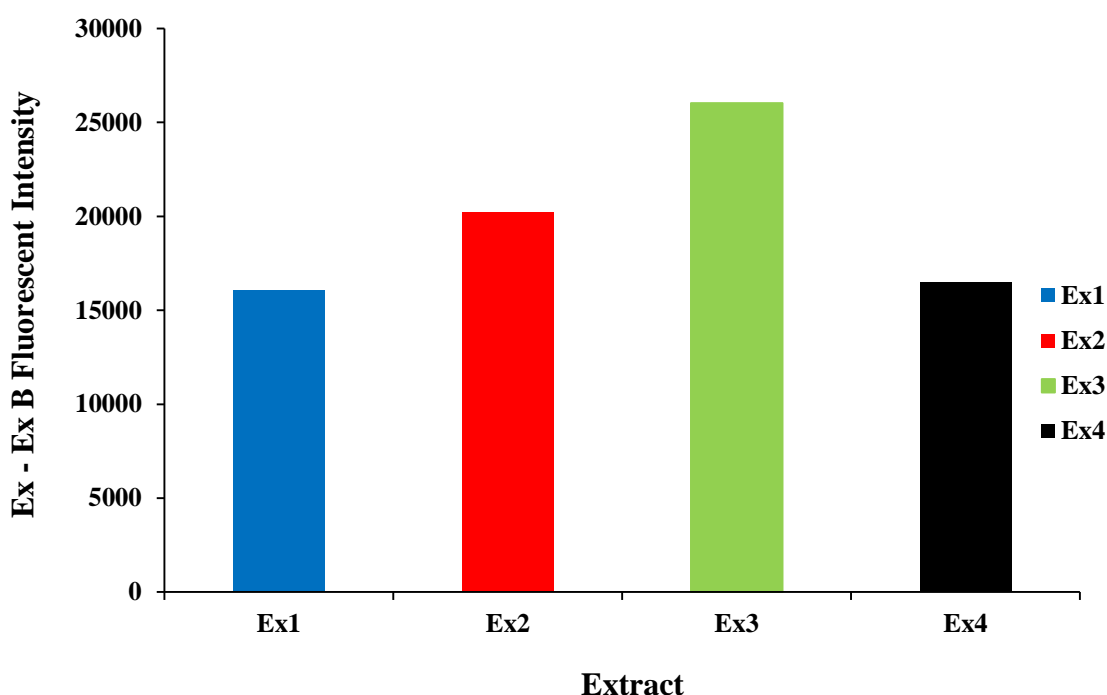


Figure App.2: Fluorescent intensity of contaminated DDGS extracts containing AFB₁ extracts (Ex 1, Ex 2, Ex 3 and Ex 4) after subtraction of blank DDGS extracts free of AFB₁ (Ex 1B, Ex 2B, Ex 3B and Ex 4B).

Extractions of T-2 toxin from Dried Distillers Grain with Solubles

Extraction method 2 (described in Table App.1) was implemented for the isolation of T-2 toxin from contaminated DDGS samples and also for the extraction of blank DDGS samples (known to be free of T-2 toxin) to produce a DDGS representative matrix. To determine if the extraction method was effectual, the extracted blank DDGS matrix was spiked with doubling dilutions of known T-2 toxin concentrations to generate a standard curve in an indirect competitive inhibition ELISA format. The T-2 toxin extracted from the contaminated DDGS samples was then calculated using the T-2 toxin standard curve. This process established whether a) T-2 toxin was successfully extracted from contaminated DDGS samples using extraction method 2 and b) if the competitive inhibition format would be functional in the extraction method 2 aqueous-based matrix. Figure App.3 indicates that a standard curve was produced by spiking the obtained blank DDGS matrix with known concentrations of T-2 toxin. From this curve the extracted T-2 toxin contaminated DDGS samples was calculated to contain 5.01 ng/mL calculated as 6.72 µg/kg of T-2 toxin. Previous analysis of this sample by the Global Research Institutes in

Health and Food Security, Queens University, Belfast using LC/MS-MS methods indicated that this sample contained 9 $\mu\text{g/kg}$ of T-2 toxin. Therefore, there is a decrease in the concentration of T-2 toxin being recovered by extraction method 2. This may be due to the low concentration of methanol in the aqueous-based extraction solvent (20%) or alternatively the result may be limited by use of the indirect competitive inhibition ELISA detection method. However, this result demonstrates that T-2 toxin was successfully extracted from contaminated DDGS samples and provided a suitable level of contaminated sample for a ‘proof-of-concept’ analysis on the MBio detection system. Furthermore, the fluorescent detection of the MBio platform may provide a more sensitive detection of T-2 toxin than the ELISA method. The ability to extract both mycotoxins using the 80:20% (v/v) water:methanol solution established conditions which enabled the use of these extracts for multiplex detection in the MBio detection system.

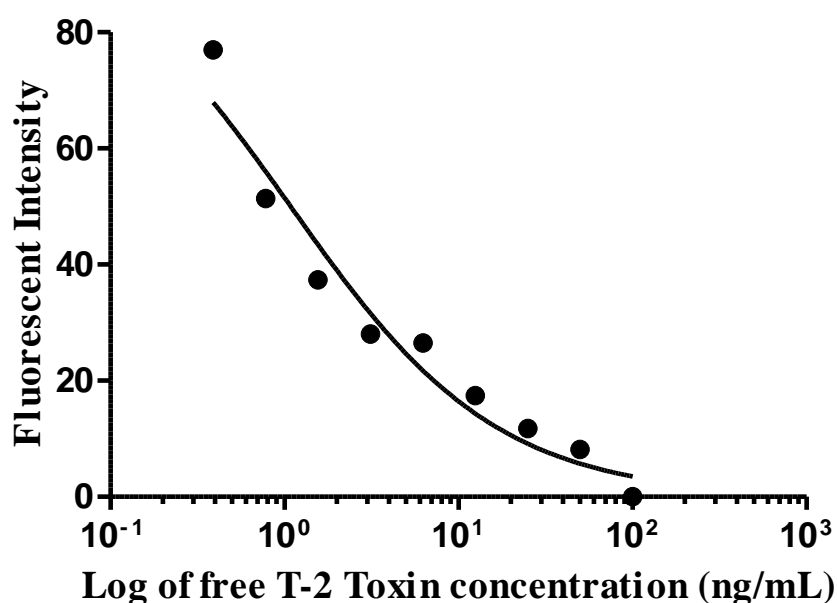


Figure App.3: Indirect Competitive Inhibition ELISA with anti-T-2 toxin polyclonal antibody against immobilised T-2 toxin-BSA (20 $\mu\text{g/mL}$). T-2 toxin was diluted with PBS and coated on an ELISA plate. Doubling dilutions of free T-2 toxin from 100 – 0.39 ng/mL were prepared in PBS and allowed to incubate with a 1/500 dilution of anti-T-2 toxin polyclonal antibody in PBST with 1% (w/v) Milk Marvel. A HRP-labelled anti-HA secondary antibody diluted 1/1,000 in PBST with 1% (w/v) Milk Marvel was added, followed by TMB substrate. The reaction was stopped with 10% (v/v) HCl and absorbance was measured at 450 nm using a Tecan Safire™ 2 plate reader.